DISSOLUTION OF IRON OXIDES BY OXALIC ACID

A thesis submitted for the degree of

Doctor of Philosophy

by

SUNG OH LEE

M.Sc (Resources Recycling Engineering)
B.Sc (Mineral and Resources Engineering)
Chonnam National University, KOREA

THE UNIVERSITY OF NEW SOUTH WALES

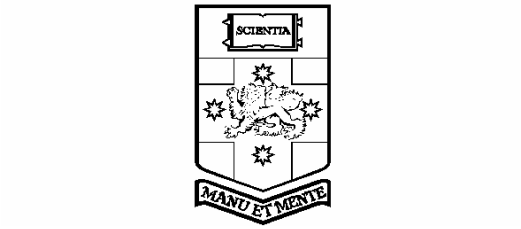

School of Chemical Engineering and Industrial chemistry
Faculty of Engineering

Sydney, Australia

September, 2005

PLEASE TYPE

THE UNIVERSITY OF NEW SOUTH WALES
Thesis/Project Report Sheet

Surname or Family name: LEE

First name: SUNG OH Other name/s:

Abbreviation for degree as given in the University calendar: Ph.D

School: Chemical Engineering & Industrial Chemistry Faculty: Engineering

Title: DISSOLUTION OF IRON OXIDES BY OXALIC ACID

Abstract 350 words maximum: (PLEASE TYPE)

The iron content of industrial minerals can be reduced by physical and chemical processing. Chemical processing is very efficient to achieve a high degree of iron removal at minimum operating cost. Both inorganic acids and organic acids have been used for clay refining. However, due to environmental pollution and contamination of products with the SO_4^{2-} and Cl^-, inorganic acids should be avoided as much as possible. This research investigated the use of oxalic acid to dissolve iron oxides and the dissolution characteristics of natural iron oxides.

The dissolution of iron oxides in oxalic acid was found to be very slow at temperatures ranging from 25℃ to 60℃, but increased rapidly at a temperature above 90°C with increasing oxalic acid concentration, whereas the pH caused the reaction rate to decrease at pH>2.5 and improved the rate from pH 1 to pH 2.5. The iron oxides such as goethite (α-FeOOH), lepidocrocite (γ-FeOOH) and iron hydroxide ($Fe(OH)_3$) can be dissolved faster at the presence of magnetite which exhibits an induction period at the initial stage and showed the bell-shaped curves for the dissolution.

In titration tests, however, the increase of temperature causes an increase in solubility of the oxalate complexes, resulting in an increased stability of ionized species in solution. During the addition of NaOH, $NaHC_2O_4 \cdot H_2O$ was precipitated without forming $Na_2C_2O_4 \cdot H_2O$, but it was re-dissolved at pH>4.0. On the other hand with NH_4OH, $NH_4HC_2O_4 \cdot H_2O$ and $(NH_4)_2C_2O_4 \cdot H_2O$ co-precipitated at pH 0.93, but also re-dissolved at over pH 2.03. The reaction temperature was found not to affect the removal of iron from the ferric oxalate complex solution using lime. Iron is removed as iron hydroxide and calcium oxalate is then precipitated during the iron removal step. The formation of $Fe(OH)_3$ in the solution was affected by the dissociation of $Ca(OH)_2$.

The thermodynamics of sodium, ammonium and iron oxalate complexes were investigated and the standard free energy, ΔG^o was calculated using thermodynamic data and solubility products.

The dissolution of pure hematite by oxalate was found to follow a shrinking core model of which the kinetic step of the reaction is the controlled mechanism.

Declaration relating to disposition of project report/thesis

I am fully aware of the policy of the University relating to the retention and use of higher degree project reports and theses, namely that the University retains the copies submitted for examination and is free to allow them to be consulted or borrowed. Subject to the provisions of the Copyright Act 1968, the University may issue a project report or thesis in whole or in part, in photostat or microfilm or other copying medium.

I also authorise the publication by University Microfilms of a 350 word abstract in Dissertation Abstracts International (applicable to doctorates only).

....
Signature Witness Date

The University recognises that there may be exceptional circumstances requiring restrictions on copying or conditions on use. Requests for restriction for a period of up to 2 years must be made in writing to the Registrar. Requests for a longer period of restriction may be considered in exceptional circumstances if accompanied by a letter of support from the Supervisor or Head of School. Such requests must be submitted with the thesis/project report.

FOR OFFICE USE ONLY Date of completion of requirements for Award:

Registrar and Deputy Principal

THIS SHEET IS TO BE GLUED TO THE INSIDE FRONT COVER OF THE THESIS

Sticker

ACKNOWLEDGEMENTS

I am deeply grateful to my supervisor, Associate Professor Tam Tran, for his guidance, advice, support and invaluable help over the duration of my research.

I would also like to sincerely thank my co-supervisor, Dr. Frank Lucien of the School of Chemical Engineering and Industrial Chemistry, and Associate Professor Myong Jun Kim of Chonnam National University, for their guidance, advice, support and invaluable help over the duration of my research.

I gratefully thank Mr. Jin Kon Song of the School of Chemical Engineering and Industrial Chemistry, for his encouragement, assistance in experimental work and invaluable help.

I am also grateful to the following: Young Jun Hong, Il Joon Bae, Him Chan Cho, Sang Yoon Lee, Eung Yeul Park and Eun Chul Cho, for their friendship and offers of help for my research and overseas life.

Finally, my thanks also go to my wife, Seo Jin, Seo Kyoung and all my brothers for their moral support. I would like to offer thanks to God for seeing me through my study and stay in Australia.

LIST OF PUBLICATIONS

1. Sung Oh LEE, Tam TRAN, Yi Yong PARK and Myong Jun KIM, Dissolution of iron oxide using oxalic acid, paper submitted to J. of Int. Min. Proc. (October 2005).

2. Sung Oh LEE, Tam TRAN, Yi Yong PARK and Myong Jun KIM, Study on the kinetics of dissolution of iron oxide, paper submitted to Hydrometallurgy (October, 2005).

3. Sung Oh LEE, Jong Kee OH and Bang Sup SHIN, Dissolution Of Iron Oxide Rust Materials Using Oxalic Acid, *Journal of MMI of Japan*, Vol.115, No.11, (1999).

4. Sung Oh LEE, Myong Jun KIM, Jong Kee OH and Bang Sup SHIN, Removal of Ferric Ions from Iron (III) Oxalato Complexes Reacted with Calcium Hydroxide in Solution, *Journal of MMI of Japan,* Vol.115, No.11, (1999).

5. Sung Oh LEE, Sung Kyu KIM, Jong Kee OH and Bang Sup SHIN, Dissolution Characteristics of Hematite and Magnetite with Oxalic acid, *Journal of the Korean Inst. of Mineral and Energy Resources Engineering,* Vol.35, No.6, (1998)-(in Korean).

6. Sung Oh LEE, Wan Tae KIM, Jong Kee OH and Bang Sup SHIN, Iron-removal of Clay Mineral with Oxalic Acid, *Journal of MMI of Japan,* Vol.113, No.11, (1997).

ABSTRACT

The iron content of industrial minerals can be reduced by physical and chemical processing. Chemical processing is very efficient to achieve a high degree of iron removal at minimum operating cost. Both inorganic acids and organic acids have been used for clay refining. However, due to environmental pollution and contamination of products with the SO_4^{2-} and Cl^-, inorganic acids should be avoided as much as possible. This research investigated the use of oxalic acid to dissolve iron oxides and the dissolution characteristics of natural iron oxides.

The dissolution of iron oxides in oxalic acid was found to be very slow at temperatures ranging from 25℃ to 60℃, but increased rapidly at a temperature above 90°C with increasing oxalic acid concentration, whereas the pH caused the reaction rate to decrease at pH>2.5 and improved the rate from pH 1 to pH 2.5. The iron oxides such as goethite (α-FeOOH), lepidocrocite (γ-FeOOH) and iron hydroxide ($Fe(OH)_3$) can be dissolved faster at the presence of magnetite which exhibits an induction period at the initial stage and showed the bell-shaped curves for the dissolution.

In titration tests, however, the increase of temperature causes an increase in solubility of the oxalate complexes, resulting in an increased stability of ionized species in solution. During the addition of NaOH, $NaHC_2O_4 \cdot H_2O$ was precipitated without forming $Na_2C_2O_4 \cdot H_2O$, but it was re-dissolved at pH>4.0. On the other hand with NH_4OH, $NH_4HC_2O_4 \cdot H_2O$ and $(NH_4)_2C_2O_4 \cdot H_2O$ co-precipitated at pH 0.93, but also re-dissolved at over pH 2.03. The reaction temperature was found not to affect the removal of iron from the ferric oxalate complex solution using lime. Iron is removed as iron hydroxide and calcium oxalate is then precipitated during the iron removal step. The formation of $Fe(OH)_3$ in the solution was affected by the dissociation of $Ca(OH)_2$.

The thermodynamics of sodium, ammonium and iron oxalate complexes were investigated and the standard free energy, ΔG^o was calculated using thermodynamic data and solubility products.

The dissolution of pure hematite by oxalate was found to follow a shrinking core model of which the kinetic step of the reaction is the controlled mechanism.

TABLE OF CONTENTS

LIST OF FIGURES

LIST OF TABLES

CHAPTER ONE

INTRODUCTION

1.1 BACKGROUND

The dissolution of metal oxides is of practical importance as it is used to clean iron oxide from the iron metal surface and to remove the iron from mineral concentrates. Industrial processes related to dissolution of iron oxides include acid leaching of iron ores, removal of corrosion products from industrial equipment and heat exchangers (e.g. cooling coils in water-cooled nuclear reactors), as well as removal of the associated oxides, hydroxides and hydrated oxides of ferric iron (hematite, goethite and lepidocrocite etc.) from industrial minerals.

The iron content in industrial minerals can be reduced by physical, physicochemical and chemical processing. Of these processes, chemical processing to remove the contaminated iron oxides in industrial minerals is ideal as it is found to be efficient (Cornell and Schwertmann, 1996; Blesa et al., 1994). Chemical methods involve leaching of minerals using inorganic and organic acids. In most industrial processes, inorganic acids such as hydrochloric acid and sulphuric acid are used due to higher leaching rates. Nevertheless, many researchers have studied the use of oxalic acid to dissolve iron oxides, as this acid can be obtained cheaply as a by-product from other industrial processes (Ambikadevi and Lalithambika, 2000; Blesa et al., 1987; Cornell and Schindler, 1987).

Corrosion chemists and metallurgists place their emphasis on the electrochemical aspects of dissolution of iron oxides, in particular on the effect of the applied oxidation potential. This aspect of the dissolution of iron oxides has been studied by Vermilyea (1966), Diggle (1973), Segal and Sellers (1984), Frenier and Growcock (1984), Jepson (1988), Chiarizia and Horwitz (1991), Blesa et al. (1994), Cornell and Schwertmann (1996) and Panias et al. (1996).

The other approach, which is emphasized in this study, considers the effect of solution parameters on the rate of dissolution; aiming at elucidating the principal dissolution mechanisms involved and on the basis of this, developing deterministic dissolution models.

The use of different inorganic and organic acids (in complexing or reductive reactions) for the dissolution of iron compounds have been major subjects of study (Sidhu et al., 1981; Lim-Nunez and Gilkes, 1987; Borghi et al., 1989; Cornell and Giovanoli, 1988a; Blesa et al., 1994; Segal and Sellers, 1980). Most of these studies focused on the mechanism of the dissolution of hematite and magnetite, under various chemical and experimental conditions using synthetic materials (Baumgartner et al., 1982; Frenier and Growcock, 1984; Cornell et al., 1976; Blesa and Maroto, 1986). However, their unoptimized results cannot be used for the design of an industrial process for removing iron from natural minerals.

The aim of this study is to investigate the characteristics of dissolution of natural iron oxides (hematite, magnetite and iron rust materials), which are common iron–bearing minerals found in industrial minerals. The study was conducted to optimize reaction parameters, such as oxalic acid concentration, temperature, and pH of the solution.

In addition, a thermodynamic analysis of the above reactions including those involved in the formation of iron oxalate complexes was evaluated. For this purpose, the speciation of oxalic acid, and the formation of sodium, ammonium and iron oxalate complexes and their thermodynamic properties of appropriate representative chemical reactions have also been investigated.

The main objective of this study is to clarify the characteristics of leaching of iron oxide from industrial minerals with oxalic acid. Reaction conditions will be optimized for the development of a process which is more efficient and environmentally acceptable than the current practice.

1.2 OBJECTIVES OF THE STUDY

The specific objectives of this research are:

- To examine and characterize the iron oxides and mineral ores used for the

dissolution tests.

- To investigate the factors affecting the dissolution of iron such as reaction temperature, acid concentration, agitation speed and solution pH.
- To study the dissolution characteristics and elucidate the mechanism of the leaching of Fe(II/III) oxides under different reaction conditions.
- To study the thermodynamics of the reaction of iron oxides and sodium/ammonium oxalate complexes.
- To re-evaluate the solubility product (K_{sp}) and free energy of the dissolution of iron oxides in oxalic acid solution, the formation of sodium/ammonium oxalate complexes and their solubility.
- To study the reaction and the precipitation of the sodium/ammonium oxalate.
- To study the decomposition of iron oxalate ion in solution and the formation of calcium oxalate.

CHAPTER TWO

LITERATURE REVIEW

2.1 INTRODUCTION

Most of the iron is in the form of immobile Fe(III) oxides in natural systems, although a large amount of iron circulates in all parts of the ecosystem through biota, water and soil systems. Processes of iron dissolution or precipitation are crucial for the formation of iron ores and ferricretes in soils and for the cycling of iron in natural waters (Stumm and Sulzberger, 1992; Stumm, 1992; Rasmussen and Nielsen, 1996). Dissolution processes are also relevant to the interconversions in a solution. The rate at which an iron precursor dissolves can have a pronounced effect on the type and properties of the final phase.

The formation of Fe(III) oxides mainly involves aerobic weathering of surface magmatic rocks in both terrestrial and marine environments. Redistribution may involve mechanical transport by wind/water erosion from the pedosphere into the hydrosphere or atmosphere or, more importantly, reductive dissolution followed by oxidative re-precipitation. Iron ore formation and iron oxide precipitation in the biota are important examples of such redistribution processes.

Industrial processes related to the dissolution of iron oxides include acid leaching of iron ores, removal of corrosion products from equipment and scales (on surfaces such as cooling coils in water-cooled nuclear reactors), removal of impurities from industrial minerals such as clay, kaoline, the stabilising of passive layers on iron and, the pickling of steel. In extractive metallurgy, iron ores are leached to recover the metal and produce the efficiency of the extraction process depends upon the leachability of the ore (Warren and Roach, 1971; Veglio et al., 1994). The removal of iron oxide deposits from the inner surfaces of boilers, steam generators and pipes improves heat transfer, reduces pitting corrosion and prolongs the service life of the equipment. Such corrosion products and scales from steel surface are usually removed using strong acids or acid/complexant mixtures. Sodium dithionite and organic acid are used to bleach kaolin

and clay minerals, remove the staining iron oxides and thereby improve its whiteness for use in porcelain (Jepson, 1988; Lee et al., 1997).

The dissolution of iron oxides was studied in the following areas:

1) Corrosion chemists and metallurgists place emphasis on the electrochemical aspects, in particular, the effect of the applied potential. This aspect of the dissolution of iron oxides has been studied by Vermilyea (1966), Diggle (1973), Segal and Sellers (1984), Frenier and Growcock (1984) and Chiarizia and Horwitz (1991).

2) The other approach considers the effect of operating parameters on the rate of dissolution; aiming at elucidating the principal dissolution mechanisms involved and on the basis of this, developing deterministic dissolution models.

The factors affecting the dissolution behaviour of iron oxides are surface area and, in some cases, crystal morphology. Surface area is considered important because for a heterogeneous reaction involving processes at the solid/liquid interface its rate is a function of surface area. Even after taking surface area into consideration, however, oxides having different crystal structures and different samples of the same oxide can behave quite differently. To date, only limited attempts to study these differences have been made (Cornell et al., 1974; Schwertmann, 1984a; Lim-Nunez and Gilkes, 1987; Allen et al., 1988; Stumm, 1992; Stumm and Sulzberger, 1992; Cornell and Giovanoli, 1993; Casey, 1995).

2.2 DISSOLUTION OF IRON OXIDES

The Eh-pH diagram of the oxygen and iron binary system (Pourbaix, 1981) shows that only three oxides are thermodynamically stable, namely wustite ($Fe_{1-x}O$), magnetite (Fe_3O_4) and hematite (α-Fe_2O_3). However, metastable phases and hydrated forms are commonly found in nature and when these are included, the list of iron (hydrous) oxides enlarges considerably. Tables 2.1 and 2.2 summarize the main properties of these compounds, compiled by gathered by Schwertmann and Cornell (1991) and re-produced herewith.

Table 2.1 Selected properties of crystalline iron oxides (according to Schwertmann and Cornell (1991))

	Name of naturally occurring mineral	Crystal system (space group)	Structural relationships	ΔG^{o}_{f} [kJ (mol Fe)$^{-1}$	Solubility at pH 7 and 25^{o}C (-logC_{Fe})	E^{o}_{H+} at pH 7(V)
Fe(III)	Hematite (α-Fe_2O_3)	*R3c*	*hcp*	371.4	12.5	-0.48
	Maghemite (γ-Fe_2O_3)	*$p4_1(p4_3)$*	*ccp*	363.7	≅10	-0.38
	Goethite (α-FeOOH)	*Pbnm*	-	489.0	13.5	-0.52
	Akagnetite (β-FeOOH)	-	*ccp*	-	-	-
	Lepidocrocite (γ-FeOOH)	*Aman*	*ccp*	476.5	≅10	-0.35
Fe(II /III)	Magnetite (Fe_3O_4)	*Fd3m*	*ccp*	338.1	2	-0.59
Fe(II)	Wustite (FeO)	*Fm3m (Fd3m)*	*ccp*	251	0.8	-
	Amakinite $Fe(OH)_2$	*P3m1*	*hcp*	492	0.7	-

Table 2.2 Selected properties of less crystalline forms of iron oxides (according to Schwertmann and Cornell (1991))

Oxidation state	III			II
Name	Ferrihydrites	Feroxyhydrite	Spiro ball	Green rust
Approximate composition	$Fe_5O_{12}H_9$	δ-FeOOH	$Fe_{16}O_{16}$ $(OH)_{12}$ $(SO_4)_2$	Fe_xO_y $(OH)_z$Y·xH_2O Y=CO_3^{2-}, Cl^-, SO_4^{2-}
Structural features	Trigonal *a* = 0.508 *c* = 0.940	Hexagonal *a* = 0.293 *c* = 0.460	Tetragonal *a* = 1.065 *c* = 0.604	Hexagonal

2.2.1 Dissolution mechanisms

The principles of dissolution have been reviewed earlier by Bloom and Nater (1991), Blesa et al. (1994) and Casey (1995). The driving force for dissolution is the extent of undersaturation with respect to the iron oxides. Therefore, undersaturation is a necessity for dissolution as is supersaturation for precipitation. When other factors are equal, the rate of reaction increases as the degree of undersaturation rises. The extent of undersaturation varies from one system to the next. Dissolution of anodic films often takes place in nearly saturated solutions, whereas extraction of iron from its ores requires markedly undersaturated solutions in order to be efficient. In most natural systems, (soils and waters) the aqueous phase is fairly close to saturation with respect to iron oxides and resulting in slow dissolution. The dissolution process can also be accelerated by a redox process in the presence of chelating ligands.

The dissolution process is usually considered to take place in a reverse step of the process of crystal growth, i.e. an ion or molecule at a crystal surface is first detached from its neighbours, diffuses over the crystal surface and finally enters the bulk solution. Each of these steps can be rate-determining.

The dissolution rate (and mechanism) is frequently established on the basis of data corresponding to the release of no more than a few percent of the total iron (e.g. Stumm et al., 1985). In the initial stage of dissolution, the amount of iron released is often a linear function of time, so the initial dissolution rate can be expressed as the amount of iron dissolved per unit weight or unit area of the oxide. However, this small proportion of the reaction does not fully represent the behaviour of the bulk oxide as other processes taking place later on will hinder or promote the dissolution.

While most studies on dissolution concentrate on establishing the reaction mechanism, there are few studies in which different oxides have been compared to provide information on the effect of oxide properties. In fact, Blesa and Maroto (1986) concluded that there is no unique reactivity which can be attributed to a tested iron oxide. If this is the case, what differences there are between oxides and even between different samples of the same oxide, can probably be associated with structural factors. Natural crystal surfaces are seldom smooth on a microscopic scale with high energy on the surface. Such irregularities are caused by point defects, dislocations, microfractures,

kinks, domain boundaries, corners, ledges and edges. Therefore, the dissolution behaviour of an iron oxide sample strongly depends on the preparation and the source. For this, Schott et al. (1989) suggested that the rate of dissolution is closely related to the concentration of micro-scale defects.

The factors affecting the rate of dissolution of iron oxides are properties of the overall system (e.g. temperature), composition of the solution phase (e.g. pH, redox potential, concentration of acids, reductants and complexing agents) and properties of the oxide (e.g. stoichiometry, crystal structure, crystal habit and presence of defects or guest ions) (Cornell and Schwertmann, 1996; Blesa et al., 1994). However, only the composition of the solution and the tendency of ions in solution to form surface complexes are considered important in mechanistic studies (Blesa et al., 1994).

Additives in a solution affect dissolution of iron oxides significantly. Additives may act in solution (via complexation), but more often adsorb on the surface of iron oxides and influence the energy of attachment between the surface ions and those of the interior. In some cases, adsorbed additives may inhibit dissolution (Blesa et al., 1994).

The pH conditions strongly influence the dissolution of iron oxides. The high affinity of protons with structural O^{2-} assists the release of iron particularly at a low pH. It is the release of the cation, rather than the anion which is likely to be rate-limiting. The pH also influences the electrochemical surface potential and hence redox processes. The surface potential is determined largely by surface charge, which in turn, depends upon pH (Cornell and Schwertmann, 1996). In this chapter, the three mechanisms of dissolution are discussed.

2.2.1.1 Protonation reaction

The general reaction between protons and Fe(III) oxides can be written as

$$FeOOH_{aq} + nH^{+} \rightarrow [Fe(OH)_{(3-n)}]_{aq}^{n+} + (n-1)H_2O \qquad (2\text{-}1)$$

A detailed mechanism of this reaction has been proposed by Stumm and Furrer (1987). In this model, starting with a surface Fe atom coordinated to a neutral OH/OH_2 pair, the first step involves adsorption of a proton by the surface OH group thus transforming the surface $\equiv FeOHOH_2$ entity into a positively charged $\equiv Fe(OH_2)_2^{+}$. Subsequently, two

more protons per one Fe atom are adsorbed. The adsorption of proton weakens the Fe-O bond, probably by polarizing it and so, promotes detachment of Fe from the bulk oxide. In this step, the activation energies (E_a) show the highest values; as the detachment step is rate-limiting.

The rate of dissolution by protonation can usually be described by the relationship, $R = k[H^+_{aq}]^n$, with n ranging between 0 and 1 and k being a constant. This arises from the similar relationship between $[H^+]_{aq}$, and adsorbed protons. Classical adsorption models, such as the Langmuir model, also describe R as a function of adsorbate concentration, $[H^+]_{ads}$, n is often close to 0.5, but a linear relationship between R and $[H^+_{aq}]$ ($n = 1$) has been found for the initial stage of goethite dissolution (Cornell and Schwertmann, 1996; Cornell et al., 1976).

The same principle may hold for anions accompanying protons. Anions replace surface OH groups and thereby assist in the release of Fe. Cl^- ions have a strong dissolution promoting effect, whereas ClO_4^-, which has a much lower affinity with the oxide surface is less effective. These anions have a similar effect on the dissolution of both natural and synthetic goethite (Surana and Warren, 1969; Cornell et al., 1976).

The rate of dissolution of goethite in HCl is described by the following equation (Cornell et al., 1976),

$$\frac{dFe}{dt} = k[H^+]\frac{K[N][Cl^-]}{(1+K[Cl^-])} \qquad (2\text{-}2)$$

where k = reaction rate constant, K = adsorption constant for Cl^- and [N] = number of sites. The concentration of the surface Cl complex is described by a Langmuir equation which accounts for the fact that the rate is insensitive to solution chloride concentrations above which the surface is fully saturated with adsorbed chloride ions. The effect of chloride was explained as follows; its adsorption lowers the positive surface charge and thus facilitates protonation and in addition, the surface Fe-Cl complex causes weakening of the bond between Fe and neighbouring ions in the bulk oxide. The activation energy for goethite dissolution in HCl and in $HClO_4$ was 96kJ mol^{-1}. It was suggested that dissolution was faster in HCl because the observed E_a also contained a contribution

from the adsorption energy of Cl^- and hence, was, in fact, significantly lower than that for $HClO_4$.

2.2.1.2 Complexation reaction

The complexation of both organic and inorganic ligands with the surface functional groups may accelerate, retard, or even block dissolution. However, as shown for oxalate ions (Fig. 2.1), ligands can substantially increase the rate of dissolution of iron oxides. The general reaction for ligand-promoted dissolution may be written as follows,

$$\equiv Fe(III)-OH + L^- + H^+ \rightarrow \equiv Fe(III)L + H_2O \rightarrow Fe(III)L_{aq} + H_2O \qquad (2\text{-}3)$$

The ligand is first adsorbed on the surface of the Fe oxide and this weakens the Fe-O bonds to neighbouring atoms and eventually leads to detachment of the Fe(III) complex (Cornell and Schwertmann, 1996).

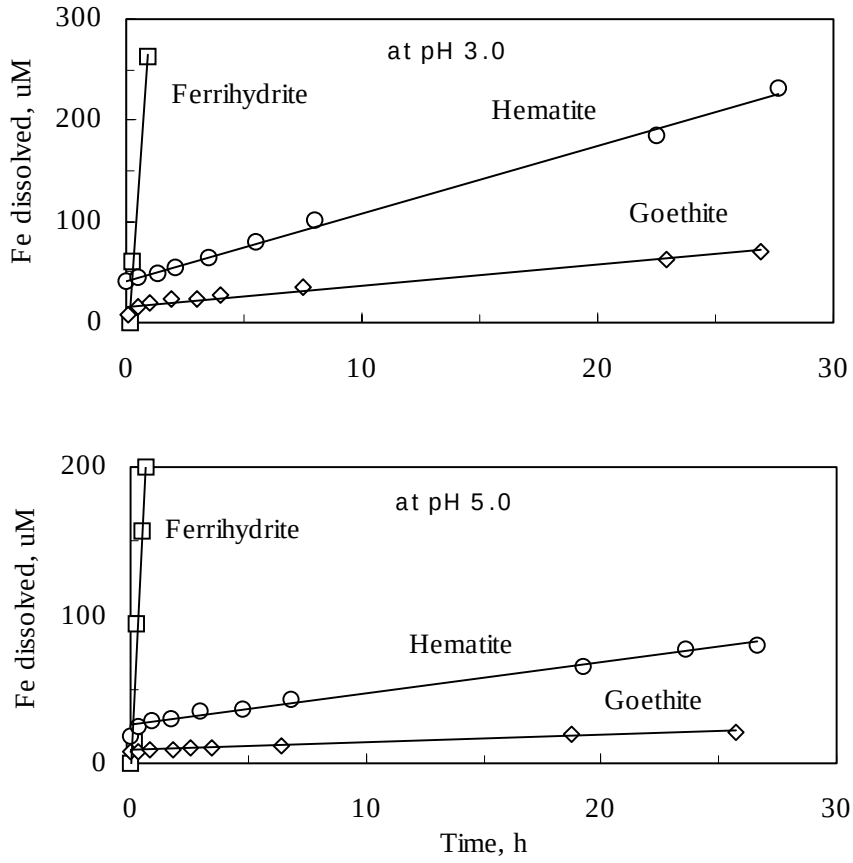

Figure 2.1: Initial stages of dissolution of ferrihydrite, goethite and hematite in the presence of 10^{-3}M oxalate at pH 3.0 and 5.0 (Stumm et al., 1985).

Figure 2.1 shows this effect for oxalate which promotes dissolution of goethite, hematite and ferrihydrite over the pH range 3-5, but in the absence of the ligand, dissolution at this pH is essentially zero (Stumm et al., 1985).

Complexing agents may act in solution as well as through adsorption. Chang and Matijevic (1983) showed that as the pH varied, the mechanism by which hematite dissolved in EDTA changed. In acid media, dissolution by adsorption predominated, whereas in moderately alkaline media, dissolution involved complexation of Fe in solution.

Stumm and Furrer (1987) proposed that dissolution of an M(III) oxide by an organic ligand involved three consecutive reactions, namely, ligand adsorption, metal detachment and proton adsorption/surface restoration as shown in Figure 2.2.

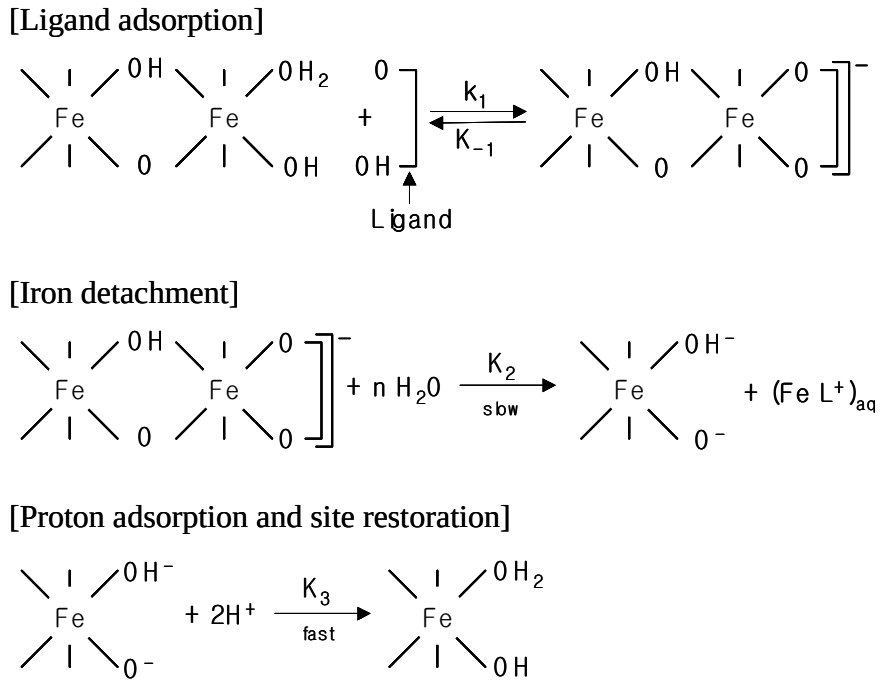

Figure 2.2: The three subsequent reaction steps of the dissolution of a Fe(III) oxide by an organic ligand: ligand adsorption, iron detachment and proton adsorption (site restoration) (Stumm and Furrer, 1987).

Protons facilitate the dissolution process by protonating the OH groups, thereby contributing to a weakening of the Fe-O bond, and, to a lesser extent, act by increasing the positive charge of the oxide surface thus promoting ligand adsorption. On the other

hand, as the pH falls, protonation of the ligands in solution increases, the extent of their adsorption falls and the rate of dissolution by complexation decreases. As a result of these two opposing processes, i.e. surface protonation and change of ligand speciation, there is often an optimum pH at which the dissolution rate in the presence of an organic ligand is at a maximum. For example, according to Zhang et al. (1985) the dissolution of hematite in citric acid is at a maximum at pH 4-5, whereas with oxalic acid, the rate starts decreasing from pH 2.0 (Figure 2.3).

Although citrate forms a more stable complex with Fe(III), oxalic acid appears to be a more efficient dissolving agent, presumably because adsorption at a particular pH is greater and also because detachment of the Fe-oxalate complex requires breakage of fewer bonds (Zhang et al., 1985). Oxalate adsorption on goethite is constant over the pH range 2-4 and the HOx^- species predominates in solution at pH 2; the dissolution rate is at a maximum at pH 2.6 (Cornell and Schindler, 1987).

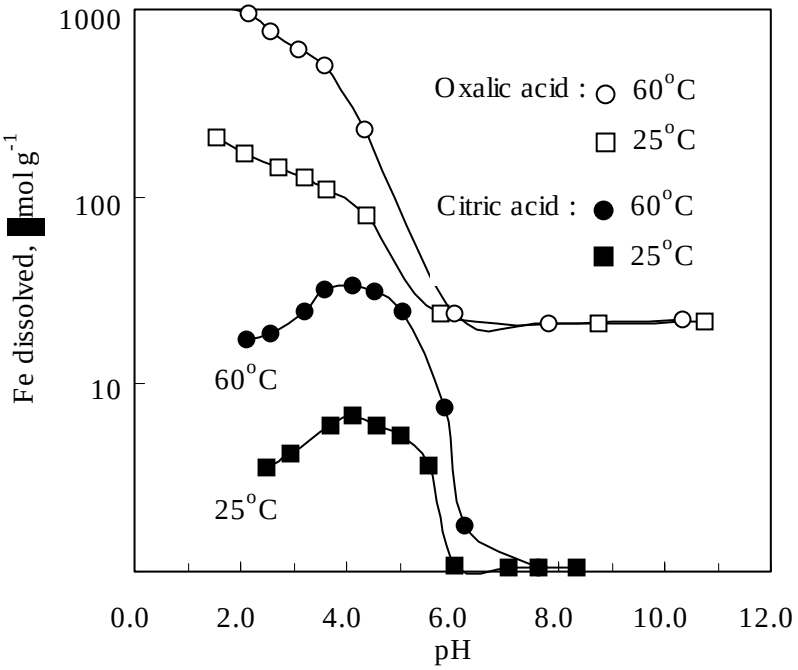

Figure 2.3: Fe dissolved from haematite in oxalic and citric acid at 25°C and 60°C as a function of pH (Zhang et al., 1985).

Ligands which promote dissolution are thought to form mononuclear surface complexes, whereas those that inhibit the process form binuclear (or even trinuclear) surface complexes (Cornell and Schwertmann, 1996: Blesa et al., 1994). The former

assist detachment of Fe from the surface, whereas the latter are firmly anchored. An inhibiting effect was displayed by EDTA which almost completely blocked dissolution of goethite (Rueda et al., 1985) and dissolution of akageneite at pH < 6 where EDTA adsorbed strongly (Rubio and Matijevic, 1979). With these polymorphs of FeOOH, EDTA appeared to promote dissolution only by complexation in solution.

2.2.1.3 Reductive dissolution

In a natural environment, reductive dissolution is by far the most important dissolution mechanism (Blesa et al., 1994; Cornell and Schwertmann, 1996). It is mediated both biotically and abiotically. The most important electron donors, particularly in near surface ecosystems, result from metabolic oxidation of organic compounds under O_2 deficient conditions. In anaerobic systems, therefore, the availability of Fe oxides may control the degradation of dead biomass and organic pollutants in the ground water zone. Reductive dissolution is also often applied to the removal of corrosion products from piping in industrial equipment and for bleaching kaolin.

The mechanism by which the structural bonds between Fe atoms in iron oxides may be weakened, involves reduction of structural Fe(III) to Fe(II) (Cornell and Schwertmann, 1996; Blesa et al., 1994). The reductive dissolution of Fe oxides has been widely studied (Blesa et al., 1994; Cornell and Schwertmann, 1996). Reductants investigated include dithionite, thioglycolic acid, thiocyanate, hydrazine, ascorbic acid, hydroquinone, H_2S, H_2, Fe^{2+}, tris(picolinato)-V(II), fulvic acid, fructose, sucrose and biomass/bacteria. Under appropriate conditions, reductive dissolution may also be affected photochemically. As with protonation, the extent of reduction may be strongly influenced by ligand and proton adsorption on the oxide surface (Cornell and Schwertmann, 1996; Blesa et al., 1994).

Sodium dithionite ($Na_2S_2O_4$) is a reductant that is commonly used for the extraction of Fe oxides from kaolin and from soils both to determine the total amount of Fe oxides and to improve the dispersibility of the clay minerals (Mehra and Jackson, 1960). The overall reaction may be written as,

$$2FeOOH + S_2O_4^{2-} + 4H^+ \rightarrow 2Fe^{2+} + 2HSO_3^- + 2H_2O \qquad (2\text{-}4)$$

This reduction reaction is accompanied by the disproportion of dithionite, i.e.

$$2S_2O_4^{2-} + H_2O \rightarrow S_2O_3^{2-} + 2HSO_3^- \qquad (2\text{-}5)$$

The rate of disproportion increases with decreasing pH and rising temperature, which also favour oxide reduction. To achieve a reasonable rate of dissolution, one has to determine the optimum pH, which varies from one system to another. A pH of 3.0 is used in kaolin bleaching (Jepson, 1988), whereas in soil analysis the system is usually buffered with citrate and bicarbonate at ca. pH 7 (Mchra and Jackson, 1960).

Citrate also complexes the dissolved Fe(II) and prevents its precipitation as Fe(II) sulphide. For the dithionite/EDTA system, Rueda et al. (1992) found maximum dissolution at pH 5-6 and an activation energy of 70 kJmo1^{-1} for goethite.

Chloride was used as a complexant for the reductive dissolution of hematite and magnetite by Cr^{2+} and wustite and magnetite by V^{3+} (Valverde, 1976). Synergistic effects were displayed in the reduction of ferrihydrite and goethite by Fe^{2+} (Fischer, 1972, 1976, 1983) and of goethite by ascorbic acid (Stumm et al., 1985), both in the presence of oxalate. The initial (ca. 2%) dissolution rate was a direct function of the level of adsorbed oxalate. Because both the complexing ligand (oxalate) and the reductant must be adsorbed before they interact with the oxide, their surface complexation constants strongly influence the dissolution rate (Rueda et al., 1992). Sucrose was found to be an effective reductant for the dissolution of haematite in sulphuric acid (Veglio et al., 1994). This process is used for bleaching of kaolin and quartz-bearing sands.

Reducing agents such as thioglycolic acid (Baumgartner et al., 1982), oxalic acid (Baumgartner et al., 1983) and tris(picolinato)-V(II) (Segal and Sellem, 1982) are used, or have the potential to be used, to decontaminate pipes in water-cooled nuclear reactors. Hematite and magnetite have been studied as model oxides. The first step in the process involves adsorption of the reductant. Thioglycolic acid dissolution of magnetite is at a maximum at pH 4-5. This is the result of the opposing effects between two parameters - the free thioglycolate concentration, which increases with rising pH, and the positive surface charge which rises as pH falls (Baumgartner et al., 1982).

Another effective reductant is bivalent iron. It has been known for years that Fe^{2+} ions accelerate the dissolution of slowly dissolving compounds such as Fe oxides and also $Fe_2(SO_4)_3$. Increasing $[Fe^{2+}]$ increased the rate of dissolution of ferrihydrite in oxalate at pH3 (Figure 2.4) with the initial rate being linearly related to $[Fe^{2+}]$ (Fischer, 1972). The same effect was observed for goethite dissolution (Figure 2.5, left) (Suter et al., 1991).

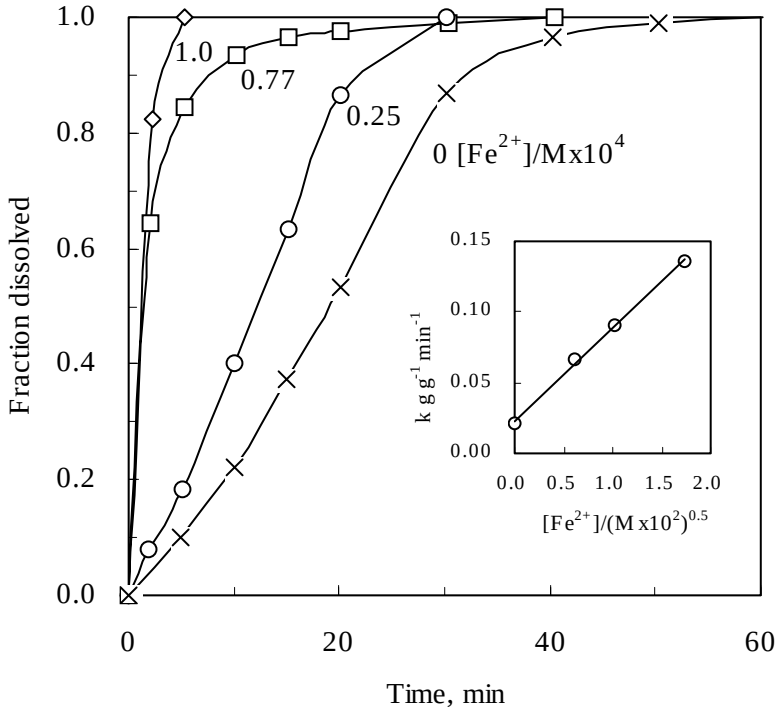

Figure 2.4: Dissolution-time curves of ferrihydrite in 0.2M $NH_4C_2O_4$, pH3.0 in the presence of various $[Fe^{2+}]$ (0-1.3 $\cdot 10^{-4}$M) at room temperature. Inset: initial rate of dissolution, k, as a function of $[Fe^{2+}]^{0.5}$ (Fischer, 1972).

For goethite dissolution (Fig. 2.5, left) although the rate increased initially with rising $[Fe^{2+}]$, it levelled off at higher concentrations. The rate also increased as the pH rose from 2 to 4 owing to the increasing deprotonation of oxalic acid which facilitates adsorption (Figure 2.5, right). It is generally agreed that in the Fe^{2+}/oxalate system, the first step is formation of a soluble Fe(II) oxalate complex which adsorbs at a surface Fe(III) site. The Fe(II)-oxalate complex is considered to be a much stronger reductant than Fe^{2+} alone. Upon adsorption, an electron is transferred from the Fe(II)-$(Ox)_n^{(2n-1)}$ surface complex to a surface Fe(III) site thus inducing detachment of Fe and creation of a new surface site. A similar mechanism has been proposed for the photochemical

dissolution of goethite in the presence of oxalate and Fe^{2+} (Cornell and Schindler, 1987).

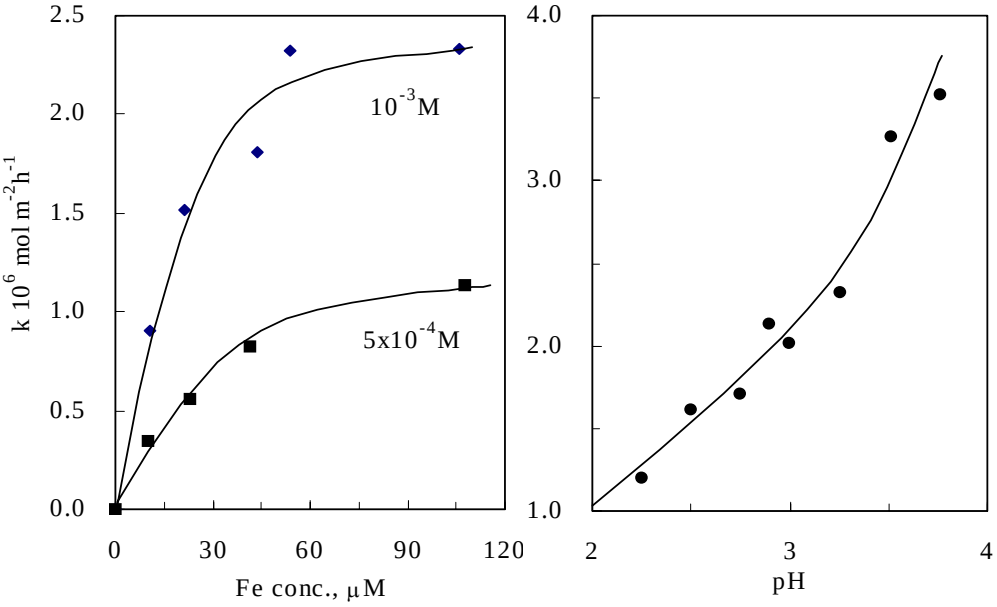

Figure 2.5: Left: dissolution rate of goethite at 25°C in 10^{-3} and $5{\cdot}10^{-4}$M oxalate at pH 3.0 as a function of $[Fe^{2+}]$. Right: same as a function of pH ($[Fe^{2+}]$: $5{\cdot}10^{-3}$M, oxalate: 10^{-3}M (Suter et al., 1991).

The dissolution of iron oxides was also accelerated in the presence of Fe^{2+} (Sulzberger et al., 1989) in malonate and citrate leaching systems. Fe^{2+} also promotes the dissolution of magnetite in sulphuric acid (Bruyere and Blesa, 1985). Small amounts of Fe^{2+} in solution speed up the transformation of ferrihydrite to goethite at 50°C by promoting the dissolution of ferrihydrite (Fischer 1972). Adsorption of Fe is a necessary first step in the dissolution process. Only a small amount of Fe^{2+} is required for the reaction to proceed to completion because, upon re-oxidation of the detached Fe^{2+} in solution to form goethite, the electron is again available for further interaction with ferrihydrite.

Therefore, reductive dissolution may be more complex than the two previous mechanisms in that it involves electron transfer processes. Formation of ≡Fe(II) via reductive dissolution can be effected by adsorption of an electron donor, by the cathodic polarization of an electrode supporting the iron oxide and by the transfer of an electron to a surface Fe(III). Addition of Fe(II) to a system containing a ligand such as oxalate

promotes electron transfer via a surface complex and thus markedly accelerates dissolution (Fischer, 1976).

As in the case of protonation, the detachment of Fe is likely to be rate determining, but it cannot be ruled out that, as has been suggested for Mn oxides, electron transfer is rate limiting in some cases (Stone and Morgan, 1987). The reduction of Fe(III) to Fe(II) destabilizes the coordination sphere of the iron both as a result of the loss of charge and because of the larger size of the bivalent Fe(II) (0.078nm vs 0.064 nm) and thus induces detachment of iron as Fe(II) (Stone and Morgan, 1987). The release of Fe(II) from the structure is energetically more favourable than that of Fe(III) (Stone and Morgan, 1987). It is often difficult to determine, experimentally, the step involving the formation of Fe(II). In a kinetic study on the dissolution of magnetite by mercapto-carboxylic acids, Borghi et al. (1991) concluded that it was difficult to distinguish between the two processes involved in the dissolution, namely the reduction of structural Fe(III) in a surface Fe(III)-L complex followed by Fe(II) detachment or the formation of a soluble Fe(III)-L complex followed by its reduction in solution as the two processes are kinetically equivalent.

Detachment of structural Fe(III) is facilitated by the protonation of the metal site. Because the reducing ligand is usually a charged species, pH will, through its effect on ligand adsorption, have a strong effect on the rate of reductive dissolution. The dissolution rate will be a function of both pH and the concentration of ligand in solution. Borghi et al. (1991) considered that the strong pH dependence of the rate of reductive dissolution of magnetite in mercapto-carboxylic acids (maximum at pH 3-4) indicates that moderately strong attachment of the ligand to the surface is optimal for the polarization of the Fe-O bond. A too strong bonding of the ligand lowers the dissolution rate by immobilizing a surface site (Cornell and Schwertmann, 1996).

It is to be expected that reductive dissolution of Fe oxides becomes faster as the electron activity increases, i.e. the lower the redox potential (Eh) of the aqueous system is, the faster the dissolution. In most experiments, however, Eh has not been measured. A rare example is given by Fischer (1987) who dissolved goethite in an Eh range of between ca. -0.3 and +0.1 V with the Eh being measured with a Pt/H_2 electrode and a range of partial pressures of H_2. As expected, the rate was an exponential function of Eh (Figure

2.6). Organic and inorganic additives that shift the redox potential toward a more negative direction will accelerate the dissolution of iron oxides (Frenier and Growcock, 1984).

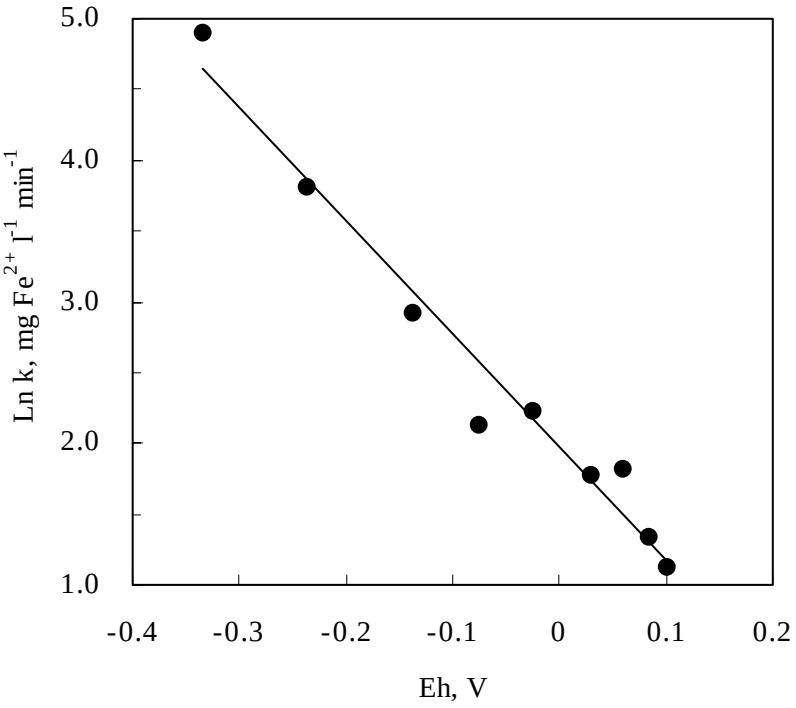

Figure 2.6: Rate of dissolution of a synthetic goethite as a function of redox potential (Eh) in a H_2 system at pH3.0 and room temperature (Fischer, 1987).

2.2.1.4 Comparison of the three different types of dissolution reactions

There are only a few cases where the dissolution of an iron oxide by all three types of processes under comparable conditions has been investigated. Banwart et al. (1989) found that at pH3, the rate of dissolution of hematite increased in the order protonation < complexation < reduction with a factor of 350 between the extremes. A similar factor (400) was found for goethite as shown Figure 2.7 (Zinder et al., 1986).

Hematite dissolution processes were also compared in the pH range similar to that found in slightly acidic (pH3) environments as shown Figure 2.8. Again, dissolution by simple protonation was extremely slow, whereas reduction, especially when aided by Fe(III) complexing ligands, was particularly effective (Banwart et al., 1989). Thus, It can be concluded that reduction, particularly when assisted by protonation and complexation, will be the main mechanism for Fe oxide dissolution.

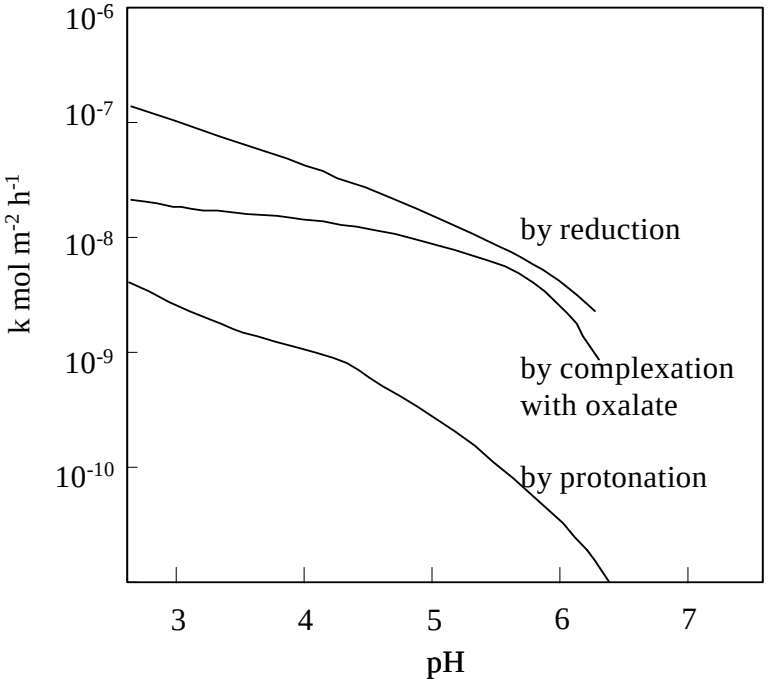

Figure 2.7: Dissolution rate of goethite by protonation, complexation with oxalate and reduction by ascorbic acid as a function of pH (Stumm and Furrer, 1987).

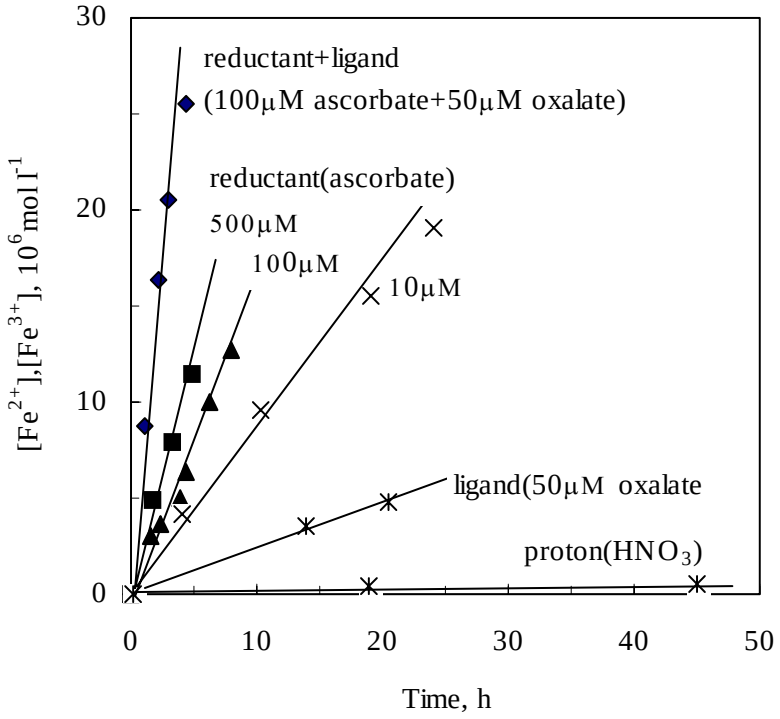

Figure 2.8: Comparison of the dissolution of hematite at pH3 by protonation (HNO_3), complexation (50µM oxalate), reduction (100µM ascorbic acid) and combined complexation-reduction (Banwart et al., 1989).

2.2.2 Dissolution kinetics

The rate of dissolution reactions may be either transport-controlled (i.e. diffusion) or surface-controlled (Segal and Sellers, 1984). In the transport-controlled mechanism, the concentration of dissolved species (c) immediately adjacent to the surface corresponds to the equilibrium solubility (c_e) of the solid phase, increases with the square root of time, t, i.e.

$$c = c_e + 2k_d t^{1/2} \qquad (2\text{-}6)$$

k_d being the rate constant.

An example of this type of reaction is the very rapid dissolution of hematite by the tris(picolinato)-V(II) species. The surface-controlled mechanism is so fast that diffusion is the rate determining step (Segal and Sellers, 1980, 1982). The acid leaching of iron oxides from bauxite also appears to be controlled by the slow diffusion of acid through the pores created by the initial removal of the haematite (Patermarakis and Paspaliaris, 1989).

In many systems, it is the chemical reaction at the solid/liquid interface that is rate-determining. Such dissolution reactions usually have an activation energy greater than 25kJmol^{-1}, whereas diffusion-controlled reactions have lower activation energies. When investigating dissolution reactions, it is essential to provide sufficient agitation to ensure that a contribution to the rate from slow diffusion is avoided. Where surface control is rate-determining, the instantaneous rate must be proportional to the surface area of the solid, i.e.

$$rate = \frac{dc}{dt} = k_A A \qquad (2\text{-}7)$$

where k_A (M s^{-1} m^{-2}) is the kinetic rate constant and A is the surface area. At any time, t, the rate will be a function of the surface area left and a first order type of equation may be followed, i.e.

$$(1-\alpha) = e^{-kt} \qquad (2\text{-}8)$$

where α is the proportion dissolved at time t and k is the rate constant (time^{-1}). This equation is based on the assumption that the binding strengths of the ions in the solid are

all the same. Information on the kinetics of heterogeneous reactions, including dissolution, is provided by Brown et al.(1980). Table 2.2 shows a number of rate equations that are commonly applied to dissolution processes.

Table 2.2 Rate equations applicable to dissolution.

Equation	Type	Physical meaning
$\alpha^2 = kt$	Deceleratory	One-dimensional diffusion
$(1-\alpha)\ln(1-\alpha)+\alpha = kt$	Deceleratory	Two-dimensional diffusion for a cylinder
$[1-(1-\alpha^{1/3}]^2 = kt$	Deceleratory	Three-dimensional diffusion for a sphere
$(1-2/3\alpha)-(1-\alpha)^{2/3} = kt$	Deceleratory	Three-dimensional (Ginstling-Brounstein)
$-\ln(1-\alpha) = kt$	Deceleratory	Random nucleation (first order)
$[-\ln(1-\alpha)]^{1/2} = kt$	Sigmoidal	Random nucleation 2D (Avrami-Erofejev)
$[-\ln(1-\alpha)]^{1/3} = kt$	Sigmoidal	Random nucleation 3D (Avrami-Erofejev)
$\ln\ln(1-a) = \alpha\ln k + \alpha\ln t$	Variable	Modified first order (Kabai)
$1-(1-\alpha)^{1/2} = kt$	Geometric	Phase boundary controlled for a shrinking disc
$1-(1-\alpha)^{1/3} = kt$	Geometric	Phase boundary controlled for a contracting sphere (cube root)
$\alpha^{1/n} = kt$	Acceleratory	
$\alpha^2 = kt$	Acceleratory	

∗α = extent of reaction; *a* = constant

The geometry of the solid influences the dissolution behaviour and a number of rate equations, therefore, take geometry into account. The “cube root” law (Hixon and Crowell, 1931),

$$1-(1-\alpha)^{1/3} = kt \qquad (2\text{-}9)$$

applies to a situation in which the interface moves inwards at a constant rate and implies isotropic dissolution, i.e. that the particle shape is maintained. It is also termed the

"shrinking core" model and strictly speaking should apply only to spherical and cubic particles. It has, however, been applied successfully to the dissolution of goethite and lepidocrocite by several workers who also found that their data for dissolution of goethite in HCl, HNO_3 and H_2SO_4 could equally well be described by a first order law (Cornell et al., 1975; Sidhu et al., 1981; Chiarizia and Horwitz, 1991).

The Avrami-Erofejev law, i.e.

$$(-\ln(1-\alpha))^{1/2} = kt \qquad (2\text{-}10)$$

has been applied to the dissolution of agandite (Cornell and Giovanoli, 1988a) and to haematite (Cornell and Giovanoli, 1993), both of which displayed sigmoidal dissolution curves. Another equation that has been applied to reactions with sigmoidal kinetics is the Kabai equation,

$$1-\alpha = e^{-(kt)a} \qquad (2\text{-}11)$$

where a is a materials "constant of average order" (Kabai, 1973). For $a > 1$, the kinetic curve is sigmoidal i.e. acceleratory in its first part and for $a < 1$ the curve is deceleratory throughout. For different iron oxides, a varies from 0.5 to 2 (Schwertmann et al., 1985). This equation provides a flexible way of summarizing experimental data, but does not provide a physical explanation for k and a.

A relationship which expressed the rate of dissolution as a function of changing crystal size, morphology and site density (Christofferson and Christofferson, 1976; Postma, 1993) is,

$$\frac{J}{m_0} = k\left[\frac{m}{m_0}\right]^{\gamma} \qquad (2\text{-}12)$$

where J/m_0 is the normalized rate per initial mass of oxide (m_0), m is the mass dissolved at time t and γ is a material constant covering the change in properties during dissolution. For spheres or cubes, it follows from the relationship between volume and surface area that $\gamma = 2/3$. For dissolution of ferrihydrite in ascorbic acid a value for = 1.1 was obtained and for two iron oxide mixtures in sediments γ was 4.7 and 2.75 which was interpreted as indicating a continuum of reactivities (Postma, 1993).

Gorichev and Kipriyanov (1984) found that the dissolution of powdered magnetite particles in HCI, H_2SO_4, H_3PO_4 and Na_2EDTA at temperatures of up to 80^oC displayed sigmoidal dissolution curves that could be described by,

$$-\ln(1-\alpha) = A \cdot \sinh kt \qquad (2\text{-}13)$$

For hematite and wustite in the same media, the kinetic curves were deceleratory.

The dissolution models provide a summary of the dissolution reaction and its kinetics. Usually, the correlation coefficient, r^2, for the relationship between the measured values and those predicted by the model are taken as criterium for the suitability of a particular model. Often, however, the very beginning or the very end of the dissolution curve is not included in the model - either because the data does not exist or because it does not fit. If the middle data points - say 15-85% - are used it is easy to get high r^2 values for several models. Although a model may provide some information on whether the rate-determining step is the surface reaction or diffusion of the reacting species, the fact that a reaction follows a particular rate law does not guarantee that this describes the physical processes that take place. In some cases, an apparent rate law is the result of interaction between a number of counterbalancing processes. It should also be borne in mind that the shape of the kinetic curve and the extent to which a particular rate law is obeyed are influenced by the particle size distribution of the sample. The broader the size distribution is the faster the initial stages of the reaction and the slower the latter part (Gallagher, 1965). The cube root law, for example, may be followed for up to 90% of the reaction by a mono-dispersed sample and up to only 60-70% of dissolution by the same material with a broad size distribution (Segal and Sellers, 1982).

2.3 THERMODYNAMIC ANALYSIS OF THE Fe-$H_2C_2O_4 \cdot H_2O$ SYSTEM

2.3.1 Oxalic acid and oxalates system

2.3.1.1 Speciation of oxalic acid as a function of pH

Oxalic acid has two ionisation constants, shown in Table 2.3. In oxalic acid solution, molecules of oxalic acid and its ions, $HC_2O_4^-$ and $C_2O_4^{2-}$, coexist in equilibrium. These ions have been produced by the following ionisation reactions (Bailar et al., 1989; Vincze and Papp., 1987; Chatzeioannou, 1972).

Table 2.3 Ionisation constants of oxalic acid at 25℃.

$H_2C_2O_4 \leftrightarrow H^+ + HC_2O_4^-$	$K_{a1} = 5.6 \times 10^{-2}$
$HC_2O_4^- \leftrightarrow H^+ + C_2O_4^{2-}$	$K_{a2} = 6.2 \times 10^{-5}$

$$H_2C_2O_4 \leftrightarrow H^+ + HC_2O_4^- \tag{2-14}$$

$$K_{a1} = \frac{[H^+][HC_2O_4^-]}{[H_2C_2O_4]} \tag{2-15}$$

$$HC_2O_4^- \leftrightarrow H^+ + C_2O_4^{2-} \tag{2-16}$$

$$K_{a2} = \frac{[H^+][C_2O_4^{2-}]}{[HC_2O_4^-]} \tag{2-17}$$

If C_{ox} is the initial concentration of $H_2C_2O_4$ in the solution, then the fractions of non-dissociated $H_2C_2O_4$, $HC_2O_4^-$ and $C_2O_4^{2-}$ are defined by the following equations respectively:

$$a_0 = \frac{[H_2C_2O_4]}{C_{ox}} \tag{2-18}$$

$$a_1 = \frac{[HC_2O_4^-]}{C_{ox}} \tag{2-19}$$

$$a_2 = \frac{[C_2O_4^{2-}]}{C_{ox}} \tag{2-20}$$

and:

$$C_{ox} = [H_2C_2O_4] + [HC_2O_4^-] + [C_2O_4^{2-}] \tag{2-21}$$

By combining the above equations, the fractions a_0, a_1, a_2 as a function of pH can be derived.

$$a_0 = \frac{[H^+]^2}{[H^+]^2 + K_{a1}[H^+] + K_{a1}K_{a2}} \tag{2-22}$$

$$a_1 = \frac{K_{a1}[H^+]}{[H^+]^2 + K_{a1}[H^+] + K_{a1}K_{a2}} \tag{2-23}$$

$$a_2 = \frac{K_{a1}K_{a2}}{[H^+]^2 + K_{a1}[H^+] + K_{a1}K_{a2}} \quad (2\text{-}24)$$

In Figure 2.9, the variations of the fractions of the undissociated $H_2C_2O_4$, $HC_2O_4^-$ and $C_2O_4^{2-}$ as a function of pH are shown (Huang, 2000).

It is obvious from Figure 2.9 that the $C_2O_4^{2-}$ concentration is high in alkaline solutions and low in acidic solutions. At pH less than 2, the $C_2O_4^{2-}$ concentration is negligible. In such solutions, the active species is $HC_2O_4^-$ rather than $C_2O_4^{2-}$ (Vincze and Papp., 1987).

At pH higher than 3, almost complete ionisation of oxalic acid is observed. In this region, the active species are both $HC_2O_4^-$ and $C_2O_4^{2-}$. Above pH 4 the concentration of $HC_2O_4^-$ is less than that of $C_2O_4^{2-}$, and at above pH 6 the concentration of $HC_2O_4^-$ becomes negligible.

2.3.1.2 Stability of oxalic acid and the oxalates

Figure 2.10 shows the domains of relative predominance of carbon in the form of oxalates and carbonates at 25^{o}C. According to Figure 2.10, oxalic acid and oxalates are reducing agents and are thermodynamically unstable in the water stability zone. Nevertheless, their reducing action is slow, becoming appreciable only with powerful oxidizing agents (e.g. MnO_4^-) or in the presence of a catalyst (e.g. finely divided Pt) (Pourbaix, 1958).

2.3.2 Iron oxalato complex

The well-known phenomenon of ring formation by ligand in a complex is called chelation and the ring formed is called a chelate ring. Oxalate ion ($C_2O_4^{2-}$) has two oxygen atoms with unshared pairs of electrons. These oxygen atoms have the ability to co-ordinate to the same metal atom or ion and form a ring. In the presence of ferric (Fe^{3+}) and ferrous (Fe^{2+}) ions, oxalate ions have the ability to generate five-membered rings and form complex ions. Table 2.4 shows the probable iron oxalato complexes and overall dissociation constants (K_d) (Bailar et al., 1989; Vincze and Papp, 1987).

From Table 2.4, the following conclusions can be deduced:

(a) $[Fe^{3+}(C_2O_4)_3]^{3-}$ is the most stable iron oxalato complex.

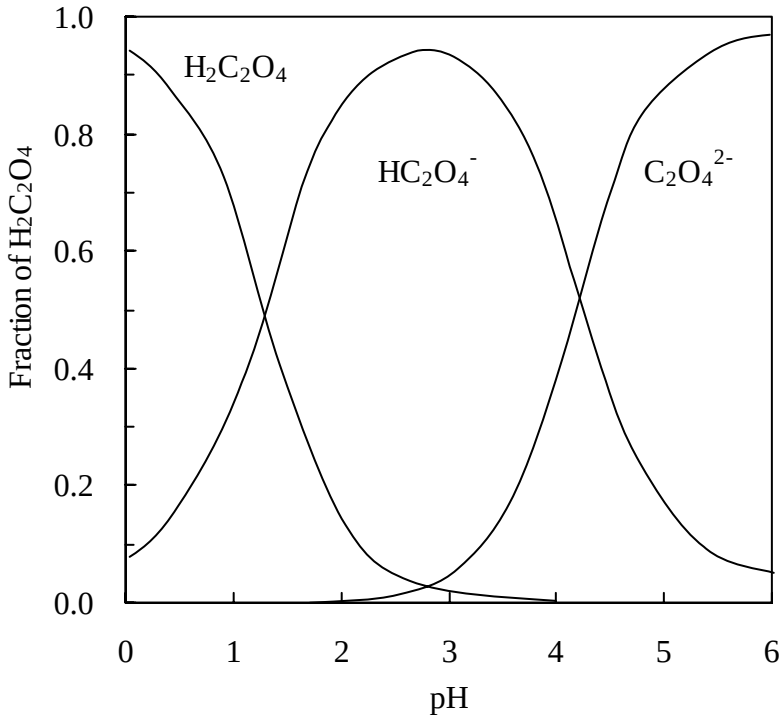

Figure 2.9: Speciation in oxalic acid solution at 25°C (Huang, 2000).

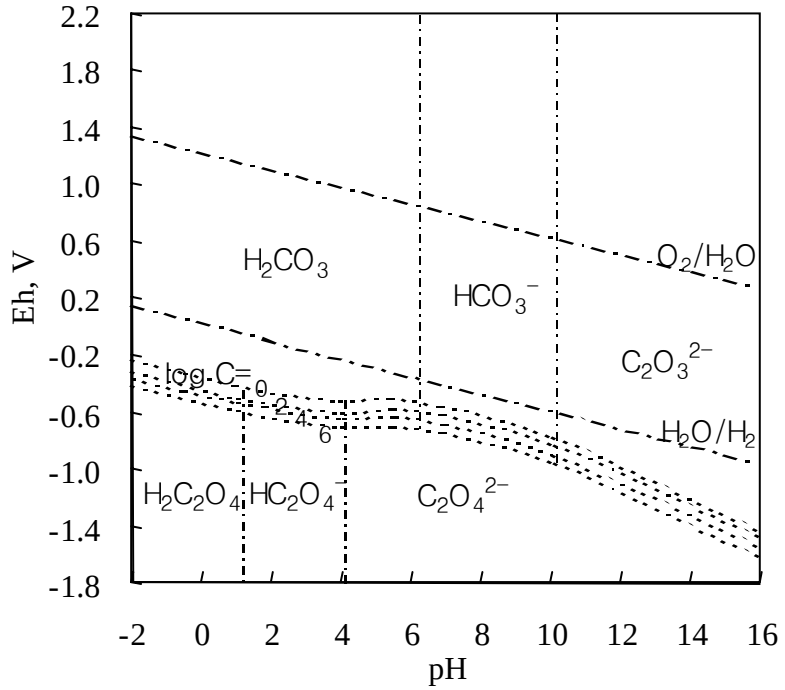

Figure 2.10: Domains of relative predominance of carbon in the form of oxalates and carbonates at 25°C (Pourbaix, 1958).

(b) all iron(III) oxalato complexes are more stable than the iron(II) oxalato complexes.

In the presence of oxalate ions, ferrous ion can form an insoluble compound, FeC_2O_4, with solubility product value K_{sp} = 2x10^{-7} (Chatzeioannou, 1972);

$$FeC_2O_4 \leftrightarrow Fe^{2+} + C_2O_4^{2-} \quad (2\text{-}25)$$

However there are also several complexes formed between iron(III), iron(II) and oxalate as listed in the following table, together with their dissociation constants (Panias et al, 1996).

Table 2.4 Iron oxalato complexes and their overall dissociation constants (K_d) at 25℃.

Complex ion	**Dissociation constants (k_d)**
$[Fe^{2+}(C_2O_4)_3]^{4-}$, (Trioxalatoferrate(II) ion)	6x10^{-6}
$[Fe^{2+}(C_2O_4)_2]^{2-}$ (Dioxalatoferrate(II) ion)	2x10^{-8}
$[Fe^{3+}(C_2O_4)_3]^{3-}$ (Trioxalatoferrate(III) ion)	3x10^{-21}
$[Fe^{3+}(C_2O_4)_2]^{-}$ (Dioxalatoferrate(III) ion)	6.31x10^{-21}
$[Fe^{3+}C_2O_4]^{+}$ (Oxalatoiron(III) ion)	3.98x10^{-10}
$[Fe^{3+}C_2O_4H]^{2+}$ (Bi-oxalatoiron(III) ion)	2.95x10^{-10}

2.3.2.1 Equilibrium diagram of iron (III) oxalato complexs

The equilibrium in iron(III) oxalate system was greatly affected by $C_2O_4^{2-}$ concentration and pH. The following species are present in an aqueous solution of Fe^{3+}-$C_2O_4^{2-}$ system, namely Fe^{3+}, $[FeC_2O_4]^+$, $[Fe(C_2O_4)_2]^-$ and $[Fe(C_2O_4)_3]^{3-}$ in the region where free oxalate ions are stable (pH2-4). Chemical equilibria in this system can be described by the three reactions given in table 2.5 (Panias et al., 1996).

Table 2.5 Chemical reactions and equilibrium constants describing the Fe^{3+}-$C_2O_4^{2}$ system at 25°C (Panias et al., 1996).

Reactions	**Equilibrium constant(*K*)**
$Fe^{3+} + C_2O_4^{2-} \leftrightarrow FeC_2O_4^{+}$	K_1=2.51x10^9
$FeC_2O_4^{+} + C_2O_4^{2-} \leftrightarrow Fe(C_2O_4)_2^{-}$	K_2=6.31x10^6
$Fe(C_2O_4)_2^{-} + C_2O_4^{2-} \leftrightarrow Fe(C_2O_4)_3^{3-}$	K_3=2.1x10^4

The equilibrium constants K_1, K_2 and K_3 of these reactions are :

$$K_1 = \frac{[FeC_2O_4^{+}]}{[Fe^{3+}][C_2O_4^{2-}]} \quad (2\text{-}26)$$

$$K_2 = \frac{[FeC_2O_4)_2^{-}]}{[FeC_2O_4^{+}][C_2O_4^{2-}]} \quad (2\text{-}27)$$

$$K_3 = \frac{[Fe(C_2O_4)_3^{3-}]}{[Fe(C_2O_4)_2^{-}][C_2O_4^{2-}]} \quad (2\text{-}28)$$

The total concentration of trivalent iron in solution, C_{Fe3+} is :

$$C_{Fe3+} = [Fe^{3+}] + [FeC_2O_4^{+}] + [Fe(C_2O_4)_2^{-}] + [Fe(C_2O_4)_3^{3-}] \quad (2\text{-}29)$$

The fraction of the total trivalent iron in solution, present as Fe^{3+}, $FeC_2O_4^{+}$, $Fe(C_2O_4)_2^{-}$ and $Fe(C_2O_4)_3^{3-}$ respectively can be defined as :

$$B_0 = \frac{[Fe^{3+}]}{C_{Fe3+}} \quad (2\text{-}30)$$

$$B_1 = \frac{[FeC_2O_4^{+}]}{C_{Fe3+}} \quad (2\text{-}31)$$

$$B_2 = \frac{[Fe(C_2O_4)_2^{-}]}{C_{Fe3+}} \quad (2\text{-}32)$$

$$B_3 = \frac{[FeC_2O_4)_3^{3-}]}{C_{Fe3+}} \quad (2\text{-}33)$$

Combining equations from (2-26) to (2-33) the fractions B_0, B_1, B_2 and B_3 can be

calculated as a function of $C_2O_4^{2-}$ concentration in the solution:

$$B_0 = \frac{1}{1K_1[C_2O_4^{2-}] + K_1K_2[C_2O_4^{2-}]^2 + K_1K_2K_3[C_2O_4^{2-}]^3} \quad (2\text{-}34)$$

$$B_1 = B_0K_1[C_2O_4^{2-}],\ B_2 = B_0K_1K_2[C_2O_4^{2-}]^2,\ B_3 = B_0K_1K_2K_3[C_2O_4^{2-}]^3$$

The fractions of different iron-oxalate complexes (B_0, B_1, B_2 and B_3) as a function of $C_2O_4^{2-}$ concentration in the solution at pH<3 are plotted in Figure 2.11 (Panias et al., 1996).

As seen from Figure 2.11, free trivalent iron Fe^{3+} ions are stable in oxalate solutions only at extremely low oxalate concentrations (below 10^{-7}M). Therefore, it is highly unlikely to find free trivalent iron ions in common oxalate solutions. Above oxalate concentration of 10^{-6}M, the complex ion $[Fe(C_2O_4)_3^{3-}]$ is formed and is the only significant complex ion existing in the solution at concentrations above 10^{-2}M.

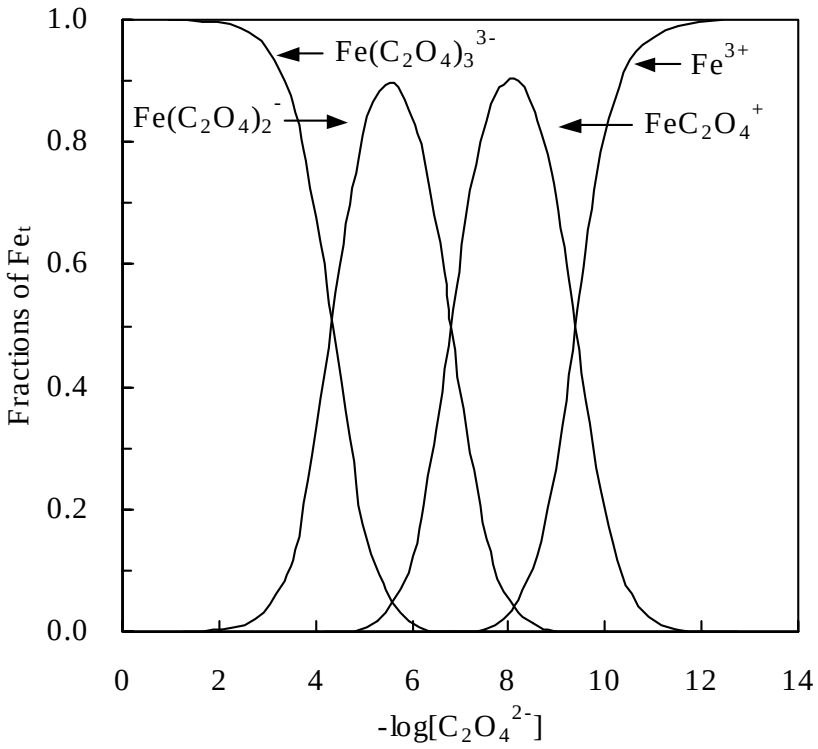

Figure 2.11: Fractions of different Fe(III)-oxalate species as a function of $C_2O_4^{2-}$ concentration in the solution (Panias et al., 1996).

On the other hand, at a lower pH range (pH0-2) another equilibrium involving ferric and bi-oxalate ions has to be taken into consideration according to Panias et al. (1996), namely:

$$Fe^{3+} + HC_2O_4^- \leftrightarrow [FeC_2O_4H]^{2+} \quad , K_4 = 3.39\text{x}10^9 \tag{2-35}$$

where:
$$K_4 = \frac{[FeC_2O_4H]^{2+}}{[Fe^{3+}][HC_2O_4^-]} \tag{2-36}$$

The total oxalic acid concentration, C_{ox} in the solution, therefore is :

$$C_{ox} = [H_2C_2O_4] + [HC_2O_4^-] + [C_2O_4^{2-}] + [Fe(C_2O_4)^+] + 2[Fe(C_2O_4)_2^-] + 3[Fe(C_2O_4)_3^{3-}] \tag{2-37}$$

Panias and co-workers [1996] studied the effect of pH and oxalic acid concentration on the speciation of various Fe(III)-oxalate complexes. Assuming that oxalic acid is in large excess in the solution, which is a valid assumption for the systems under study, the speciation of oxalic acid is not affected by the presence of ferric ion. Thus, the concentration of Fe(III)-oxalato complexes is negligible in proportion to the concentrations of oxalic acid dissociation products. As a result, eqn (2-37) is simplified to become the following:

$$C_{ox} = [H_2C_2O_4] + [HC_2O_4^-] + [C_2O_4^{2-}] \tag{2-38}$$

The total concentration of ferric ion in the solution is equal to :

$$C_{Fe3+} = [Fe^{3+}] + [FeC_2O_4^+] + [Fe(C_2O_4)_2^-] + [Fe(C_2O_4)_3^{3-}] + [FeHC_2O_4^{2+}] \tag{2-39}$$

Combining equations (2-15) and (2-17) will result in equation (2-40) from which the concentration of free $C_2O_4^{2-}$ as a function of C_{ox} and pH can be calculated:

$$[C_2O_4^{2-}] = \frac{K_{a1}K_{a2}}{[H^+]^2 + K_{a1}[H^+] + K_{a1}K_{a2}} C_{ox} \tag{2-40}$$

As with B_0, B_1, B_2 and B_3 the fraction of the Fe(III)-bioxalate ions in the solution, B_4, can be expressed by the following equations:

$$B_4 = \frac{[FeHC_2O_4^{2+}]}{C_{Fe3+}} \tag{2.41}$$

Combining equations (2-17), (2-26)-(2-28), (2-36) and (2-39), the following equations are derived by Panias et al [1996]:

$$B_0 = \frac{1}{1 + K_1[C_2O_4^{2-}] + K_1K_2[C_2O_4^{2-}]^2 + K_1K_2K_3[C_2O_4^{2-}]^3} + \frac{K_4[H^+][C_2O_4^{2-}]}{K_{a2}} \qquad (2\text{-}42)$$

$$B_1 = A_0K_1[C_2O_4^{2-}] \qquad (2\text{-}43)$$

$$B_2 = A_0K_1K_2[C_2O_4^{2-}]^2 \qquad (2\text{-}44)$$

$$B_3 = A_0K_1K_2K_3[C_2O_4^{2-}]^3 \qquad (2\text{-}45)$$

$$B_4 = A_0K_4\frac{[H^+][C_2O_4^{2-}]}{K_{a2}} \qquad (2\text{-}46)$$

Equations (2-40) and (2-42)-(2-46) describe mathematically the influence of C_{ox} and pH on the composition of the Fe^{3+}-oxalic acid system. The equilibrium composition of the Fe^{3+}-oxalic acid system is a function of both pH and oxalic acid concentration. The above set of equations was used to study the effect of pH on the composition of the solution at 1, 0.1 and 0.01 M oxalic acid concentration and the results are shown in Figure 2.12 and 2.13, respectively (Panias et al., 1996).

The concentration of Fe^{3+} in the solution as a function of pH is shown in Fig. 2.12. The Fe^{3+} concentration is extremely low, below $6x10^{-7}$M, in all cases. There are no Fe^{3+} ions in solutions with pH above 2. The concentration of $[FeC_2O_4]^+$ complex fraction is also very low at all oxalic acid concentrations.

In Figure 2.13, the fraction of $[Fe(C_2O_4)_2^-]$, $[Fe(C_2O_4)_3^{3-}]$ and $[FeH(C_2O_4)^{2+}]$ in solution as a function of pH is presented. At all oxalic acid concentrations, the fraction of $[Fe(C_2O_4)_2^-]$ in the solution is below 0.4 and gradually decreases as the concentration of oxalic acid is increased. The pH region in which $[Fe(C_2O_4)_2^-]$ is stable strongly depends on the concentration of oxalic acid. At 0.01M, $[Fe(C_2O_4)_2^-]$ is stable between pH 1-4, while at 1.0M oxalic acid concentration, it is stable between pH 0.5-2.

The $[FeH(C_2O_4)^{2+}]$ concentration in solution sharply decreases as pH increases and it is almost zero at pH higher than 2.5. At very low pH, the $[FeH(C_2O_4)^{2+}]$ is the predominant complex ion present in solution.

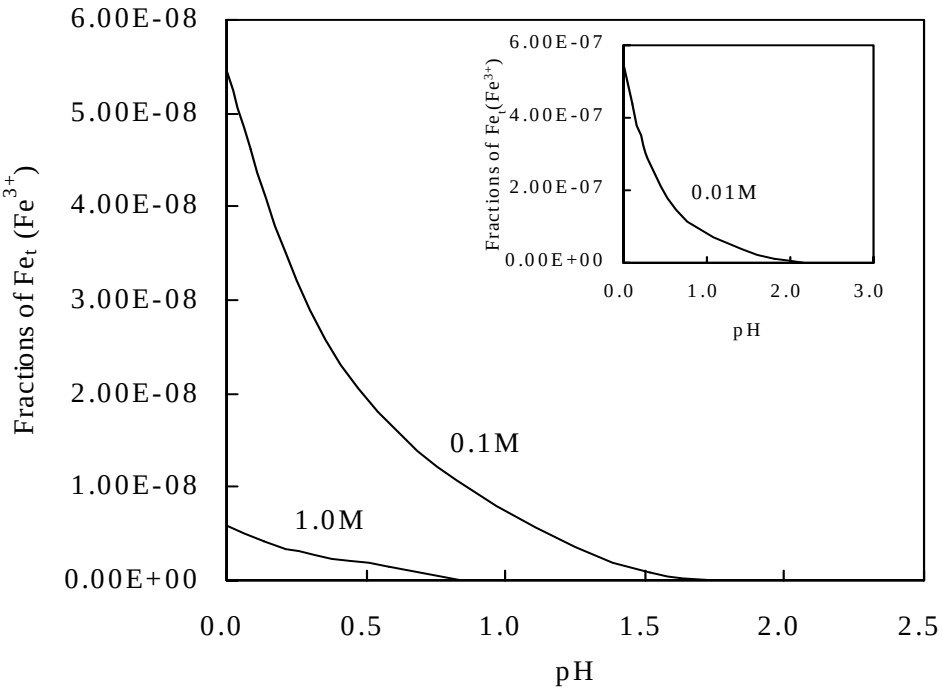

Figure 2.12: The fraction of Fe^{3+} as a function of pH at oxalic acid concentration 0.01, 0.1 and 1.0M, respectively (Panias et al., 1996).

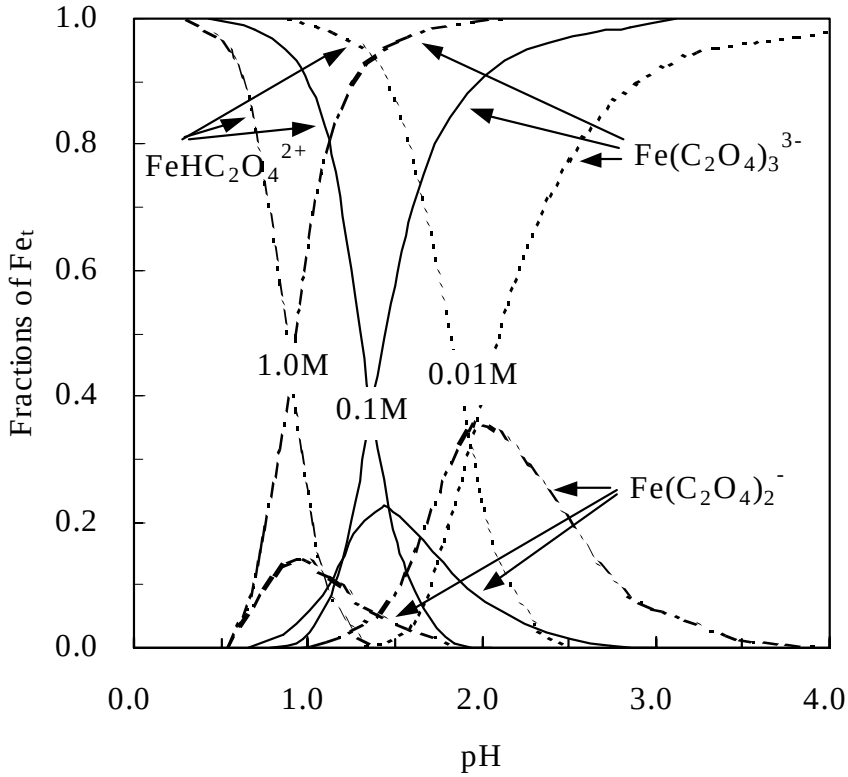

Figure 2.13: The fraction of $[Fe(C_2O_4)_2^-]$, $[Fe(C_2O_4)_3^{3-}]$ and $[FeH(C_2O_4)^{2+}]$ as a function of pH at oxalic acid concentration 0.01, 0.1 and 1.0M, respectively (Panias et al., 1996).

2.3.2.2 Equilibrium diagrams of iron (II) oxalato complexes

According to Panias et al [1996], the equilibrium reactions in iron(II) oxalate system (equations 2.47-2.49) are also greatly affected by free $C_2O_4^{2-}$ concentration, pH and total oxalic acid concentration.

$$FeC_2O_{4(s)} \leftrightarrow Fe^{2+} + C_2O_4^{2-},\ [K_{sp} = 2\text{x}10^{-7}] \tag{2-47}$$

$$Fe^{2+} + 2C_2O_4^{2-} \leftrightarrow Fe(C_2O_4)_2^{2-},\ [K_5 = 5\text{x}10^{7}] \tag{2-48}$$

$$Fe(C_2O_4)_2^{2-} + C_2O_4^{2-} \leftrightarrow Fe(C_2O_4)_3^{4-},\ [K_6 = 3.3\text{x}10^{-3}] \tag{2-49}$$

By assuming that the solution is not saturated with solid $FeC_2O_{4(s)}$, reaction (2-47) does not take place. Consequently, the chemical equilibrium in the solution is mainly described by reactions (2-48) and (2-49).

The equilibrium constants K_5 and K_6 of these reactions are given by the following equations:

$$K_5 = \frac{[Fe(C_2O_4)_2^{2-}]}{[Fe^{2+}][C_2O_4^{2-}]^2} \tag{2-50}$$

$$K_6 = \frac{[Fe(C_2O_4)_3^{4-}]}{[Fe(C_2O_4)_2^{2-}][C_2O_4^{2-}]} \tag{2-51}$$

The total iron concentration in the solution, C_{Fe2+}, is equal to:

$$C_{Fe2+} = [Fe^{2+}] + [Fe(C_2O_4)_2^{2-}] + [Fe(C_2O_4)_3^{4-}] \tag{2-52}$$

D_0, D_1 and D_2 express the fractions of iron present in the solution as Fe^{2+}, $Fe(C_2O_4)_2^{2-}$ and $Fe(C_2O_4)_3^{4-}$, respectively. Combining the equations (2-50)-(2-52), D_0, D_1 and D_2 can be calculated:

$$D_0 = \frac{[Fe^{2+}]}{C_{Fe2+}} = \frac{1}{1 + K_5[C_2O_4^{2-}]^2 + K_5K_6[C_2O_4^{2-}]^3} \tag{2-53}$$

$$D_1 = \frac{[Fe(C_2O_4)_2^{2-}]}{C_{Fe2+}} = D_0K_5[C_2O_4^{2-}]^2 \tag{2-54}$$

$$D_2 = \frac{[Fe(C_2O_4)_3^{4-}]}{C_{Fe2+}} = D_0K_6[C_2O_4^{2-}]^3 \tag{2-55}$$

The composition of Fe(II)-oxalate complexes in an unsaturated solution as a function of free $C_2O_4^{2-}$ concentration is presented in Figure 2.14. In solutions with very low free $C_2O_4^{2-}$ concentration (less than 10^{-5}M) un-complexed Fe^{2+} ions are predominant. Their concentration in the solution decreases rapidly as free $C_2O_4^{2-}$ concentration increases from 10^{-5} to 10^{-3}M. Below 10^{-3}M, un-complexed Fe^{2+} ions are unlikely to be present. In that zone, the only stable complex is The $Fe(C_2O_4)_3^{4-}$ complex also builds up in the same zone, but not at the same levels of concentration as $Fe(C_2O_4)_2^{2-}$ and thus can be neglected.

Assuming that oxalic acid is in large excess in the solution, the concentration of $C_2O_4^{2-}$ in the solution can be calculated with respect to changes in pH from the equilibria constants (K_{a1} and K_{a2} shown in equations 2.15 and 2.17) associated with the ionisation reactions of oxalic acid. As previously demonstrated, $C_2O_4^{2-}$ concentration is given by the following equation:

$$[C_2O_4^{2-}] = \frac{K_{a1}K_{a2}}{[H^+]^2 + K_{a1}[H^+] + K_{a1}K_{a2}} C_{ox} \qquad (2\text{-}56)$$

Panias and co-workers [1996] calculated the composition of a Fe^{2+}-oxalic acid system in excess oxalic acid as a function of pH and oxalic acid concentration, the result of which is shown in Figures 2.15 and 2.16, respectively. In high acid solutions, un-complexed Fe^{2+} is stable in solution (Fig. 2.15). Its stability region is strongly dependent on oxalic acid concentration. At 1.0M oxalic acid solution, Fe^{2+} is more predominant only at a pH below pH0.5. As the oxalic acid concentration decreases its stability region is extended to higher pH values. In low acid solutions (pH higher than 2), $Fe(C_2O_4)_2^{2-}$ is practically the only ion present. The stability region moves to higher pH values as the oxalic acid concentration decreases. At all oxalic acid concentrations (0.01, 0.1 and 1.0M) the fraction of $Fe(C_2O_4)_3^{4-}$ in the solution is very low (less than 0.0035) and gradually increases as the oxalic acid concentration increases (Fig. 2.16).

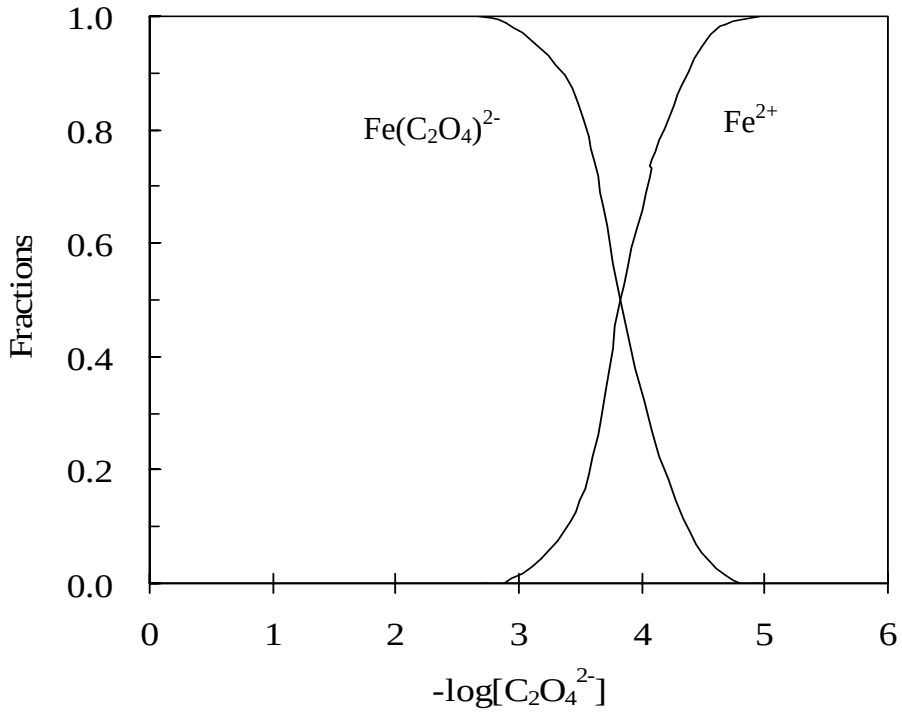

Figure 2.14: The composition of Fe(II)-oxalate complexes in an unsaturated Fe^{2+} solution as a function of $C_2O_4^{2-}$ (Panias et al., 1996).

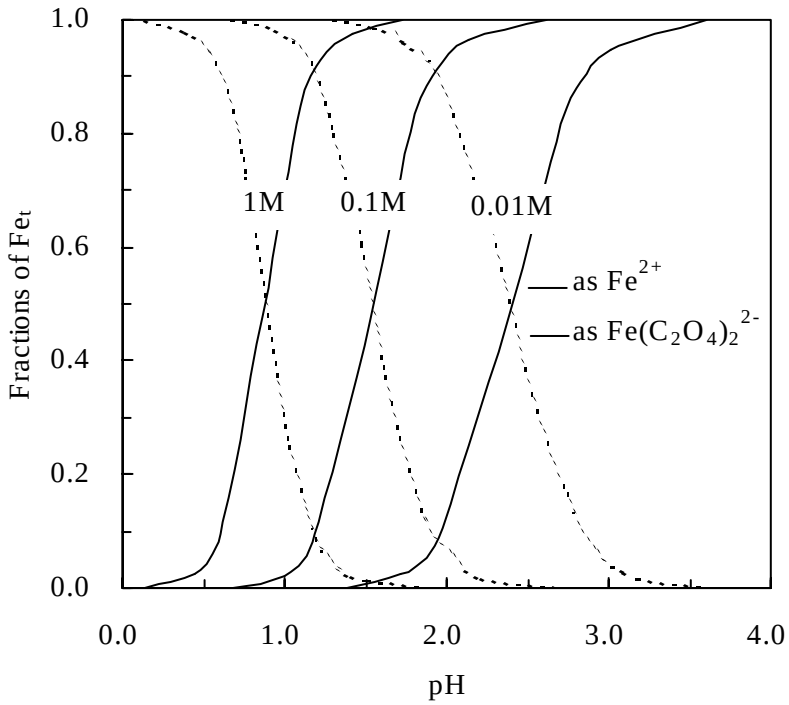

Figure 2.15: The fraction of Fe^{2+} (dotted lines) and $Fe(C_2O_4)_2^{2-}$ (continuous lines) as a function of pH (Panias et al., 1996).

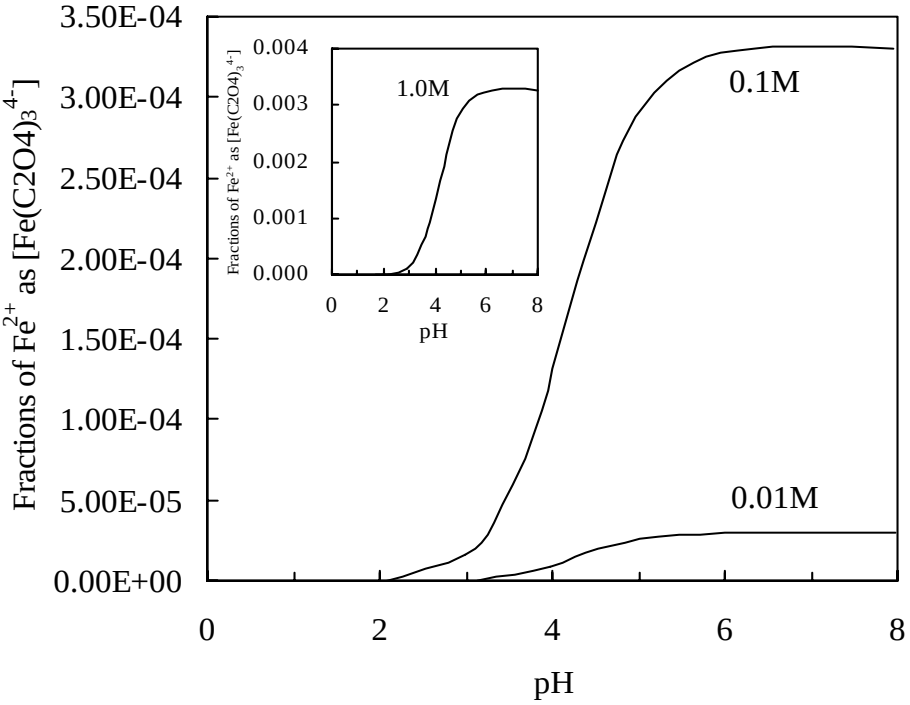

Figure 2.16 The very low fraction of $Fe(C_2O_4)_3^{4-}$ as a function of pH and oxalate concentration from 0.01M to 1.00M (Panias et al., 1996).

2.4 PASSIVITY OF IRON IN OXALATE SOLUTIONS

Sokolova et al. (1976) showed that iron in concentrated oxalic acid solutions has two regions of passivity: at E = -0. 18 to -0.4V where the formation of a passivating salt film of sparingly soluble oxalate $FeC_2O_4 \cdot H_2O$ was observed, and between 0.7 and 1.6V where there is a region of oxide passivity. These regions are separated by a sharp anodic current maximum, the origin of which remains unknown. This feature does not occur in other systems with regions of salt and oxide passivity. Thus as in the case of manganese in phosphate solutions, the transition from the salt region to the oxide region is smooth and without current extrema (Sukhotin and Osipenkova. 1978).

Sukhotin and Berezin (1982) construct and discuss the Pourbaix diagram for the $Fe\text{-}H_2C_2O_4 \cdot H_2O$ system and study the anodic polarization curves of iron in 0.21 M oxalic acid (pH =1.2) in comparison with the electrochemical behaviour of $FeC_2O_{4(s)}$. In this system, they used the following equilibrium constants, taken from Chemical Data Handbook (Rabinovich and Khavin, 1978)

$$[Fe^{2+}][C_2O_4^{2-}] = 2.1x10^{-7};\ [Fe^{3+}][C_2O_4^{2-}]\ /\ [FeC_2O_4^{+}]\ = 4x10^{-10}$$

$[Fe^{2+}][C_2O_4^{2-}]^2 / [Fe(C_2O_4)^{2-}] = 3.4x10^{-5}$; $[Fe^{3+}][C_2O_4^{2-}]^2 / [FeC_2O_4^{-}] = 6x10^{-21}$

$[Fe^{2+}][C_2O_4^{2-}]^3 / [Fe(C_2O_4)_3^{4-}] = 6x\ 10^{-6}$; $[Fe^{3+}][C_2O_4^{2-}]^3 / [Fe(C_2O_4)_3^{3-}] = 3x10^{-21}$

$[Fe^{2+}][OH^-] = 1.95xl0^{-14}$; $[Fe^{3+}][OH^-]^3 = 6.9x10^{-5}$

Table 2.6 shows the values of the potentials of the electrochemical reactions, which are important in relation to the passivity of iron in the system. For comparison it shows the equilibrium potentials of the reactions in the Fe-H_2O system which does not contains oxalate ions, on the condition that the activity of iron ions in the solution is equal to unity. Reactions involving Fe_3O_4 and γ-Fe_2O_3 are taken into account, because these are apparently the oxides which constitute the two-layer passivating film on the Fe (Gohr and Lange, 1957; Sato et al., 1974; Khentov and Sukhotin, 1979).

Eh-pH diagrams based on these data were developed by Khentov and Sukhotin (1979) as shown in Figure 2.17. The complex formation of the Fe^{2+} and Fe^{3+} ions with $C_2O_4^{2-}$, and also the stability of insoluble $FeC_2O_{4(s)}$, lead to marked differences between the diagrams in Figures 2.17 (a) and (b).

On the basis of this diagram, the processes occurring for iron when the anodic polarization is increased can be considered. Line 1, bounding the regions of stability and active dissolution of Fe in Figure 2.17(a), corresponds in Figure 2.17(b) to the formation of a passivating salt film according to the overall reaction:

$$Fe + C_2O_4^{2-} = FeC_2O_{4(s)} + 2e \qquad (2\text{-}57)$$

The equilibrium position of line 1 naturally does not depend on whether the mechanism of this reaction is of the bulk or direct electrochemical type. Line 7 corresponds to oxidation of $FeC_2O_{4(s)}$ to Fe^{3+} ions on the condition that their concentrations correspond to complete establishment of equilibrium of all the reactions of complex formation in the solution. For the assumed initial data, the equilibrium value of $[Fe^{3+}]$ is $7.1x10^{-22}$M. In practice such low concentrations are frequently not attained. Increasing $[Fe^{3+}]$, for example, to 10^{-11} would lead to shift of line 7 in Figure 2.17 (b) by 0.6V in the anodic direction.

Table 2.6 Theoretical reaction potentials (volt) for the Fe-H_2O and Fe-0.21 M $H_2C_2O_4 \cdot H_2O$ systems (Gohr and Lange, 1957; Sato et al., 1974; Khentov and Sukhotin, 1979).

No	Reaction	Fe-H_2O system	Fe-0.21 M $H_2C_2O_4 \cdot H_2O$ system	
			Range of pH in Pourbaix diagram	At pH 1.2
1	$Fe = Fe^{2+} + 2e$	-0.44	-0.62	-0.62
2	$Fe = Fe^{3+} + 3e$	-0.037	-0.45	-0.45
3	$3Fe + 4H_2O = Fe_3O_4 + 8H^+ + 8e$	-0.085 - 0.059	-0.085 - 0.059	-0.16
4	$2Fe + 3H_2O = \gamma Fe_2O_3 + 6H^+ + 6e$	-0.007 - 0.059	-0.007 - 0.059	-0.08
5	$3Fe^{2+} + 4H_2O = Fe_3O_4 + 8H^+ + 2e$	0.98 - 0.236	1.51 - 0.236	1.23
6	$2Fe^{2+} + 3H_2O = \gamma Fe_2O_3 + 6H^+ + 2e$	0.85 - 0.177	0.12 - 0.177	0.99
7	$Fe^{2+} = Fe^{3+} + e$	0.77	-0.12	-0.12
8	$Fe^{2+} + Fe_3O_4 + H_2O = \gamma Fe_2O_3 + 4H^+ + 2e$	0.71 - 0.118	0.89 - 0.118	0.75
9	$2Fe_3O_4 + H_2O = 3\gamma Fe_2O_3 + 2H^+ + 2e$	0.58 - 0.059	0.58 - 0.059	0.51
10	$Fe_3O_4 + 8H^+ = 3Fe^{3+} + 4H_2O + e$	0.35 - 0.472	-0.39 - 0.472	-2.86
11	$Fe_3O_4 = 3Fe^{3+} + 2O_2 + 9e$	1.13	0.71	0.71
12	$\gamma Fe_2O_3 = 2Fe^{3+} + 1.5O_2 + 6e$	1.24	0.78	0.78
13	$\gamma Fe_2O_3 + 6H_2O = \gamma Fe(OH)_3 + 1.5O_2 + 6H^+ + 6e$	13 - 0.059	1.23 - 0.059	1.23
14	$Fe_3O_4 + 9H_2O = Fe(OH)_3 + 2O_2 + 9H^+ + 9e$	1.23 - 0.059	1.23 - 0.059	1.16
15	$Fe^{2+} + 2H_2O = Fe(OH)_2 + 2H^+$	0.65	0.65	
16	$Fe^{3+} + 3H_2O = Fe(OH)_3 + 3H^+$	0.61	0.67	-
17	$2Fe(OH)_2 = \gamma Fe_2O_3 + H_2O + 2H^+ + 2e$	0.062 - 0.059	0.062 - 0.059	0.009
18	$Fe + 2H_2O = Fe(OH)_2 + 2H^+ + 2e$	-0.047 - 0.059	-0.047 - 0.059	0.12

Regions of stability of various iron oxides have also been changed in the presence of oxalate. The boundary of stability of magnetites at low pH values as determined in Figure 2.17 (a) (for non-oxalate systems) has been significantly shifted in the presence of oxalate (Fig. 2.17(b)).

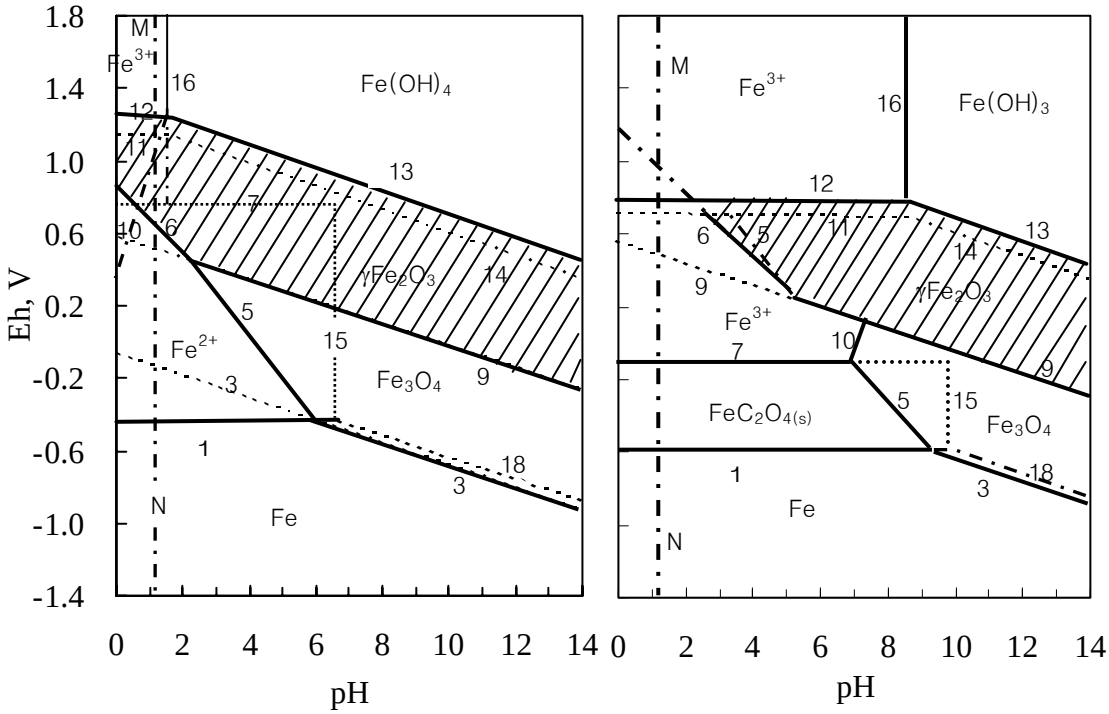

Figure 2.17: Eh-pH diagrams for systems: (a) Fe-H_2O and (b) Fe-H_2O-0.21 M $H_2C_2O_4$ (Khentov and Sukhotin, 1979).

The region of stability of γ-Fe_2O_3 in Figure 2.17 (a and b) are shaded. Line 9, corresponding to the equilibrium Fe_3O_4/γ-Fe_2O_3, does not change position and, thus, the presence of oxalate ions is not reflected in the position of the Fladet potential (passivation potential), which in acid solutions is associated with the formation of a cover of γ-Fe_2O_3 over a sublayer of Fe_3O_4 (Gohr and Lange, 1957). However, the cathodic boundary of stability of γ-Fe_2O_3 along line 6, with which in acid solution is linked to the region of complete passivation, sharply shifts toward the anodic side in the oxalate system. At pH = 2.37, line 6 in Figure 2.17 (b) intersects line 12 corresponding to the reaction of overpassivation of iron (Sukhotin and Khentov. 1980). Therefore, at pH < 2.37 γ-Fe_2O_3 is not stable in the oxalate system. The formation of a film of

γ-Fe_2O_3 by reactions 14 and 9 must be accompanied by its dissolution (reactions 6 and 12), so that it shows worse protective properties of the passivating film and a corresponding increase in the anodic current density in the region of oxide passivity. In particular, this refers to the solution of 0.21 M $H_2C_2O_4^{2-}$ (line MN in Figure 2.17 (a) and (b)).

Over the range of pH 2-4 of interest to the dissolution of iron oxides, Fig. 2.17(b) implies that the dissolution of various iron oxides will form solid ferrous oxalate in the Eh range -0.15V to -0.6V.

2.5 SUMMARY

In metallurgy, where iron ores are leached to recover the metal, the efficiency of the extraction process depends upon the leachability of the ore.

In most natural systems, the aqueous phase is fairly close to saturation with respect to iron oxides and resulting in slow dissolution. The dissolution process can be accelerated by the presence of higher levels of electrons or chelating ligands.

The dissolution rate and mechanism is frequently established on the basis of data corresponding to release of no more than a few percent of the total iron available. In the initial stage of dissolution, the amount of iron released is often a linear function of time, so the dissolution rate can be expressed as the amount of iron dissolved per unit weight or unit area of the oxide.

While most studies on iron oxide dissolution concentrate on establishing the mechanism of dissolution, there are few studies in which different oxides have been compared to provide information about the effect of oxide properties. The dissolution behaviour of an iron oxide sample strongly depends on its preparation and source.

The factors affecting the rate of dissolution of iron oxides are temperature, composition and characteristics of the solution phase (e.g. pH, redox potential, concentration of acids, reductants and complexing agents) and properties of the oxide (e.g. stoichiometry, crystal chemistry, crystal habit and presence of defects or guest ions).

Additives in the leaching solution affect the dissolution of iron oxides significantly. Additives may act in solution (via complexation), but more often adsorb on the surface of iron oxides and influence the energy of attachment between the surface ions and those of the interior. In extreme cases, adsorbed additives may inhibit dissolution.

The solution pH strongly influences the dissolution of iron oxides. The high affinity of protons with structural O^{2-} assists the release of iron particularly at low pH. It is the release of the cation, rather than the anion which is likely to be rate-limiting.

The general reaction between protons and Fe(III) oxides can be written as

$$FeOOH_{aq} + nH^{+} \rightarrow [Fe(OH)_{(3-n)}]^{n+}_{aq} + (n-1)H_2O$$

The first step involves adsorption of a proton by the surface OH. The adsorption of proton weakens the Fe-O bond, probably by polarizing it and so, promotes detachment of Fe from the bulk oxide.

The general reaction for ligand promoted dissolution may be written as follows,

$$\equiv Fe(III) - OH + L^{-} + H^{+} \rightarrow \equiv Fe(III)L + H_2O \rightarrow Fe(III)L_{aq} + H_2O$$

The ligand is first adsorbed on the surface of the Fe oxide and this weakens the Fe-O bonds to neighbouring atoms and eventually leads to detachment of the Fe(III) complex .

In natural environments, reductive dissolution is by far the most important mechanism. The mechanism by which the structural bonds in iron oxides may be weakened, involves reduction of structural Fe(III) to Fe(II).

For iron oxide dissolution from mineral samples reductants investigated include dithionite, thioglycolic acid, thiocyanate, hydrazine, ascorbic acid, hydroquinone, H_2S, H_2, Fe^{2+}, tris(picolinato)-V(II), fulvic acid, fructose, sucrose and biomass/bacteria.

Dissolution reactions may be either transport-controlled (i.e. diffusion) or surface-controlled. However, in many systems, the chemical reaction at the solid/liquid interface is rate-determining.

Iron in concentrated oxalic acid solutions has two regions of passivity: at Eh in the range -0.18 to -0.4V, the formation of a passivating salt film of $FeC_2O_4(s)$ is observed, and between 0.7 and 1.6V there is a region of oxide passivity.

Equilibrium diagrams show that in low acid solutions (higher than pH3) the only thermodynamically stable complex ions of bivalent and trivalent iron are $[Fe(C_2O_4)_2]^{2-}$ and $[Fe(C_2O_4)_3]^{3-}$. As the oxalic acid concentration increases the stability region of the above complex ions is extended to more acidic regions.

Un-complexed Fe^{2+} ion is stable only in high acid solutions, while un-complexed Fe^{3+} ion is not likely to buildup in oxalic acid solutions. $[Fe^{3+}(C_2O_4)_2]^-$ is stable in the pH range 1-2, while $[Fe^{3+}C_2O_4]^+$ is stable in the same region but at lower concentrations compared with the other complex ions.

At pH less than 1, the $[Fe^{3+}HC_2O_4]^{2+}$ complex ion is very stable in comparison with the other ions in the solution. Thus in such solutions $[Fe^{3+}HC_2O_4]^{2+}$ is the only ion existing.

CHAPTER THREE

THERMODYNAMIC ANALYSIS OF THE REACTIONS OF SODIUM, AMMONIUM AND IRON OXALATE COMPLEXES AND THEIR SOLUBILITY

3.1 INTRODUCTION

The dissolution of pure iron oxide or the removal of iron oxide from industrial minerals such as clay, kaoline and quartz by organic acids has been extensively studied (Blesa et al., 1994, Afonso et al., 1990, Sellars and Williams, 1984; Lee, 1997). Among the organic acids, oxalic acid ($H_2C_2O_4 \cdot 2H_2O$) is used widely for the dissolution of iron due to its effectiveness as a complexant.

The activity of oxalic acid depends strongly on temperature, agitation speed and the amount of solution in a reaction system. The maximum solubility of oxalic acid is about 1.0 M in water at 25^{o}C at pH less than 1.0. The activity of oxalate increases with the increase in pH. When the pH of an oxalate solution is in the range of pH2 to 4, its efficiency for iron leaching increases significantly. It has been known that the major factor affecting leaching efficiency is pH in a solution, while the effect of the concentration of oxalic acid in a solution, particular at low temperatures is minimal.

To control the pH of an oxalic acid leaching solution, sodium hydroxide and ammonium hydroxide are often used. However, they easily form oxalate complexes and precipitate in saturated solution in the forms such as $NaHC_2O_4 \cdot H_2O$ or $Na_2C_2O_4 \cdot H_2O$, and $NH_4HC_2O_4 \cdot H_2O$ or $(NH_4)_2C_2O_4 \cdot H_2O$.

In this study, a thermodynamic analysis of the above reactions in an oxalic acid solution will be presented. This involves study on 1) the reactions involved in the formation of iron oxalate complexes 2) solubilities of sodium or ammonium-oxalate complexes in an

oxalic solution and 3) precipitation of sodium, potassium or ammonium-oxalate complexes. For these purposes, the speciation of oxalic acid and sodium, potassium ammonium and iron oxalate complexes and the standard free energy changes of representative chemical reactions were reviewed and discussed.

3.2 EXPERIMENTAL

3.2.1 Materials

The following reagent-grade chemicals were used in this study:

1) Oxalic acid: $H_2C_2O_4 \cdot 2H_2O$ (99%), analytical reagent, which was used as a leaching solvent.

2) Sodium hydroxide and sodium oxalate: NaOH (99%) and $Na_2C_2O_4$ (99%), analytical reagent.

3) Ammonium hydroxide and ammonium oxalate: NH_4OH (99%) and $(NH_4)_2C_2O_4$ (99%), analytical reagent.

4) All solutions were prepared by dissolving or diluting analytical grade reagents in distilled water.

3.2.2 Procedures

A 250 ml 3–necked cylindrical pyrex reaction vessel was used as the reactor for the experiments. The reactor was kept in a temperature-controlled water bath. Temperature was controlled to within ± 0.5℃. Agitation was achieved by using a teflon coated stirrer. The speed of the stirrer was kept constant at 300 rpm throughout all experiments. A pH meter (ORION, Model-520A) was used to measure the pH of a solution.

The concentrations of Na^+ and Fe^{3+} in a solution were measured by atomic absorption spectroscopy (AAS, Varian, Spectra AA-20). NH_4^+ concentration in a solution was measured by UV-visible spectrophotometer (UV-VIS, Model -160A, SHIMADZU).

The morphology or crystalline structure of the precipitates was examined by a scanning electron microscope (SEM, JSM-5400).

3.3. RESULTS AND DISCUSSION

3.3.1 Speciation of oxalic acid

The ionization of oxalic acid includes two reactions with ionisation constants K_{a1} and K_{a2} as shown in Table 3.1. In an oxalic acid solution, molecules of oxalic acid and its ions, $HC_2O_4^-$ and $C_2O_4^{2-}$, coexist in equilibrium. These ions are produced by the following ionisation reactions (3-1) to (3-4) (Bailar et al.,1989; Panias et al., 1996).

Table 3.1 Ionisation constants of oxalic acid at 25℃.

$H_2C_2O_4 \leftrightarrow H^+ + HC_2O_4^-$	$K_{a1} = 5.6 \times 10^{-2}$
$HC_2O_4^- \leftrightarrow H^+ + C_2O_4^{2-}$	$K_{a2} = 6.2 \times 10^{-5}$

$$H_2C_2O_4 \leftrightarrow H^+ + HC_2O_4^- \tag{3-1}$$

$$K_{a1} = \frac{[H^+][HC_2O_4^-]}{H_2C_2O_4} \tag{3-2}$$

$$HC_2O_4^- \leftrightarrow H^+ + C_2O_4^{2-} \tag{3-3}$$

$$K_{a2} = \frac{[H^+][C_2O_4^{2-}]}{HC_2O_4^-} \tag{3-4}$$

The fractions of non-dissociated $H_2C_2O_4$, $HC_2O_4^-$ and $C_2O_4^{2-}$ are defined by the following equations, respectively:

$$a_0 = \frac{[H_2C_2O_4]}{C_{ox}} \tag{3-5}$$

$$a_1 = \frac{[HC_2O_4^-]}{C_{ox}} \tag{3-6}$$

$$a_2 = \frac{[C_2O_4^{2-}]}{C_{ox}} \tag{3-7}$$

where:

$$C_{ox} = [H_2C_2O_4] + [HC_2O_4^-] + [C_2O_4^{2-}] \tag{3-8}$$

Combining equations (3-2) and (3-4)-(3-8) the fractions a_0, a_1, a_2 as a function of pH

can be derived.

$$a_0 = \frac{[H^+]^2}{[H^+]^2 + K_{a1}[H^+] + K_{a1}K_{a2}} \quad (3\text{-}9)$$

$$a_1 = \frac{K_{a1}[H^+]}{[H^+]^2 + K_{a1}[H^+] + K_{a1}K_{a2}} \quad (3\text{-}10)$$

$$a_2 = \frac{K_{a1}K_{a2}}{[H^+]^2 + K_{a1}[H^+] + K_{a1}K_{a2}} \quad (3\text{-}11)$$

The variations of the undissociated $H_2C_2O_4$ and dissociated fractions of $HC_2O_4^-$ and $C_2O_4^{2-}$ as a function of pH are shown in Figure 2.9 (Chapter 2) (Huang, 2000).

It is obvious from Figure 2.9 that the $C_2O_4^{2-}$ concentration is high in alkaline solutions and low in acidic solutions. In a solution of pH less than 2.0, the $C_2O_4^{2-}$ concentration is negligible. In such solutions, the active species is $HC_2O_4^-$ rather than $C_2O_4^{2-}$. At pH higher than 3.0, almost complete ionisation of oxalic acid is observed. In this region, the active species are both $HC_2O_4^-$ and $C_2O_4^{2-}$. When the pH of a solution is higher than 4.0, the concentration of $HC_2O_4^-$ is less than that of $C_2O_4^{2-}$, and at above pH 6.0 the concentration of $HC_2O_4^-$ becomes negligible.

3.3.2 Formation of sodium, ammonium and iron oxalate complexes

The well-known phenomenon of ring formation by ligands in a complex is called chelation. The ring is called a chelate ring. Oxalate ion ($C_2O_4^{2-}$) becomes negatively charged and has two oxygen atoms with pairs of electrons donated from carbon atoms. These two oxygen atoms become negatively charged and have the ability to co-ordinate to metal atoms or ions and form a ring. Therefore in the presence of metal (M^{x+}) ions, oxalate ions have the ability to form strong complex ions. Table 3.2 shows the reactions involved in the formation of sodium, ammonium and iron oxalate complexes and their thermodynamic data. Their solubility products (K_{sp}), dissociation constants (K_d) and equilibrium constants (K_c) are also given in Table 3.2. The solubility products of sodium and ammonium oxalates were obtained from this study. Other dissociation constants and equilibrium constants were obtained from Donald et al.(1982); Huang, (2000); Bailar et al.(1989), Vincze and Papp (1987) and Lide, et al.(1997).

Table 3.2 The formation of sodium, ammonium and iron oxalate complexes, and their overall solubility products (K_{sp}), equilibrium constant (K_c) and dissociation constants (K_d) for iron complexes at 25℃(Donald et al.,1982; Huang, 2000; Bailar et al., 1989; Vincze and Papp, 1987; Lide, et al., 1997)

$Na_2C_2O_4 \leftrightarrow 2Na^+ + C_2O_4^{2-}$	K_{sp} = 7.76 x 10^{-2}	(3-12)
$NaHC_2O_4 \leftrightarrow Na^+ + HC_2O_4^-$	K_{sp} = 2.37 x 10^{-2}	(3-13)
$Na^+ + C_2O_4^{2-} \leftrightarrow NaC_2O_4^-$	K_c = 1.808 x 10^4	(3-14)
$(NH_4)_2C_2O_4 \leftrightarrow 2NH_4^+ + C_2O_4^{2-}$	K_{sp} = 0.2446	(3-15)
$NH_4HC_2O_4 \leftrightarrow NH_4^+ + HC_2O_4^-$	K_{sp} = 1.012	(3-16)
$[Fe^{2+}(C_2O_4)_3]^{4-}$	K_d = 6x10^{-6}	(3-17)
$[Fe^{2+}(C_2O_4)_2]^{2-}$	K_d = 2x10^{-8}	(3-18)
$[Fe^{3+}(C_2O_4)_3]^{3-}$	K_d = 3x10^{-21}	(3-19)
$[Fe^{3+}(C_2O_4)_2]^-$	K_d = 6.31x10^{-21}	(3-20)
$[Fe^{3+}C_2O_4]^+$	K_d = 3.98x10^{-10}	(3-21)
$[Fe^{3+}C_2O_4H]^{2+}$	K_d = 2.95x10^{-10}	(3-22)

From K_{sp} values, it can be predicted that ammonium oxalate solid is less stable than sodium oxalate. Ammonium oxalate $NH_4HC_2O_4$ therefore dissolves readily to form NH_4^+ and $HC_2O_4^-$.

3.3.3 Calculations of standard free energy, ΔG^o

3.3.3.1 Sodium hydroxide – oxalic acid system

In this study, the solubility products (K_{sp}), dissociation constants (K_d) and equilibrium constants (K_c) were adopted to calculate thermodynamic data, ΔG^o. The calculation of ΔG^o is based on Hess' law.

In Table 3.2, the reactions involved in the formation of sodium oxalate in water or oxalic acid solution are shown as (3-12) to (3-14).

The overall reaction of the formation of sodium oxalate can be described as the equation (3-23).

$$2NaOH_{(s)} + C_2O_4^{2-}{}_{(aq)} + 2H^+{}_{(aq)} \rightarrow Na_2C_2O_{4(s)} + H_2O_{(l)} \quad (3\text{-}23)$$

In an acidic solution, the speciation of oxalate is predominated by $HC_2O_4^-$ because the dissociation of oxalic acid depends on the pH of the solution. Therefore, in an acidic solution (<pH 3.5), the following reaction can be assumed:

$$NaOH_{(s)} + HC_2O_4^-{}_{(aq)} + H^+ \rightarrow NaHC_2O_{4(s)} + H_2O_{(l)} \quad (3\text{-}24)$$

However, at a pH higher than 3.5, other reactions can be assumed, represented by equations (3-25) and (3-26):

$$NaHC_2O_{4(s)} + Na^+_{(aq)} + OH^-_{(aq)} \rightarrow Na_2C_2O_{4(s)} + H_2O_{(l)} \quad (3\text{-}25)$$

$$NaOH_{(s)} + C_2O_4^{2-}{}_{(aq)} + H^+{}_{(aq)} \rightarrow NaC_2O_{4(aq)}^- + H_2O_{(l)} \quad (3\text{-}26)$$

In the case of high alkaline solution (reaction 3-26), $NaHC_2O_4$ ionizes into $HC_2O_4^-$ and Na^+ ions. $HC_2O_4^-$ further dissociates into H^+ and $C_2O_4^{2-}$ ion. The hydrogen ion released from $HC_2O_4^-$ reacts with OH^- ion in the solution and is consumed. Thus, the representative reaction in a saturated solution can be assumed by the equation (3-25) and the precipitated solid forms include $Na_2C_2O_4 \cdot H_2O$ and $NaHC_2O_4 \cdot H_2O$, respectively.

The values of ΔG^o for an appropriate series of reactions in this system are given in Table 3.3. The ΔG°values were calculated by thermodynamic data developed by Bailar et al. (1989), Vincze and Papp (1987), Huang (2000) and Lide et al.(1997).

The ΔG°values for reaction (3-32), (3-33) and (3-34) were calculated according to the following equation :

$$\Delta G^o_{298} = -RT\ln(K)$$

For reactions (3-32) and (3-33), the K_{sp} values for reactions (3-12) and (3-13) were used, the K_c value in reaction (3-14) was used for reaction (3-34).

Table 3.3 ΔG°values for some reactions at 25℃.(Bailar et al., 1989; Vincze and Papp,

1987; Huang, 2000 and Lide et al., 1997).

Reaction	ΔG^o (kJ/mol)	
$H_{2(g)} + 1/2O_{2(g)} \leftrightarrow H_2O_{(l)}$	-237.13	(3-27)
$1/2H_{2(g)} \rightarrow H^+_{(aq)} + e^-$	0	(3-28)
$H_2C_2O_4 \leftrightarrow H^+ + HC_2O^-_{4(s)}$	-698.3	(3-29)
$HC_2O_4^- \leftrightarrow H^+ + C_2O_4^{2-}$	-673.9	(3-30)
$Na^+_{(ao)} + OH^-_{(ao)} \leftrightarrow NaOH_{(ao)}$	-419.15	(3-31)
$Na^+_{(ao)} + HC_2O_4^- \leftrightarrow NaHC_2O_{4(s)}$	-9.28	(3-32)
$2Na^+_{(ao)} + C_2O_4^{2-} \leftrightarrow Na_2C_2O_{4(s)}$	-6.34	(3-33)
$Na^+_{(ao)} + C_2O_4^{2-} \leftrightarrow NaC_2O_4^-$	-24	(3-34)

The calculated ΔG^o values for the reactions (3-24), (3-25) and (3-26) were evaluated by the data in Tables 3.2 and 3.3 as follows:

$\Delta G^o_{298} = -89.1 kJ/mol$ (reaction 3-24)

$\Delta G^o_{298} = -39.8 kJ/mol$ (reaction 3-25)

$\Delta G^o_{298} = -100 kJ/mol$ (reaction 3-26)

From the calculated results, the negative value of ΔG^o of each reaction indicates it is a spontaneous reaction at standard states. However, the reactions in an industrial system depend strongly on the kinetics rather than the thermodynamic stability.

3.3.3.2 Ammonium hydroxide – oxalic acid system

In an acidic solution (pH<3.0), the speciation of oxalate is predominated by $HC_2O_4^-$. The predominant reaction when saturation is reached is that of ammonium and bi-oxalate ions according to:

$$NH_4^+ + HC_2O^-_{4\,(aq)} + \rightarrow NH_4HC_2O_{4(s)} \quad (3\text{-}35)$$

On the other hand, in a solution with pH higher than 3.5, $NH_4HC_2O_{4(s)}$ would not be

stable, especially at the increase in the concentration of free $C_2O_4^{2-}$. As shown in Chapter 2, $C_2O_4^{2-}$ ion is predominant in a high-pH solution (pH>4.0). The addition of ammonium hydroxide to such a solution causes the reaction of $C_2O_4^{2-}$ ion with ammonium ion, resulting in the formation of ammonium oxalate ($(NH_4)_2C_2O_4$). The overall reaction of ammonium hydroxide and oxalate at high pH's (in the region where free oxalate is stable pH>4.0) forming ammonium oxalate can be expressed as the equation (3-35):

$$2NH_4^+ + C_2O_{4\,(aq)}^{2-} \rightarrow (NH_4)_2C_2O_{4(s)} \qquad (3\text{-}36)$$

The possible precipitates formed in saturated solutions of ammonium and oxalate ions within the range pH2-4 are $(NH_4)_2C_2O_4 \cdot H_2O$ and $NH_4HC_2O_4 \cdot H_2O$. The conversion from $NH_4HC_2O_4 \cdot H_2O$ to $(NH_4)_2C_2O_{4(s)}$ at high pH's can be described by the reaction (3-37).

$$NH_4HC_2O_{4\,(s)} + NH_{4(aq)}^+ + OH_{(aq)}^- \rightarrow (NH_4)_2C_2O_{4(s)} + H_2O_{(l)} \qquad (3\text{-}37)$$

The ΔG^o values for the above equilibrium reactions were calculated from thermodynamic data quoted by Bailar et al. (1989), Vincze and Papp (1987), Donald et al. (1982), Huang (2000) and Lide et al. (1997).

$\Delta G_{298}^o = -0.03 kJ/mol$ (for reaction 3-35)

$\Delta G_{298}^o = +3.49 kJ/mol$ (for reaction 3-36)

$\Delta G_{298}^o = -52.0 kJ/mol$ (for reaction 3-37)

The free-energy value calculated for Reaction 3-36 indicated that the precipitation of $(NH_4)_2C_2O_4$ will not proceed at 25°C.

3.3.3.3 Iron oxides (Hematite and Goethite)-oxalic acid system

The dissolution of iron from hematite in oxalic acid can proceed via two different pathways which are reductive and non-reductive, respectively.

The non-reductive pathway shows the presence of iron in the form of iron(III) oxalate complexes in the solution. As discussed in Chapter 2, the trioxalatoferrate(III) ion

$[Fe(C_2O_4)_3]^{3-}$ is the most stable among iron(III) oxalate complexes. Thus, hematite (α-Fe_2O_3) could be dissolved according to the reaction of equation (3-41), representing the non-reductive pathway which predominates in a solution at a pH higher than 4.0.

$$\alpha - Fe_2O_{3(s)} + 6C_2O_{4(aq)}^{2-} + 6H_{(aq)}^{+} \rightarrow 2[Fe(C_2O_4)_3]_{(aq)}^{3-} + 3H_2O_{(l)} \qquad (3\text{-}41)$$

However, in a slightly acidic solution (pH2.0-4.0), the active species is $HC_2O_4^-$ ion, as presented in Figure 2.9 (Chapter 2). Therefore, the complex ion $[FeHC_2O_4]^{2+}$ can probably be formed in the solution, as described by the equation (3-42).

$$\alpha - Fe_2O_{3(s)} + 2HC_2O_{4(aq)}^{-} + 6H_{(aq)}^{+} \rightarrow 2[FeHC_2O_4]_{(aq)}^{2+} + 3H_2O_{(l)} \qquad (3\text{-}42)$$

The ΔG^o values of reactions (3-41) and (3-42) could be calculated, yielding:

$\Delta G_{298}^o = -212.8 kJ/mol$ (for reaction 3-41)

$\Delta G_{298}^o = -87.3 kJ/mol$ (for reaction 3-42)

Other equilibria of interest to the systems studied are tabulated in Table 3.4, with free energy data calculated and reported in the literature by several workers (Donald et al., 1982; Vincze and Papp, 1987; Bailar et al., 1989).

Table 3.4 ΔG°values for some reactions at 25°C.(Donald et al., 1982; Vincze and Papp, 1987; Bailer et al., 1989)

Reaction	ΔG^o (kJ/mol)
$\alpha - Fe_2O_{3(s)} + 6C_2O_{4(aq)}^{2-} + 6H_{(aq)}^{+} \rightarrow 2[Fe(C_2O_4)_3]_{(aq)}^{3-} + 3H_2O_{(l)}$	-212.8
$\alpha - Fe_2O_{3(s)} + 2HC_2O_{4(aq)}^{-} + 6H_{(aq)}^{+} \rightarrow 2[FeHC_2O_4]_{(aq)}^{2+} + 3H_2O_{(l)}$	-87.3
$Fe_{(aq)}^{3+} + 3C_2O_{4(aq)}^{2-} \leftrightarrow [Fe(C_2O_4)_3]_{(aq)}^{3-}$	-117.14
$Fe_{(aq)}^{3+} + HC_2O_{4(aq)}^{-} \leftrightarrow [FeHC_2O_4]_{(aq)}^{2+}$	-54.40

On the other hand, the reductive dissolution pathway involves a redox reaction taking place on the hematite surface. For a solution at pH>4.0 the reaction is most likely to involve hematite reduction to form Fe(II)-oxalate and oxidation of oxalate ($C_2O_4^{-2}$) to form carbon dioxide. $[Fe(C_2O_4)_2]^{2-}$ complex is the most predominant iron(II) oxalate complex in this pH range. The reduction of hematite therefore can be represented by:

$$\alpha - Fe_2O_{3(s)} + 5C_2O_{4(aq)}^{2-} + 6H_{(aq)}^{+} \rightarrow 2[Fe(C_2O_4)_2]_{(aq)}^{2-} + 2CO_{2(g)} + 3H_2O_{(l)} \qquad (3\text{-}43)$$

for which the free energy could be calculated to be $\Delta G^{o}_{298} = -153.9 kJ/mol$.

In the range of pH from pH2.0-4.0, although the predominant oxalate species is bi-oxalate ($HC_2O_4^-$), the reduction of hematite under these conditions are similar to the above.

Goethite (α-FeOOH) has a slightly different free energy of formation and the thermodynamics of goethite dissolution was investigated by Cornell and Swertmann (1996). In solution predominated by $C_2O_4^{2-}$ at pH>4.0 the non-reductive dissolution can be described by the following reaction (3-44).

$$\alpha FeOOH + 3C_2O^{2-}_{4(aq)} + 3H^{+}_{(aq)} \rightarrow [Fe(C_2O_4)_3]^{3-}_{(aq)} + 2H_2O_{(l)} \qquad (3\text{-}44)$$

However, in a slightly acidic solution (pH2.0-4.0), the dissolution of goethite is represented by the following equation:

$$\alpha FeOOH + HC_2O^{-}_{4(aq)} + 3H^{+}_{(aq)} \rightarrow [FeHC_2O_4]^{2-}_{(aq)} + 2H_2O_{(l)} \qquad (3\text{-}45)$$

the ΔG^{o} values for reaction (3-44) and (3-45) were calculated, respectively as:

$\Delta G^{o}_{298} = -215.0 kJ/mol$ (for reaction 3-44)

$\Delta G^{o}_{298} = -89.5 kJ/mol$ (for reaction 3-45)

On the other hand, the reductive pathway of goethite dissolution with oxalic acid can be described by the following reaction:

$$FeOOH + 2.5C_2O^{2-}_{4(aq)} + 3H^{+}_{(aq)} \rightarrow [Fe(C_2O_4)_2]^{2-}_{(aq)} + CO_{2(g)} + 2H_2O_{(l)} \quad \text{-- (3-46)}$$

The ΔG^{o} value of reaction (3-46) was calculated to be:

$\Delta G^{o}_{298} = -156.1 kJ/mol$ (for reaction 3-46)

Free energy data however did not give indications on the kinetics of dissolution. As a matter of fact, as reviewed in Chapter 2 and as later reported in the experimental chapters of this study, the dissolution of goethite is faster than that of hematite.

3.3.4 Reactions of oxalic acid with the sodium and ammonium hydroxide

In this section, the overall procedures for an acid-base titration between oxalic acid and sodium or ammonium hydroxide were adopted to observe the patterns of precipitation and re-dissolution of Na-oxalate or NH_4-oxalate solids in an oxalic acid solution.

3.3.4.1 Effect of concentration

Figures 3.1 and 3.2 show the titration curves for titrating 100 mL of oxalic acid at different concentrations (0.2, 0.6 and 1.0 M $H_2C_2O_4 \cdot H_2O$) with various bases (1.0M NaOH, 1.0M KOH and 1.0M NH_4OH). The reaction temperature of the solution was 27^oC and the titrant of NaOH, KOH or NH_4OH solution was added slowly to a solution of oxalic acid from a burette.

In this system, when the pH of a solution at different stages of a titration was plotted *vs.* the volume of the added NaOH titrant, a "titration curve" with several "end-points" and deflections was obtained.

Fig. 3.1 shows the variation of pH at different levels of addition of NaOH to various solutions of oxalic acid (from 0.20 to 1.0M oxalic acid). For the 0.2M, 0.6M and 1.0M oxalic acid, a total addition of 40mL, 60mL and 100mL, respectively of 1.0M NaOH caused the precipitation of $NaHC_2O_{4(s)}$ at a 1:1 molar ratio (buffer region A1, B1 and C1, respectively) to reach completion. The pH would be buffered in this precipitation zone (pH1-4) as shown and in this pH range the predominant species is $HC_2O_4^-$ [Panias et al, 1996]. The solubility of $NaHC_2O_{4(s)}$ is 17g/L and 210g/L at 25 and 100^oC, respectively [CRC Handbook of Chemistry and Physics, 1982]. As further NaOH was added, another less soluble precipitate was also formed at pH>4.0 where oxalate ion predominates, namely $Na_2C_2O_{4(s)}$ of which the solubilities are 37g/L and 63.3 g/L at 25 and 100^oC, respectively. The 'end point" was reached at A2, B2 and C2, when the reaction between NaOH and oxalic acid reached completion as shown in Fig. 3.1. Theoretically at these "end points" of the reaction, 2 moles of NaOH would have reacted with 1 mole of oxalic acid ($H_2C_2O_4.\ 2H_2O$), according to the reaction represented by Eq.3.47, before

re-dissolution of the precipitate takes place:

$$H_2C_2O_4 \cdot 2H_2O_{(aq)} + 2NaOH_{(aq)} \rightarrow Na_2C_2O_{4(s)} + 4H_2O_{(aq)} \qquad (3\text{-}47)$$

Due to the slow dissolution of the precipitate slightly extra acid was used (overshooting of the end point determination). Nevertheless the clear buffer zone where precipitation of sodium-oxalate solids took place (A1, B1 and C1) was demonstrated in each case as shown in Fig. 3.1.

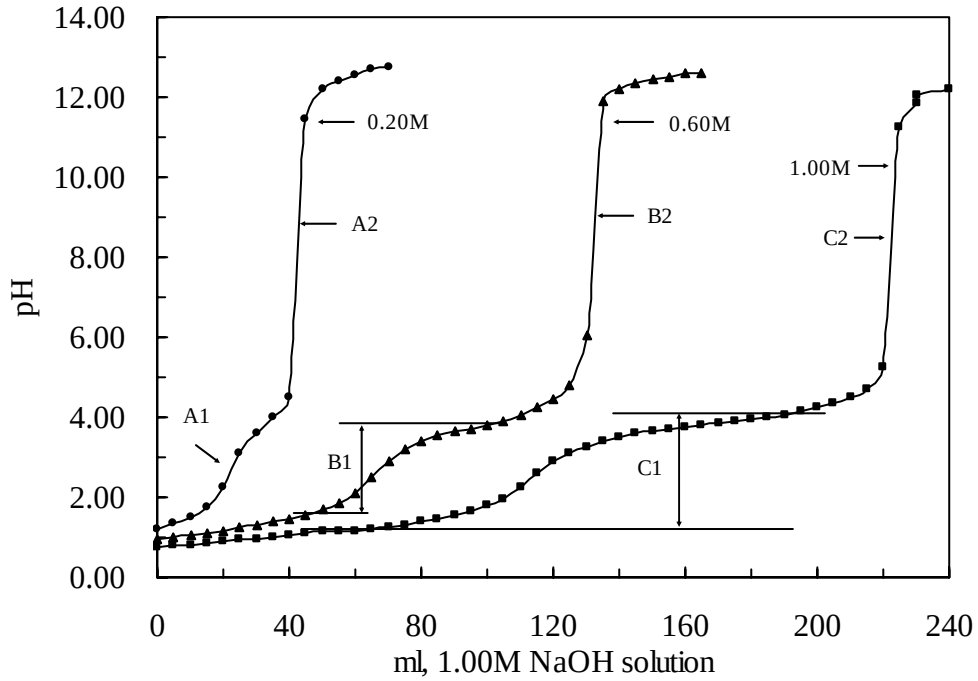

Figure 3.1 The titration curve for titrating oxalic acid (0.2, 0.6 and 1.0 M $H_2C_2O_4 \cdot H_2O$) with 1.0M NaOH solution at 27^{o}C.

The titration results imply that within the pH 2-4 range, the precipitate formed is $NaHC_2O_{4(s)}$. In the range of pH2-4, $HC_2O_4^-$ forms precipitate with Na^+, producing $NaHC_2O_4^-{}_{(s)}$. At the pH range of interest to the dissolution of iron oxide (ie pH 2-4) the availability of $HC_2O_4^-$ is governed by the solubility of $NaHC_2O_4$.

The same pattern was also observed for titration of oxalic acid by another strong base, KOH as show in Figure 3.2. where pH buffer zones were observed between pH1-4. .

However, for the NH_4OH system (Fig. 3.3), although the precipitate would re-dissolve quickly with further addition of ammonia, especially at low concentration of oxalic acid (0.2M). There is only one "end point" corresponding to the 1:1 reaction (3-48) as a result.

$$H_2C_2O_4 \cdot 2H_2O_{(aq)} + NH_4OH_{(aq)} \rightarrow (NH_4)HC_2O_{4(s)} + 4H_2O_{(aq)} \qquad (3\text{-}48)$$

The 1:1 requirement for the NH_4OH-oxalic acid system indicates that there are stable soluble ammonia-bioxalate complexes (holding back one hydrogen ion) compared to the other two systems of NaOH- and KOH-oxalic acid. The precipitation zones (A1, B1 and C1) for the NH_4OH-oxalic acid system were found not to be as large as with the NaOH- and KOH-oxalate systems. The solubilities for $(NH_4)_2C_2O_{4(s)}$ of 25.4g/L and 118g/L at 25 and 50^{o}C, respectively (CRC Handbook of Physisc and Chemistry, 1982) are higher than for their counterparts of the NaOH-oxalic acid system. Although the ammonia-bioxalate $NH_4HC_2O_{4(s)}$ solid is very soluble as stated in the CRC Handbook of Physics and Chemistry (1982) (although no figure is given on its solubility) its re-dissolution must form stable and soluble ammonium-bioxalate complexes.

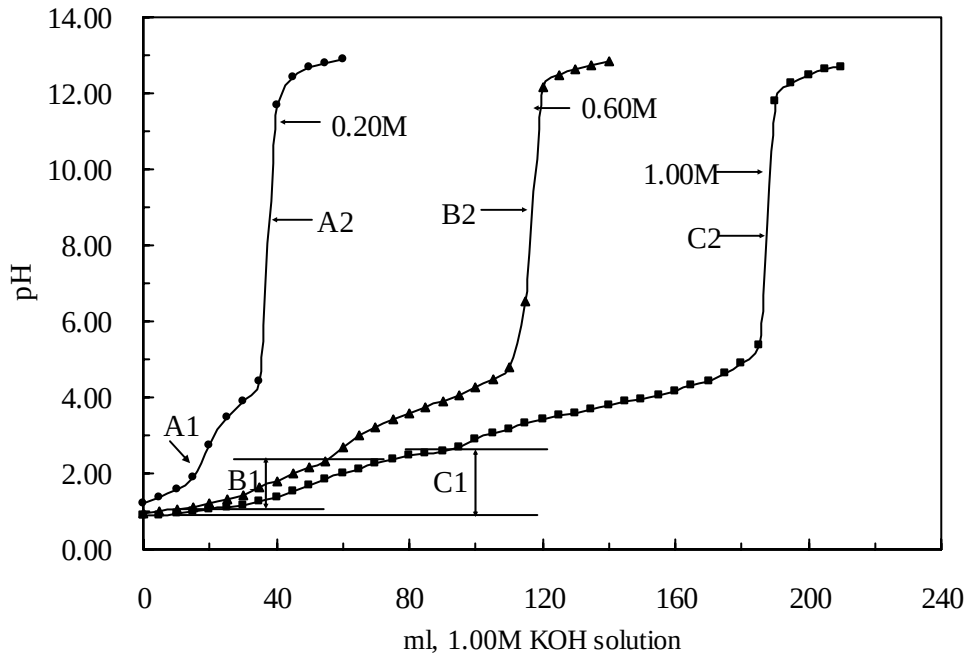

Figure 3.2 The titration curve for titrating oxalic acid (0.2, 0.6 and 1.0 M $H_2C_2O_4 \cdot H_2O$) with 1.0M KOH solution at 27^{o}C.

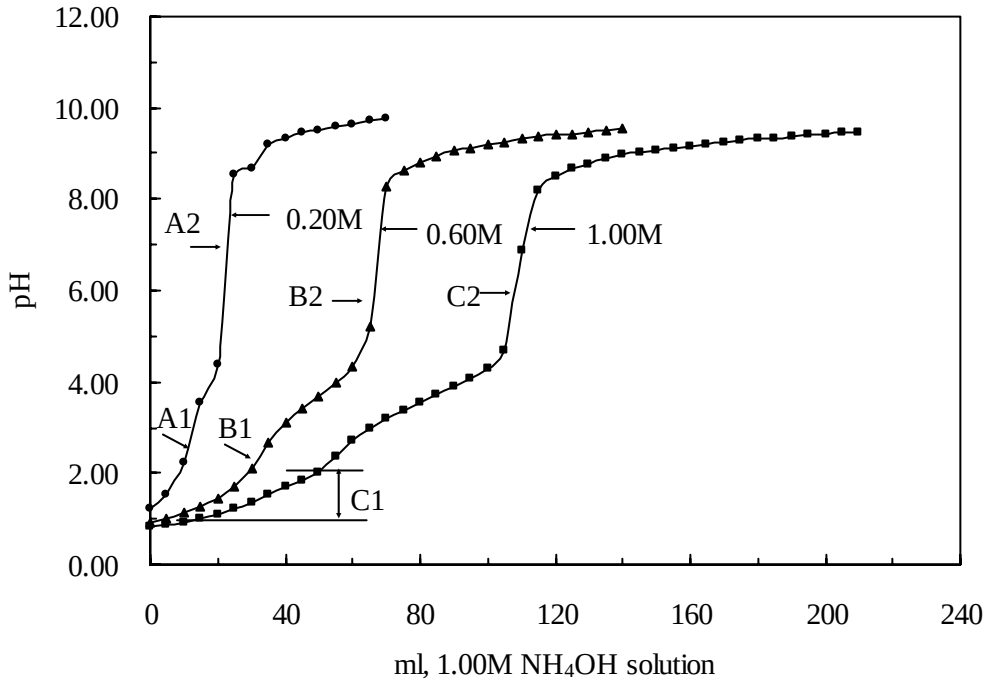

Figure 3.3 The titration curve for titrating oxalic acid (0.2, 0.6 and 1.0 M $H_2C_2O_4 \cdot H_2O$) with 1.0M NH_4OH solution at 27^oC.

3.3.4.2 Effect of temperature

Figures 3.4 to 3.6 show the effect of reaction temperature on the titration of 100mL of 1.0 M oxalic acid solution with the addition of 1.0M NaOH and 1.0M NH_4OH, respectively. To study the effect of temperature in a solution, tests were conducted at 27, 50 and 80^oC with slow addition of a titrant.

Figure 3.4 shows the effect of reaction temperature on the addition of NaOH titrant. The increase of reaction temperature increased the dissociation of oxalic acid in a solution and the dissolution of precipitated crystal, which was sodium oxalate, due to the high activities of the ionized species of H^+, $HC_2O_4^-$ and $C_2O_4^{2-}$. The precipitation zone at 50^oC was smaller than that at 27^oC, which occurred at pH 2.15. The precipitate formed at 50^oC easily re-dissolved at pH 3.40. However, at 80^oC, oxalate crystals from the titration were not formed under the same conditions within the whole range of pH studied.

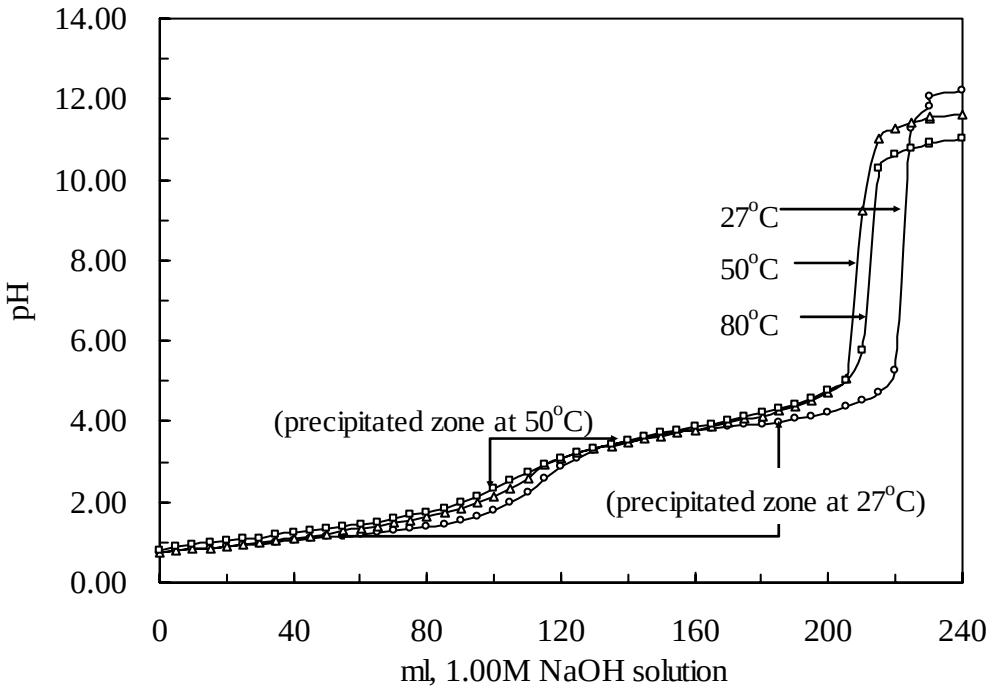

Figure 3.4 The effect of temperature on the addition of NaOH titrant (1.0 M)

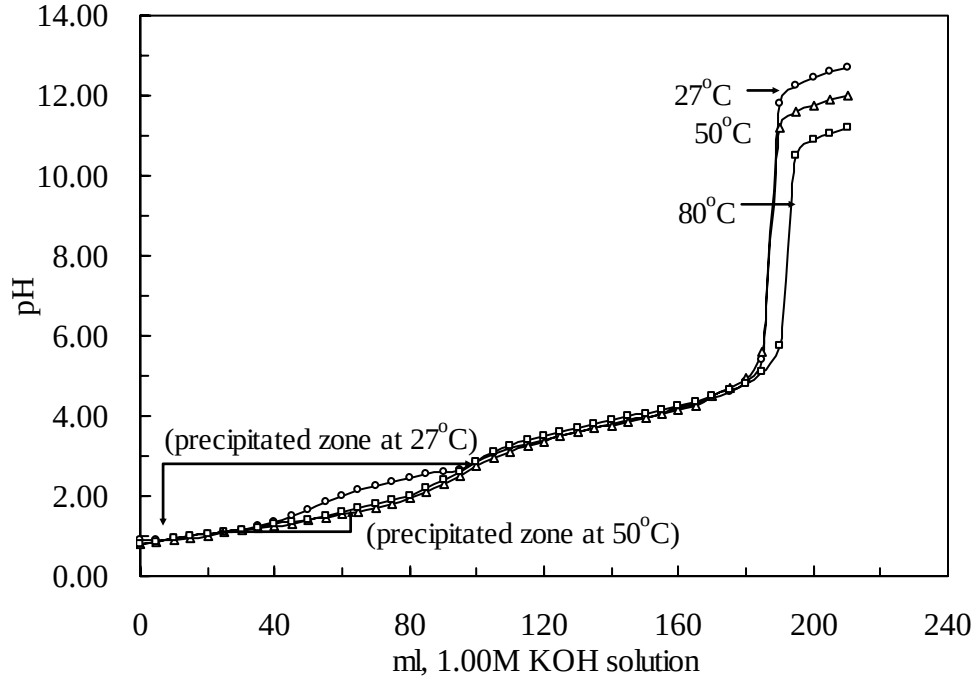

Figure 3.5 The effect of temperature on the addition of KOH titrant (1.0 M $H_2C_2O_4 \cdot H_2O$ and 1.0M KOH).

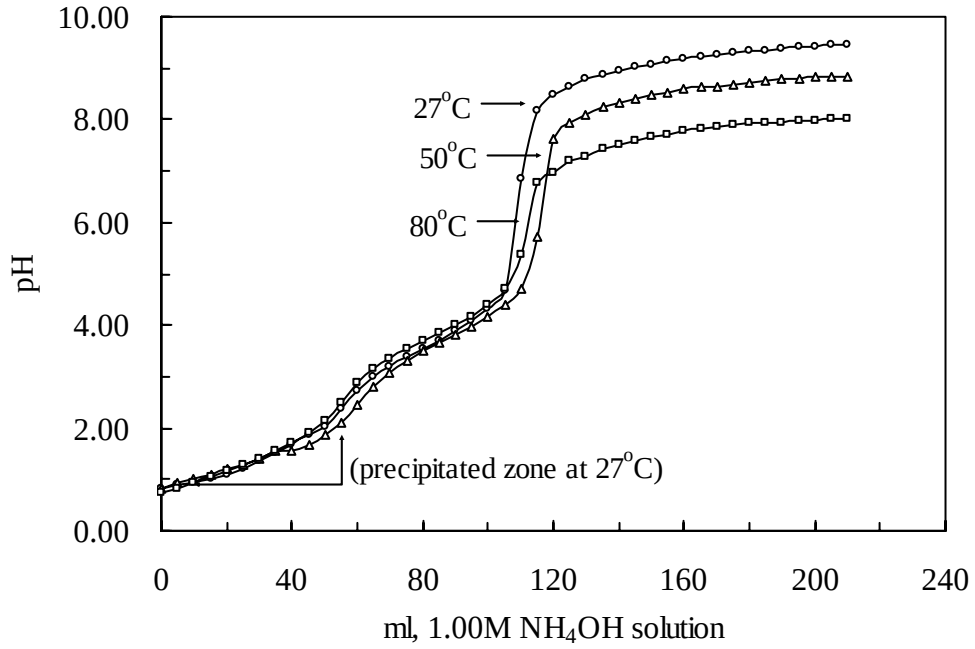

Figure 3.6 The effect of temperature on the addition of NH_4OH titrant (1.0 M $H_2C_2O_4 \cdot H_2O$ and 1.0M NH_4OH).

The addition of NH_4OH titrant (Figure 3-6) showed a similar trend for titration, however, it did not show the formation of oxalate crystals at both 50 and 80°C. These results indicate that the increase of temperature causes an increase in the solubility of the ammonium-oxalate solid compounds, increasing the formation of ionized species in solution. The NH_4OH as a pH control reagent is better than the NaOH which enhances the formation of soluble oxalate species in solution.

3.3.4.3 Properties of precipitated oxalate complexes

Figure 3.7 shows the soluble species of oxalate remaining from 1M oxalic acid solution after the addition of 1.0M of NaOH or NH_4OH. The concentration of soluble oxalate ions at low pH in solution was sharply decreased with the addition of both NaOH and NH_4OH, due to precipitation of oxalate compounds as indicated earlier.

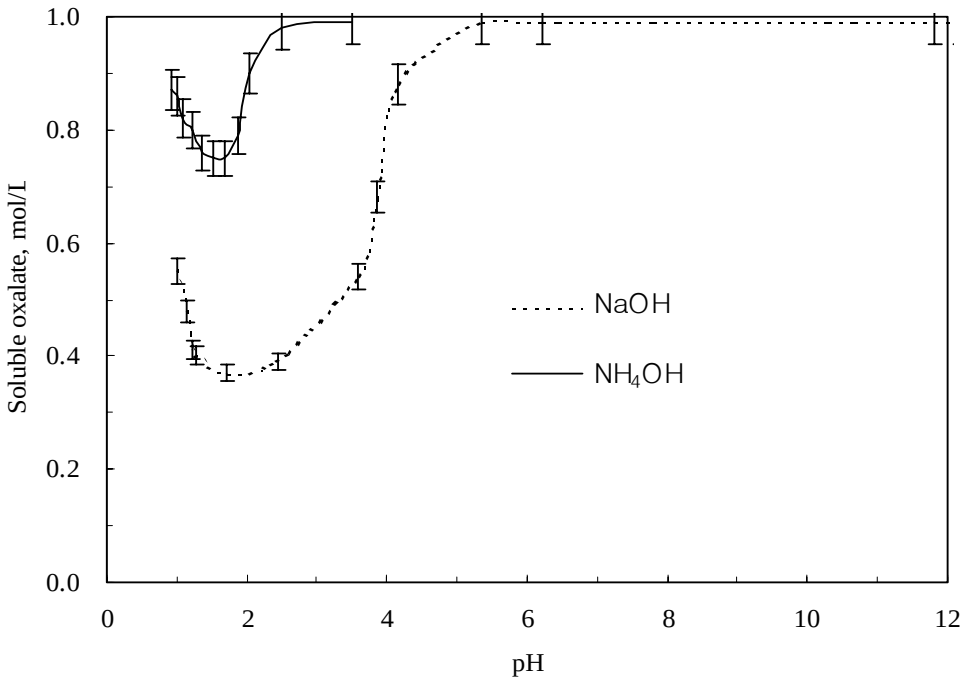

Figure 3.7 The speciation of soluble oxalate ion in 1.0 M $H_2C_2O_4 \cdot H_2O$ with various titrants at 27^oC (1.0M NaOH and 1.0M NH_4OH solution).

However, the increasing of the dissolution of precipitated oxalate compounds occurs at pH higher than 2.03 for NH_4OH and at pH higher than 3.00 for NaOH. As equations (3-12) to (3-16) predict, experiments show that the ammonium oxalate solid had higher solubility than the sodium oxalate complex.

3.4 CONCLUSIONS

An analysis on the thermodynamic properties of sodium, ammonium and iron oxalate complexes was conducted and the standard free energies ΔG^o were calculated from published thermodynamic data and solubility products.

In titration tests, the increasing temperature increased the solubility of various Na-, K- or NH_4-oxalate solids, resulting in an increase in the formation and stability of ionized species in solution. At low temperature, high concentrations of oxalic acid are not favourable for the dissolution of iron oxides as they promote the formation of

precipitates with NaOH, KOH or NH_4OH within the range pH2-4, which was the optimum range for the dissolution. The NH_4OH titrant is a better reagent that can be used to control the pH of the leaching solutions than NaOH and KOH. This is due to the formation of stable ammonium-oxalate ionized species in solution.

The concentrations of $C_2O_4^{2-}$ ions in solution were sharply decreased with the addition of both NaOH and NH_4OH, due to the formation of oxalate complexes. However, the precipitate starts redissolving at pH>2.03 for NH_4OH and at pH>3.00 for NaOH systems, respectively, especially at high temperatures (>50^oC).

CHAPTER FOUR

DISSOLUTION OF IRON OXIDE RUST MATERIALS

4.1 INTRODUCTION

The dissolution of metal oxides is of practical importance as it can be used to clean iron oxide on the iron metal surface and remove the iron from mineral concentrates (Kim et al. (1997); Lee et al. (1997); Tsimas (1995)). Oxalic acid is a reagent commonly used in dissolving iron oxide from a wide range of host minerals such as clay or silicate and has been studied extensively.

The basic concept of dissolving iron oxide by oxalic acid was put forward by Engell (1956), Valverde and Wagner (1976) and later was reviewed by Diggle (1973). Blesa and co-workers (1987) studied the mechanism of oxalic acid dissolution of magnetite at 30^{o}C and found that the reaction is controlled by an electrochemical transfer between the Fe(II)-and Fe(III) oxalate complexes.

The optimum pH was found to be around 2.5, above which the dissolution will decrease in rate. The dissolution of magnetite and hematite by other carboxylic acid was also studied in great details by many other investigators (Afonso et al., 1990, Sellars and Williams, 1984, Blesa et al., 1994 and Panias et al., 1996).

The dissolution of iron oxide by oxalic acid involves complexation of the dissolved iron (either Fe(II) or Fe(III)) by oxalate and a redox process. In this case, oxalate acts as a complexant and a reductant in the dissolution process. Both hydrogen ions and oxalate appear to be involved in the dissolution process, whereas the addition of Fe(II) seems to accelerate the initial induction of the reaction. This indicates that the slow induction step is affected by the complexation of oxalate with the Fe(II) species. In the latest work, Panias et al. (1996) concluded that the dissolution consists of three distinctive steps: (a) adsorption of organic acid on the iron oxide surface, (b) non-reductive dissolution and

(c) reductive dissolution. The reductive dissolution takes place in two stages of induction and autocatalytic reaction.

The interaction of UV light in photochemical reaction between goethite and oxalic acid was also studied by Cornell and Schindler (1987). It was found that UV irradiation seems to promote the release of Fe(III) oxalate from the reaction surface.

Past investigations, however, did not deal with natural materials found in ores or in iron oxide rust materials. This work is different from others since it aimed to evaluate the efficiency of oxalic acid in dissolving iron oxide selected from iron ores and from iron oxides rust materials.

The aim of this study is to investigate the dissolution characteristics of natural iron oxides (hematite, magnetite and iron rusts materials) which are common iron–bearing phases in industrial minerals for the optimization of reaction parameters, such as oxalic acid concentration, temperature, and pH of solution.

4.2. EXPERIMENTAL

4.2.1 Materials and reagents

The sample, used in this experiment, was hematite (Fe_2O_3, obtained from a mine in the U.S.A). An adequate amount of rust was also collected from waterworks zinc plated tubes selected and ground by a tungsten carbide Jaw crusher (Leatch Co. Ltd). The samples were wet-separated by -100/+140mesh (105～149㎛) sieves, and dried at 100℃ for 24 hours to be used in dissolution experiments.

Chemical analysis of hematite sample, using XRFS and AAS, confirmed the composition of 98.2% Fe_2O_3, <1% of SiO_2 and Al_2O_3. Magnetite (Fe_3O_4, 99.33%), used in comparative dissolution, was prepared under the same conditions. BET tests (N_2-sorption technique) revealed that the specific surface areas of samples were 5.35㎡/g and 6.01㎡/g, respectively. Oxalic acid ($H_2C_2O_4{\cdot}2H_2O$) 99% was used, and the pH was controlled by the use of aqueous ammonia (NH_4OH). The iron rust materials contained 90.3% Fe_2O_3. XRD analysis of this material confirmed major phases of iron as goethite (α-FeOOH) and lepidochrosite (γ-FeOOH) and iron hydroxide ($Fe(OH)_3$). Iron rust and

pure hematite samples were added at 3 g/L.

4.2.2 Experimental methods

The dissolution tests were carried out in the 1 liter -3 necked flask immersed in a water bath, and the dissolution characteristics were investigated as functions of the dissolution reaction time, pH, concentration of oxalic acid and velocity of agitation.

The temperature of the bath was controlled to within 0.5℃. The dissolution characteristics were investigated, while fixing the amount of samples to 3g/L and changing the concentration of oxalic acid from 0.048M to 0.476M, dissolution reaction temperature from 25 to 100℃, and initial pH from about 1.0 to 4.5. The agitation speed was fixed at 450 rpm throughout the series of experiments.

The dissolution was studied by following the percentage of the dissolution with reaction time during the experiments. 2mL of dissolved solution were withdrawn to analyze Fe by the atomic absorption spectrophotometry at the predetermined time intervals. The surface of particles dissolved as a function of initial pH was examined by scanning electron microscope.

4.3. RESULTS AND DISCUSSION

Table 4.1 presents the chemical composition of the ion rust samples, showing that the iron content reaches 90.3% while other major elements such as Zn, Al, Na, Mg, etc. are less than 2% each.

Table 4.1 Chemical composition of the iron oxide rust samples

Element	Fe	Zn	Al	Na	Mg	Ca
Assay (wt.%)	90.3	0.43	0.85	1.74	0.17	1.83

The iron rust sample when analysed by XRD, showed the presence of three iron oxide phases, namely goethite (α-FeOOH), lepidocrocite (γ-FeOOH) and iron trihydroxide ($Fe(OH)_3$) as presented in Fig. 4.1.

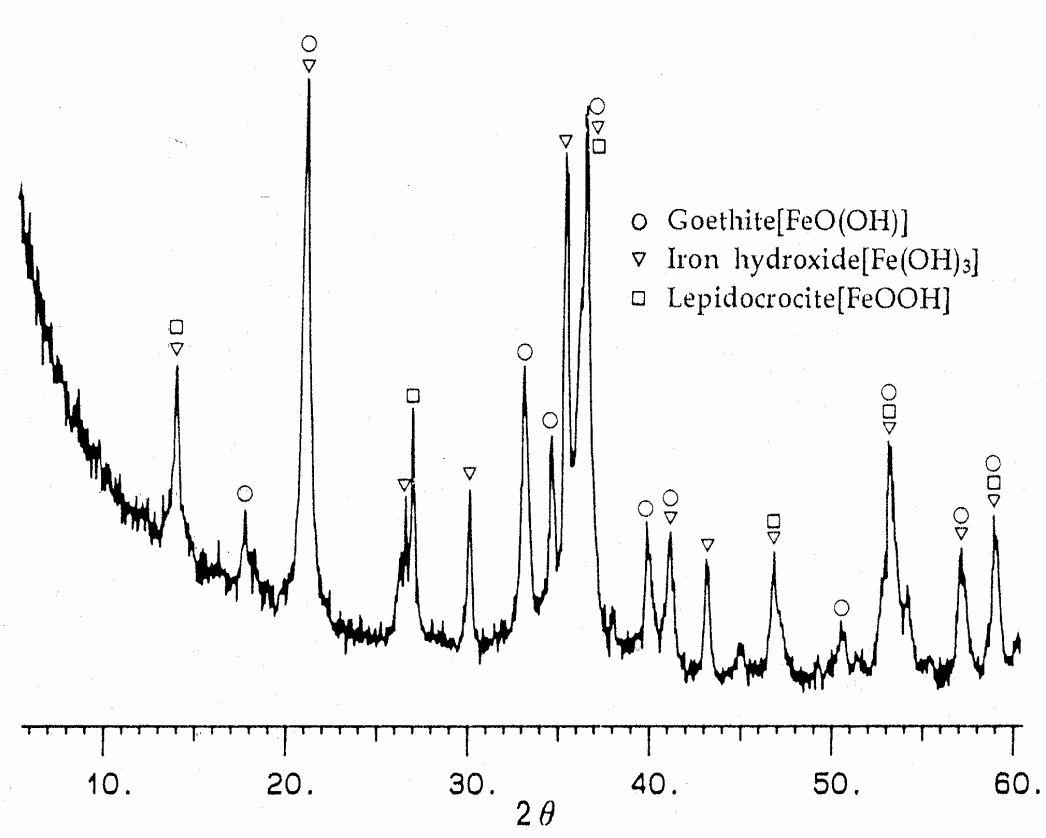

Figure 4.1: XRD pattern of the iron rust sample showing peaks belonging to different iron oxide phases.

The dissolution rate of rust materials was compared with the dissolution of hematite under different conditions and the results are discussed in the following sections.

4.3.1 Effect of oxalic acid concentration

The dissolution of iron oxide, either as hematite or iron rust materials increased with an increase of oxalic acid concentration. Figures 4.2 (a) & (b) show the dissolution characteristics of both materials over a range of acid concentration from 0.048M to 0.476M.

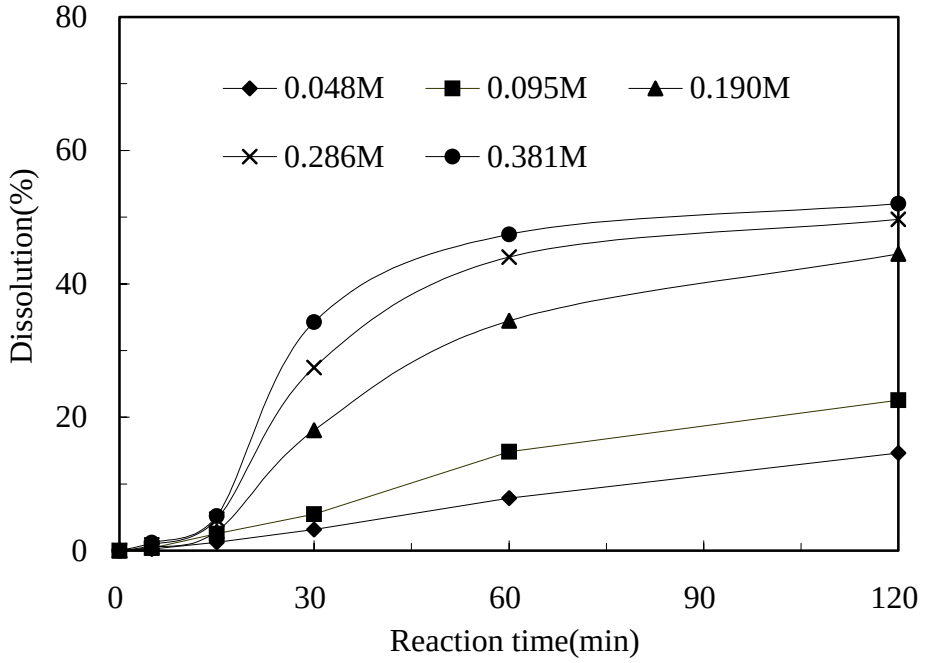

(a)

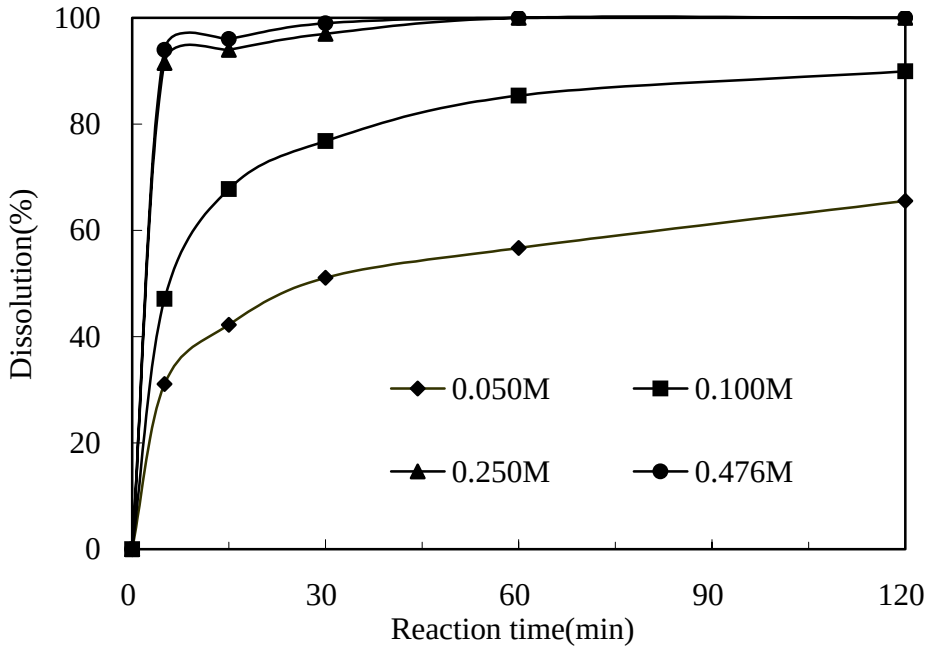

(b)

Figure 4.2 Effect of oxalic acid concentration on the dissolution of (a) hematite and (b) iron oxide rust (Temperature: 100℃, initial pH: 2.5, impeller speed: 450 rpm and particle size: 105～149㎛)

At 100^{o}C and a concentration of 0.095M or less, the dissolution rate of hematite is low, compared to higher concentrations. However these conditions this did not significantly affect the dissolution of iron oxide rust materials as 84% of dissolution still took place within 60mins (Figure 4.2(a)). The dissolution rate is higher with iron oxide rust and complete reaction also took place within 60 minutes for 0.250M oxalic acid or higher (Figure 4.3(b)).

There is a significant difference in both types of dissolution in that there is an absence of the induction period for iron rust dissolution. Gibbs free energy changes of the chemical dissolution reactions on the oxalic acid leaching of iron oxides are calculated by Hess law (Cornell and Schwertmann, Panias et al., 1996) with thermodynamic data shown in equation (4-1) to (4-3).

$$Fe_2O_3 + 6HC_2O_4^- \leftrightarrow 2Fe(C_2O_4)_3^{3-} + 3H_2O \qquad \Delta G^o_{298} = -26.67 \text{ kJ/mol} \quad (4\text{-}1)$$

$$\alpha\text{-FeOOH} + 3HC_2O_4^- \leftrightarrow 2Fe(C_2O_4)_3^{3-} + 2H_2O \quad \Delta G^o_{298} = -43.54 \text{ kJ/mol} \quad (4\text{-}2)$$

$$\gamma\text{-FeOOH} + 3HC_2O_4^- \leftrightarrow 2Fe(C_2O_4)_3^{3-} + 2H_2O \quad \Delta G^o_{298} = -54.54 \text{ kJ/mol} \quad (4\text{-}3)$$

The free energy changes imply that the chemical dissolution (non-reductive) reaction involving iron oxide rust (α-FeOOH or γ-FeOOH) is naturally more spontaneous compared to hematite (eq. 4-1), which means that iron oxides with loose crystallinity such as α- and/or γ-FeOOH may be much more easily chemically-dissolved than hematite. The loose structure of iron rust is also comfirmed later in the morphology study section.

In this study, non-hematite iron oxides in the iron rust materials were found to dissolve faster than hematite, confirming previous studies by other workers. The dissolution of hematite seemed to be either affected by a passivation mechanism due to the formation of ferrous oxalate on the oxide surface or be governed by its precipitation from the bulk solution, confirming Khentov and Sukhotin's study in 1979. Fig. 2.17 (Chapter 2) shows the possible formation of the solid ferrous oxalate for iron - 0.21M oxalic acid system. After 30 minute of leaching in this study, the dissolution of iron reached a plateau corresponding to <50% iron dissolution, especially at a high oxalate concentration (>0.286M).

The results found in this study are also in accordance with other studies on the dissolution of different forms of iron oxides. By studying the electrochemical dissolution of hematite (α-Fe_2O_3), maghemite (γ-Fe_2O_3), goethite (α-FeOOH) and lepidochrocite (γ-FeOOH) in hydrochloric and oxalic acid using voltammetry, Cepria and his co-workers [2003] found that the hydroxy-oxides of FeOOH could be dissolved also via soluble Fe(III) species (formed from chemical dissolution first) at 0.6-0.8V (vs Ag-AgCl), whereas hematite and maghemite dissolved only via direct reduction of the solid at -0.55V to -0.60V (vs Ag-AgCl). This fundamental study confirms the electrochemical nature of hematite reductive dissolution. It further explains why hydroxyl-oxides such as goethite or lepidochrocite can dissolve in oxalic acid via reduction and complexation [Stumm and Furrer, 1987] whereas hematite dissolves mainly via solid reduction [Banwart et al, 1989].

The predominant chemical (non-reductive) dissolution of non-hematite iron oxides further explains why the iron rust material could be almost completely dissolved in this study. Since minimum Fe(II) species was formed from the reductive dissolution step, less chance of solid ferrous oxalate was formed during the dissolution of iron rust materials compared with hematite where the reduction of its solid surface is the predominant reaction.

4.3.2 Effect of pH

The effect of pH on the dissolution of hematite was studied at 100℃ with 0.190M oxalic acid concentration and iron oxide rust materials at 95℃ with 0.250M oxalic acid concentration, and with pH values varying between 1 and 4.5. The results are shown in Figures 4.3 (a) & (b). With the temperature fixed, the acidity at varied pH is very important in determining the rate of dissolution, as it has influence on the solution complexation equilibria and the rate of reaction (Blesa et al., 1994). That is to say, when oxalic acid dissociates, $H_2C_2O_4$ and $HC_2O_4^-$ are at the same fraction of 50% at pH around 1.0, whereas $HC_2O_4^-$ reaches the maximum of 90% at pH 2.3, $HC_2O_4^-$ and $C_2O_4^{2-}$ show the same fraction pH 3.5, whereas $C_2O_4^{2-}$ exists as major ion in a higher pH solution (Oh et al., 1998; Panias et al., 1996).

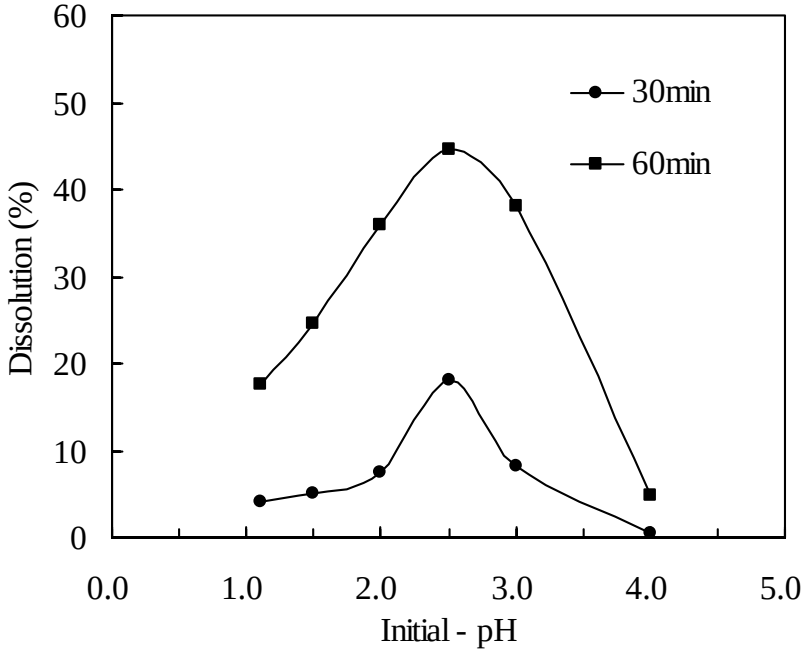

(a)

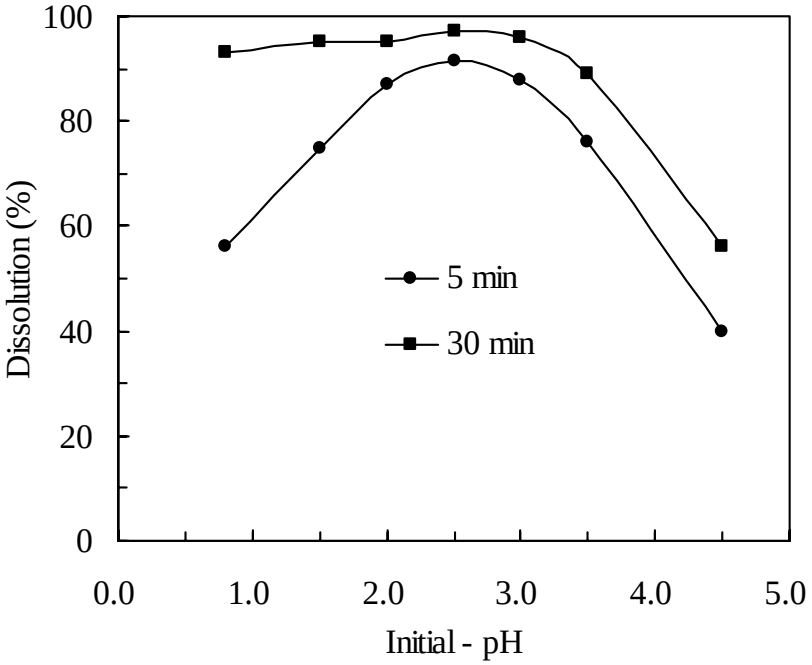

(b)

Figure 4.3 The effect of initial pH on dissolution of (a) hematite at 100℃ with 0.190M oxalic acid concentration and (b) iron oxide rust at 95℃ with 0.250M oxalic acid concentration (Impeller speed: 450 rpm and particle size: 105～149㎛).

As inferred from the result, the initial dissolution rate was significantly affected by the pH for both iron oxide rust materials and hematite. The dissolution rate is highest at pH 2.3, while in more and less acidic solutions, it was decreased as shown by the bell-shaped curves especially at the early stage of dissolution. The solution chemistry of oxalic acid shows that the concentration of $HC_2O_4^-$ is maximized at pH 2.5 (Blesa et al., 1994; Panias et al., 1996; and Oh et al., 1998). At this maximum, $HC_2O_4^-$ produces both H^+ and $C_2O_4^{2-}$ required for both dissolution of iron oxide and complexation of the Fe^{3+} released. The reaction steps could be divided into equation (4-4) to (4-6).

$$HC_2O_4^- \leftrightarrow H^+ + C_2O_4^{2-} \quad (4\text{-}4)$$

$$Fe_2O_3 \text{ (or FeOOH)} + 6H^+ \leftrightarrow 2Fe^{3+} + H_2O \quad (4\text{-}5)$$

$$Fe^{3+} + 3C_2O_4^{2-} \leftrightarrow Fe(C_2O_4)_3^{3-} \quad (4\text{-}6)$$

These sequential reactions mean that the hydrogen ion and oxalate ion are necessary in order to dissolve the iron oxides. It can be easily concluded that hydrogen oxalate ion ($HC_2O_4^-$) plays an important role for the dissolution of iron oxides and there exist an optimum pH which the concentration of $HC_2O_4^-$ is maximised. At pH over than 2.5 there is not enough $C_2O_4^{2-}$ for complexation whereas at higher pH there is a depletion of H^+ ions.

4.3.3 Effect of temperature

To study the effect of temperature on hematite and iron oxide rust materials dissolution, tests were conducted at 25-100℃ under the condition of a constant pH of 2.5, oxalic acid concentration of 0.190 M and 0.250M, respectively.

Figures 4.4 (a) shows the effect of temperature on hematite reaction with oxalic acid. Dissolution rate is seen to be dependent on temperature. For hematite at 90℃, the dissolution is slow reaching 14% at 120 minutes, while at 100℃ it is fast and reaches up to 46% at the same reaction time. The result can be explained as follows. The reaction is controlled by non-reductive dissolution which removes only the more reactive sites of the oxide surface at high temperature by hydrogen ion in solution (Blesa et al., 1994). But, at lower temperatures below 90℃, the reaction did not proceed at a reasonable dissolution rate at all for hematite.

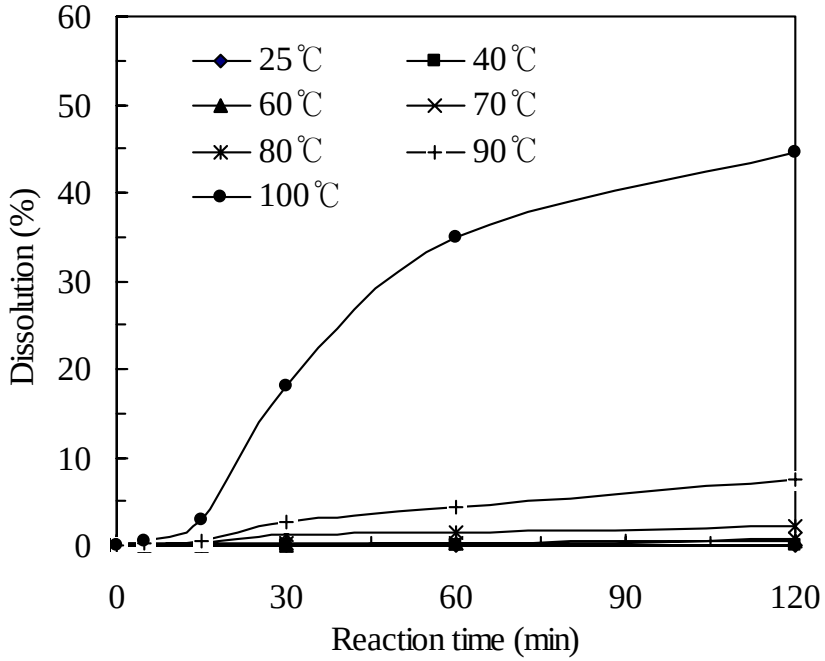

(a)

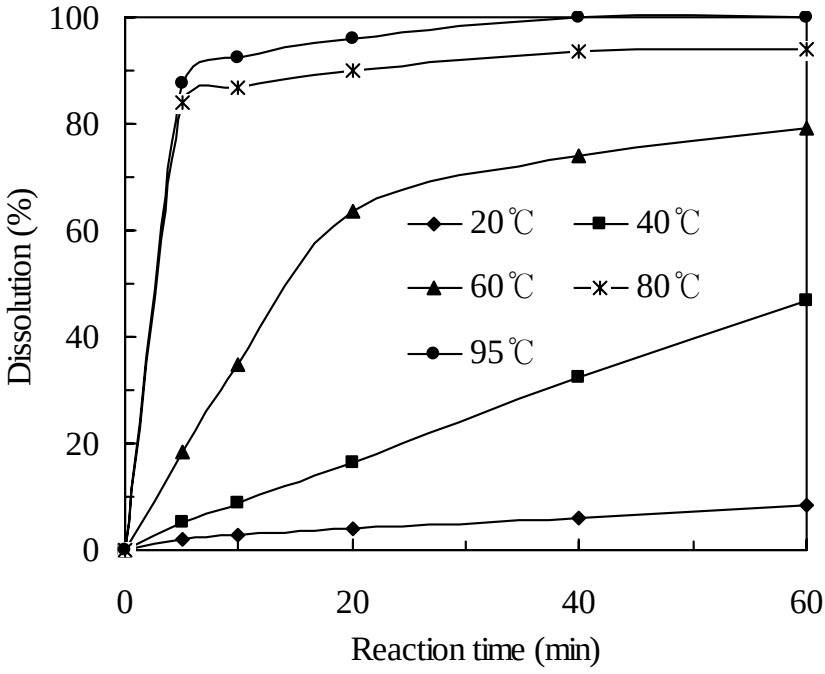

(b)

Figure 4.4 The effect of temperature on the dissolution of (a) hematite at 0.190M oxalic acid concentration and (b) iron oxide rust at 0.250M oxalic acid concentration (Initial pH: 2.5, impeller speed: 450 rpm and particle size: +105-149㎛).

On the other hand, Figure 4.4 (b) shows that there is no delayed effect of the induction period in this series for iron rust material due to the different crystallinity existing with the iron rust material of another dissolution process is more predominant in this case. It is also noticed that the induction period is only obvious at 100^{o}C, indicating that only at a high temperature a shift from one reaction step to another predominant one is observed. For a lower dissolution (<10%) the shift (the induction period) is not clearly seen.

4.3.4 Morphology Study

Figure 4.5 shows the surface of dissolved particles by scanning electron microscope under of (a & b) hematite at 100℃ with 0.190M oxalic acid concentration and (c & d) iron rust at 95℃ with 0.250M oxalic acid concentration.

The nature of the surface changes during dissolution. Hematite particle shows (a) the regular pits forming at initial reaction and (b) the pits are enlarged as a result of attack at grain boundaries as the reaction proceeds. However, the iron rust particle shows somewhat different dissolving types as forming (c) regular pits or (d) showing the rod-like types and plate structure by the dissolution of grain boundary (Lee et al., 1998). Smaller grains and more disintegrated particles were observed early (15 mins for (d)) for iron rust compared to larger clumps still observed for hematite after 120 minutes (Micrographs b).

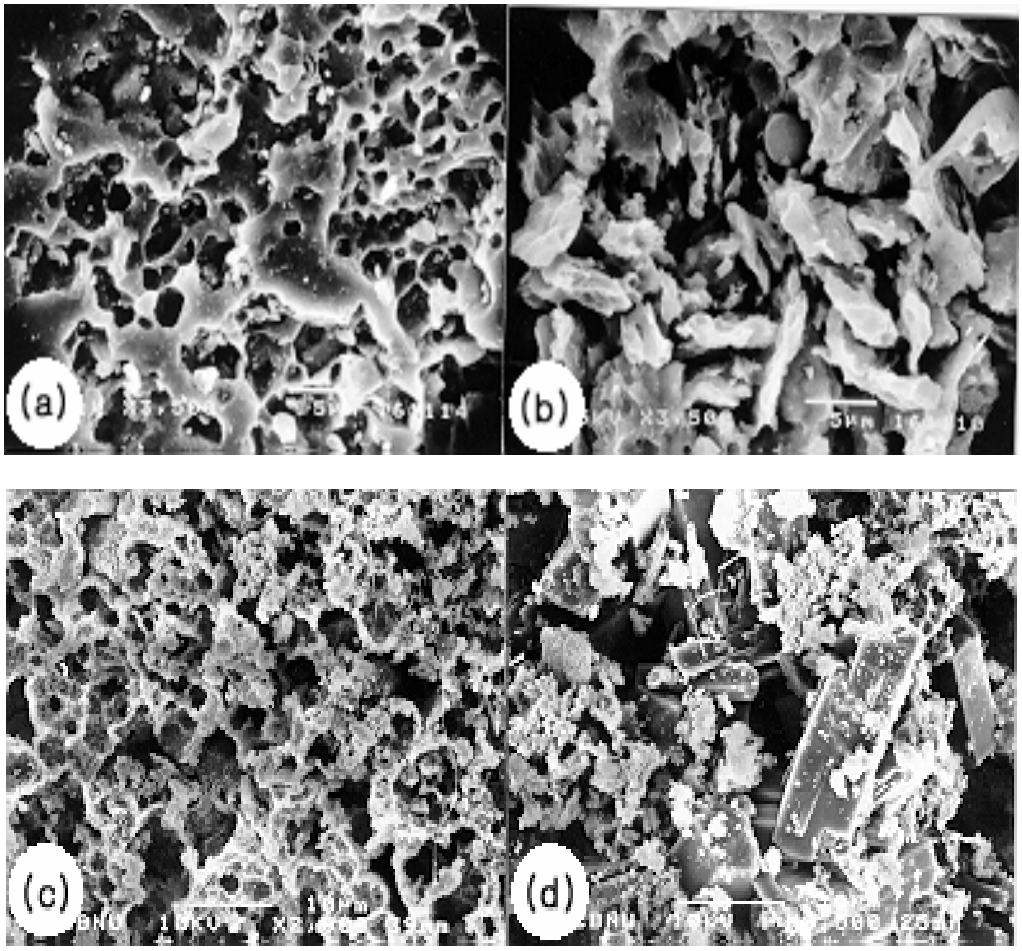

Figure 4.5 Scanning electron micrographs of the dissolved (a & b) hematite at 100℃ with 0.190M oxalic acid concentration and (c & d) iron oxide rust at 95℃ with 0.250M oxalic acid concentration (Impeller speed: 450 rpm, particle size: 105～149㎛ and intial pH: 2.5). (a) reacted for 5mins (b) 120mins (c) 5mins (d) 15mins

4.3.5 Comparison of the dissolution reaction of hematite and magnetite

Figure 4.6 shows the dissolution rate of hematite and magnetite with 0.1M oxalic acid concentration (pH = 1.66) at 95℃. The dissolution of both hematite and magnetite increases linearly within 180 minute reaction, but the dissolution rate of magnetite was twice higher than that of hematite under the same experimental condition.

As noted in Chapter 2, the general scheme for the dissolution of iron oxides by carboxylic acids includes two types of direct leaching: non-reductive dissolution (equation 4-7) and reductive dissolution (equation 4-8). At a certain point, reductive dissolution by the Fe(III)-L eventually becomes dominant. Therefore, it is this

mechanism which explains the steps involved. When iron dissolves in oxalic acid solution, a free oxalate complex adsorbs on iron surface and detachment of iron from the iron ore surface through a redox reaction (Blesa et al., 1994).

$$\equiv Fe(III) - L \xrightarrow{H^+} Fe(III) - L_{(aq)} \quad (4\text{-}7)$$

$$\equiv Fe(III) - L \xrightarrow{H^+} Fe^{2+}{}_{(aq)} + \text{oxidation products of ligand} \quad (4\text{-}8)$$

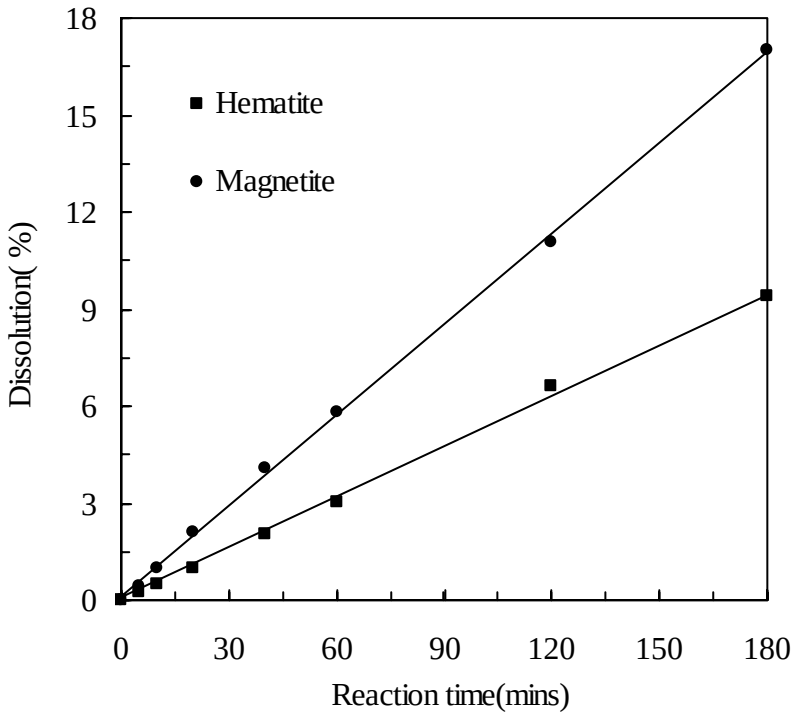

Figure 4.6 The dissolution of hematite and magnetite with 0.10M oxalic acid concentration (Temperature: 95℃, initial pH: 1.66, impeller speed: 450 rpm, particle size, -16/+20mesh)

As shown in Figure 4.6, the fast dissolution of magnetite by oxalic acid could be auto-acceleratory by Fe^{2+} in magnetite, however the reduction of Fe^{3+} to Fe^{2+} in oxalic acid solution was the rate-determining step. A similar behavior was observed in the dissolution of magnetite and hematite by malonic acid and by EDTA, iminodiacetic, and N(2-hydroxyethyl) iminodiacetic acids at 100^{o}C (Blesa et al., 1994). When Fe(II)

ions existed in a reaction system, the reaction rate was accelerated owing to high electron activity on the surface of iron oxide by the activity of ferrous oxalate complexes. The species involved in the auto-acceleration of the dissolution reaction is Fe(II) ion which is transferred from the solid to the solution. In the absence of Fe(II) ions, the generation of Fe(II) ions in solution can be described by equations 4-7 and 4-8. When sufficient ferrous oxalate was formed in this dissolution system, the secondary reductive dissolution step became dominant and the whole process was by equation (4-9)

$$Fe_3O_4 + 8HC_2O_4^- \rightarrow 2Fe(C_2O_4)_3^{3-} + Fe(C_2O_4)_2^{2-} + 4H_2O \qquad (4\text{-}9)$$

For all that, though the leaching rate of magnetite was not as high as hematite with inorganic acid solution, it was quickly reacted in an organic acid (Blesa et al. 1994). They explained that the dissolution of hematite was dominated by a reduction reaction (Equation 4-10) at high temperature, The overall reaction therefore is dependant on the redox potentials of half-cell reactions involving Fe-oxalate complexes. Thus, magnetite which has a Fe(II,III)-O structure can be quickly dissolved, comparing with hematite (Fe(III)-O structure) in an oxalic acid solution as shown in Figure 4-6.

$$Fe_2O_{3(s)} \xrightarrow{\text{reductant},H^+} Fe^{2+}{}_{(aq)} \qquad (4\text{-}10)$$

Figure 4.7 shows the scanning electron micrograph of hematite and magnetite particles. In a hematite sample reacted for 180 minutes, partially leached materials showed a shape of regular pits with clear grain boundary, while the magnetite showed a cubic structure, forming stepped or rectangular structure. When magnetite containing Fe^{2+} and hematite only composed of Fe^{3+} were reacted in the same condition, the different crystal structure resulted in different microstructure. The analysis of surface area on the above samples showed that the surface area of the raw hematite was 5.35m^2/g, and 13.20m^2/g after reaction, while that of raw magnetite was 6.0 m^2/g, and 10.68 m^2/g after reaction. This showed that surface area of a sample did not affect the reaction rate of hematite and magnetite.

On the other hand, as shown in Figure 4.4, the dissolution rate was strongly dependent on reaction temperature. At 25^{o}C, the dissolution rate was only 1% and at 90^{o}C it was

below 10% after 120 minutes, while at 100^{o}C it reached up to 46% at the same reaction time. The result can be explained by that fact that the initial reaction was controlled by non-reductive dissolution at high temperature, which removed more reactive sites of the oxide surface by the hydrogen ion in solution (Blesa et al., 1994). It showed that the dissociation of oxalic acid depended strongly on the reaction temperature and its increase enhanced the activity of oxalate species in oxalic acid solution. This is due to the fact that oxalic acid was not completely dissociated at low temperature and in the acidic pH range of weak acid.

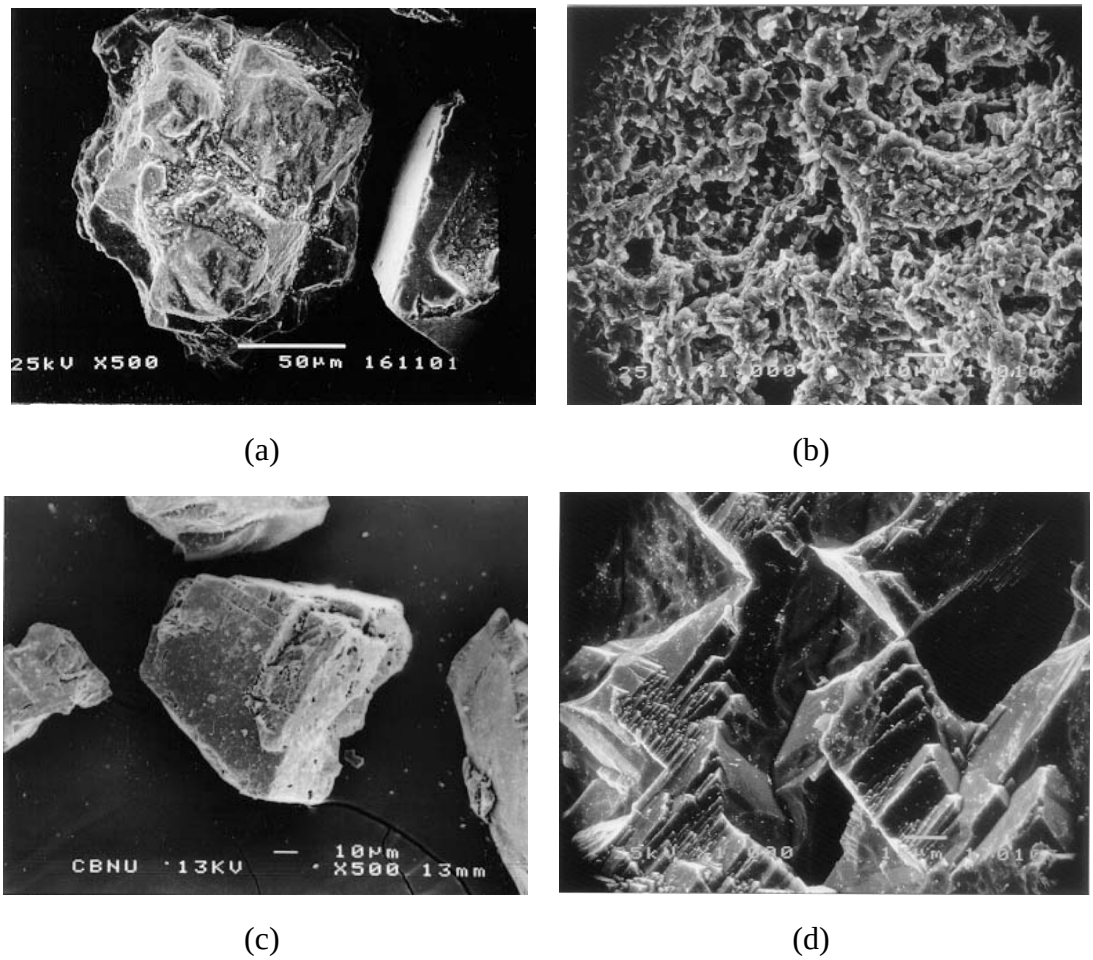

(a) (b)

(c) (d)

Figure 4.7 Scanning electron micrographs of hematite and magnetite particles. (Temperature: 95^{o}C: reaction time: 180mins, initial pH: 1.66; 0.10M oxalic acid, 450 rpm, particle size: -16/+20mesh) (a) Raw hematite (b) Reacted hematite (c) Raw magnetite (d) Reacted magnetite

As discussed in Chapter 2, the dissolution rate at low temperature was dominated by the formation of surface speciation on surface of hematite for reaction, while at high temperature, it was affected by a reduction process.

4.4. CONCLUSIONS

The study has confirmed that oxalic acid can be used to dissolve various iron oxide phases. One of the direct applications is that the technique can be used to remove iron oxide rust from the metal surfaces as one method for cleaning.

The dissolution of iron oxide rust (which contains goethite, iron trihydroxide and lepidocrocite) is faster compared to that observed for hematite without a slow induction period at the beginning of the dissolution process. The dissolution process is affected by the pH of the initial solution, oxalic acid concentration and temperature. In particular, the temperature and initial pH of solution controlled the dissolution rate of hematite rather than that of iron oxide rust. The nature of the particle surface changes during dissolution and the hematite particle shows regular pits forming, but the iron oxide rust particles shows different type of dissolution.

The dissolution rate of magnetite turned out to be twice that of hematite under the same experimental conditions.

CHAPTER FIVE

REMOVAL OF IRON FROM CLAY MINERALS

5.1 INTRODUCTION

The dissolution of ferric oxides has been considered important in several fields such as the removal of oxide deposits from metal surface, the extraction of metals from ores, and the beneficiation of industrial minerals such as kaolin, pottery stone and clays. In fact, most clays like kaolin are usually contaminated with ferric and ferrous iron which are detrimental impurities that greatly decrease the whiteness of the products sintered at high temperatures (Sumner, 1963; Park et al., 1974). The contamination of ferrous iron is considered particularly serious in the ceramic industry because it is oxidized to ferric iron in the burning phase and the ferric iron imparts an orange color to products in that condition (Marabini et al., 1993). The iron content of industrial minerals can be reduced by physical, physicochemical and chemical processing. Chemical processing is favourably considered for achieving a high degree of iron removal at minimum operation cost.

Thus, the chemical processing is often applied to get a highly refined product (Shin et al., 1990). Both inorganic acids (sulphur dioxide and sodium dithionite, hydrochloric acid) and organic acids (oxalic acid, citric acid) have been used for clay refining. However, due to the environmental pollution and to contamination of products with the SO_4^{2-} and Cl^-, inorganic acids should be avoided as much as possible. Organic acids have, therefore, been tried and being employed. Some researchers reported that oxalic acid is more preferable in dissolution of iron contaminants (Shin et al., 1990; Marabini et al., 1993; Tsimas et al., 1995; Baumgartner, 1983; Blesa and Maroto, 1986; Borghi et al., 1989; Segal and Sellers, 1984), as it has higher leachability for different types of iron oxides.

The objective of this study is to clarify the characteristics of leaching of iron oxide from clay mineral with oxalic acid. It was conducted as part of the development of alternative technological methods for removing iron using an organic-acid leaching system which may be more effective and environmentally acceptable in Jang-San Mine, Korea.

5.2 EXPERIMENTAL

5.2.1 Materials and reagents

The sample used for the present experiment was clay mineral from Jang-San mine which have been used as raw materials by Haengnam China Ware Co. Ltd. in Korea. Samples were crushed by a Jaw-crusher and divided into two types; coarse parts (-16/+100mesh; J-A) and fines (-100mesh; J-B) for the leaching tests. The result of the chemical analysis is shown in Table 5.1. Oxalic acid ($H_2C_2O_4 \cdot 2H_2O$) of 99 - 100 percent purity was used as a solvent.

5.2.2 Experimental methods and analysis

A three-necked flask of 1L in volume was employed as a leaching reactor, with a temperature controlled water bath and a stirrer. Leaching conditions were as follows:

- Reaction temperature: 25, 50, 75 and 100℃.
- Concentration of the oxalic acid: 0.19, 0.38 and 0.48 M
- Agitating speed: fixed at 500 rpm, the optimal speed determined through pretests

During the experiments, aliquots of 3mL of reacted solution were withdrawn at known time intervals to analyze Fe by the atomic absorption spectrophotometry at the predetermined time intevals. The leached clay was examined by XRD, SEM and XRF, and briquetted to disks of 50 mm. in diameter, and sintered at 1260℃ for 60min to measure their whiteness (whiteness of the standard with MgO set at 88.3%, Spectrophotometer SP88, X-Rite, USA).

5.3 RESULTS AND DISCUSSION

5.3.1 Compositions and Components

Table 5.1 shows the chemical compositions of the clay samples used for experiments which consist of aluminum silicate (90-94% of $SiO_2 + Al_2O_3$) and 2.2-3.89% of ($Na_2O + K_2O$). The coarser J-A sample contained less amounts of both Fe_2O_3 and Al_2O_3, than J-B, but slightly higher in SiO_2 content.

When the sample was used as a raw material for ceramic production, the ferrous oxide caused the yellowing of the product after heat treatment. In nature, the iron oxide in the raw samples could react with basic elements existing in the clay during hydrothermal

alteration or dissolution by incursion of ground water, forming small iron-encrusted openings in the clay (Park, 1974). These were observed under optical microscopy shown in Figure 5.1. Figure 5.1 (a) exhibits small openings (circled dark areas), and Figure 5.1 (b) shows the iron-rich zone easily crushed than in the coarse grained sample J-A (see Table 5.1). Free silica can be seen in area (c) and the impurity-free area (d) is mostly composed of coarse particles.

To identify the mineralogical iron oxide component contained in the clay, XRD was used to analyse the concentrates of both non-magnetic and magnetic materials separated by means of a high intensity magnetic separator (HIMS) (Figure 5.2).

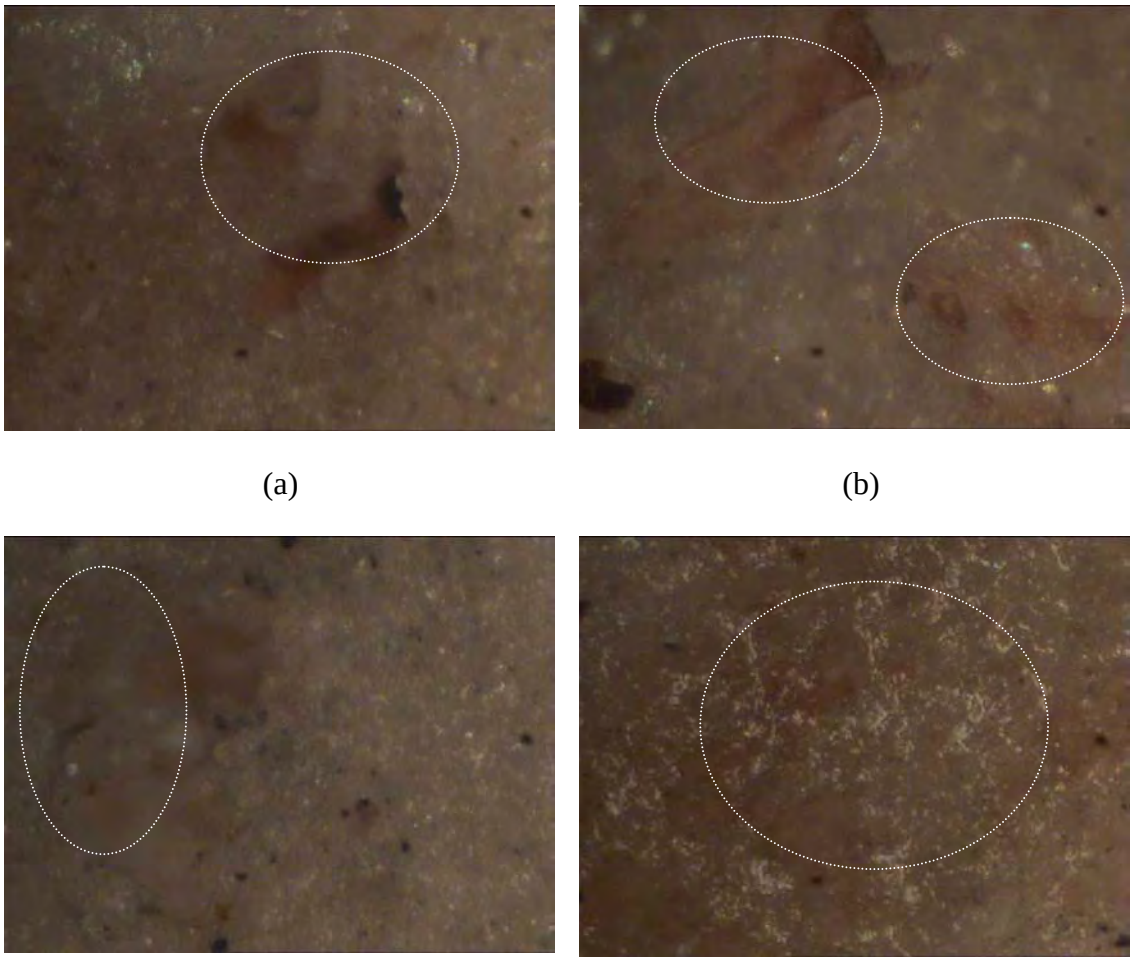

(a) (b)

(c) (d)

Figure 5.1 Optical micrographs of Jan-San clay samples

Table 5.1 Chemical analysis of the samples in weight percentages

Comp. (%)	SiO_2	Al_2O_3	Fe_2O_3	CaO	MgO	TiO_2	Na_2O	K_2O	MnO	P_2O_5	I.L.
J-A	86.40	8.23	0.58	0.16	0.10	0.32	0.20	2.00	0.01	0.09	1.61
J-B	76.30	14.79	1.06	0.35	0.18	0.39	0.30	3.59	0.01	0.17	2.66

(J-A : -16/+100mesh, J-B : -100mesh) I.L. : Ignition loss

In Figure 5.2, (a) a non-magnetic concentrate with iron content of 0.3% Fe_2O_3 consists of mainly sericite and α -quartz. However, the magnetics with iron content of 5.5% Fe_2O_3 as tailing (b) shows the x-ray pattern of hydrated iron oxides and iron aluminum silicate rather than that of magnetite or hematite. This suggests that it is difficult to remove the iron to a desired level (<0.1% Fe_2O_3 for achieving >90% whiteness) using a magnetic separator, and thus a chemical process must be used for removing the iron components.

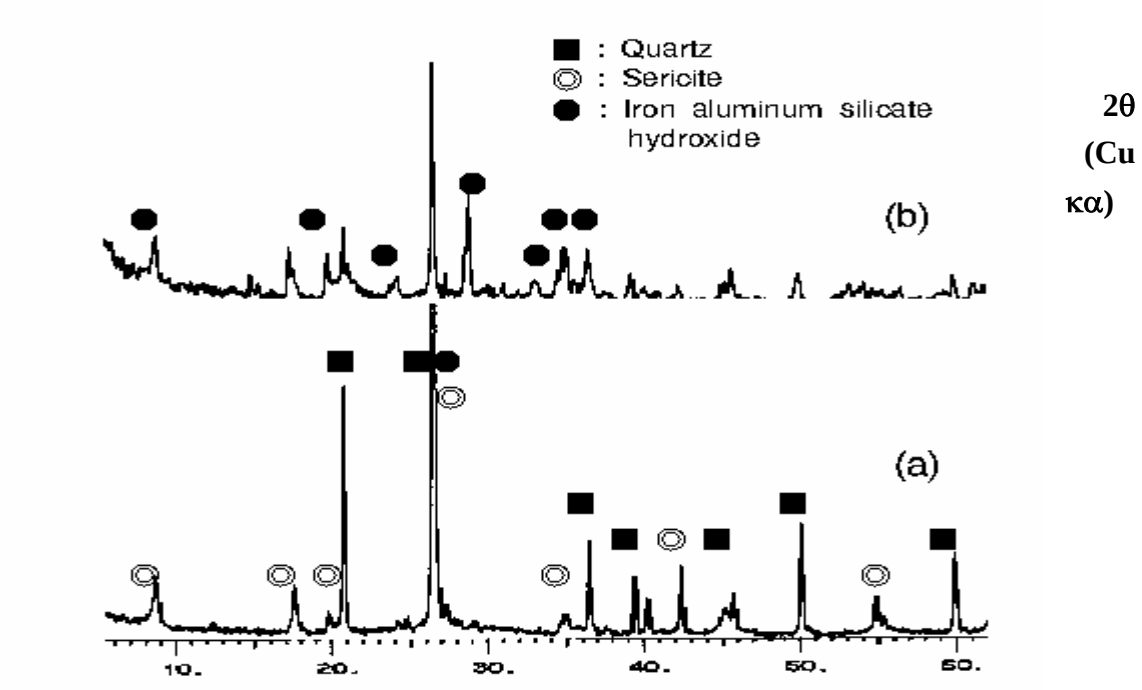

Figure 5.2 XRD patterns of the sample separated by HIMS at 1.5 Tesla.

(a) non-magnetic concentrate fraction (b) magnetic tailing fraction

5.3.2 Chemical leaching of iron

Of all the possible complexing carboxylic acids, oxalic acid appears to be the most efficient for iron removal. The oxalates are decomposed by heating into carbon monoxide/dioxide and carbonates (Baumgartner et al., 1983; Marabini et al., 1993). The redox reaction in an aqueous solution is expressed in equation (5-1) (Charlot, 1954), and the mechanism of chemisorption of oxalic acid on surface ferric cations is expressed in Figure 5.3 (Blesa et al., 1987).

$$H_2C_2O_4 \rightarrow 2CO_2 + 2H^+ + 2e \qquad E_o = \text{-0.49volt} \qquad (5\text{-}1)$$

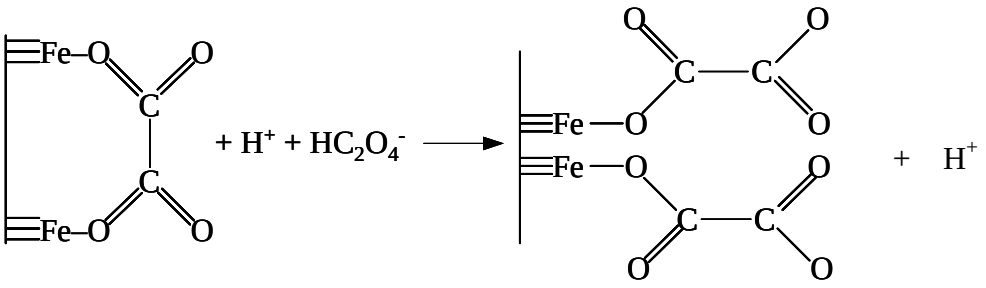

Figure 5.3 Chemisorption of oxalic acid on surface ferric cations

In the case of iron(III) oxide, the reduction of Fe(III) to Fe(II) brings about a great increase in the rate of dissolution (Segal and Sellers, 1982). The origin of the enhancement is the greater lability of Fe(II)-O bonds as compared to Fe(III)-O bonds (Baumgartner et al., 1983). The dissolution process involves reactions on the particle surface and linear dependence on [$C_2O_4^{2-}$] that serves to a valence electron-transfer to Fe(III) ions on the surface as shown in equation (5-2):

$$C_2O_4^{2-} + 2Fe(III) \rightarrow 2CO_2 + 2Fe(II) \qquad (5\text{-}2)$$

From the experimental result, the oxalate phase precipitated from the leaching solution was found to be the ferrous oxalate of $FeC_2O_4 \cdot 2H_2O$ (2θ: 18.7, 23.2, 24.9, 29.9, 34.3, 50.4) which was identified on the XRD pattern. Accordingly, the mechanism of leaching reaction in this experiment can be expressed as equation (5-3) for the overall reaction between hydrated ferric oxide and oxalic acid:

$$2FeOOH + 3H_2C_2O_4 \cdot 2H_2O \rightarrow 2FeC_2O_4 + 2CO_2 + 4H_2O \qquad (5\text{-}3)$$

5.3.2.1 Effect of temperature

Figures 5.4 and 5.5 show the leaching curves of samples J-A and J-B respectively as a function of the reaction temperature at 0.38 M oxalic acid, 500 rotation speed and liquid/solid ratio (L/S) of 5:1 at various temperatures of 25, 50, 75 and 100℃. As shown in Figure 5.4 for sample J-A, Fe dissolution reaches 11% at 25℃ but goes up to 63% at 100℃ in 10 min In two-hours, the percentage leaching reaches 39% at 25^{o}C and 83% at 100℃. For the sample J-B shown in Figure 5.5, an increased leaching efficiency was obtained in the temperature range of 25^{o}C to 100^{o}C. The result means that liberation degree or exposure of iron components due to smaller particle size must be a significant parameter for the leaching of iron from clays. The larger the particle size of the sample is the lower the leaching efficiency of iron due to less liberation of iron minerals from the ore particles (Fogler, 1992).

5.3.2.2 Effect of oxalic acid concentration

In order to clarify the effect of oxalic acid concentration, the leaching was conducted in the presence of various oxalic acid concentrations of 0.19, 0.38 and 0.48 M at 100℃ at a L/S of 5:1 and stirring rate of 500 rpm.

Figure 5.6 shows the leaching percentage increases at a higher concentration of oxalic acid for the J-A sample. The leaching percentage appears lower within 40 min of leaching especially at a higher concentration of oxalic acid. Excellent leaching results were obtained at 0.38 M oxalic acid. However, for sample J-B as shown in figure 5.7, a leaching efficiency of 96% was obtained at 0.19 M oxalic acid after 120 min, of which the result appeared better than those at higher concentrations of the solvent, i.e., 0.38 M or higher concentration of oxalic acid. This finding, once again, seems to support the observations in several studies that an oxalate concentration higher than 0.21M (Fig. 2.17, Chapter 2) would induce the precipitation of solid ferrous oxalate which could passivate the reaction interface.

5.3.2.3 Effect of liquid/solid ratio

Figures 5.8 and 5.9 show the effect of slurry density on the leaching of iron from clay samples (J-A and J-B) respectively. As shown in the figures, the initial leaching rate appeared very fast for both J-A and J-B. After about 10 min, the leaching rate decrease as shown in this figure. However, a higher the leaching efficiency of iron was observed for a lower pulp density as expected. For the J-A sample shown in figure 5.8,

dissolution of iron reached about 60 % or more in 20 min and about 70 % in 60 min. For the J-B sample as shown in figure 5.9, 85 % or more of iron was dissolved within 10 min a pulp density lower than L/S ratio of 6.7 and about 95 % of iron was leached in 40 min.

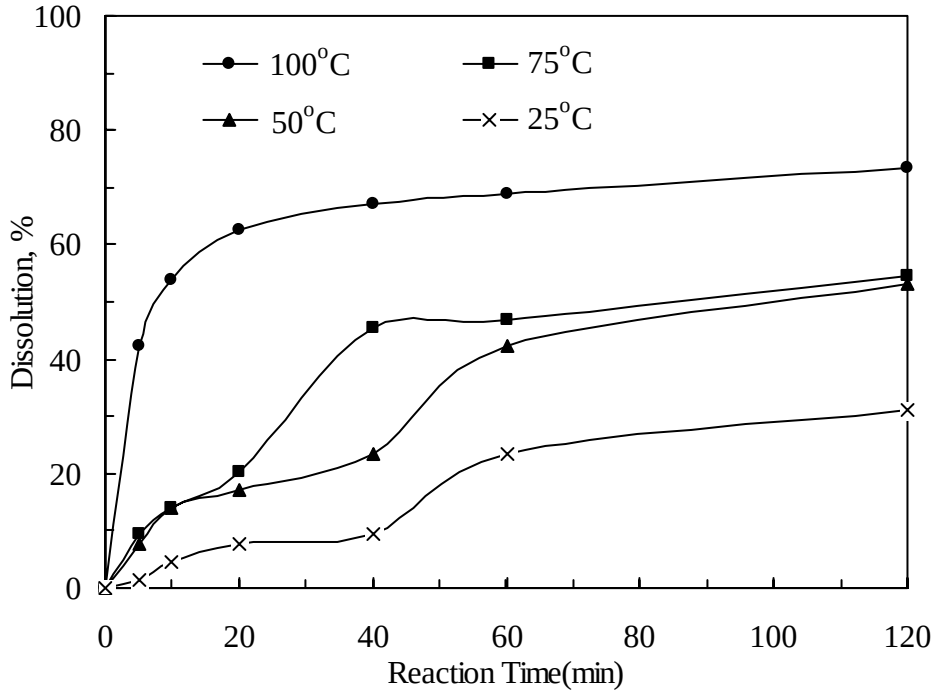

Figure 5.4 Leaching tests on J-A as a function of reaction temperatures (Oxalic acid concentration: 0.38 M, L/S: 5:1, Agitation: 500 rpm).

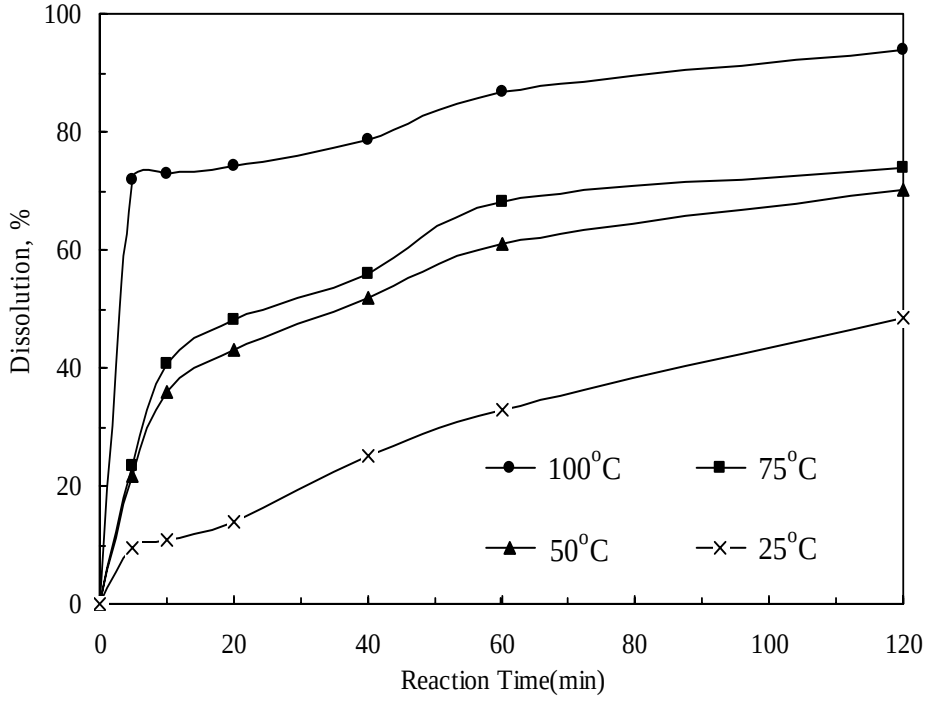

Figure 5.5 Leaching tests on J-B as a function of reaction temperatures (Oxalic acid concentration: 0.38 M, L/S: 5:1, Agitation: 500 rpm).

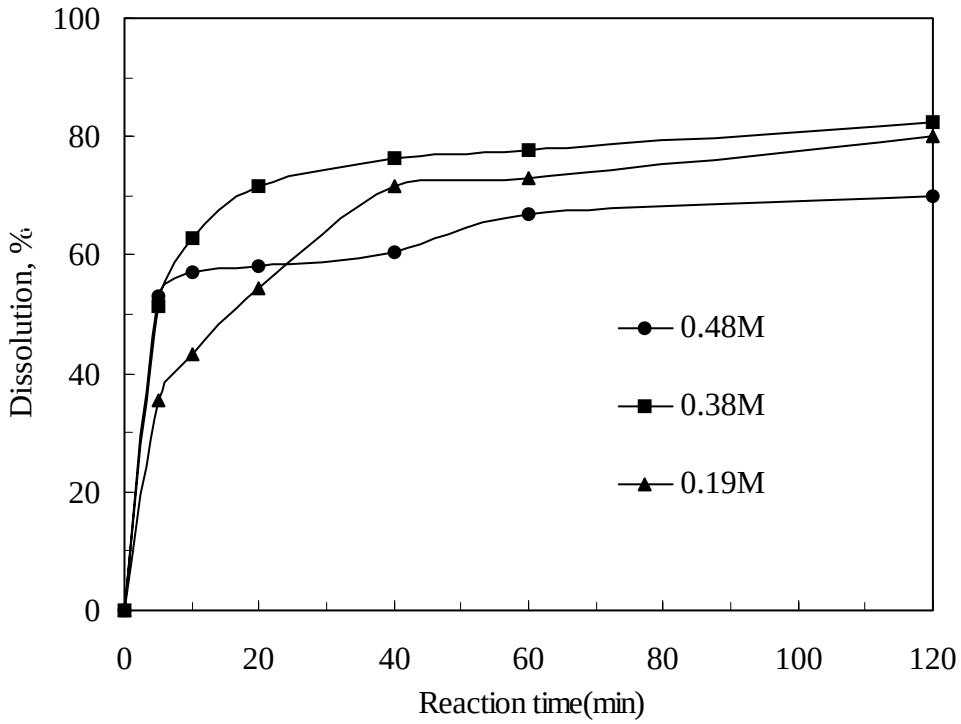

Figure 5.6 Leaching tests on J-A as a function of Oxalic acid concentration (Temperature: 100℃, L/S: 5:1, Agitation: 500 rpm).

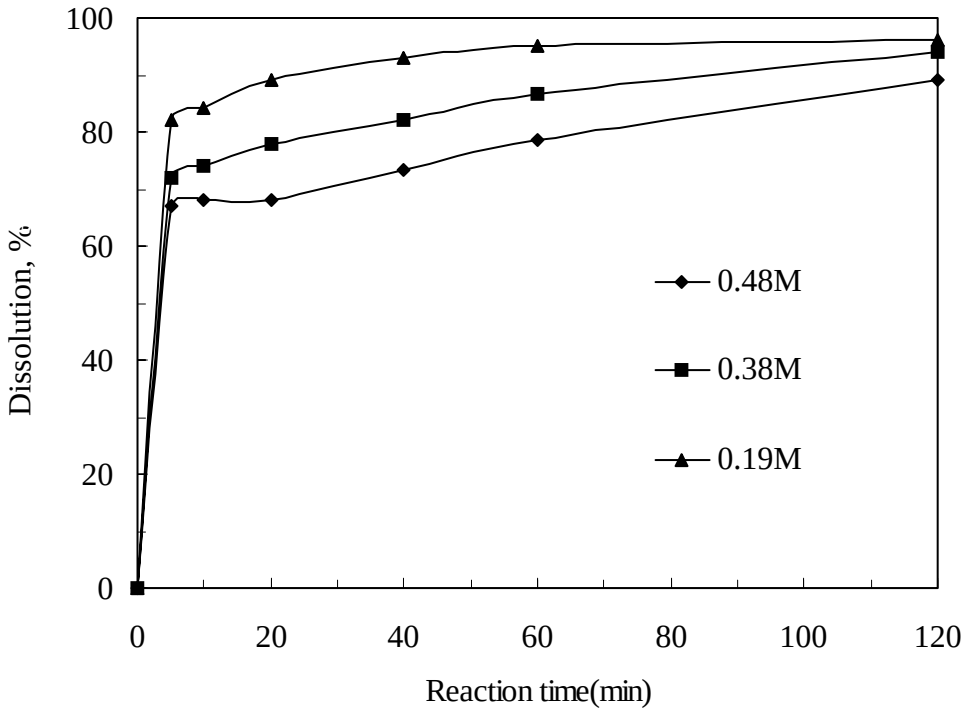

Figure 5.7 Leaching tests on J-B as a function of Oxalic acid concentration (Temperature: 100℃, L/S: 5:1, Agitation: 500 rpm).

The lower pulp density is effective enough to dissolve iron in clay. Because the J-B sample has high specific surface area as compared to the most J-A sample, the leaching rate and efficiency are greater for materials with small particles.

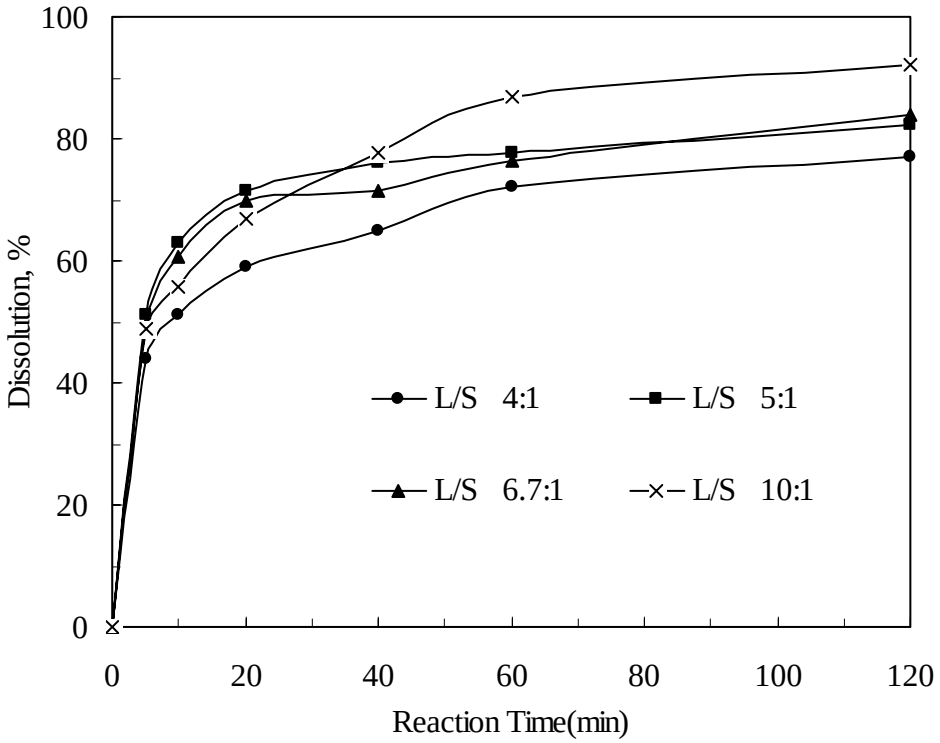

Figure 5.8 Leaching tests on J-A as a function of L/S ratio (Oxalic acid concentration: 0.38 M, Temperature: 100℃, Agitation: 500 rpm).

5.3.3 Properties of leached sample

Table 5.2 shows the chemical analysis results of the leached clays through further removal of magnetic particles by magnetic separation after leached samples were washed twice. The total removal of Fe from the clays reached 86.2% and 89.6% for J-A and J-B samples respectively, at 100℃, L/S ratio of 5:1 and 500 rpm stirring speed after two-hour leaching with 0.38 M oxalic acid for the J-A sample and 0.19 M oxalic acid for J-B sample. As shown in table 5.1 and table 5.2 the silica contents increased slightly, while the alumina was decreased after the leaching with oxalic acid. However, the iron contents of the clay a decreased from 0.58 % to 0.08 % for J-A sample and from 1.06 % to 0.11 % for the J-B sample respectively. The sintered briquettes of the refined clays show whiteness of 88-90 % for both clay samples in table 5.3. These optical properties meet the standard for high grade ceramic products.

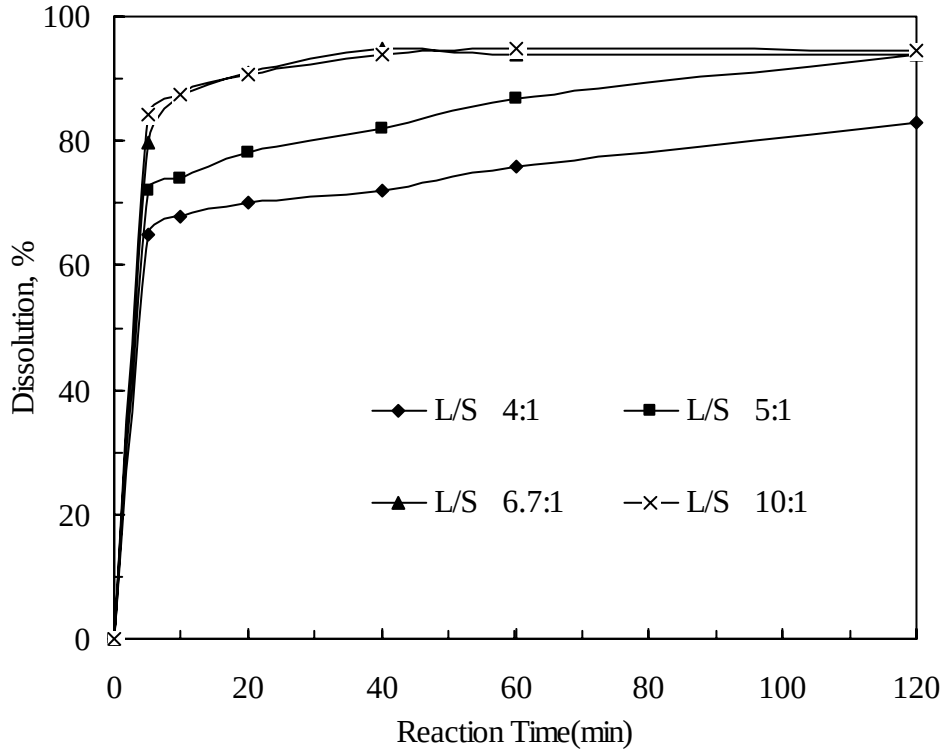

Figure 5.9 Leaching tests on J-B as a function of L/S ratio (Oxalic acid concentration: 0.38 M, Temperature: 100℃, Agitation: 500 rpm).

Table 5.2 Chemical analysis of leached samples in weight percent.

Comp. (%)	SiO_2	Al_2O_3	Fe_2O_3	CaO	MgO	TiO_2	Na_2O	K_2O	MnO	P_2O_5	I.L
J-A	89.82	6.00	0.08	0.11	0.07	0.30	0.22	1.55	0.01	0.04	1.15
J-B	78.88	14.15	0.11	0.10	0.15	0.38	0.30	3.41	0.01	0.07	2.15

(J-A : -16/+100mesh, J-B : -100mesh), I.L : Ignition loss

Table 5.3. The whiteness of the samples.

	Whiteness, %
Raw clay	69.0
Non-magnetic conc. by HIMS at 1.5 Tesla	78.3
J-A sample*	88.7
J-B sample*	90.0

* refined by leaching and magnetic separation

5.4 CONCLUSIONS

The mineralogical investigation of the tested samples showed sericite and α-quartz as the main components of clay samples containing high iron oxides. Hydrated iron oxide was found to be a major iron impurity and aluminum silicate hydroxide [$K(Fe,Al)_2(Si,Al)_4O_{10}(OH)_2$] appeared to be the second phase of Fe-contaminants of the clay samples. Optimum leaching could be obtainable in the presence of 0.38 M oxalic acid for J-A sample and of 0.19 M for J-B sample at 100℃, a L/S ratio 5:1 and 500 rpm stirring rate within 60 min The leaching percentage for J-A and J-B samples reached 83% and 96%, respectively. The overall removal of iron from the clays was obtained to be 86.2% and 89.6% for J-A and J-B, respectively. A lower pulp density and smaller particle size improved the leaching efficiency of iron. The final refined clay products had a whiteness of about 90 %, which meet the standard of high-class ceramic products. This quality was approved by Haengnam China Ware Co. Ltd. in Korea who produces fine ceramic kitchenware.

CHAPTER SIX

REMOVAL OF FERRIC IONS FROM IRON (Ⅲ) OXALATO COMPLEXES REACTED WITH CALCIUM HYDROXIDE IN SOLUTION

6.1 INTRODUCTION

Large amounts of solution with iron (III) oxalate complexes would have been disposed from the metal cleaning processes, chemical leaching of clay minerals, and radioactive waste treated with organic acids (Ladd and Miller, 1988; Lee et al., 1997; Moon et al., 1997). The removal and recovery of metal ions from waste water containing metal complexes are of major environmental concern in view of keeping water clean from contamination and recycling of valuable metals. The waste waters containing iron (III) oxalato complexes generated from chemical leaching of clay materials and tube flushing solutions have stable ferric oxalato complexes in various pH ranges. The main metallic components in the waste water generated from the chemical leaching of clay are Fe (III), Ca(II), Mg(II) and Al (III) metal oxalate in the pH range of 2.5～3.5 (Lee et al., 1998).

Recently, several studies were reported on the treatment of industrial waste waters using calcium hydroxide (Noyes, 1993; Tehobanoglous and Rurton, 1993).

The present study investigated the removal of ferric ions from an iron oxalate complex solution using calcium hydroxide. The water regenerated in this process is to be recycled for use in the process.

Several experiments were conducted to study the effect of temperature, concentration of oxalic acid, concentration of Fe (III) ion and the initial pH. Emphasis was also placed on the behavior of Fe (III) on the addition of calcium hydroxide.

This investigation compliments the leaching of iron contaminants from clay minerals using organic acid.

6.2 EXPERIMENTAL

6.2.1 Chemicals

The oxalato-ferric complex solution was prepared by dissolving oxalic acid ($H_2C_2O_4 \cdot 2H_2O$, EP grade) and ferric chloride ($FeCl_3 \cdot 6H_2O$) into distilled and deionized water. Calcium hydroxide ($Ca(OH)_2$) was used as a neutralizer and sodium hydroxide (NaOH) as a pH modifier. All were first grade chemicals. The leach solutions were produced according to the procedures reported in the previous chapter (Lee et al., 1997), and each solution was prepared just prior to the experiment.

6.2.2 Experimental procedures

A three-necked 1L flask incorporating a stirrer was used as the reactor where temperature is controlled by a water bath. The experimental conditions were as follows:

- Reaction temperature : 27, 40, 60 and 85℃
- Concentration of oxalic acid (OxA) : 0.05, 0.1 and 0.3M
- Concentration of calcium hydroxide : 0.027, 0.040, 0.054, 0.067 and 0.081M
- Concentration of iron chloride ($FeCl_3 \cdot 6H_2O$) : 0.008, 0.01, 0.03 and 0.06M
- Initial pH range : 1.55, 2.55 and 3.52
- Agitating speed : 350 rpm

The pH of the solutions was measured using a pH meter (TOA Co). The efficiency of removal Fe (III) was calculated from the Fe (III) concentration in the residual solutions, sample 2mL of the solution were taken for analysis of Fe (III) by the ICP Spectrometer (JOBIN-YVON Co.).

The efficiency of removal (%) was calculated according to the following equation (6-1)

$$= \quad 100 \ (\grave{}C_i - C_{f'}) / C_i \qquad (6\text{-}1)$$

where C_i is the initial concentration of the total M (III) ion in the solution and C_f is the final concentration of total M (III) ion in the batch experiments.

6.3 RESULTS AND DISCUSSION

6.3.1 Reaction of $Ca(OH)_2$ and iron (III) oxalato complexes

The formation of metal complexes from the reaction of Fe (III) ion and oxalic acid was affected by the ionic activity of oxalate and pH-value of the solution. When the oxalic acid and Fe (III) ion co-existed in the solution without other elements, they formed iron (III) oxalato complexes as $Fe(C_2O_2)_n^{3-2n}$ (n=1, 2, 3), as shown in equations (6-2), (6-3) and (6-4). Under these conditions, the active species is $HC_2O_4^-$ rather than $C_2O_4^{2-}$, forming $FeH(C_2O_4)^{2+}$ complex ion as shown in equation (6-5). The equilibrium constants calculated at the ionic strength of 1.0 and 25°C, are also shown with these equations (Martell and Smith, 1996; Panias et al., 1996).

$$Fe^{3+} + C_2O_4^{2-} \leftrightarrow Fe(C_2O_4)^{1+}_{(aq)} \qquad K_1 = 10^{7.58} \qquad (6\text{-}2)$$

$$Fe(C_2O_4)^{1+} + C_2O_4^{2-} \leftrightarrow Fe(C_2O_4)_2^{1-}{}_{(aq)} \qquad K_2 = 10^{6.23} \qquad (6\text{-}3)$$

$$Fe(C_2O_4)_2^{1-} + C_2O_4^{2-} \leftrightarrow Fe(C_2O_4)_3^{3-}{}_{(aq)} \qquad K_3 = 10^{4.79} \qquad (6\text{-}4)$$

$$Fe^{3+} + HC_2O_4^- \leftrightarrow FeH(C_2O_4)^{2+}_{(aq)} \qquad K_4 = 10^{9.53} \qquad (6\text{-}5)$$

According to Panias et al. (1996) and Martell and Smith (1996), when the pH of the solution is adjusted in the range of 2.5～3.0, the most stable reaction is equation (6-4), a result of the increasing of oxalate activity. Otherwise, when the pH decreases to below 2.5, equation (6-5) will dominate in decreasing oxalate activity, and could co-exist with the free oxalic acid. Therefore, the reaction of $Ca(OH)_2$ and iron (III) oxalato complex in solution to remove the ferric ions are shown in following equations.

$$Ca(OH)_2 + H_2O \leftrightarrow Ca^{2+} + 2OH^- + H_2O \qquad K_{sp} = 6.5\times10^{-6} \qquad (6\text{-}6)$$

$$Ca^{2+} + C_2O_4^{2-} \leftrightarrow CaC_2O_4 \qquad K_f = 1.0\times10^{3} \qquad (6\text{-}7)$$

$$FeH(C_2O_4)^{2+} + Ca(OH)_2 \leftrightarrow CaC_2O_4 + Fe^{3+} + H_2O + OH^- \qquad K_f = 2.5\times10^{7} \qquad (6\text{-}8)$$

$$Fe(C_2O_4)_3^{3-} + 3Ca(OH)_2 \leftrightarrow 3CaC_2O_4 + Fe(OH)_3 + 3OH^- \qquad K_f = 1.5\times10^{16} \qquad (6\text{-}9)$$

According to the above equations, the overall reaction can be expressed by equation (6-8) in a solution at pH<2.5, whereas in the range of pH 2.5～3.0, equation (6-9) represent the predominant process, because the free oxalate species is dominant in the solution in this case (Dean, 1992, and Brady and Holum, 1996). The calcium ((II)

oxalate and iron (III) hydroxide were simultaneously precipitated in the solution. XRD test of the products showed the formation of $CaC_2O_4 \cdot H_2O$, although $Fe(OH)_3$ was not detected by XRD due to its amorphous nature and only a small amount of $Fe(OH)_3$ precipitate is formed. However ESCA tests confirmed its presence.

6.3.2 Effect of calcium hydroxide addition

Figure 6.1 shows the change of pH with the concentration of added calcium hydroxide, and the reaction time. The starting solution was prepared with 0.010M of Fe dissolved in 0.100M of oxalic acid solution, adjusted to an initial pH of 2.5 at 25℃.

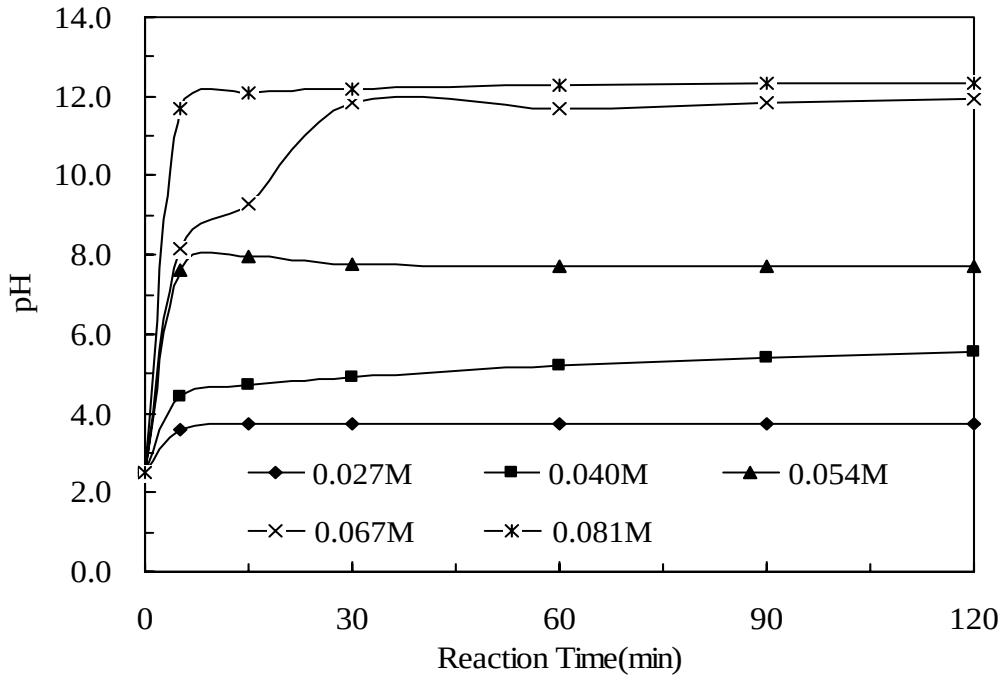

Figure 6.1 The change of pH with the amount of calcium hydroxide added (M: mol/L) (Oxalic acid conc. : 0.100M, Fe : 0.010M, pH : 2.5, Temp. : 25℃).

Figure 6.1 shows that the change of pH in the solution with 0.027 mol/L of calcium hydroxide added is very slow. However when the amount of calcium hydroxide was increased to 0.054 mol/L, the pH reached 7.5 within 5 minutes. Of special concern is the fact that the pH of the solution showed a dramatic increase to 11.34 within 30 minutes by adding 0.067 mol/L of calcium hydroxide. Calcium and hydroxide react with oxalate and ferric ions to form calcium oxalate and ferric hydroxide, respectively.

Figure 6.2 shows the effect of the concentration of calcium hydroxide on the efficiency of Fe removal under similar experimental conditions as those shown in Figure 6.1. The concentration of Fe in the solution was decreased with the addition of calcium hydroxide, and the removal efficiency reached 50% and 56% within 5 minutes with 0.027 mol/L and 0.040 mol/L of calcium hydroxide added, respectively. On the other hand, the iron removal was increased rapidly to 90% within 5 minutes at 0.054 mol/L calcium hydroxide added, and completed within 15 minutes at 0.067 mol/L added.

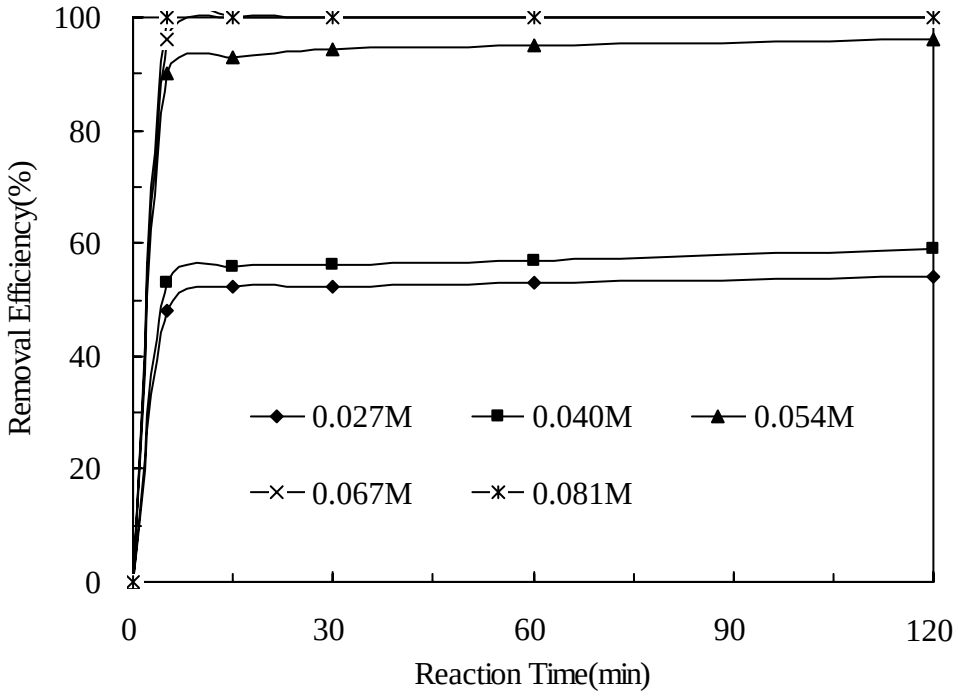

Figure 6.2 Effect of calcium hydroxide additions (as M: mol/L) on the removal % of Fe (Oxalic acid concentration: 0.100M, Fe : 0.010M, pH : 2.5, Temp. : 25℃).

6.3.3 Effect of reaction temperature

Figure 6.3 shows the efficiency of Fe removal at different temperatures when 0.010M of Fe dissolved in 0.100M of oxalic acid solution at the initial pH of 2.5. The experiments were conducted with the temperature range from 25℃ to 85℃, at a constant addition of 0.054 mol/L $Ca(OH)_2$. No effect of temperature was observed in this series of tests, indicating that the precipitation process can be conducted at 25℃.

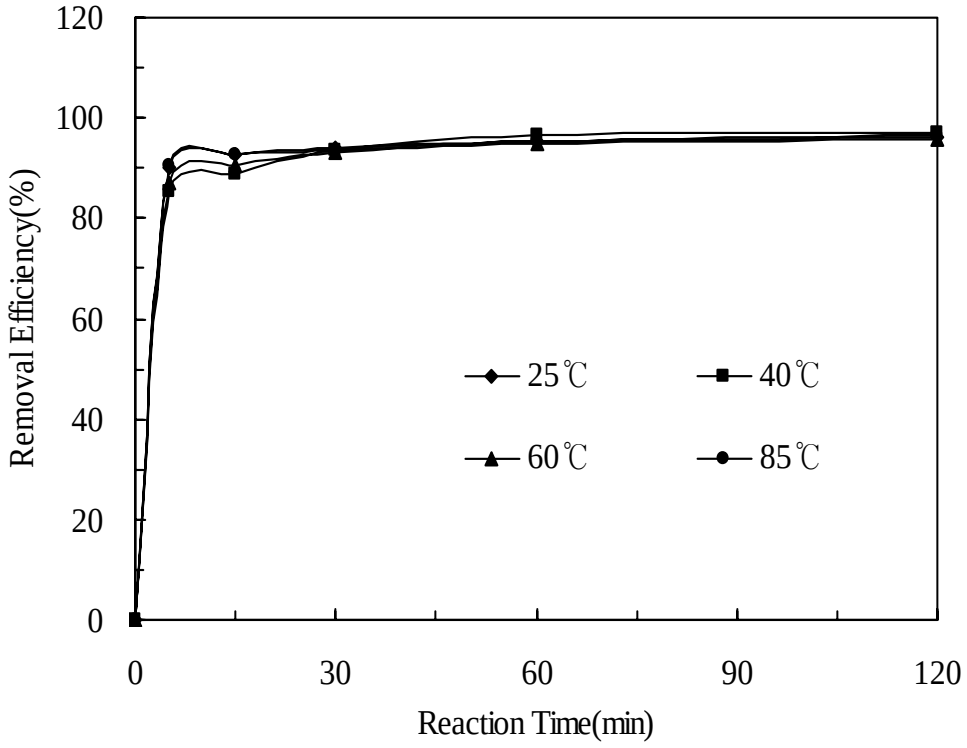

Figure 6.3 Effect of reaction temperature on the removal % of Fe (Calcium hydroxide addition: 0.054 mol/L, Oxalic acid conc. : 0.100M, Fe : 0.010M, pH : 2.5).

6.3.4 Effect of oxalic acid and Fe concentration

Figure 6.4 shows the efficiency of Fe removal under different oxalic acid concentrations with 0.054 mol/L of calcium hydroxide added at 25℃. The starting solution was prepared by adding 0.010M of Fe to solution of various oxalic acid concentrations from 0.050M to 0.300M and the initial pH was adjusted to about pH of 2.5. The efficiency of Fe removal in 0.100M of oxalic acid solution reached 90% within 5 minutes. The efficiency was increased to 99% in the same duration when the oxalic acid concentration was decreased to 0.050M. It indicated that the increase of oxalic acid concentration increased the addition amount of calcium hydroxide due to the free oxalate species produced in the solution at the fixed concentration of ferric ions.

This result also can be seen in Figure 6.5. When the ferric ion concentration was increased in 0.100M oxalic acid in solution, the efficiency of Fe removal was increased with the increase of ferric iron concentration. Therefore, the increase of oxalic acid concentration in solution decreased the removal efficiency of Fe and increased the

amount of calcium hydroxide required under the same conditions.

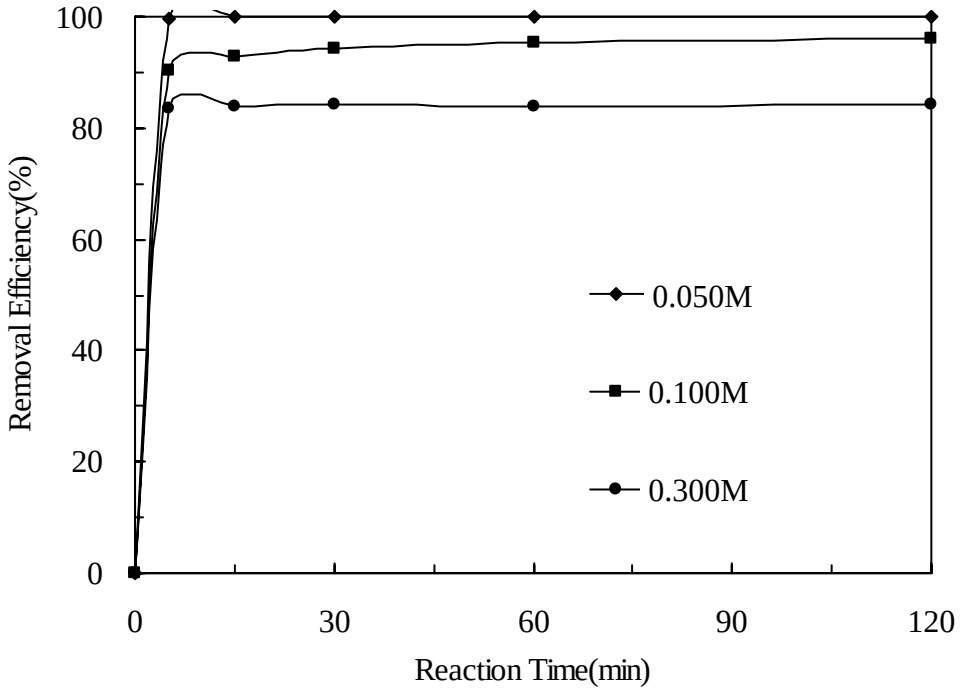

Figure 6.4 Effect of oxalic acid concentration on the removal % of Fe (Calcium hydroxide added at 0.054 mol/L, Fe : 0.010M, pH : 2.5, Temp. : 25℃).

From equation 6.8 and 6.9, 2 or 3 moles of $C_2O_4^{2-}$ is required for each mole of Fe. Therefore if the molar ratio of oxalate/Fe is increased, more stable iron oxalate complex will exist in the solution. Therefore for 0.1 M oxalic acid, when ferric ion concentration was lower than 0.03 M, the oxalate/ferric ion molar ratio was higher than 3, indicating stable ferric-oxalate complexes existed in the solution. In these conditions, 80-100 mg/L Fe(III) remained in the solution. It seems that it was harder to remove these complexes by calcium hydroxide. Free Fe^{3+} ions are required for $Fe(OH)_3$ precipitation (as in the cases at high concentration of Fe(III)) first, probably to act as nuclei for other precipitate to form.

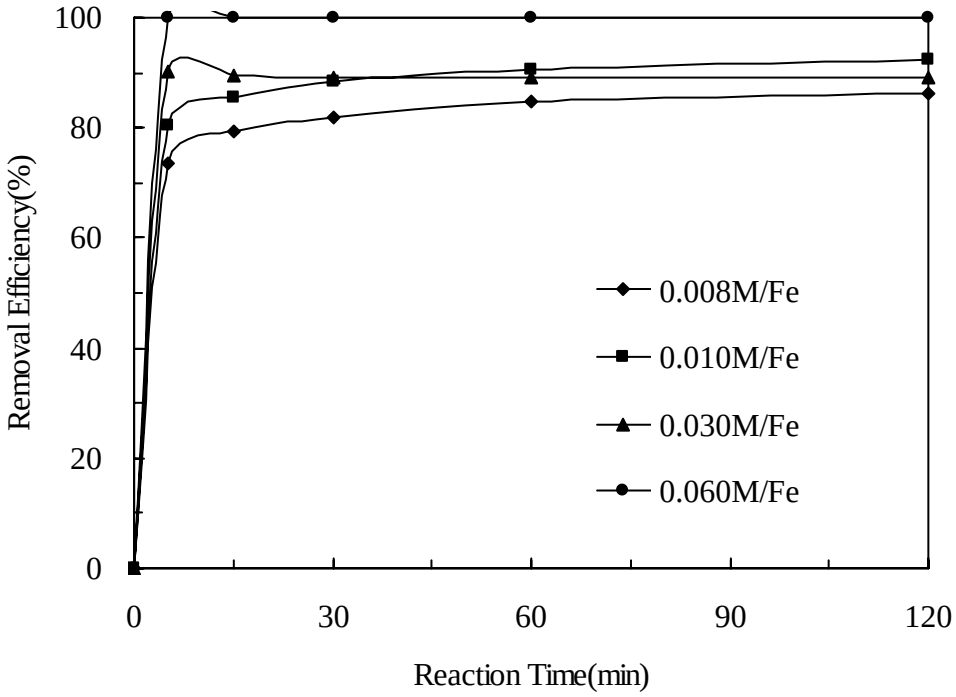

Figure 6.5 Effect of iron (III) concentration on the removal % of Fe (Oxalic acid conc. : 0.100M, Calcium hydroxide addition: 0.054 mol/L, pH : 2.5, Temp. : 25℃).

6.3.5 Effect of initial pH and reuse of sludge

Figure 6.6 shows the effect of the initial pH-value with 0.010M of Fe dissolved in 0.100M of oxalic acid at 25^{o}C. The initial pH of the starting solution was adjusted from 1.55 to 3.52. The pH-value, when the 0.054 mol/L of calcium hydroxide added to the solution, was sharply increased to pH8.0-11.5 within 5 minutes and the efficiency of Fe removal shows about 90-91%. In a strongly acidic solution, the change of pH was low and the removal efficiency decreased to 59%. In an acidic solution of pH 1.15 at room temperature, an excess of calcium hydroxide is needed to change the pH and to increase the efficiency of Fe removal rather than other initial pH. At pH1.15, it seems that more soluble Fe(III)-oxalate complex, $FeHC_2O_4^{2+}$, are still predominant whereas at higher pH's $Fe(C_2O_4)_3^{3-}$ is more predominant.

Figure 6.7 shows the change of pH on the number of reuse of the precipitated sludge. The sludge was filtered each time through 1.2 glass fiber micro filter and dried at room

temperature without the removal of iron hydroxide. When the sludge was reused two or more times, the activity was sharply decreased, showing a change of pH from 8.5 after the first use to 3.2 after the second use, within the 15 minutes and with 0.067 mol/L initial addition of calcium hydroxide. Sludge samples used more than twice were affected by the change of pH in the solution because it consisted mainly of $CaC_2O_4 \cdot H_2O$ and only a small amount of $Ca(OH)_2$ remained.

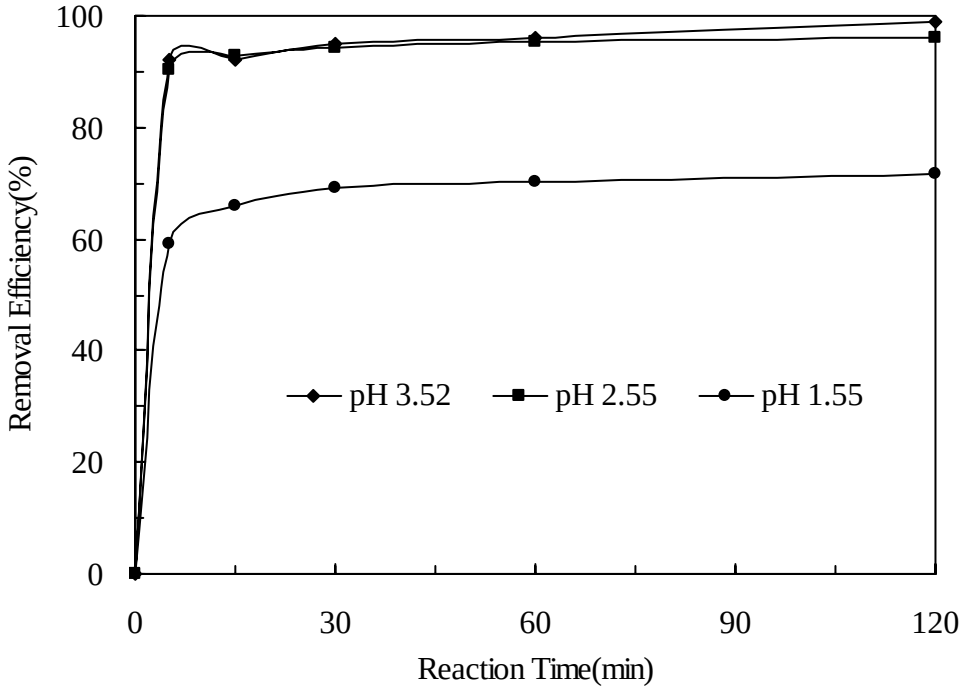

Figure 6.6 Effect of various initial pH on the removal % of Fe (Oxalic acid conc. : 0.100M, Fe : 0.010M, Calcium hydroxide addition.: 0.054 mol/L, Temp. : 25^{o}C).

6.3.6 Application to the clay leaching solution

Figure 6.8 shows the efficiency of Fe removal and change of the pH-value with the concentration of calcium hydroxide to the clay leaching solution at 25^{o}C or 85 ^{o}C. When 0.338 mol/L of calcium hydroxide was added to the solution at 25 ^{o}C, the removal efficiency of Fe is about 2% within 30 minutes at the final pH value of 4.0. When the reaction temperature increased to 85^{o}C, the removal increased to 99% at the pH-value of 12.5. The clay leaching solution with oxalic acid contains Fe (III), Al (III) Ca (II), Na (I) and Mg (II) ions, forming oxalato-metalic complexes, for example, as $M(C_2O_4)_n^{3-2n}$ (n=1, 2 ,3). The removal efficiency of Fe and Al as a function of the reaction temperature is shown in Figure 6.9. In the case of the artificial solution, the increase of

the reaction temperature decreased the removal efficiency of ferric ion from iron (III) oxalato complexes. Al ion was also removed according to the increase of pH and temperature. The solution can be recycled into the treatment and the sludge as $CaC_2O_4 \cdot H_2O$ produced can be used for other industrial processes.

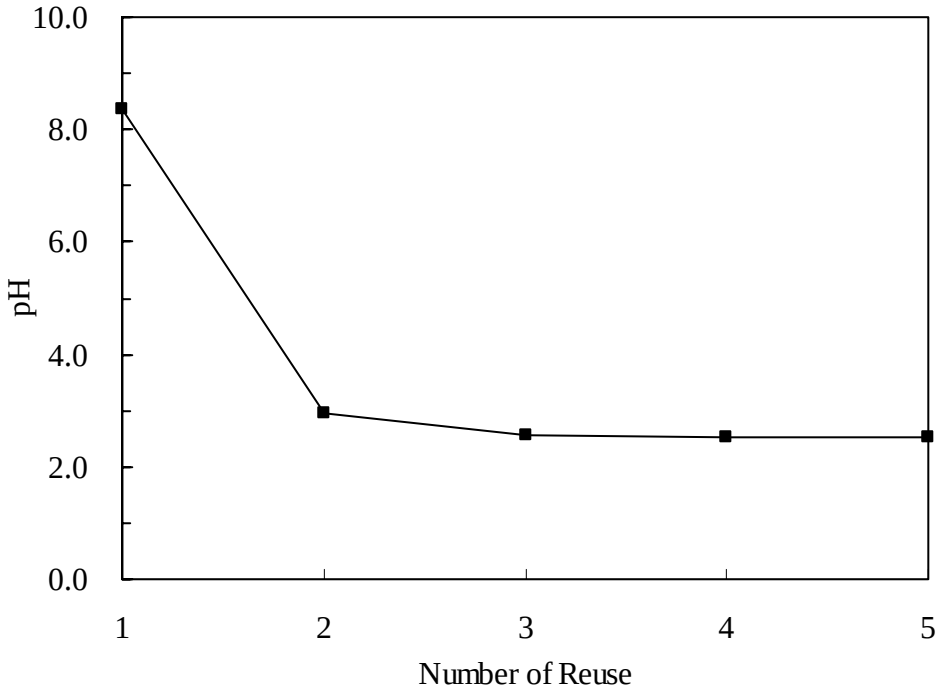

Figure 6.7 The change of pH on number of reusing times of the precipitated sludge (Oxalic acid conc.: 0.100M, pH : 2.5, Fe : 0.010M, Calcium hydroxide addition: 0.067 mol/L, Reaction time : 15min., Initial temp. : 25℃).

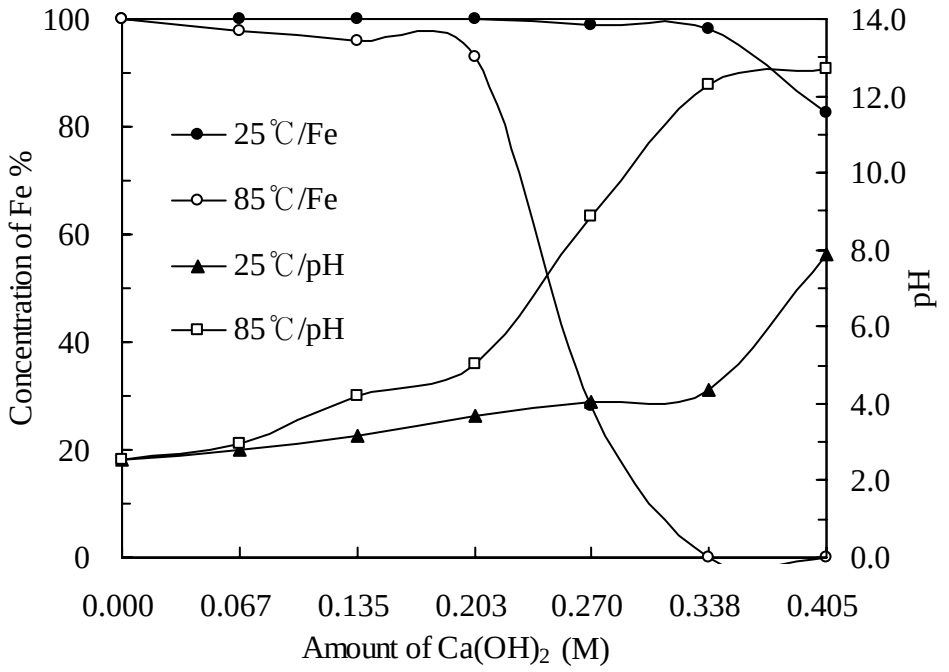

Figure 6.8 Effect of calcium hydroxide concentration on the removal of Fe and change of pH (Oxalic acid conc.: 0.100M, pH : 2.5, Fe conc. : 0.078M (4,350mg/*l*), Reaction time : 30min.).

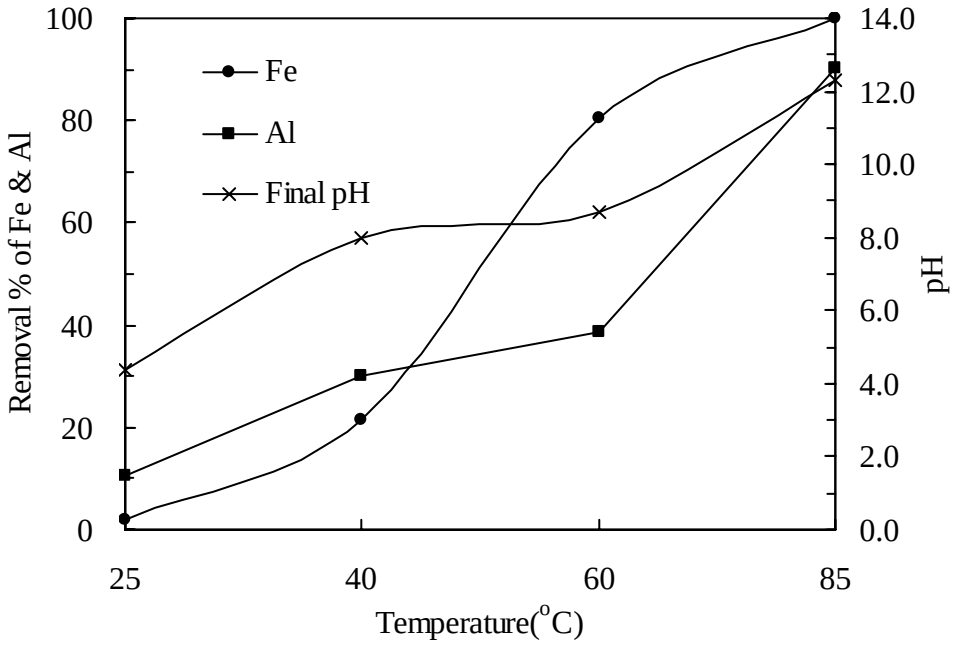

Figure 6.9 Effect of reaction temperature on the removal % of Fe and Al (Oxalic acid conc. : 0.100M, pH : 2.5, Calcium hydroxide addition: 0.338 mol/L, Reaction time : 30min., Fe conc. : 0.078M (4,350mg/L), Al conc. : 0.028M (750mg/L).

6.4 CONCLUSIONS

The experimental results obtained from the present work are summarized as follows.

The change of pH in the solution depends on the level of calcium hydroxide added, more than 0.054 mol/L of which is needed for removing Fe dissolved from the solution of 0.010M iron in 0.100M of oxalic acid. The formation of $Fe(OH)_3$ from the iron (III) oxalato complex solution was completed during the initial reaction, within about 15 minutes. The amount of calcium hydroxide added affects both the final pH and Fe concentration in the oxalic acid solution. When the sludge was used repeatedly its activity decreased because it consisted mainly of $CaC_2O_4{\cdot}H_2O$ and only a small amount of $Ca(OH)_2$ remained. The reaction temperature did not play an important role in the removal of iron from artificial ferric oxalate complex solutions, but the increase of temperature increased the removal efficiency of both Fe (III) and Al (III) from the clay leaching solution by adjusting the pH to an alkaline range with calcium hydroxide.

CHAPTER SEVEN

MODELLING OF THE KINETICS OF THE LEACHING REACTION

7.1 INTRODUCTION

7.1.1 Scope

The previous chapters report the outcome of several practical leaching systems involving oxalate and different types of iron oxide. Although these studies have demonstrated the effect of various parameters influencing the leaching reaction, strict control of these parameters has not yet been implemented. The modeling of the reaction kinetics therefore is restricted. Another issue of concern is that iron oxide can be dissolved via two mechanisms, either via chemical dissolution where Fe(III) will be formed, or if a reductive dissolution is more predominant, then Fe(II) is the major product.

The first objective for work reported in this chapter is to implement a technique to analyze iron (II) concentration colorimetrically using a UV-visible spectrophotometer, by complexing iron (II) with orthophenanthroline, an agent imparting a bright red colour for the Fe(II) complex. The measurement for the absorption of the red color of iron (II)-orthophenanthroline will in turn be used to determine the concentration of iron (II) in the solution. Moreover, this method will be extended to measure total iron content available by reducing all iron (III) to iron (II) with a reducing agent before adding the coloring agent. In this way, both iron (II) and iron (III) concentration can be determined for the same sample.

The second part of the research work aims to dissolve iron (III) oxides in oxalic acid under various conditions. The reaction system was conducted using particles of narrow size ranges, known oxalic acid concentration at controlled pH and

temperature. In several experiments the enhancement of the reaction rate was also demonstrated when magnetite was added to the leaching system.

Controlled experiments will yield reliable data for reaction kinetic modeling. For homogeneous systems the reaction kinetics is usually based on the shrinking core model. For such systems, the solid particles are assumed to be spherical which shrink as the reaction interface move to the inner core of the particles. The reaction kinetics can then be controlled by either (i) the diffusion of reactants through a product layer formed during the reaction, or (ii) the kinetic step of the electrochemical reaction involved during leaching.

7.1.2 Shrinking Core Model

Several textbooks have described the fundamental aspects related to the shrinking core models (Levenspiel, 1972). As the dissolution could take place via chemical and/or reductive dissolution, the heterogeneous reaction can only be represented by the general form as shown:

$$aOx_{(f)} + bH^{+}_{(f)} + cFe_2O_{3(s)} \rightarrow dFe_{(f)} + eCarb_{(f)} + H_2O \qquad (7\text{-}1)$$

where:

Ox	:	soluble oxalate species
H^+	:	hydrogen ions
$Fe_{(f)}$	:	soluble Fe species, either Fe(III) oxalate or Fe(II) oxalate
$Carb_{(f)}$	:	carbonate species as product of oxalate oxidation

As there is no solid formed as product from the dissolution, the model tested is the surface reaction model, of which conversion-time relationship is given as:

$$1-(1-x)^{(1/3)} = (V/r_o)\, k\, [Ox]^m\, [H^+]^n\, t \qquad (7\text{-}2)$$

where:

x	:	percentage of dissolution
V	:	volume of solution
r_o	:	initial average radius of the particles

In order to test the surface reaction, the percentages of iron extraction obtained at all parameters were substituted into $1-(1-x)^{(1/3)}$ and plotted against reaction time. The gradients attained for different particle sizes, pH and oxalate concentration are plotted against log of hydrogen and oxalate concentration, respectively.

7.2 EXPERIMENTAL

7.2.1 Analytical Techniques

A colorimetric technique was adopted for the determination of Fe(II) in the system. This analytical method will detect iron by measuring the amount of light absorbed by iron (II) –phenanthroline at 510nm. In general, uncomplexed iron (II) exhibits little color in solution and has zero absorptivity in visible light. [1] Hence, 1, 10-phenanthroline was added to complex with Fe(II), producing an orange-red color solution. The structure of this compound is shown as below:

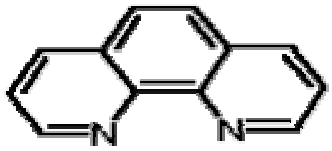

1,10-phenanthroline

The red colored complex formed is exceptionally stable and is free from variations in color, due to minor changes in pH or temperature.

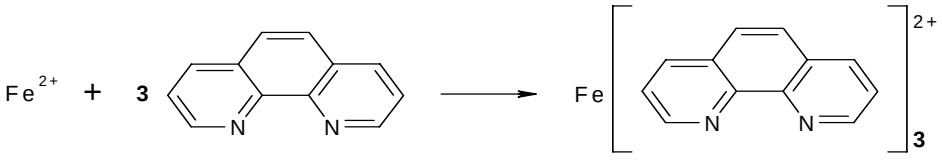

1, 10-phenanthroline Iron (II)-1, 10-phenanthroline complex

Thus, the amount of iron can be selectively determined spectrophotometrically. Measuring the concentration of iron (II)-orthophenanthroline is equivalent to the measuring the concentration of iron (II) available. Fundamentally, it is the only phenanthroline complex, having a strong absorption of light at 510nm, which is due to iron (ll), and independent of the presence of other cations or complexes.

Concentrated sulphuric acid will destroy the structure of iron oxalate by freeing iron from the oxalate. Hydroxylamine hydrochloride intercepts oxygen and prevents oxidation of ferrous iron to ferric iron. This is because the ion has to be iron (IIl) before the formation of the red complex. The reaction for this reduction is shown below:

$$2HONH_3^+Cl^- + 4Fe^{3+} <===> N_2O + 4Fe^{2+} + H_2 + 6H^+ + 2Cl^-$$

Then, the complex formation reaction can be best described:

$$Fe^{2+} + 3\ C_{12}H_2N_2\ (aq) \rightarrow [(C_{12}H_2N_2)3Fe]^{2+}\ (aq)\ \text{an orange-red complex}$$

7.2.2 Experimental Techniques and Methods

1M ammonium acetate, 10% hydroxylamine hydrochloride and 0.3% 1, 10 phenanthroline were prepared to be added into various iron solutions. 6M sulphuric acid was prepared and added into iron (II) and/or iron (III) oxalate, to prepare the stock solutions.

Preparation of 500ml iron (II) oxalate:
Dissolve 1.68g of sodium oxalate and 1.74g iron (II) sulphate in distilled water. Pipette 5ml of concentrated sulphuric acid into the beaker.

Preparation of 500ml oxalate solution (blank):
Dissolve 1.68g sodium oxalate in distilled water. Pipette 5ml of concentrated sulphuric acid.

Preparation of 500ml iron (III) oxalate:
Dissolve 1.25g of iron (III) sulphate/ammonium ferric sulphate and 1.68g of sodium oxalate in distilled water. Pipette 5ml of concentrated sulphuric acid

Preparation of standard solutions:
Standards were prepared by taking known aliquots of standard iron solution of 1mg/ml into a 250ml of volumetric flask. Measure 2 ml of the iron standard into a 100ml volumetric flask. Add 1ml of ammonium acetate and 1 ml of hydroxylamine

hydrochloride. Followed by 10 ml of 1, 10 phenanthroline. Repeat using 4, 6, 8, 10, 20, 30, 40, 50 and 60 ml of the iron solution.

Preparation of solutions of iron (II)/iron (III) oxalate:
Transfer 428.6ml of iron (II)/iron (III) oxalate into a 1000ml volumetric flask. Add 25 ml of 6M H_2SO_4. Use a pipette and transfer 10ml of this liquid to a 100ml volumetric flask. Add 1 ml of ammonium acetate, 1ml of hydroxylamine hydrochloride and 10 ml of 1, 10 phenanthroline. Repeat using 2, 4, 6 and 8 ml of this solution.

Preparation of 100ml oxalate solution (blank):
1ml of ammonium acetate, 1ml of hydroxylamine hydrochloride and 10ml of 1, 10 phenanthroline were added.

7.2.3 Leaching experiments

The leachant was prepared by dissolving 1.34g sodium oxalate in distilled water. Addition of sulphuric acid was required to adjust the pH to the value required. Each reaction run was conducted for 2 hours and samples were taken out at 10, 30, 60 and 120 minutes.

For each sample 1ml of liquor was withdrawn into a 25ml of volumetric flask. This was followed by addition of 1ml of 1M ammonium acetate, 1ml of 10% hydroxylamine hydrochloride and 10ml of 0.3% phenanthroline.

Samples were then subjected to absorption measurement at 510nm, following a calibration curve produced with standards prepared as per previous procedures.

7.3 RESULTS AND DISCUSSION

For all conditions studied, analysis of the samples taken through out the course of the reaction confirmed that there was no Fe(III) existing in the solution. This implied that the dissolution of hematite was via a reductive mechanism. The overall reaction was therefore a redox reaction, formed by two half cells:

- Oxidation of oxalate to form carbonic acid or carbon dioxide:

$$HC_2O_4^{1-} = H^+ + 2CO_2 + 2e^- \quad (7\text{-}3)$$

- Reduction of hematite forming Fe(II) oxalate:

$$2H^+ + Fe_2O_3 + 4HC_2O_4^{1-} + 2e^- = 2Fe(C_2O_4)_2^{2-} + 3H_2O \quad (7\text{-}4)$$

The overall reaction is therefore:

$$H^+ + Fe_2O_3 + 5HC_2O_4^{1-} = 2Fe(C_2O_4)_2^{2-} + 3H_2O + 2CO_2 \quad (7\text{-}5)$$

The reaction indicates that species involved in the leaching would be hydrogen ions, oxalate and iron oxide (hematite particles). It is expected that the reaction kinetics be governed by solution pH, concentration of oxalate and the nature of iron oxide particles.

7.3.1 Effect of Particle Size

Effect of particle dimension on the dissolution rate were compared by using different size fractions while other parameters remained constant. It could clearly be observed in Figure 7.1 that the dissolution of iron oxide was dependent on different particle size ranges over the test (2 hours at 103^{o}C and pH3). As inferred from the results, the dissolution of iron oxide increases with decreasing particle average radius. This is due to the increase in surface area that can be attacked by oxalic acid. Even at the fine range of 45-71 micron, only around 16% of iron oxide was dissolved within 2 hours, limiting the scope of full dissolution within reasonable time for practical application. At the coarsest range (160-210 micron) less than 5% of the iron oxide was dissolved, showing a very slow rate of reaction, even at 103 deg.C. For larger size ranges the dissolution of hematite is much less as shown in Figure 7.1B. The relationship of equation 7.2 when tested shows reasonable linearity (correlation coefficient, R^2 >0.98) for most conditions shown in Fig. 7.2.

7.3.2 Effect of Oxalic Acid Concentration

The effect of oxalic acid on dissolution rate was determined at the following molar ratio, 4:1, 8:1 and 12:1, corresponding to oxalic concentrations of 3.36g/L, 6.72g/L and 10.1g/L or 0.037M, 0.074M and 0.112M, respectively. As expected, the rate of dissolution of iron oxide increases with oxalate concentration as shown in Figure 7.3.

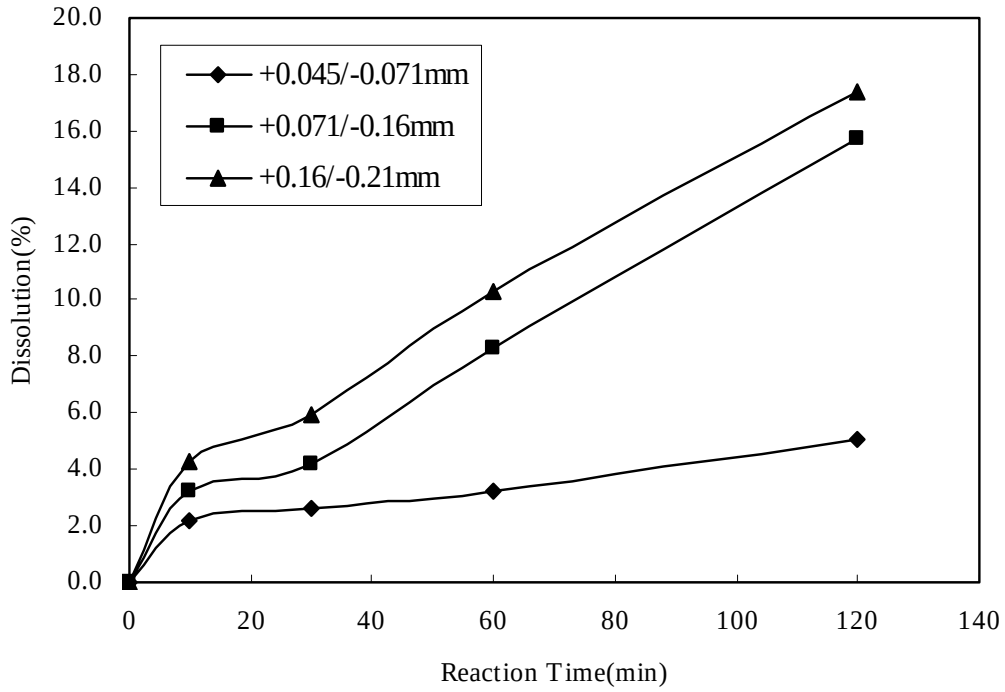

(A)

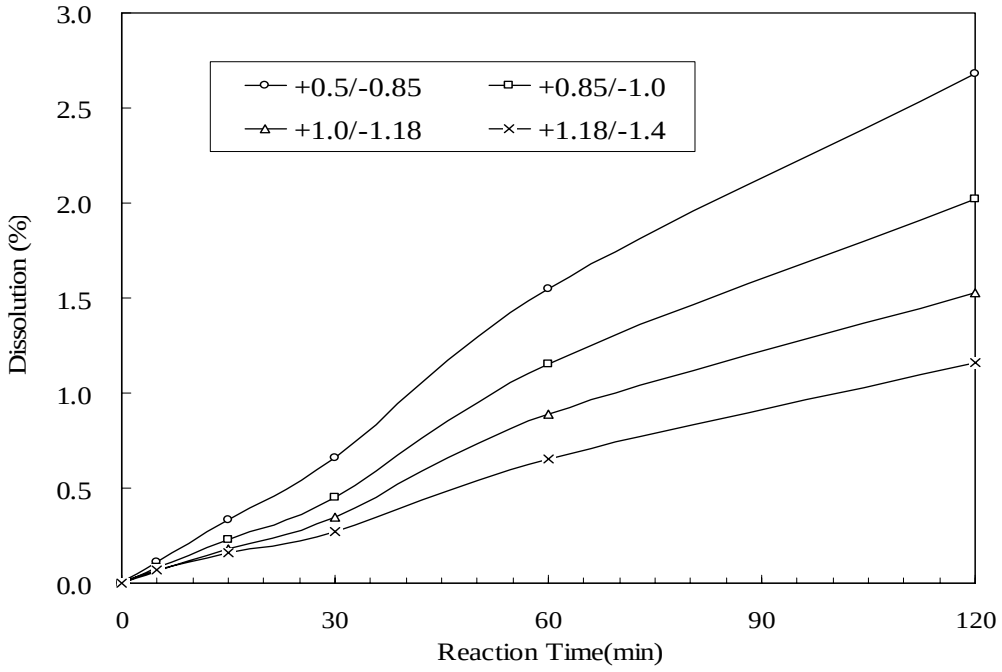

(B)

Figure 7.1 Dissolution of iron oxide (hematite) (Molar Ratio: 4:1, pH: 3.0 and Temperature: 103^{o}C) at different particle size ranges: (A) micron size range and (B) mm size range.

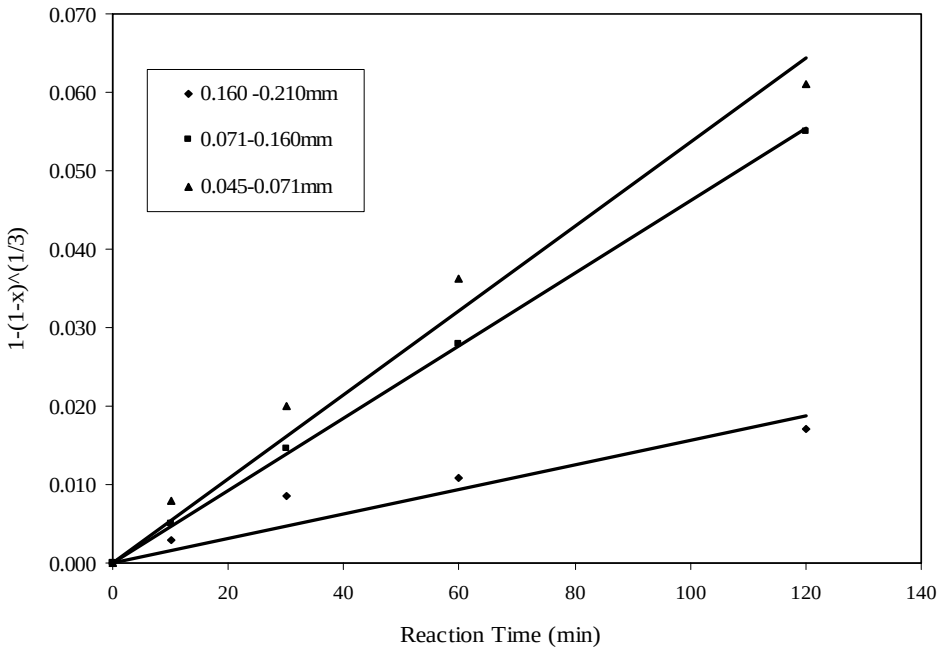

y = 1.57E-04x
R^2 = 8.74E-01

y = 4.61E-04x
R^2 = 1.00E+00

y = 5.36E-04x
R^2 = 9.79E-01

(A)

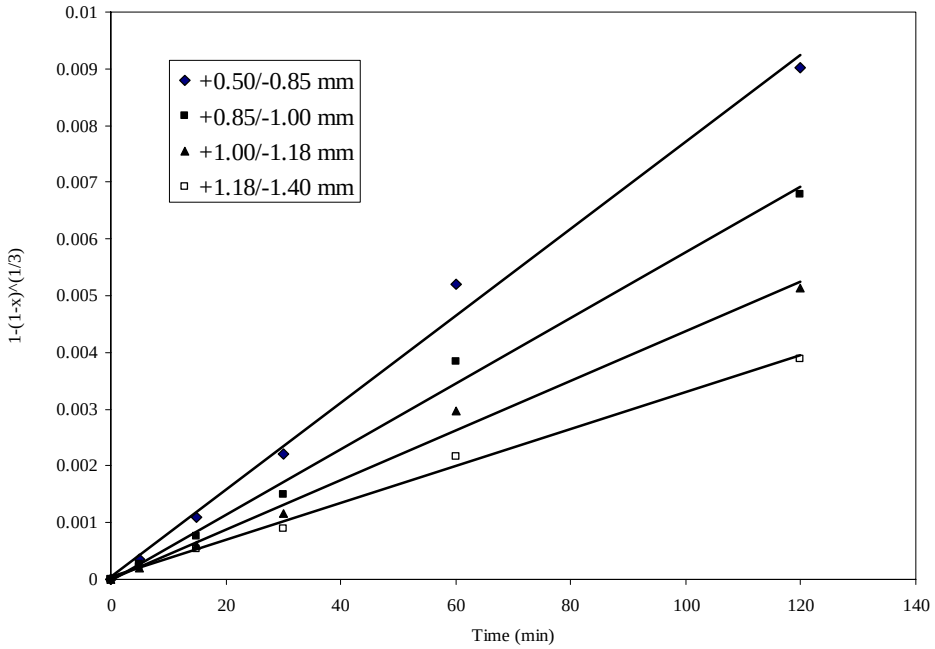

y = 6E-05x - 2E-05
R^2 = 0.9934

y = 4E-05x - 1E-06
R^2 = 0.9919

y = 8E-05x + 4E-05
R^2 = 0.9937

y = 3E-05x + 4E-05
R^2 = 0.9953

(B)

Figure 7.2 Comparison of rate-time equations of different particle sizes.

Rate plots also confirmed the linearity of Equation 7-2 as shown in Figure 7.4. From the Ln (gradient of rate expression) vs Ln (concentration of oxalate) one can also derive the value of m in the rate equation represented by equation 7-2. This plot shows a straight line relationship yielding m of 0.81.

7.3.3 Effect of pH

The effect of pH has been demonstrated in previous chapters on the leaching of industrial materials. The reaction kinetics could be improved significantly in the practical range of pH 1.5-3.0 as shown with hematite materials in this series of test. The linearity of equation 7-2 above was also confirmed as shown in Figure 7.5 for dissolution of up to 5% in the best case (pH 3.0) for test conditions of 4:1 molar ratio of oxalate and iron (II) oxide as hematite, 103 deg. C).

From the slopes of these straight lines, gradients were determined and then plotted against [H+] on a Ln-Ln plot as shown in Figure 7.6. The straight line yielded a slope of 5.9, which is the value of n in the rate equation 7-2.

The very high slope indicates the sensitivity of pH during the reaction. The dual role of hydrogen ion in protonating the –OH group on the oxide surface (Fig 2.2) and the protonation of the oxalate ligand as the pH drop (discussed in detail in section 2.2.1.2) could explains for this high slope.

This significant effect of $[H^+]$ or pH indicates that speciation of $HC_2O_4^-$ to form H^+ and $C_2O_4^{2-}$ required for both reactions as discussed on equation 4.4 is a critical step.

7.3.4 Effect of Fe(III) oxide

The dissolution of Fe(III) oxide as hematite follows a kinetic control shrinking core model as shown in the above sections, under controlled test conditions. For most test conditions the dissolution has been extremely slow, reaching less than 20% in 2 hours at pH 3.0 and 103 deg.C using particles of -160 +210 micron size range. Such a slow rate is not practical for commercial application as materials have to be finely ground and a high temperature has to be employed.

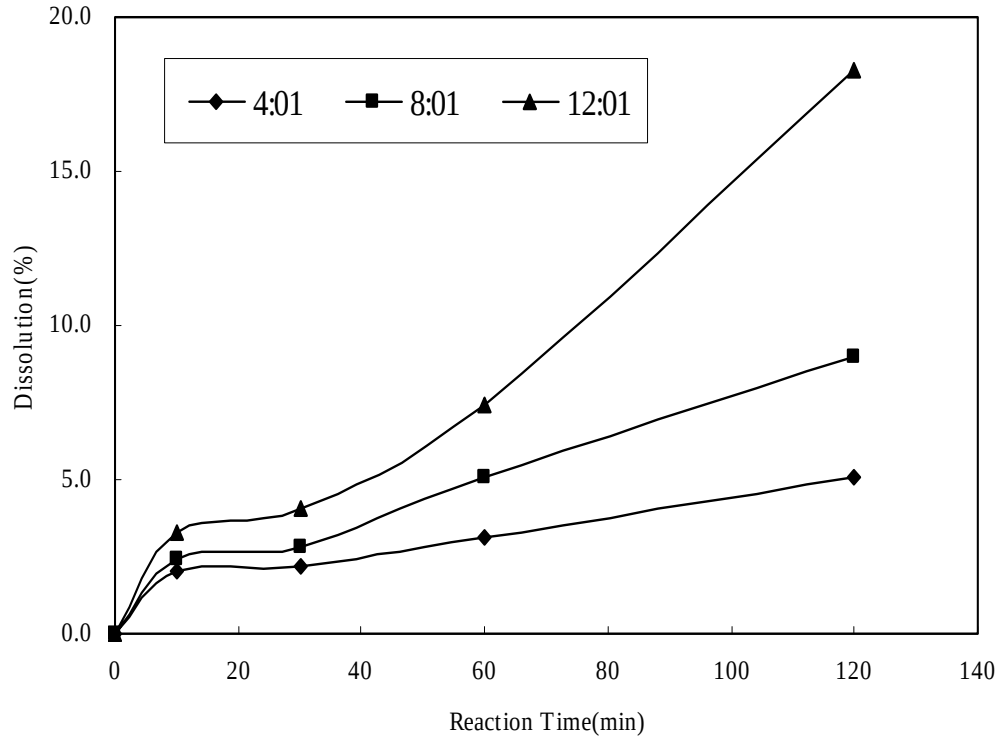

(A)

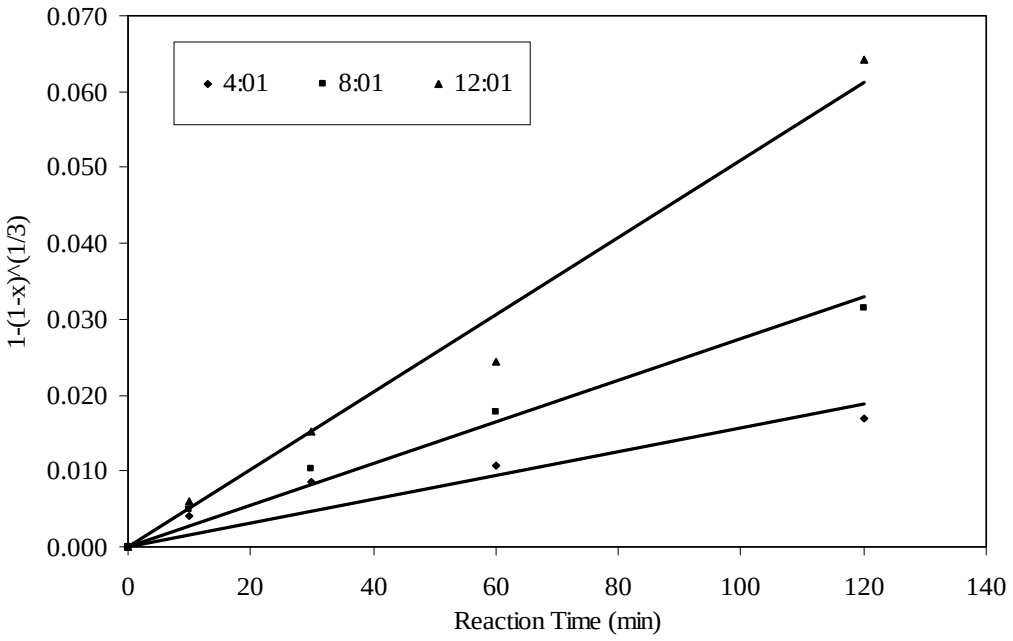

(B)

Figure 7.3 Dissolution at different oxalate concentrations of 0.37M, 0.74M and 0.112M corresponding to molar ratio of 4:1, 8:1 and 12:1, respectively (Particle size (+160/-210) micron, pH 3.0 and Temperature: 103^{o}C).

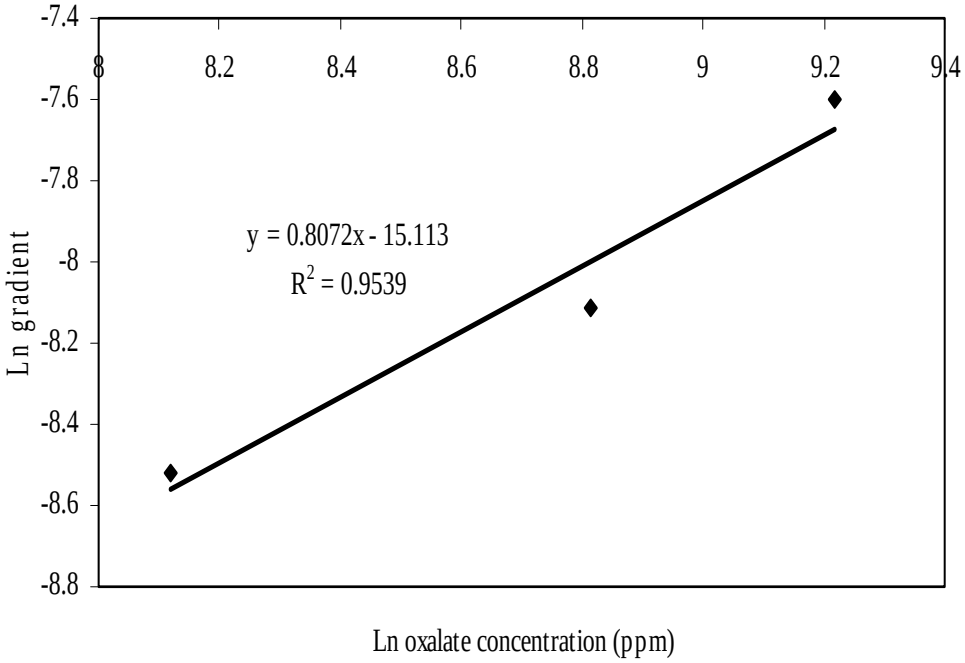

Figure 7.4 Dissolution at different oxalate concentrations of 0.37M, 0.74M and 0.112M corresponding to molar ratio of 4:1, 8:1 and 12:1, respectively (Particle size: -160/+210 micron, pH 3.0 and Temperature: 103^{o}C).

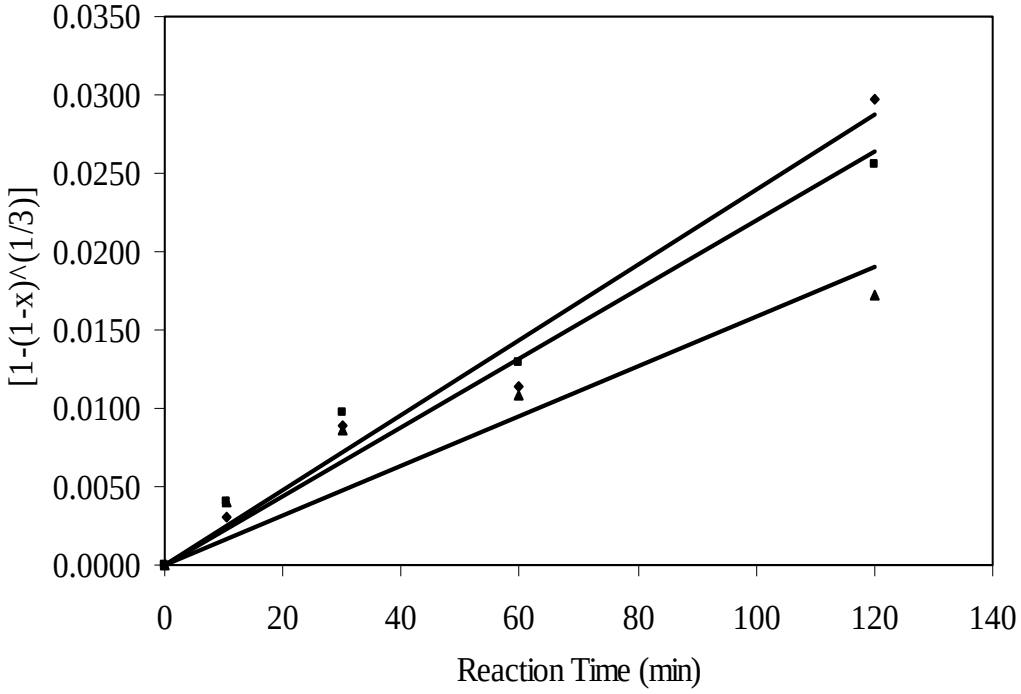

Figure 7.5 Plot of rate expression showing linearity of kinetic control rate reation (Test conditions: pH 1.5 (triangle) , pH 2.0 (square) and pH 3.0 (diamond), 103 deg.C, molar ratio 4:1, particle size range +160/-212 microns).

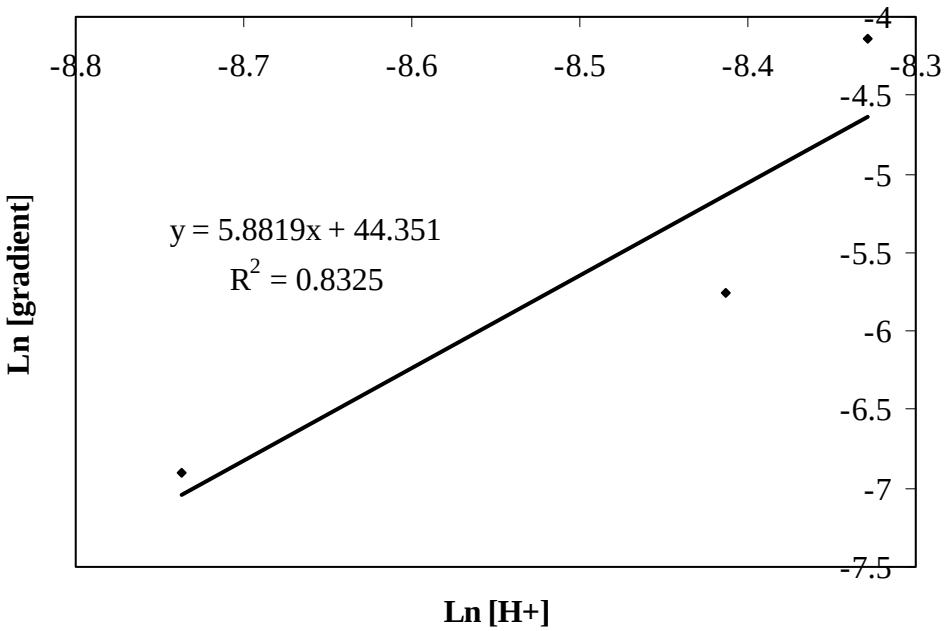

Figure 7.6 Plot of Ln [gradient] vs Ln [H+] yielding the coefficient m for [H+] in the rate equation 7-2.

However, it has also been confirmed in these controlled experiments that the dissolution was significantly improved if magnetite (Fe_3O_4) was added. As shown in the following series of tests for coarser materials (mm size range), the dissolution within 2 hours has been accelerated.

Figure 7.7 shows a 10-fold increase in dissolution compared with the same cases when no magnetite was added (Figure 7.1B). Temperature is still a critical parameter as shown in Figure 7.8, where reasonable rate can only be achieved at 100. ^{o}C.

Deviation from the kinetic control mechanism of the shrinking core model was shown in Figure 7.9 for different size ranges and Figure 7.10 for different temperatures. Typical linear plots of the rate expression of $[1-1(1-x)^{1/3}]$ vs time could no longer be observed.

Such behaviour indicates that magnetite not only improves the reaction rate significantly, it also changes the controlling mechanism of the rate determining step.

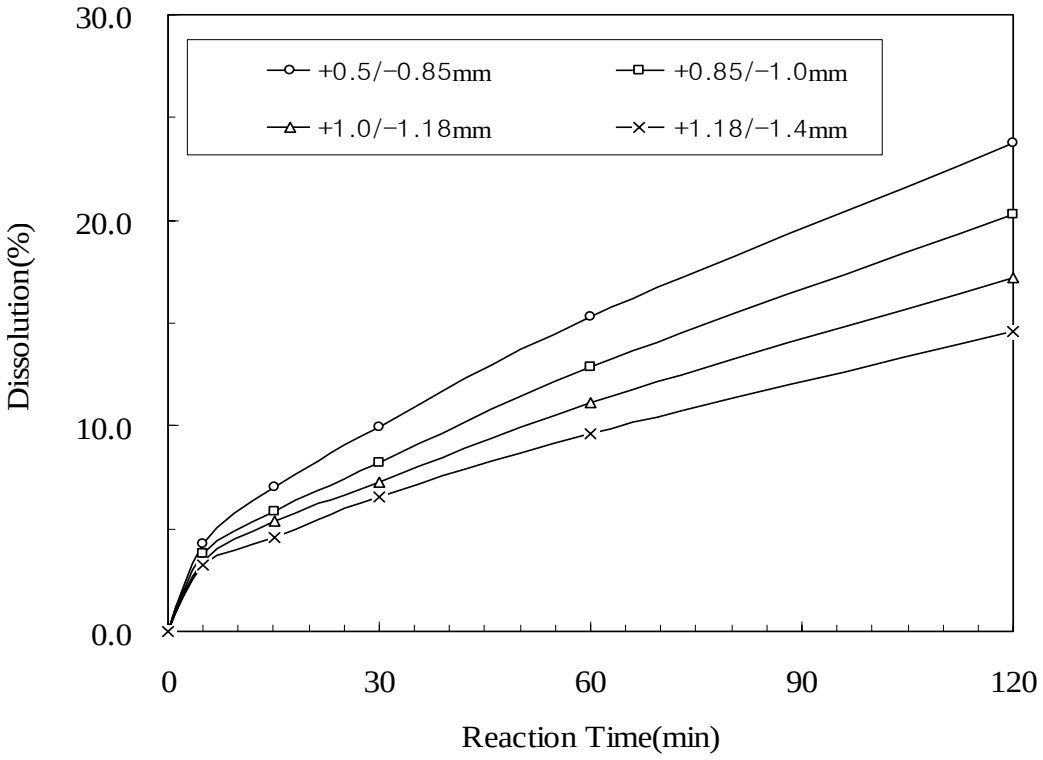

Figure 7.7 Dissolution vs time plots for different size ranges at 103 deg.C, 4:1 molar ratio, pH 3.0, , 4 g/L Fe_2O_3 + 0.4 g/L Fe_3O_4).

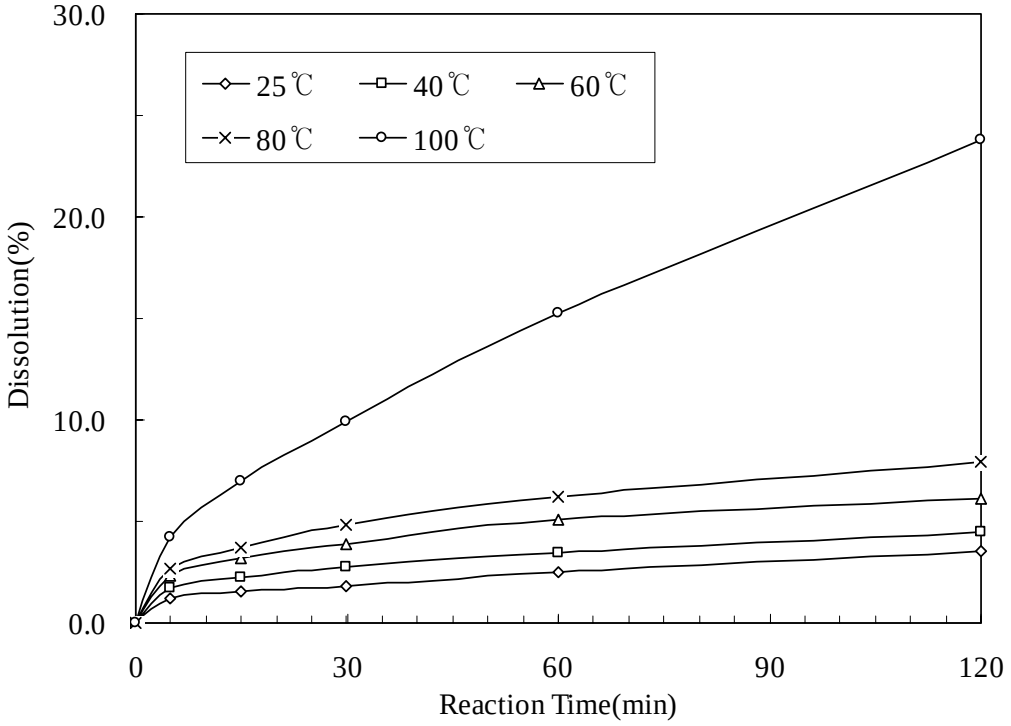

Figure 7.8 Dissolution vs time plots for different temperatures (pH 3.0, particle size: -0.500/+0.85 mm, 4:1 molar ratio, 4 g/L Fe_2O_3 + 0.4 g/L Fe_3O_4).

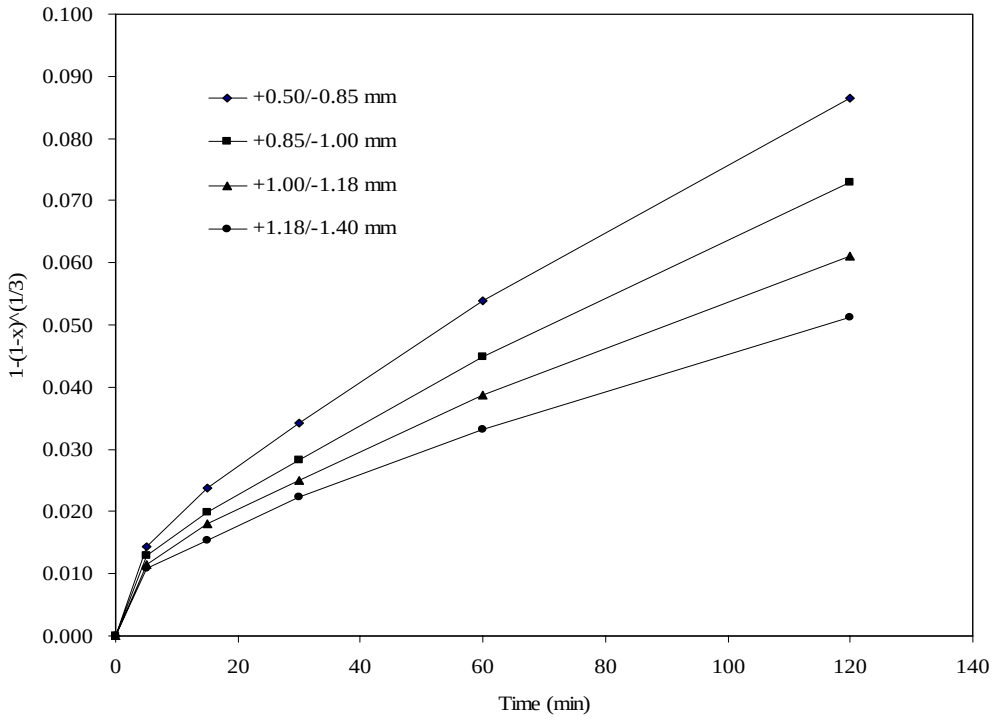

Figure 7.9 Rate expression $[1-1(1-x)^{1/3}]$ vs time plots for different size ranges at 103 deg.C, 4:1 molar ratio, pH 3.0, 4 g/L Fe_2O_3 + 0.4 g/L Fe_3O_4).

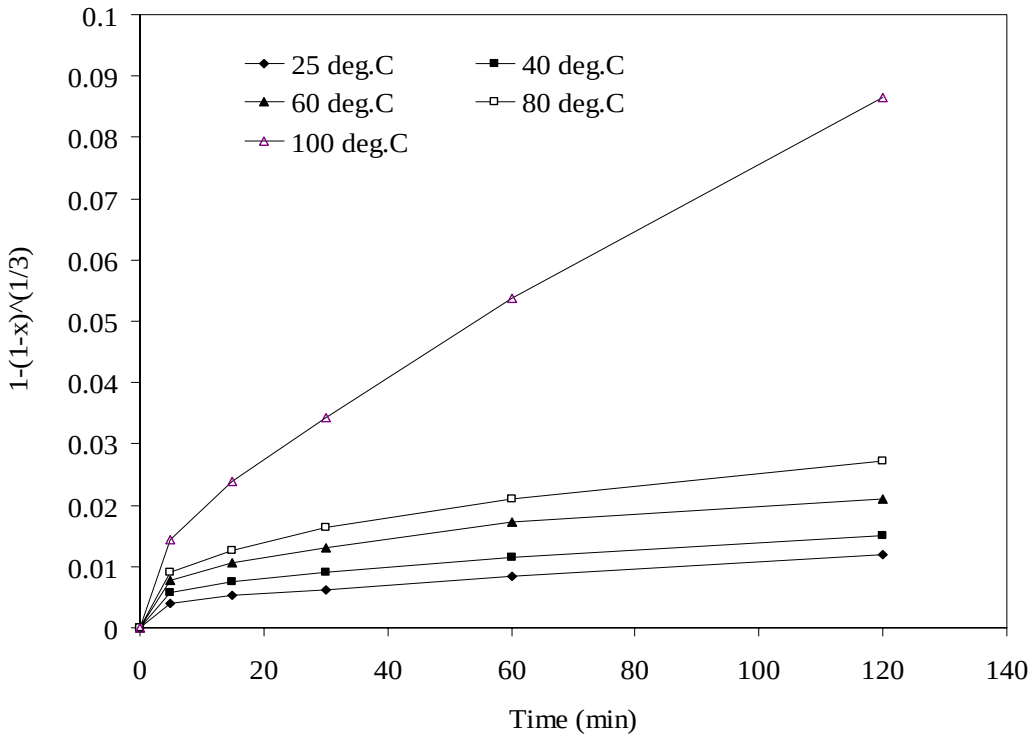

Figure 7.10 Rate expression $[1-1(1-x)^{1/3}]$ vs time plots for different temperatures, particle size: -0.500/+0.850 mm,4:1 molar ratio, pH 3.0, 4 g/L Fe_2O_3 + 0.4 g/L Fe_3O_4).

7.4 CONCLUSIONS

Kinetic studies using different types of iron oxide of narrow particles size ranges have shown:

- The dissolution of hematite follows a kinetic control shrinking core model. The rate expression relating conversion to time:

  $$1-(1-x)^{(1/3)} = (V/r_o)\, k\, [Ox]^n\, [H^+]^m\, t$$

  shows linearity for pure hematite systems, where n is 0.85 and m is 5.9.

- The dissolution rate is significantly improved when magnetite containing iron (II) oxide was added to the leaching system, showing the catalytic effect of Fe-Oxalate complex during the reaction as experienced and shown in chapter 4.

- Reasonable reaction rate can only be achieved at high temperatures (80-100 deg.C) and coarse iron oxide particles can be dissolved in a reasonable time only when magnetite is added. However, it seems that magnetite changes the process controlling the reaction kinetics and the kinetic-controlled mechanism no longer applies in this case.

CHAPTER EIGHT

CONCLUSIONS AND RECOMMENDATIONS

8.1 CONCLUSIONS

The experimental results obtained from the present work are summarized as follows:

The thermodynamic analysis of reactions involving sodium, ammonium and iron oxalate complexes were investigated and the value of standard free energy, ΔG^o was calculated by using thermodynamically data tables and tested solubility products.

In titration tests, the increase of temperature causes the increasing of solubility of sodium, potassium or ammonium-oxalate solids, resulting in the increasing stability of ionized species in solution. When NaOH was added, the precipitated solid was found to be $NaHC_2O_4 \cdot H_2O$ and $Na_2C_2O_4 \cdot H_2O$. With the increasing of pH by NaOH titrant, the $NaHC_2O_4 \cdot H_2O$ was stable until pH 3.5 but with further increase in pH $Na_2C_2O_4 \cdot H_2O$ is more stable. However, in NH_4OH, the $NH_4HC_2O_4 \cdot H_2O$ precipitate is more stable than $(NH_4)\ {}_2C_2O_4 \cdot H_2O$. These precipitates however are not stable and all redissolved at pH>2,.5. The use of NH_4OH for pH control is therefore better than for NaOH.

The dissolution of iron oxide rust (which contains goethite, iron trihydroxide and lepidocrocite) is faster compared to that observed for hematite without a slow induction period at the beginning of the dissolution process. For iron rust materials, their mainly chemical dissolution process is also affected by the pH of the initial solution, oxalic acid concentration and temperature. In particular, the temperature and initial pH of solution controlled the dissolution rate of hematite rather than that of iron oxide rust. The nature of the particle surface changes during dissolution and the hematite particle shows regular pits forming, but the iron oxide rust particles shows finer structure for dissolution. Hematite predominantly dissolved via a redox process, and the formation of ferrous oxalate solid on the hematite surface could be the reason slowing down the dissolution of hematite.

The dissolution rate of magnetite was found to be twice higher than that of hematite under the same experimental conditions. The dissolution rate of hematite was remarkably low at 25-90℃, but increased rapidly at 100℃. At 100℃, there was an induction period in the beginning of the reaction. The increase of oxalic acid concentration, in turn, increased the dissolution rate, especially above 0.095 M. The surface of hematite particles was dissolved differently depending on the initial pH. The dissolution characteristics exhibited the bell-shaped curves of dissolution vs time. While the dissolution under pH 1.1 was due to the attack of hydrogen ion (H^+), the regular pits formed initially were changed into the plates at pH 2.5, observed for the reductive dissolution process. The degree of dissociation of oxalic acid was affected by reaction temperature. The initial pH also had an effect on the dissolution of hematite.

The mineralogical investigation of the tested clay sampls resulted found sericite and α-quartz as main components. Hydrated iron oxide was found to be a major iron impurity and aluminum silicate hydroxide [$K(Fe,Al)_2(Si,Al)_4O_{10}(OH)_2$] appeared to be a second phase of Fe-contamination of the clay samples. The optimum leaching could be obtained using 0.38 M oxalic acid for two clay samples at 100℃, a L/S ratio 5:1 and 500 rpm stirring rate within 60 min. The leaching percentage for J-A (coarse fraction) and J-B (fine fraction) samples reached 83% and 96%, respectively. The overall removal of iron from the clays was obtained to be 86.2% and 89.6% for J-A and J-B, respectively. The lower pulp density and smaller particle size improve the leaching efficiency. The finally refined clay products had a whiteness of about 90 %, which means they can be used for making high-class ceramic products.

The change of pH in the solution depends on the concentration of calcium hydroxide added, more than 0.054 mol/L addition of which is needed for removing Fe from dissolved solution of 0.010M iron in 0.100M of oxalic acid. The formation of $Fe(OH)_3$ from the iron (Ⅲ) oxalato complex solution was completed during the initial reaction, within about 15 minutes. The concentration of calcium hydroxide added effects both pH and Fe concentration in the oxalic acid solution. When the sludge was used repeatedly, the activity was decreased, because it consists mainly of $CaC_2O_4{\cdot}H_2O$ and the small amount of $Ca(OH)_2$ remained. The reaction temperature does not play an important role in the removal of iron from artificial ferric oxalato complex solutions, but the increase of temperature increased the removal efficiency of both Fe (Ⅲ) and Al (Ⅲ) from the

clay leaching solution by adjusting the pH-value to an alkaline range with calcium hydroxide.

The kinetics of dissolution of Fe(Ⅲ) oxide was controlled by solution pH, concentration of oxalate, particle size and the nature of the iron oxide. In pure systems, the reaction is controlled by a kinetic step, following the shrinking core model. However, in the presence of Fe_3O_4 (magnetite) the shrinking core model no longer holds, although the reaction rate is significantly increased.

8.2 RECOMMENDATIONS

Future study should focus on the following aspects:

1) Further extensive investigation on the chemical behavior of sodium and ammonium oxalate complexes speciation in oxalic acid system including:

- Investigation of the probable oxalate complexes species which are solid or liquid species in solution.
- Determination of the free energy of formation of probable oxalate complexes species and identification of the compound by applying analytical instruments such as SEM, XRD, AA and FTIR.
- Extensive study on the formation of iron oxalate complexes with the effects of existing cation (Na^+ and NH_4^+) in solution by added titrants and the chemical behavior of cations in solution.
- Solubility study of the probable oxalate complexes species and precipitates obtained in different experimental conditions.
- Development of stability diagram for Na^+-NH_4^+-Fe(II/III) oxalate complexes in oxalic acid solution system.

2) Study on the kinetics of the destruction of oxalate ion by oxidation/reduction reagent or electrochemistry methods.

3) Finally, study on the determination of mass balance for plant design and the

modeling of the process for simulation of the utilization of oxalic acid as a common leaching reagent.

CHAPTER NINE

REFERENCES

Afonso, M. D. S., Morando, P. J., Blesa, M. A., Banwart, S. and Stumm, W., (1990), The Reductive Dissolution of Iron Oxides by Ascorbate, J. of Colloid and Interface Science, Vol. 138, No. 1, p. 74-82.

Allen, G. C., Kirby, C. and Sellers, R. M., (1988), The Effect of the Low-oxidation-state Metal Ion Reagent Tris-picolinatovanadium (II) Formate on the Surface Morphology and Composition of Crystalline Iron Oxides, J. Chem. Soc. Faraday Trans. (I) Vol. 84, p. 355-364.

Ambikadevi, V. R. and Lalithambika, M., (2000), Effect of Organic Acids on Ferric Iron Removal from Iron-stained Kaolinite, Applied Clay Science Vol. 16, p.133-145.

Bailar, J. C. et al., (1989), Chemistry, 3rd edn. HBJ. Publishers, p. A21-A24..

Banwart, S., Davies, S. and Stumm, W., (1989), The Role of Oxalate in Accelerating the Reductive Dissolution of Hematite(α-Fe_2O_3) by Ascorbate, Colloids and Surfaces, Vol. 39, p. 303-309.

Baumgartner, E. C., Blesa, M. A. and Maroto, A. J. G., (1982), Kinetics of the Dissolution of Magnetite in Thioglycolic Acid Solutions, J. Chem. Soc. Dalton Trans., p. 1649-1654.

Baumgartner, E. C., Blesa, M. A., Marinovich, H. A. and Maroto, A. J. G., (1983), Heterogeneous Electron Transfer as a Pathway in the Dissolution of Magnetite in Oxalic Acid Solutions, Inorg. Chem., Vol. 22, p. 2224-2226.

Blesa, M. A. and Maroto, A. J. G., (1986), Dissolution of Metal Oxides, J. Chem. Phys., Vol. 83, p. 757-764.

Blesa, M. A., Marinovich, H. A., Baumgartner, E. C. and Maroto, A. J. G., (1987), Mechanism of Dissolution of Magnetite by Oxalic Acid - Ferrous Ion Solutions, Inorg. Chem., Vol. 26, p. 3713-3717.

Blesa, M. A., Morando, P. J. and Regazzoni, A. E., (1994), Chemical Dissolution of Metal Oxides, CRC Press Inc. p. 269-308.

Bloom, P. R. and Nater, E. A., (1991), Kinetics of Dissolution of Oxide and Primary Silicate minerals, In; Spark, D. L. and Suarez, D. L. (Eds.), Rates of Soil Chemical Processes, Soil Sci. Soc. Am. Spec. Publ., Vol. 21, p. 151-189.

Borghi, E. B. Morando, P. J. and lesa, M. A., (1991), Dissolution of Magnetite by Mercaptocarboxylic Acids, Langmuir, Vol. 7, p. 1652-1659.

Borghi, E.B., Regazzoni, A.E., Maroto, A.J.G. and Blesa, M.A., 1989, Redctive Dissolution of Magnetite by Solutions Containing EDTA and Fe(II): J. Colloid Interface Sci., Vol. 130, No. 2, p. 299-310.

Brady. J. E. and Holum. J. R., (1996), Chemistry: The study of Matter and Its Changes, 2nd Ed., John Wiley & Sons Inc..

Brown, W. E. B., Dollimore, D. and Galwey, A. K., (1980), Reactions in the Solid State, In: Bamford, C. H. and Tipper, C. F. H. (Eds), Comprehensive Chemical Kinetics, Elsevier Amsterrdam, Vol. 22, p. 41-109.

Bruyere, V. I. E. and Blesa, M. A., (1985), Acidic and Reductive Dissolution of Magnetite in Aqueous Sulphuric Acid: Site-binding Model and Experimental Results, J. Electroanal. Chem., Vol. 182, p. 141-156.

Casey, W. H., (1995), Surface Chemistry During the Dissolution of Oxide and Silicate Materials, In: Vaughan, D. J. and Pattrick, R. A. D. (Eds), Mineral Surfaces, Min. Soc. Series 5, Chapman and Hall, London, p. 185-217.

Cepria, G., Uson, A., Perez-Arantegui, J. and Castillo, J.R., 2003, Identification of iron (III) oxide and hydroxyl-oxides by voltammetry of immobilized microparticles, Analytical Chim. Acta, 477, 157-168.

CRC Handbook of Chemistry and Physics, Ed: Weast R. and Astle, M.J., pub: CRC Press, Florida, USA

Chang, H. C. and Matijevic, E., (1983), Interactions of Metal Hydrous Oxides with Chelating Agents, IV. Dissolution of Hematite, J. Colloid Interface Sci., Vol. 92, p. 479-488.

Charlot, G., (1954), Qualitative Inorganic Analysis - A New Physico-Chemical Approach (trans. from the French by R.C.Murray), John Wiley & Sons, INC., p. 307-309.

Chatzeioannou, Th. P., (1972), Qualitative Analysis and Chemical Equilibrium. Athens, p. 591.

Chiarizia, R. and Horwitz, E. P., (1991), New Formulations for Iron Oxides Dissolution, Hydrometallurgy, Vol. 27, p. 339-360.

Cornell, R. M. and Giovanoli, R., (1988a), Acid Dissolution of Akaganeite and Lepidocrocite: The Effect on Crystal Morphology, Clays Clay Min. Vol. 36, p. 385-390.

Cornell, R. M. and Giovanoli, R., (1993), Acid Dissolution of Hematites of Different Morphologies, Clay Min., Vol. 28, p. 223-232.

Cornell, R. M. and Schindler, P. W., (1987), Photochemical Dissolution of Goethite in Acid/Oxalate Solution, Clays Clay Miner., Vol. 35, No. 5, p. 347-352.

Cornell, R. M. and Schwertmann, U., (1996), The Iron Oxides, VCH Publishers, New York (USA), p. 175.

Cornell, R. M., Posner, A. M. and Quirk, J. P., (1974), Crystal Morphology and the Dissolution of Goethite. J. Inorg. Nucl. Chem., Vol. 36, p. 1937-1946.

Cornell, R. M., Posner, A. M. and Quirk, J. P., (1975), The Complete Dissolution of Goethite, J. Appl. Chem. Biotechnol., Vol. 25, p. 701-706.

Cornell, R. M.; Posner, A. M. and Quirk, J. P., (1976), Kinetics and Mechanisms of the Acid Dissolution of Goethite (α-FeOOH), J. Inorg. Nucl. Chem., Vol. 38, p. 563-567.

Dean, J. A, (1992), Lange's Handbook of Chemistry, McGraw-Hill, Inc., 14th Ed., p. 6.1

Diggle, J. W., (1973), Dissolution of Oxide Phases, In: Diggle, J. W. (Ed.), Oxides and Oxide Films, Vol. 2, Marcel Dekker, New York, p.281-386.

Engell, H. J., (1956), The Solution of Oxides in Dilute Acids - The Electrochemistry of Ion Crystals, Z. physik. Chem. (Frankfurt) [N.F.], Vol. 7, No. 2, p. 158-181.

Fischer, W. R., (1972), Die Wirkung von Zweiwertmann Eisen auf Losung und Umwandlung von Eisen(III)-hydroxiden, In: Schliching E. and Schwertmann, U., (Eds.), Pseudogley and Gley., Trans. Comm. Vand VI Int. Soil. Sci. Soc., VCH Weinheim, p. 37-44.

Fischer, W. R., (1976), Differentiation of Oxalate Soluble Iron Oxides, Z. Pflanzenernaehr. Bodenkd., Vol. 139, No. 5, p. 641-646.

Fischer, W. R., (1987), Standard Potentials (E_o) of Iron (III) Oxides under Reducing Conditions, Z. Pflanzenerahr. Bodenk, Vol. 150, p. 286-289.

Fischer, W. R.., (1983), Theoretical Considerations of the Reductive Dissolution of Iron(III) Oxides, Z. Pflanzenernaehr. Bodenkd., Vol. 146, No. 5, p. 611-622.

Fogler, H. S., (1992), Elementals of Chemical Reaction Engineering, 2nd Ed., Prentice-

Hall, Inc.

Frenier, W. W. and Growcock, F. B., (1984), Mechanism of Iron Oxides Dissolution, A Review of Recent Literature, Corrosion NACE Vol. 40, p. 663-668.

Gallagher, K. J., (1965), The Effect of Particle Size Distribution on the Kinetics of Diffusion Reactions in Powders, In: Schwab, G. M. (Ed), Reactivity of Solids, Elservier, Amsterdam, p. 201-203.

Giovanoli, R. and Brutsch, R., (1975), Kinetics and Mechanisms of the Dehydration of γ-FeOOH, Thermochim. Acta, Vol. 13, p. 15-36.

Gohr, H. and Lange, E., (1957), Interpretation of Passivity, and Especially of the Flade Standard Potential, of Iron, Z. Elektrochem., Vol. 61, No. 10, p. 1291-1301.

Gorichev, I. G. and Kipriyanov, N. A., (1984), Regular Kinetic Features of the Dissolution of Metal Oxides in Acidic Media, Russian Chem. Rev., Vol. 53, p. 1039-1061.

Hidalgo, MdV., Katz, N. E., Maroto, A. J. G. and Blesa, M. A., (1988), The Dissolution of Magnetite by Nitrilotriacetatoferrate (II), J. Chem. Soc. Faraday Trans. (I), Vol. 84, No. 1, p. 9-18.

Hixon, A. W. and Crowell, J. H., (1931), Dependence of Reaction Velocity upon Surface Agitation, Ind. Eng. Chem., Vol. 23, p. 923-981.

Huang, H. H., (2000), Stabcal-Stability Calculation for Aqueous Systems.

Jepson, W. B., (1988), Structural Iron in Kaolinites and in Associated Ancillary Minerals, In; Stucki, J. W., Goodman, B. A. and Schwertmann, U., (Eds), Iron in Soils and Clay Minerals, D. Reidel Publ. Co., Dordrecht, Holland, NATO ASI Ser, Vol. 217, p. 467-536.

Kabai, J., (1973), Determination of Specific Activation Energies of Metal Oxides and Metal Oxide Hydrates by Measurment of Rate of Dissolution, Acta Chem. Acad. Sci. Hung., Vol. 78, p. 57-73.

Khentov, A. I., Sukhotin, A. M., (1979), Reduction Potential of γ-ferric Oxide in 0.5M Sulfuric Acid, Zashch. Met., Vol. 15, No. 1, p. 66-67.

Kim, S. G., Kwon, K. J., Lee H. Y. and Oh, J. K., (1997), Leaching of Iron from Domestic Low-Grade Halloysite with Oxalic Acid, J. of The Korean Inst. of Mineral and Energy Resources Eng., Vol. 34, p. 94-101.

Ladd, J. A. and Miller, M. J., (1988), US Patent No. 5196580.

Lee, S. O., Kim, S. G., Oh, J. K. and Shin, B. S., (1998), Dissolution Characteristics of

Hematite and Magnetite with Oxalic Acid, J. of The Korean Inst. of Mineral and Energy Resources Eng., Vol. 35, p. 520-526.

Lee, S. O., Kim, W. T, Oh, J. K. and Shin, B. S., (1997), Iron Removal of Clay Minerals with Oxalic Acid, J. of the Mining and Materials Processing Institute of Japan, Vol. 113, No. 11, p. 847-851.

Lee, S. O., Oh, J. K. and Shin, B. S., (1999), Dissolution of Iron Oxide Rust Materials using Oxalic Acid, J. of the Mining and Materials Processing Institute of Japan, Vol. 115, No. 11, p. 815-819.

Levenspiel, O., 1972, Chemical Reaction Engineering, Published Wiley International.

Lide, D. R., et al., (1996-97), CRC handbook of Chemistry and Physics, 77th, CRC Press, INC., p.5-86.

Lim-Nunez, R. and Gilkes, R. J., (1987), Acid Dissolution of Synthetic Metal-containing Goethites and Hematites, In: Schultz, L. G., Van Olphen, H. and Mumpton, F. A., (Eds), Proc. Int. Clay Conf. Denver, (1985), Clay Min. Soc. Bloomington, Indiana, p. 197-204.

Marabini, A. M., Falbo, A., Passariello, B., Esposito, M. A. and Barbaro, M., (1993), Chemical Leaching of Iron Industrial Minerals, XVlll International Mineral Processing Congress, Sydney, p. 23-28.

Martell. A. E. and Smith, R. M., (1996), Crystal Stability Constants: Other Organic Ligands, Plenum Press, New York and London, Vol. 3, p. 284-332.

Mehra, O. P. and Jackson, M. L., (1960), Iron Oxide removal from Soils and Clays by Dithionite-citrate System Buffered with Sodium Bicarbonate, Clays Clay Min., Vol. 7, p. 317-327.

Moon, J. K., Park, S. Y., Jung, C. H., Lee, J. W. and Oh, W. Z., (1997), A Study on the Recycling of Radioactively Contaminated Metal Waste, J. of Korean Inst. of Resources Recycling, Vol. 6, No. 3, p. 22-27.

Noyes, R., (1994), Unit Operation in Environmental Engineering, Noyes Publications.

Oh, J. K. and Shin B. S., et al., (1998), Development of New Chemical Leaching Process for the Removal of Iron from Clay Minerals, 96R-NM01-P-06 (a Report of Research in Korea).

Panias, D., Taxiarchou, M., Douni, I., Paspaliaris, I. and Kontopoulos, A., (1996), Thermodynamic Analysis of the Reactions of Iron Oxides: Dissolution in Oxalic Acid, Canadian Metallurgical Quarterly, Vol. 35, No. 4, p. 363-373.

Panias, D., Taxiarchou, M., Paspaliaris, I. and Kontopoulos, A., (1996), Mechanisms of Dissolution of Iron oxides in Aqueous Oxalic Acid Solutions: Hydrometallurgy, Vol. 42, p. 257-265.

Park, K. C., Choi, S. C. and Park, Y. K., (1974), A Study on Iron Compounds Accompanied in Korean Kaolin Minerals, J. of the Korean Ceramic Society, Vol. 11, No. 2, p.22-30.

Patermarakis, G. and Paspaliaris, Y., (1989), The Leaching of Iron Oxides in Boehmite-bauxite by Hydrochloric Acid, Hydrometallurgy, Vol. 23, p. 77-90.

Postma, D., (1993), The Reactivity of Iron Oxides in Sediments: A Kinetic Approach, Geochim. Cosmochim. Acta., Vol. 57, p. 5027-5034.

Pourbaix, M. (1958), Atlas of Electrochemical Equilibria in Aqueous Solution, Pergamon Press.

Pourbaix, M. and Pourbaix, A. (1981): Diagrams of Chemical and Electrochemical Equilibria, Cebelcor, Brussels, p.35-42.

Rabinovich, V. A. and Khavin, Z. Ya., (1978), Short Chemical Handbook, 2nd Ed., pp. 392.

Rasmussen, H. and Nielsen, R. H., (1996), Iron Reduction in Activated Sludge Measured with Different Extraction Techniques, Water Research, Vol. 30, No. 3, 551-558.

Rubio, J. and Matijevic, E., (1979), Interactions of Metal Hydrous Oxides with Chelating Agents, I. β-FeOOH-EDTA, J. Colloid Interface Sci., Vol. 68, p. 408-421.

Rueda, E. H., Ballesteros, M. C., Grassi, R. L. and Blesa, M. A., (1992), Dithionite as a Dissolving Reagent for Goethite in the presence of EDTA and Citrate, Application to Soil Analysis. Clays Clay Min., Vol. 40, p. 575-585.

Rueda, E. H., Grassi, R. L. and Blesa, M. A., (1985), Adsorption and Dissolution in the System Goethite/Aqueous EDTA, J. Colloid Interface Sci., Vol. 106, p. 243-246.

Sato, N., Noda, T. and Kudo, K., (1974), Thickness and Structure of Passive Films on Iron in Acidic and Basic Solution, Electrochim. Acta, Vol. 19, p. 471-475.

Schott, J., Brantley, S., Crerar, D., Guy, Ch., Borsik, M. and Willaime, Ch., (1989), Dissolution Kinetics of Strained Calcite, Geochim. Cosmochim. Acta, Vol. 53, p. 373-382.

Schwertmann, U. and Cornell, R. M. (1991) : Iron Oxides in the Laboratory, VCH

Publishers, New York

Schwertmann, U., (1984a), The Influence of Aluminium on Iron Oxides, IX. Dissolution of Al-Goethites in 6M HCl, Clay Min., Vol. 19, p. 9-19.

Schwertmann, U., Cambier, P. and Murad, E., (1985), Properties of Goethites of Varying Crystallinity, Clays Clay Min., Vol. 33, p. 369-378.

Segal, M. G. and Sellers, R. M., (1980), Reactions of Solid Iron(III) Oxides with Aqueous reducing Agents, J. Chem. Soc. Chem. Comm., p. 991-993.

Segal, M. G. and Sellers, R. M., (1982), Kinetics of Metal Oxide Dissolution-Reductive Dissolution of Nickel Ferrite by Tris(picolinato)vanadium (II), J. Soc. Faraday Trans. (I), Vol.. 78, p. 1149-1164.

Segal, M. G. and Sellers, R. M., (1984), Advances in Inorganic and Bioinorganic Mechanisms, Ed : Sykes, A. G., Academic Press : London, Vol. l. No. 3, p. 97.

Sellers, R. M. and Williams, W. J., (1984), High-temperature Dissolution of Nickel Chromium Ferrites by Oxalic Acid and Nitrilotriacetic Acid, Faraday Discuss. Chem. Soc., Vol. 77, p. 265-274.

Shin, B. S., Kook, N. P., Choi, J. M., Cheung, M. K. and Kim, Y. J., (1990), A Study on the Benefication of Low Grade Pottery Stone-Sepatation Process by H.I.M.S. and Refining, J. of The Korean Inst. of Mineral and Energy Resources Eng., Vol. 27, No. 3, p. 184-192.

Sidhu, P. S., Gilkes, R. J., Cornell, R. M., Posner, A. M. and Quirk, J. P., (1981), Dissolution of iron Oxides and Oxyhydroxides in Hydrochloric and Perchloric Acids, Clays Clay Min., Vol. 29, p. 269-276.

Sokolova, L. A., Kossyi, G. G., Ovcharenko, V. I. and Kolotyrkin, Ya. M., (1976), On the Passivation of Iron in Oxalate Solutions, Zashch. Met., Vol. 12, No. 2, p. 145-153.

Stone, A. T. and Morgan, J. J., (1987), Reductive Dissolution of Metal Oxides, In: Stumm, W., (Ed.), Aquatic Surface Chemistry J., Wiley and Sons, New York, p. 221-254.

Stumm, W. and Furrer, G., (1987), The Dissolution of Oxides and Aluminum Silicates: Examples of Surface-coordination-controlled Kinetics, In: Stumm, W., (Ed.), Aquatic Surface Chemistry J., Wiley and Sons, New York, p. 197-219.

Stumm, W. and Sulzberger, B., (1992), The Cycling of Iron in Natural Environments: Considerations Based on Laboratory Studies of Heterogeneous Redox Processes, Geochim. Cosmochim. Acta, Vol. 56, p. 3233-3257.

Stumm, W., (1992), Chemistry of the Solid-water Interface, Wiley and Sons Inc, New York, p. 428.

Stumm, W., Furrer, G., Wieland, E. and Zinder, B., (1985), The Effects of Complex-forming Ligands on the Dissolution of Oxides and Aluminosilicates, In: Drever, J. I., (Ed.), The Chemistry of Weathering, D. Reidel, Dordrecht, The Netherlands, p. 55-74.

Sukhotin, A. M. and Berezin, M. Yu., (1982), Passivity of Iron in Oxalate Solutions, Zashch. Met., Vol. 18, No. 4, p. 511-515.

Sukhotin, A. M. and Khentov, A. I., (1980), Anodic Behavior of Iron Oxides and Repassivation of Iron in Acid Solutions, Elektrokhimiya, Vol. 16, No. 7, p. 1037-1041.

Sukhotin, A. M. and Osipenkova, I. G., (1978), Anodic Behavior of Manganese in Alkaline Solutions, Zh. Prikl. Khim.(Leningrad), Vol. 51, No. 4, p. 830-832.

Sukhotin, A. M., Khentov, A. I., Motornyi, A. V. and Shtarkman, M. A., (1980), Cathodic Behavior of γ-ferric Oxide in Acid Solutions, Leningr. Politekh. Inst., Leningrad, USSR. Zashch. Met., Vol. 16, No. 5, p. 567-571.

Sulzberger, B., Suter, C., Siffert, S., Banwart, S. and Stumm, W., (1989), Dissolution of Fe(III) (Hydr)oxides in Natural Waters: Laboratory Assessment on the Kinetics Controlled by Surface Coordination, Marine Chemistry, Vol. 28, p. 127-144.

Sumner, M. E., (1963), Effect of Iron Oxides on Positive and Negative Charges in Clays and Soils, Clay Minerals Bulletin, Vol. 5, p. 218-226.

Surana, V. S. and Warren, I. H., (1969), The Leaching of Goethite, Trans. Inst. Min. Metall., Sect. C: Min. Process. Extr. Metall., p. C133-CI39.

Suter, D., Banwart, S. and Stumm, W., (1991), Dissolution of Hydrous Iron(III) Oxides by Reductive Mechanisms. Langmuir, Vol. 7, p. 809-813.

Tehobanoglous, G. and Rurton, F., (1993), Waste Water Engineering, 3rd Ed., Metcalf and Eddy INC..

Tsimas, S. G., Komiotou, M. A., Moutsatsou, A. K. and Parissakis, G. K., (1995), Reducing the Iron Content of Kaolin from Milos, Greece, by a Hadrometallurgical Process, Trans. Instn. Min. Metall.(Sect. C: Mineral Process. Extr. Metall.), Vol. 104, C110-114

Valverde, N. and Wagner, C., 1976, Considerations on the Kinetics and the Mechanism of the Dissolution of Metal Oxides in Acidic Solutions, Ber. Bunsenges. Phys. Chem., Vol. 80, No. 4, p. 330-333.

Valverde, N., (1976), Investigations on the rate of Dissolution of Metal oxides in Acidic Solutions with Additions of Redox Couples and Complexing Agents, Ber Bunserges, Phys. Chem., Vol. 80, p. 333-340.

Veglio, F., Passariello, B., Barbaro, M., Plescia, P. and Marabini, A. M., (1998), Drum Leaching Tests in the Iron Removal from Quartz using Oxalic Acid and Sulphuric Acids, Int. J. Mineral Processing, Vol.54, p.183-200.

Veglio, F., Passariello, B., Toro, L., Marabini, A. M., (1996), Development of a Bleaching Process for a Kaoline of Industrial Interest by Oxalic, Ascorbic and Sulphuric Acids: Preliminary Study using Statistical Methods of Experimental Design, Ind. Eng. Chem. Res., Vol. 35, p. 1680-1687.

Vermilyea, D. A., (1966), The Dissolution of Ionic Compounds in Aqueous Media, J. Electrochem. Soc., Vol. 113, p. 1067-1070.

Vincze, L. and Papp, S., (1987), Individual Quantum Yields of $Fe^{3+}OX^{n2-}H^{m+}$ Complexes in Aqueous Acidic Solutions (OX^{2-} = $C_2O_4^{2-}$, n = 1-3, m = 0,1), J. Photochem., Vol. 36, No. 3, p. 289-296.

Vincze, L. and Papp, S., (1987), Individual Quantum Yields of $Fe^{3+}(HCO_2^-)^n$ Complexes (n = 1-4) in Aqueous Acidic Solutions, J. Photochem., Vol. 36, No. 3, p. 279-287

Weast, R. C. and Astle. M. J. (1983), CRC Handbook of Chemistry and Physics, CRC Press INC., p. B-101.

Zhang, Y., Kallay, N. and Matijevic, E., (1985), Interactions of Metal Hydrous Oxides with Chelating Agents, VII. Hematite - Oxalic and Citric Acid Systems, Langmuir, Vol. 1, p. 201-206.

APPENDIX 1: DATA FOR FIGURES

APPENDIX 1: DATA FOR FIGURES

Data for figure 3.1 : Titration of oxalic acid with NaOH at 27^{o}C.

NaOH (mL)	Change of pH in the different oxalic acid solution(100mL)		
	0.20M	**0.60M**	**1.00M**
0	1.21	0.96	0.76
5	1.34	1	0.79
10	1.51	1.05	0.82
15	1.76	1.11	0.86
20	2.24	1.17	0.9
25	3.1	1.23	0.94
30	3.59	1.31	0.95
35	3.98	1.39	0.99
40	4.48	1.44	1.03
45	11.46	**1.57**	1.08
50	12.2	**1.7**	**1.13**
55	12.4	**1.87**	**1.13**
60	12.57	**2.11**	**1.17**
65	12.68	**2.49**	**1.22**
70	12.74	**2.89**	**1.27**
75		**3.18**	**1.32**
80		**3.4**	**1.39**
85		**3.53**	**1.46**
90		**3.63**	**1.55**
95		**3.72**	**1.66**
100		**3.79**	**1.79**
105		3.92	**1.97**
110		4.07	**2.23**
115		4.24	**2.59**
120		4.46	**2.9**
125		4.79	**3.1**
130		6.06	**3.26**
135		11.89	**3.41**
140		12.18	**3.5**
145		12.34	**3.58**
150		12.44	**3.65**
155		12.52	**3.71**
160		12.58	**3.76**
165		12.62	**3.82**
170			**3.86**
175			**3.9**
180			**3.94**
185			**3.99**
190			4.06
195			4.14

200			4.24
205			4.35
210			4.5
215			4.72
220			5.27
225			11.27
230			11.84
230			12.07
240			12.21

Data for figure 3.2 : Titration of oxalic acid with NH_4OH at 27^oC.

NH_4OH(mL)	Change of pH in the different oxalic acid solution(100mL)		
	0.20M	**0.60M**	**1.00M**
0	1.23	0.93	0.83
5	1.52	1.02	0.88
10	2.23	1.13	0.93
15	3.54	1.28	**1**
20	4.39	1.46	**1.09**
25	8.52	1.71	**1.21**
30	8.67	2.09	**1.35**
35	9.18	2.67	**1.52**
40	9.33	3.11	**1.69**
45	9.44	3.42	**1.86**
50	9.52	3.69	**2.03**
55	9.59	3.97	2.37
60	9.65	4.33	2.71
65	9.71	5.2	2.98
70	9.76	8.26	3.19
75		8.62	3.38
80		8.82	3.54
85		8.95	3.71
90		9.05	3.88
95		9.13	4.07
100		9.2	4.31
105		9.26	4.68
110		9.31	6.86
115		9.36	8.18
120		9.4	8.48
125		9.43	8.65
130		9.47	8.78
135		9.5	8.88
140		9.53	8.96
145			9.02
150			9.08
155			9.13
160			9.17
165			9.21
170			9.25
175			9.29
180			9.32
185			9.35
190			9.38
195			9.4
200			9.43
205			9.45

Data for figure 3.3 : Titration of oxalic acid with KOH at 27^{o}C.

KOH(mL)	Change of pH in the different oxalic acid solution(100mL)		
	0.20M	**0.60M**	**1.00M**
0	1.23	0.93	0.88
5	1.37	0.98	**0.92**
10	1.58	**1.04**	**0.95**
15	1.92	**1.10**	**0.98**
20	2.72	**1.19**	**1.03**
25	3.46	**1.30**	**1.09**
30	3.91	**1.44**	**1.17**
35	4.43	**1.61**	**1.26**
40	11.67	**1.78**	**1.37**
45	12.42	**1.98**	**1.51**
50	12.66	**2.14**	**1.66**
55	12.79	**2.33**	**1.83**
60	12.89	2.67	**1.98**
65		3.00	**2.13**
70		3.23	**2.26**
75		3.42	**2.36**
80		3.59	**2.45**
85		3.74	**2.53**
90		3.89	**2.59**
95		4.05	2.67
100		4.24	2.87
105		4.46	3.03
110		4.81	3.18
115		6.53	3.30
120		12.17	3.41
125		12.47	3.51
130		12.63	3.60
135		12.74	3.70
140		12.82	3.79
145			3.88
150			3.97
160			4.18
170			4.44
180			4.87
185			5.39
190			11.80
195			12.26
200			12.47
210			12.70

Data for figure 3.4 : Titration of oxalic acid (1.0 M) with 1.0M NaOH

NaOH(mL)	Change of pH in the different temperature in solution(100mL)		
	27°C	**50°C**	**80°C**
0	0.76	0.74	0.81
5	0.79	0.78	0.88
10	0.82	0.82	0.92
15	0.86	0.86	0.99
20	0.9	0.91	1.04
25	0.94	0.96	1.07
30	0.95	1.01	1.11
35	0.99	1.05	1.17
40	1.03	1.1	1.22
45	1.08	1.16	1.27
50	1.13	1.21	1.32
55	**1.13**	1.27	1.39
60	**1.17**	1.33	1.45
65	**1.22**	1.4	1.51
70	**1.27**	1.47	1.6
75	**1.32**	1.55	1.67
80	**1.39**	1.64	1.76
85	**1.46**	1.74	1.86
90	**1.55**	1.85	1.98
95	**1.66**	1.98	2.13
100	**1.79**	**2.15**	2.32
105	**1.97**	**2.35**	2.53
110	**2.23**	**2.57**	2.74
115	**2.59**	**2.94**	2.94
120	**2.9**	**3.09**	3.09
125	**3.1**	**3.21**	3.22
130	**3.26**	**3.31**	3.33
135	**3.41**	**3.4**	3.43
140	**3.5**	3.48	3.53
145	**3.58**	3.55	3.62
150	**3.65**	3.63	3.7
155	**3.71**	3.71	3.78
160	**3.76**	3.79	3.87
165	**3.82**	3.87	3.94
170	**3.86**	3.96	4.02
175	**3.9**	4.05	4.11
180	**3.94**	4.14	4.2
185	**3.99**	4.25	4.31
190	4.06	4.37	4.43
195	4.14	4.53	4.57
200	4.24	4.73	4.75
205	4.35	5.07	5.03
210	4.5	9.22	5.77

215	4.72	11.01	10.27
220	5.27	11.26	10.6
225	11.27	11.41	10.76
230	11.84	11.51	10.87
230	12.07	11.58	10.94
240	12.21	11.64	11

Data for figure 3.5 : Titration of oxalic acid (1.0 M) with 1.0M NH_4OH.

NH_4OH(mL)	Change of pH in the different temperature in solution(100mL)		
	27°C	**50°C**	**80°C**
0	0.83	0.8	0.73
5	0.88	0.92	0.81
10	**0.93**	1	0.92
15	**1**	1.09	1.04
20	**1.09**	1.19	1.16
25	**1.21**	1.3	1.27
30	**1.35**	1.42	1.4
35	**1.52**	1.54	1.54
40	**1.69**	1.55	1.7
45	**1.86**	1.69	1.89
50	**2.03**	1.87	2.14
55	2.37	2.12	2.49
60	2.71	2.46	2.87
65	2.98	2.81	3.14
70	3.19	3.09	3.35
75	3.38	3.31	3.53
80	3.54	3.49	3.69
85	3.71	3.65	3.84
90	3.88	3.81	4.02
95	4.07	3.97	4.18
100	4.31	4.15	4.39
105	4.68	4.38	4.69
110	6.86	4.7	5.36
115	8.18	5.71	6.78
120	8.48	7.61	6.96
125	8.65	7.93	7.18
130	8.78	8.11	7.29
135	8.88	8.24	7.42
140	8.96	8.34	7.52
145	9.02	8.42	7.6
150	9.08	8.47	7.67
155	9.13	8.53	7.72
160	9.17	8.58	7.77
165	9.21	8.62	7.81
170	9.25	8.65	7.86
175	9.29	8.69	7.91
180	9.32	8.72	7.93
185	9.35	8.75	7.95
190	9.38	8.78	7.95
195	9.4	8.81	7.96
200	9.43	8.82	7.97
205	9.45	8.83	8

Data for figure 3.6 : Titration of oxalic acid (1.0 M) with 1.0M KOH.

KOH(mL)	Change of pH in the different temperature in solution(100mL)		
	27°C	**50°C**	**80°C**
0	0.88	0.79	0.8
5	**0.92**	0.84	0.87
10	**0.95**	0.89	0.94
15	**0.98**	0.95	0.99
20	**1.03**	**1.02**	1.03
25	**1.09**	**1.08**	1.09
30	**1.17**	**1.13**	1.13
35	**1.26**	**1.18**	1.21
40	**1.37**	**1.24**	1.28
45	**1.51**	**1.31**	1.35
50	**1.66**	**1.38**	1.42
55	**1.83**	**1.45**	1.5
60	**1.98**	1.53	1.59
65	**2.13**	1.61	1.68
70	**2.26**	1.7	1.78
75	**2.36**	1.81	1.89
80	**2.45**	1.94	2.02
85	**2.53**	2.09	2.18
90	**2.59**	2.28	2.38
95	2.67	2.5	2.62
100	2.87	2.74	2.87
105	3.03	2.94	3.08
110	3.18	3.12	3.25
115	3.3	3.25	3.39
120	3.41	3.37	3.51
125	3.51	3.48	3.62
130	3.6	3.58	3.71
135	3.7	3.68	3.81
140	3.79	3.77	3.89
145	3.88	3.86	3.98
150	3.97	3.95	4.07
155	4.07	4.04	4.16
160	4.18	4.14	4.26
165	4.3	4.25	4.36
170	4.44	4.51	4.48
175	4.62	4.7	4.63
180	4.87	4.97	4.81
185	5.39	5.61	5.08
190	11.8	11.2	5.76
195	12.26	11.58	10.52
200	12.47	11.77	10.89

Figure 4.2 Effect of oxalic acid concentration on the dissolution of (a) hematite and (b) iron oxide rust (Temperature: 100℃, initial pH: 2.5, impeller speed: 450 rpm and particle size: 105～149㎛).

(a) hematite

Time (min)	0.048M	0.095M	0.190M	0.286M	0.381M
0	0	0	0	0	0
5	0.24	0.36	0.49	0.86	1.21
15	1.25	2.56	2.86	4.71	5.20
30	3.17	5.48	18.03	27.44	34.28
60	7.89	14.82	34.47	44.00	47.42
120	14.63	22.54	44.47	49.68	52.00

(b) iron oxide rust

Time (min)	0.050M	0.100M	0.250M	0.476M
0	0	0	0	0
5	31.11	47.12	91.50	94.00
15	42.22	67.78	94.00	96.00
30	51.11	76.79	97.00	99.00
60	56.67	85.33	100.00	100.00
120	65.56	89.91	100.00	100.00

Figure 4.3 The effect of initial pH on dissolution of (a) hematite at 100℃ with 0.190M oxalic acid concentration and (b) iron oxide rust at 95℃ with 0.250M oxalic acid concentration (Impeller speed: 450 rpm and particle size: 105～149㎛).

(a) hematite

pH	30min	60min
1.1	4.10	17.50
1.5	4.99	24.69
2.0	7.48	36.00
2.5	18.03	44.47
3.0	8.23	38.00
4.0	0.60	4.90

(b) iron oxide rust

pH	5 min	30 min
0.8	56.02	93.53
1.5	75.44	95.20
2.0	87.83	95.28
2.5	91.50	97.00
3.0	88.05	96.45
3.5	76.00	89.22
4.5	40.27	56.99

Figure 4.4 The effect of temperature on the dissolution of (a) hematite at 0.190M oxalic acid concentration and (b) iron oxide rust at 0.250M oxalic acid concentration (Initial pH: 2.5, impeller speed: 450 rpm and particle size: 105～149㎛).

(a) hematite

Time (min)	25℃	40℃	60℃	70℃	80℃	90℃	100℃
0	0	0	0	0	0	0	0
5	0.02	0.03	0.05	0.08	0.12	0.19	0.49
15	0.03	0.03	0.07	0.13	0.23	0.43	2.86
30	0.03	0.05	0.12	0.20	1.10	2.57	18.03
60	0.04	0.07	0.20	0.35	1.35	4.42	34.97
120	0.04	0.11	0.52	0.84	2.12	7.40	44.47

(b) iron oxide rust

Time (min)	20℃	40℃	60℃	80℃	95℃
0	0	0	0	0	0
5	1.86	5.09	18.52	84.11	87.76
10	2.82	8.82	34.67	86.80	92.44
20	4.06	16.29	63.52	90.00	96.11
40	6.04	32.54	74.09	93.50	100.00
60	8.26	47.00	79.14	94.01	100.00

Figure 4.6 The dissolution of hematite and magnetite with 0.10M oxalic acid concentration (Temperature: 95℃, initial pH: 1.66, impeller speed: 450 rpm, particle size, -16/+20mesh).

Time (min)	Hematite	Magnetite
0	0	0
5	0.24	0.45
10	0.49	0.99
20	0.98	2.09
40	2.03	4.11
60	3.06	5.80
120	6.60	11.05
180	9.40	17.00

Figure 5.4 Leaching tests on J-A as a function of reaction temperatures (Oxalic acid concentration: 0.38M, L/S: 5:1, Agitation: 500 rpm).

Time (min)	100°C	75°C	50°C	25°C
0	0	0	0	0
5	42.18	9.38	7.81	1.56
10	54.00	14.06	14.06	4.69
20	62.50	20.31	17.19	7.81
40	67.19	45.31	23.44	9.38
60	68.75	46.86	42.19	23.44
120	73.44	54.69	53.13	31.25

Figure 5.5 Leaching tests on J-B as a function of reaction temperatures (Oxalic acid concentration: 0.38M, L/S: 5:1, Agitation: 500 rpm).

Time (min)	100°C	75°C	50°C	25°C
0	0	0	0	0
5	72.00	23.44	21.86	9.38
10	72.75	40.63	35.94	10.94
20	74.08	48.00	43.00	14.06
40	78.50	56.00	52.00	25.00
60	86.70	68.00	60.94	32.81
120	93.95	74.00	70.31	48.44

Figure 5.6 Leaching tests on J-A as a function of Oxalic acid concentration (Temperature: 100℃, L/S: 5:1, Agitation: 500 rpm).

Time (min)	0.48M	0.38M	0.19M
0	0	0	0
5	53.00	51.20	35.60
10	57.00	63.00	43.40
20	58.00	71.50	54.30
40	60.50	76.20	71.50
60	66.80	77.80	73.10
120	69.90	82.40	80.00

Figure 5.7 Leaching tests on J-B as a function of Oxalic acid concentration (Temperature: 100℃, L/S: 5:1, Agitation: 500 rpm).

Time (min)	0.48M	0.38M	0.19M
0	0	0	0
5	67.18	72.00	82.25
10	68.18	74.00	84.38
20	68.18	78.00	89.06
40	73.44	82.00	93.00
60	78.44	86.70	95.00
120	89.06	93.95	96.00

Figure 5.8 Leaching tests on J-A as a function of L/S ratio (Oxalic acid concentration: 0.38M, Temperature: 100℃, Agitation: 500 rpm).

Time (min)	L/S 4:1	L/S 5:1	L/S 6.7:1	L/S 10:1
0	0	0	0	0
5	44.00	51.20	49.40	49.00
10	51.00	63.00	60.60	55.80
20	59.00	71.50	69.90	66.80
40	65.00	76.20	71.50	77.80
60	72.00	77.80	76.50	87.00
120	77.00	82.40	84.00	92.00

Figure 5.9 Leaching tests on J-B as a function of L/S ratio (Oxalic acid concentration: 0.38M, Temperature: 100℃, Agitation: 500 rpm).

Time (min)	L/S 4:1	L/S 5:1	L/S 6.7:1	L/S 10:1
0	0	0	0	0
5	65.00	72.00	79.68	84.38
10	68.04	74.00	87.50	87.50
20	70.33	78.00	91.10	90.63
40	72.45	82.00	95.00	94.00
60	76.01	86.70	94.00	95.00
120	83.00	93.95	94.00	94.50

Figure 6.1 The change of pH with the concentration of calcium hydroxide (Oxalic acid conc. : 0.100M, Fe : 0.010M, pH : 2.5, Temp. : 25℃).

Time (min)	0.027M	0.040M	0.054M	0.067M	0.081M
0	2.50	2.50	2.50	2.50	2.50
5	3.57	4.41	7.6	8.13	11.71
15	3.71	4.72	7.94	9.03	12.06
30	3.73	4.93	7.76	11.86	12.16
60	3.74	5.2	7.72	11.68	12.27
90	3.74	5.39	7.71	11.86	12.32
120	3.74	5.53	7.71	11.92	12.35

Figure 6.2 Effect of calcium hydroxide concentration on the removal % of Fe (Oxalic acid conc. : 0.100M, Fe : 0.010M, pH : 2.5, Temp. : 25℃).

Time (min)	0.027M	0.040M	0.054M	0.067M	0.081M
0	0.00	0.00	0.00	0.00	0.00
5	48.00	53.00	90.28	95.95	100.00
15	52.19	55.80	92.80	99.85	100.00
30	52.30	56.27	94.18	100.00	100.00
60	52.95	57.03	95.21	100.00	100.00
120	54.00	59.00	96.12	100.00	100.00

Figure 6.3 Effect of reaction temperature on the removal % of Fe (Calcium hydroxide conc.: 0.054M, Oxalic acid conc. : 0.100M, Fe : 0.010M, pH : 2.5).

Time (min)	25℃	40℃	60℃	85℃
0	0.00	0.00	0.00	0.00
5	90.28	85.28	87.15	90.70
15	92.80	89.00	90.61	92.74
30	94.18	93.56	92.96	93.63
60	95.21	96.42	94.73	95.52
120	96.12	97.00	95.58	96.60

Figure 6.4 Effect of oxalic acid concentration on the removal % of Fe (Calcium hydroxide conc.: 0.054M, Fe : 0.010M, pH : 2.5, Temp. : 25℃).

Time (min)	0.050M	0.100M	0.300M
0	0.00	0.00	0.00
5	99.66	90.28	83.47
15	100.00	92.80	83.74
30	100.00	94.18	84.14
60	100.00	95.21	84.00
120	100.00	96.12	84.08

Figure 6.5 Effect of iron (Ⅲ) concentration on the removal % of Fe (Oxalic acid conc. : 0.100M, Calcium hydroxide conc.: 0.054M, pH : 2.5, Temp. : 25℃).

Time (min)	0.008M*l* Fe	0.010M*l* Fe	0.030M*l* Fe	0.060M*l* Fe
0	0.00	0.00	0.00	0.00
5	73.53	80.56	90.13	100.00
15	79.51	85.59	89.60	100.00
30	81.93	88.35	89.20	100.00
60	84.75	90.41	89.05	100.00
120	86.39	92.24	89.02	100.00

Figure 6.6 Effect of various initial pH on the removal % of Fe (Oxalic acid conc. : 0.100M, Fe : 0.010M, Calcium hydroxide conc.: 0.054M, Temp. : 25℃).

Time (min)	pH 3.52	pH 2.55	pH 1.55
0	0.00	0.00	0.00
5	92.00	90.28	59.00
15	92.00	92.80	66.02
30	95.00	94.18	69.32
60	96.04	95.21	70.40
120	98.87	96.12	71.71

Figure 6.7 The change of pH on number of reusing times of the precipitated sludge (Oxalic acid conc. : 0.100M, pH : 2.5, Fe : 0.010M, Calcium hydroxide conc.: 0.067M, Reaction time : 15min., Temp. : 25℃).

Number of Reuse	pH	Temp.(^{o}C)
1	8.37	27.4
2	2.94	26.3
3	2.57	26.2
4	2.52	26.0
5	2.52	25.9

Figure 6.8 Effect of calcium hydroxide concentration on the removal of Fe and change of pH (Oxalic acid conc.: 0.100 M, pH : 2.5, Fe conc. : 0.078 M (4,350mg/L), Reaction time : 30min.).

$Ca(OH)_2$, (M)	25℃/Fe	85℃/Fe	25℃/*p*H	85℃/pH
0	100	100	2.52	2.52
0.067	100	97.86	2.8	2.96
0.135	100	96	3.15	4.19
0.203	100	93	3.67	5.04
0.270	99	28	4.03	8.87
0.338	98.02	0.1	4.37	12.3
0.405	82.54	0	7.89	12.7

Figure 6.9 Effect of reaction temperature on the removal % of Fe and Al (Oxalic acid conc.: 0.100M, pH : 2.5, Calcium hydroxide conc. 0.338 M, Reaction time : 30min., Fe conc. : 0.078M (4,350mg/L), Al conc. : 0.028M (750mg/L).

Temp.(^{o}C)	Fe (%)	Al (%)	Final pH
25	1.98	10.50	4.37
40	21.64	29.97	7.98
60	80.50	38.81	8.68
85	99.90	90.39	12.30

Figure 7.1 Dissolution of iron oxide (hematite) (Molar Ratio: 4:1, pH: 3.0 and Temperature: 103^{o}C) at different particle size rnages: (A) micron small size range and (B) mm size range (Conditions : Temp. 100℃, Volume: 250ml, Fe_2O_3 : 1g, Fe_3O_4 : 0.1g, pH : 3.01, Stoichiometry : (4:1) 9.92 g/L oxalate).

(A)

Reaction Time(min)	+0.045/-0.071um	+0.071/-0.16um	+0.16/-0.21um
0	0	0	0
10	2.2	3.2	4.3
30	2.6	4.2	5.9
60	3.2	8.3	10.3
120	5.1	15.7	17.4

(B)

Reaction Time(min)	+0.5/-0.85	+0.85/-1.0	+1.0/-1.18	+1.18/-1.4
0	0	0	0	0
5	0.11	0.08	0.06	0.07
15	0.33	0.23	0.18	0.16
30	0.66	0.45	0.35	0.27
60	1.55	1.15	0.89	0.65
120	2.68	2.02	1.53	1.16

Figure 7.2 Comparison of rate-time equations of different particle sizes

0	+ 0.5/−0.85	+0.85/-1.0	+1.0/-1.18	+1.18/-1.4
0.00036676	5	0.00026671	0.00020002	0.00023336
0.0011011	15	0.00076718	0.0006003	0.00053356
0.00220464	30	0.00150211	0.00116791	0.00090072
0.00519308	60	0.00384774	0.00297521	0.00217116
0.00901345	120	0.00677851	0.00512572	0.00388133

Figure 7.3 Dissolution at different oxalate concentrations of 0.37M, 0.74M and 0.112M corresponding to molar ratio of 4:1, 8:1 and 12:1, respectively (Particle size: -160/+210 micron, pH 3.0 and Temperature: 103^{o}C)

Reaction Time (min)	[1-(1-a)^(1/3)]		
	4:01	8:01	12:01
0	0	0	0
10	2.01	2.4	3.3
30	2.2	2.8	4.1
60	3.1	5.05	7.4
120	5.04	9.02	18.3

Figure 7.4 Dissolution at different oxalate concentrations of 0.37M, 0.74M and 0.112M corresponding to molar ratio of 4:1, 8:1 and 12:1, respectively (Particle size: -160/+210 micron, pH 3.0 and Temperature: 103^{o}C)

Modelling for molar ratio

Reaction Time (min)	Based on [1-(1-a)^(1/3)]		
	4:01	8:01	12:01
120	0.017	0.032	0.064
60	0.011	0.018	0.024
30	0.009	0.010	0.015
10	0.007	0.009	0.011
0	0	0	0

Concentration (g/L)	3.36	6.72	10.08
Concentration (ppm)	3360	6720	10080

Ln concentration (ppm)	8.1197	8.8128	9.2183
gradient	0.0002	0.0003	0.0005
Ln gradient	-8.5172	-8.1117	-7.6009

Ln concentration (ppm)	Ln gradient
8.119696253	-8.51719319
8.812843434	-8.11172808
9.218308542	-7.60090246

Figure 7.5 Plot of rate expression showing linearity of kinetic control rate reaction (Test conditions: pH 1.5 (triangle) , pH 2.0 (square) and pH 3.0 (diamond), 103 deg.C, molar ratio 4:1, particle size range +160/-212 microns)

Reaction Time (min)	[1-(1-a)^(1/3)]		
	pH 1.8	pH 2.5	pH 3.0
120	0.0297	0.0256	0.0173
60	0.0114	0.0129	0.0108
30	0.0089	0.0097	0.0086
10	0.0071	0.0079	0.0073
0	0.0000	0.0000	0.0000

Figure 7.6 Plot of Ln [gradient] vs Ln [H^+] yielding the coefficient n for [H^+] in the rate equation 7.2

Modelling for pH

Reaction Time (min)	[1-(1-a)^(1/3)]		
	pH 1.8	pH 2.5	pH 3.0
120	0.0297	0.0256	0.0173
60	0.0114	0.0129	0.0108
30	0.0089	0.0097	0.0086
10	0.0071	0.0079	0.0073
0	0.0000	0.0000	0.0000

	pH 1.8	pH 2.5	pH 3.0
Gradient	0.0002	0.0002	0.0002
Ln gradient	-8.3286	-8.4133	-8.7366

H^+	0.0158	0.0032	0.0010
Ln H^+	-4.1447	-5.7565	-6.9078

Ln gradient	Ln H^+
-8.328641085	-4.144653226
-8.413283728	-5.756462733
-8.736593756	-6.907755279

Figure 7.7 Dissolution vs time plots for different size ranges at 103^{o}C, 4:1 molar ratio, pH 3.0, 4 g/L Fe_2O_3 + 0.4 g/L Fe_3O_4).(Conditions : Temp. 100℃, Volume: 250mL, Fe_2O_3 : 1g, Fe_3O_4 : 0.1g, pH : 3.01, Stoichiometry : (4:1) 9.92 g/L oxalate)

(Unit : %extraction)

	+0.5/−0.85	+0.85/-1.0	+1.0/-1.18	+1.18/-1.4
0	0	0	0	0
5	4.25	3.82	3.42	3.23
15	6.99	5.86	5.33	4.55
30	9.92	8.24	7.29	6.54
60	15.29	12.85	11.15	9.66
120	23.76	20.31	17.25	14.6

Figure 7.8 Dissolution vs time plots for different temperatures (pH 3.0, particle size: -0.50/+0.85mm, 4:1 molar ratio, 4 g/L Fe_2O_3 + 0.4 g/L Fe_3O_4).(Conditions : Temp. 25, 40, 60, 80, 100℃, Fe_2O_3 : 1g, Fe_3O_4 : 0.1g, pH : 3.01, Average particle size : 0.5-0.85mm, Stoichiometry : (4:1) 9.92 g/L)

(Unit : ppm)

	25℃	40℃	60℃	80℃	100℃
0	0	0	0	0	0
5	1.19	1.71	2.29	2.68	4.25
15	1.56	2.23	3.18	3.72	6.99
30	1.83	2.72	3.88	4.85	9.92
60	2.49	3.41	5.12	6.19	15.29
120	3.52	4.47	6.16	7.97	23.76

Figure 7.9 Rate expression $[1-1(1-x)^{1/3}]$ vs time plots for different size ranges at 103°C, 4:1 molar ratio, pH3.0, 4 g/L Fe_2O_3 + 0.4 g/L Fe_3O_4).

	+0.5/-0.85	+0.85/-1.0	+1.0/-1.18	+1.18/-1.4
0	0.0000	0.0000	0.0000	0.0000
5	0.0144	0.0129	0.0115	0.0109
15	0.0239	0.0199	0.0181	0.0154
30	0.0342	0.0283	0.0249	0.0223
60	0.0538	0.0448	0.0386	0.0333
120	0.0865	0.0729	0.0612	0.0512

Figure 7.10 Rate expression $[1-1(1-x)^{1/3}]$ vs time plots for different temperatures, particle size: -0.500/+0.850 mm,4:1 molar ratio, pH3.0, 4 g/L Fe_2O_3 + 0.4 g/L Fe_3O_4).

0	25℃	40℃	60℃	80℃	100℃
5	0.00398211	0.00573223	0.00769159	0.00901345	0.01437081
15	0.00522676	0.00748854	0.01071332	0.01255577	0.02386265
30	0.00613698	0.00914923	0.013103	0.01643368	0.03422127
60	0.00836903	0.01149723	0.0173648	0.02107226	0.05380504
120	0.01187258	0.01512619	0.02096793	0.02730278	0.08645161

APPENDIX 2: PUBLICATIONS

1. Iron-removal of Clay Mineral with Oxalic Acid, Journal of MMI of Japan, Vol.113, No.11, (1997)

2. Dissolution Of Iron Oxide Rust Materials Using Oxalic Acid, Journal of MMI of Japan, Vol.115, No.11, (1999)

3. Removal of Ferric Ions from Iron (Ⅲ) Oxalato Complexes Reacted with Calcium Hydroxide in Solution, Journal of MMI of Japan, Vol.115, No.11, (1999)

資源と素材 (Shigen-to-Sozai)
Vol. 113 p. 847－851 (1997)

論文

Iron-removal of Clay Mineral with Oxalic Acid*

by Sung-Oh LEE[1], Wan-Tae KIM[2], Jong-Kee OH[3] and Bang-Sup SHIN[4]

Leaching characteristics of iron bearing impurities contained in clay mineral, have been investigated by using oxalic acid (OxA). Two types of samples with different particle size fractions (J-A ; －16/＋100 mesh and J-B ; －100 mesh) were prepared for the experiment. The main components of the clay sample were identified to be sericite, α-quartz, and hydrated iron oxides as main contaminants of iron and iron aluminum silicate hydroxide $[K(Fe, Al)_2(Si, Al)_4O_{10}(OH)_2]$ as a second phase of Fe-contamination. With a reaction temperature 100 ℃, a L/S ratio 5 : 1, a spin rate of 500 rpm, a reaction time of 120 min., the optimum leaching percentage was obtained at 0.38 mol/l oxalic acid concentration for J-A and at 0.19 mol/l for J-B. Leaching percentages for J-A and J-B were then 83 % and 96 %, respectively. The substantial removal of iron reached to 86.2 % and 89.6 % as Fe_2O_3, respectively. Instead of high leaching efficiency of iron from the J-B, it is limited to wash out the leached iron species because of a little adsorption of iron species on the surface of clay. The whiteness of the leached clay with oxalic acid decreased with the higher content of iron in the product. The small amount of magnetic materials remained after oxalic acid leaching, could be removed by weakly magnetic separator and identified a mixture of ferrous oxalate by XRD pattern.

KEY WORDS : Clay Mineral, Oxalic Acid, Leaching of Iron Oxide, Iron Oxalate Hydrate

1. Introduction

The dissolution of ferric oxides has been considered important in several fields such as the removal of oxide deposits from metal surface, the extraction of metals from ores, and the beneficiation of industrial minerals such as kaolin, pottery stone and clays. In fact, most clays like kaolin are usually contaminated with ferric and ferrous iron which are serious impurities that greatly decrease whiteness of the products sintered at high temperatures (Sumner, 1963; Park et al., 1974). Ferrous iron is considered particularly serious in the ceramic industry because it oxidizes to ferric iron in the burning phase and the ferric iron imparts an orange colour to products in that condition (Marabini et al., 1993).

Thus, the chemical processing is often applied with physical processes to get a highly refined product (Shin et al., 1993). Both inorganic acids (sodium hypochlorite, sulphur dioxide and sodium dithionite, hydrochrolic acid) and organic acids (oxalic acid, citric acid) have been available for the clay refining. However, due to the environmental pollution and to contamination of products with the SO_4^{2-} and Cl, inorganic acids should be avoidable as far as possible. Organic acids have, therefore, been tried being employed with/without inorganic acid. Oxalic acid is reported to be more preferable in dissolution of iron contaminants (Shin et al., 1993; Marabini et al., 1993; Tsimas et al., 1995; Baumgartner, 1983; Blesa and Maroto, 1986; Borghi et al., 1989; Segal and Sellers, 1984). However, the oxalic acid has higher leachability on severe conditions such as higher temperature, sizes of the particle, etc.

The objective of this paper is to clarify the leaching characteristics of iron oxide from clay mineral with oxalic acid and the particle size effect of the clay

2. Experimental

2・1 Materials and reagents

The sample used for the present experiment was clay mineral from Jang-San mine which have been used as raw materials by H. N. china factory in Korea. Samples were crushed by a Jaw-crusher and divided into two types; coarse parts (－16/＋100 mesh; J-A) and fines (－100 mesh; J-B) for the leaching tests. The result of the chemical analysis is shown in **Table 1**. Oxalic acid ($H_2C_2O_4 \cdot 2H_2O$; abbreviated as OxA) of 99 to 100 per cent purity was used as a dissolvent and distilled water was used.

2・2 Experimental methods and analysis

A three-necked flask of 1 l in volume was employed as a leaching reactor, with a temperature controllable water bath, and a stirrer. Leaching conditions were as follows:

－Reaction temperature : 25, 50, 75 and 100 ℃

－Concentration of the oxalic acid : 0.19, 0.38 and 0.48 mol/l

－Agitating speed : fixed at 500 rpm, the optimal speed determined through pretests

During the experiments, 3 ml of reacted solution was

* Received March 10, 1997 : accepted for publication August 18, 1997
1. T. A., M. Sc., College of Eng., Chonnam Nat'l Univ., Korea
2. Course of Ph. D, College of Eng., Chonnam Nat'l Univ., Korea
3. Principal Researcher, KIST, Dr., Korea
4. Membership of MMIJ, Prof., Dr., College of Eng., Chonnam Nat'l Univ., Korea
[For correspondence] FAX 82－62－512－1257 (Chonnam Nat'l Univ.)

withdrawn to analyze Fe by the atomic absorption spectrophotometry at the predetermined time intevals. The leached clay was examined by XRD, SEM and XRF, and briquetted to disk with 50 mm. in diameter, and sintered at 1,260 ℃ for 60 min. to measure whiteness (whiteness of the standard : 88.3 %).

3. Results and discussion

3・1 Compositions and components

Table 1 shows chemical compositions of clay samples used for experiments. The main components were aluminum silicate which consisted of 93 % of SiO_2 + Al_2O_3 and 3.4 % of R_2O. When the sample is used as a raw material for ceramic production, the ferrous oxide causes yellowing of the product after heat treatment. The coarser J-A sample contained less amounts of both Fe_2O_3 and Al_2O_3, than J-B, but slightly higher in SiO_2 content.

The iron oxide in raw sample can react with basic elements existing in the clay on the condition of hydrothermal alteration or dissolution by incursion of ground water, forming small iron-encrusted openings in the clay (Park, 1974). These typical shapes were observed under optical microscopy shown in **Fig. 1**. Fig. 1(a) exhibits small openings, and Fig. 1(b) shows the iron-rich zone easily crushed than in thecoarse grained sample J-A (see Table 1). Free silica can be seen in area (c) and the impurity-free area (d) is mostly composed of coarse particles, while the impurities are crushed in the contaminated zones (a) and (b).

To identify the mineralogical component of iron oxide contained in the clay, XRD, was used to analyse concentrates of both non-magnetic and magnetic materials separated by means of a high intensity magnetic separator(HIMS)(**Fig. 2**). In Fig. 2 (a) a non-magnetic concentrate with iron content of 0.3 % Fe_2O_3 consists of mainly sericite and α-quartz. However, the magnetics with iron content of 5.5 % Fe_2O_3 as tailing (b) shows the x-ray pattern of hydrated iron oxides and iron aluminum silicate rather than that of magnetite or hematite. This suggests that it is difficult to remove the iron into desired level using a magnetic separator, and thus chemical process may be available for removing the iron components.

3・2 Chemical leaching of iron

Of all the possible complex carboxylic acids, oxalic acid appears to be the most efficient for iron removal. The oxalates are decomposed by heating into carbon monoxide/dioxide and carbonates [Baumgartner et al., 1983; Marabini et al., 1993]. The redox reaction in an aqueous solution is expressed in equation (1) (Charlot, 1954), and the mechanism of chemisorption of oxalic acid on surface ferric cations is expressed in **Fig. 3** (Blesa et al., 1987).

$$H_2C_2O_4 \rightarrow 2CO_2 + 2H^+ + 2e \quad E_0 = -0.49 \text{ volt} \quad \cdots (1)$$

In the case of iron(Ⅲ) oxide, the reduction of Fe(Ⅲ) to Fe(Ⅱ) brings about a great increase in the rate of dissolution (Segal and Sellers, 1982). The origin of the enhancement is the greater lability of Fe(Ⅱ)-O bonds as compared to Fe(Ⅲ)-O bonds (Baumgartner et al., 1983). And the dissolution process involves reactions on the particle surface and linear dependence on $[C_2O_4^{2-}]$ that serves to a valence electron-transfer to Fe(Ⅲ) ions on the surface as shown in equation (2):

$$C_2O_4^{2-} + 2Fe(Ⅲ) \rightarrow 2CO_2 + 2Fe(Ⅱ) \quad \cdots\cdots\cdots\cdots (2)$$

From the experiment result, the phase of oxalate precipitated from leaching solution was found out to be the ferrous oxalate of $FeC_2O_4 \cdot 2H_2O$ (2θ : 18.7, 23.2, 24.9, 29.9, 34.3, 50.4) which was identified by the XRD pattern. Accordingly, the mechanism of leaching reaction in this experiment can be given as the equation (3) for overall reaction between hydrated ferric oxide and oxalic acid :

$$2FeO \cdot OH + 3H_2C_2O_4 \cdot 2H_2O \rightarrow$$

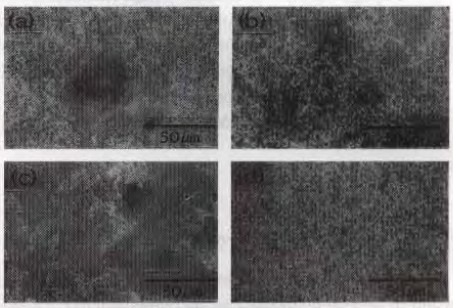

Fig. 1 Optical micrographs of raw samlpe.

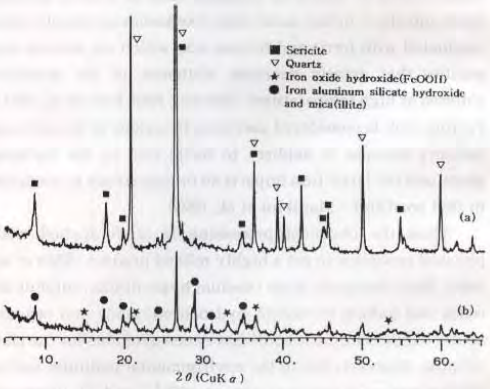

Fig. 2 XRD patterns of the sample separated by HIMS at 1.5 Tesla.
(a) non-magnetic conc. fraction
(b) magnetic tailing fraction

Table 1 Chemical analysis of the samples in weight percentages.

Composition	SiO_2	Al_2O_3	Fe_2O_3	CaO	MgO	TiO_2	Na_2O	K_2O	MnO	P_2O_5	lg.loss
J-A (−16/+100mesh)	86.40	8.23	0.58	0.16	0.10	0.32	0.20	2.00	0.01	0.09	1.61
J-B (−100mesh)	76.30	14.79	1.06	0.35	0.18	0.39	0.30	3.59	0.01	0.17	2.66

$$2FeC_2O_4 + 2CO_2 + 4H_2O \quad \cdots\cdots (3)$$

3・2・1 Effects of temperature

Figs. 4 and 5 show the leaching curves of samples J-A and J-B respectively as a function of the reaction temperature on the conditions of OxA concentration of 0.38 mol/*l*, agitation at 500 rpm, and *L*/*S* 5 : 1 at various temperatures of 25, 50, 75 and 100 ℃. As shown in Fig. 4 for sample J-A, Fe dissolution reaches 11 % at 25 ℃ but goes up to 63 % at 100 ℃ in 10 min. leaching. For two-hour leaching, the leaching percentage reaches 39 % at 25 ℃ and 83 % at 100 ℃. For the sample J-B shown in Fig. 5, a higher leaching percentage was obtainable in the whole range of temperature up to 100 ℃. The result meaned that liberation degree or exposure of iron components must be a significant parameter due to smaller particle size for the leaching of iron from clays. The larger the particle size of the sample, the lower the leaching efficiency of iron because of less liberation of iron minerals from the ore particles (Fogler, 1992).

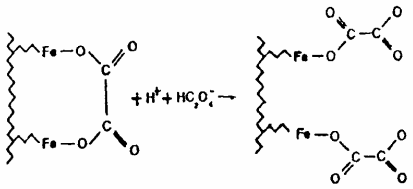

Fig. 3 Chemisorption of oxalic acid on surface ferric cations.

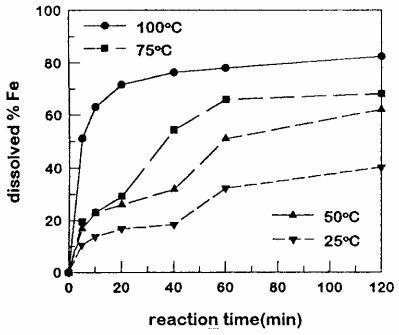

Fig. 4 Leaching tests on J-A as a function of reaction temperatures. (OxA conc. 0.38 mol/*l*, *L*/*S* 5 : 1, Agitation: 500 rpm)

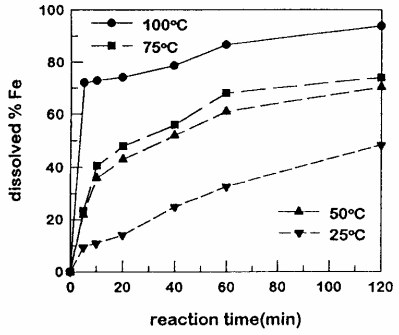

Fig. 5 Leaching tests on J-B as a function of reaction temperatures. (OxA conc. 0.38 mol/*l*, *L*/*S* 5 : 1, Agitation: 500 rpm)

3・2・2 Effects of oxalic acid concentration

In order to clarify the effect of oxalic acid concentration, the leaching was conducted in the presence of various OxA concentration of 0.19, 0.38 and 0.48 mol/*l* at 100 ℃ on the conditions of *L*/*S* = 5 : 1 and stirring rate of 500 rpm.

Fig. 6 presents the leaching percentage increases with higher concentration of oxalic acid for the J-A sample. The leaching percentage appears lower within 40 min. of leaching time, especially in the higher concentration of oxalic acid. Excellent leaching results were obtained at 0.38 mol/*l* OxA. However, for sample J-B (in Fig. 7), the leaching efficiency of 96 % was obtained by leaching at 0.19 mol/*l* OxA for 120 min., of which result appeared better than those at higher concentrations of dissolvent, i. e., 0.38 mol/*l* or higher concentration of oxalic acid. The dissolved ferric ion could be converted to ferrous ion which forms ferrous oxalate with low solubility (Weast, 1983) because the reducing power becomes stronger by oxalic acid on the conditions of denser concentration of oxalic acid and higher temperature. And hence leaching efficiency of iron from clay may decrease with higher concentration of oxalic acid than 0.38 mol/*l*.

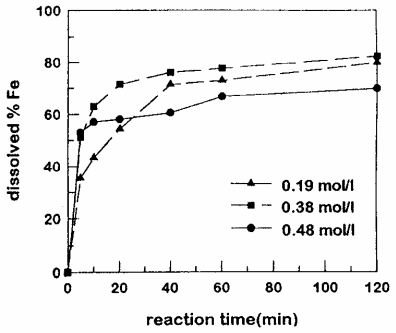

Fig. 6 Leaching tests on J-A as a function of OxA concentration. (Temp. 100 ℃, *L*/*S* 5 : 1, Agitation: 500 rpm)

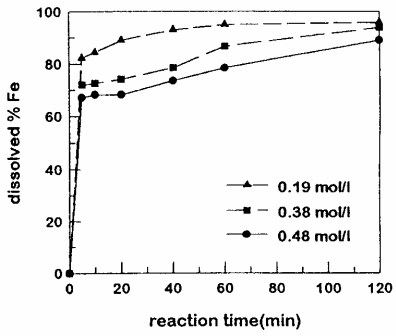

Fig. 7 Leaching tests on J-B as a function of OxA concentration. (Temp. 100 ℃, *L*/*S* 5 : 1, Agitation: 500 rpm)

3・2・3 Effect of L/S ratio

Figs. 8 and 9 show the effect of slurry density on the leaching of iron from clays of J-A and J-B, respectively. As shown in the Figures, the initial leaching rate appeared very fast for both J-A and J-B. After about 10 min., leaching efficiency was improved by a little increment on the longer reaction time. However, the lower the pulp density, the higher the leaching efficiency of iron. For J-A clay (Fig. 8), dissolution of iron reached about 60 % or more in 20 min. and about 70 % in 60 min.. For J-B clay (Fig. 9), 85 % or more of iron was dissolved within 10 min. at lower pulp density than L/S ratio of 6.7 and about 95 % of iron was leached out in 40 min. The lower pulp density is effective enough to dissolve iron in clay. Because the J-B has great specific surface area as compared to the J-A, the leaching rate and efficiency become greater for the clay with small particles.

3・2・4 Removal of ferro magnetic matters

In this experiment, small amount of iron oxalate/Fe metal composite was recovered by hand magnetic and identified through XRD analysis (Fig. 10). Generally, it is known that reduced Fe ions in the leaching solution remained stable or precipitated into forming the ferrous oxalate. From the previous result in Fig. 2, Fe metal composite was not identified. Therefore, It can be considered that residual metalic iron was impurity from crushing process and Fe metal has been considered to be insoluble than iron oxide with weak acid in reductive dissolution process and ferrous oxalate formed through leaching adhered to the surface of iron particles. Thus, in the reductive leaching of iron oxide with weak acid as oxalic acid, megnetic separation is required before or after leaching for removal of strong magnetism as metalic iron. According to the many authors like Blesa et al. (1987), Baumgartner et al. (1983), Marabini et al. (1993), and Rasmussen and Nielsen (1996), it is suggested that ferric ion can be reduced to form ferrous oxalate when iron oxides are dissolved with oxalic acid.

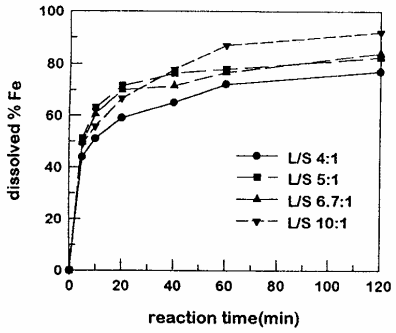

Fig. 8 Leaching tests on J-A as a function of L/S ratio. (OxA conc. 0.38 mol/l, Temp. 100 ℃, Agitation: 500 rpm)

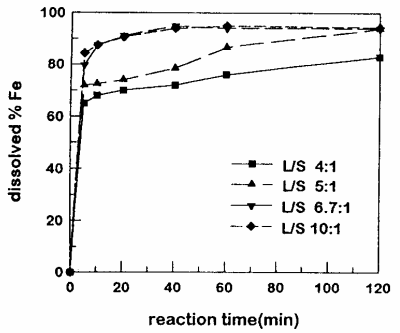

Fig. 9 Leaching tests on J-B as a function of L/S ratio. (OxA conc. 0.38 mol/l, Temp. 100 ℃, Agitation: 500 rpm)

3・3 Properties of leached clays

Table 2 shows the result of chemical analysis of the leached clays through further removal of magnetic matter by employing magnetic separator after washing the leached clays two times. Total removal of Fe from the clays reached 86.2 % and 89.6 % for J-A and J-B clays, respectively, on the conditions of 100 ℃, L/S ratio of 5 : 1 and 500 rpm stirring speed for two-hour leaching with 0.38 mol/l OxA for the sample J-A and 0.19 mol/l OxA for J-B clay. As shown in Table 1 and Table 2 silica contents goes up a little and alumina goes down a little by leaching with oxalic acid. However, iron contents of the clay greatly decreases from 0.58 % to 0.08 % for J-A and from 1.06 % to 0.11 % for the J-B on the base of ferric oxide. So overall leaching efficiencies reached 86.2 % for J-A and 89.6 % for J-B. And the sintered briquettes of the refined clays show whiteness of about 90 % for both clay samples (in Table 3). These optical properties are sufficient for the high grade ceramic products.

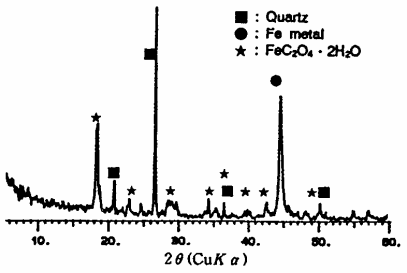

Fig. 10 XRD patterns of magentic matters obtained by magnetic saperator after reaction.

Table 2 Chemical analysis of leached samples in weight percent.

Composition	SiO_2	Al_2O_3	Fe_2O_3	CaO	MgO	TiO_2	Na_2O	K_2O	MnO	P_2O_5	lg.loss
J-A (-16/+100mesh)	89.82	6.00	0.08	0.11	0.07	0.30	0.22	1.55	0.01	0.04	1.15
J-B (-100mesh)	78.88	14.15	0.11	0.10	0.15	0.38	0.30	3.41	0.01	0.07	2.15

Table 3 The whitencess of the samples.

	Whiteness, %
Raw clay	69.0
Non-magnetic conc. by HIMS at 1.5 Tesla	78.3
J-A sample*	88.7
J-B sample*	89.0

* refined by leaching and magnetic separation

4. Conclusion

The mineralogical investigation of the tested sample resulted in sericite and α-quartz as main components. Hydrated iron oxide was found to be a major iron impurity and aluminum silicate hydroxide [$K(Fe, Al)_2(Si, Al)_4O_{10}(OH)_2$] appeared to be a second phase of Fe-contamination of the clay samples. The optimum leaching could be obtainable in the presence of 0.38 mol/l OxA for J-A and of 0.19 mol/l for J-B on the conditions of 100 ℃, a L/S ratio 5 : 1 and 500 rpm stirring rate within 60 min.. The leaching percentage for J-A and J-B reached 83 % and 96 %, respectively. The overall removal of iron from the clays was obtained to be 86.2 % and 89.6 % for J-A and J-B, respectively. The lower pulp density and smaller particle size improve the leaching efficiency of iron. The finally refined clay products had whiteness of about 90 %, which means the refined clays can be sufficiently amenable to the high-class ceramic products. The quality was approved by Haeng Nam China Ware Co. Ltd. in Korea which produces fine ceramic kitchen ware like born china. The small amount of precipitates recovered from the leach liquor for removal of iron from the clays gave the typical matter of magnetic materials, which could be proved a mixture of ferrous oxalate hydrated by XRD pattern.

Acknowledgements Authors are deeply appreciating the financial support from the Korea Institute of Science and Technology.

References

Baumgartner, E., Blesa, M. A., Marinovich, H. A. and Maroto, A. J. G. (1983) : Inorg. Chem., Vol. 22, p. 2224~2226

Blesa, M. A. and Maroto, A. J. G. (1986) : J. Chem. Phys., Vol. 83, p. 757

Blesa, M. A., Marinivich, H. A., Baumgartner, E. and Maroto, A. J. G. (1987) : Inorg. Chem., Vol. 26, p. 3713−3717

Borghi, E. B., Regazzoni, A. E., Maroto, A. J. G. and Blesa, M. A. (1989) : J. Colloid Interface Sci., Vol. 130, p. 299−310

Charlot, G. (1954) : Qualitative Inorg. Analy., New York : John Wiley & Sons, INC., p. 307−309

Cornell, R. M. and Schindeler, P. W. (1987) : Clays an Clay Minerals, Vol. 35, No. 5, p. 347−352

Fogler, H. S. (1992) : Elementals of Chemical Reaction Engineering, 2nd Edition, prentice-Hall, Inc.

Marabini, A. M., Falbo, A., Passariello, B., Esposito, M. A. and Barbaro, M. (1993) : XVIII Inter. Mineral proc. Congress, Sydney, 23−28 May, p. 1253−1259

Park, K. C., Choi, S. C. and Park, Y. K. (1974) : J. of the Korean Ceramic Society, Vol. 11, No. 2, p. 22−24

Rasmussen, H. and Nielsen, R. H. (1996) : Wat. Res., Vol. 30, No. 3, p. 551−558

Segal, M. G. and Sellers, R. M. (1984) : Advances in Inorganic and Bioinorganic Mechanisms, (Ed : A. G. Sykes) Vol. 3, p. 97, (Academic Press : London)

Shin, B. S., Kook, N. P., Choi, J. M., Cheung, M. K. and Kim, Y. J. (1990): J. of Kor. Insti. of Miner. and Energy Resour. Eng., Vol. 27, No. 3, p. 184−192

Sumner, M. E., (1963) : Clay Minerals Bulletin, Vol. 5, p. 218−226

Tsimas, S. G., Komiotou, M. A., Moutsatsou, A. K. and Parissakis, G. K. (1995) : Trans. Instn Min. Metall. (Sect. C : Mineral Process. Extr. Metall.), Vol. 104, C110−114

Weast, R. C., et al. (1983) : CRC Handbook of Chem. & Phy., p. B−101

しゅう酸による粘土鉱物の脱鉄

李 成 五[1] 金 柘 泰[2] 呉 鍾 基[3] 申 芳 燮[4]

粘土鉱物中に不純物として含有されている鉄酸化物の粒度による浸出の特性を調査するために試料を粉砕した。−16/+100 mesh (J-A) と −100 mesh (J-B) に分離し，有機酸であるしゅう酸 (OxA) により浸出した。粘土の主成分は sericite と α-quartz で構成され不純物の Fe_2O_3 成分は加水酸化鉄 (FeO・OH) と若干の含鉄加水アルミノシケリイト [$K(Fe, Al)_2(Si, Al)_4O_{10}(OH)_2$] と推定した。浸出反応温度 100 ℃，$L/S$ 5 : 1，攪拌速度 500 rpm，反応時間 120 分で J-A は OxA 濃度を 0.38 mol/l に，J-B は 0.19 mol/l で浸出した結果，おのおの 83 % (J-A)，96 % (J-B) の浸出率を得ることができた。精製産物の化学分析結果，Fe 除去率が各々 86.2 %，89.6 %，白色度は各々88.7，89 % であって，化学分析結果と一致する傾向を示した。しかし，J-B 試料の高い浸出率に比べて低い Fe の除去率を見せるのは粒度による洗浄の差のためであろう。また，少量のしゅう酸鉄と金属鉄は磁選によってすぐ除去された。

1．碩士 全南大学校 助教 (韓国)
2．工博過程 全南大学校 資源工学科 (韓国)
3．工博 韓国科学技術研究院 責任研究員 (韓国)
4．正会員 工博 全南大学校 教授 (韓国)
キーワード：粘土鉱物，しゅう酸，浸出率，しゅう酸鉄

資源と素材 (Shigen-to-Sozai)
Vol. 115 p. 815－819 (1999)

論文

Dissolution of Iron Oxide Rust Materials using Oxalic Acid*

by Sung-Oh LEE[1], Jong-Kee OH[2] and Bang-Sup SHIN[3]

The dissolution of iron oxides is an important hydrometallurgical process if it can be applied to industry. Some of the potential applications include cleaning of iron surface and removal of iron oxide from industrial minerals. In this study, the dissolution of hematite obtained from iron ores using oxalic acid was evaluated at different initial pHs, acid concentration and temperature. It was found that the dissolution of iron oxide rust was very slow at temperatures ranging from 25 ℃ to 60 ℃, but increased rapidly as temperature became above 90 ℃. An increase in concentration of oxalic acid in the range of 0.048～0.476 mol/l increased the dissolution rate, whereas the pH caused some passivation (at pH > 2.5) after improving the rate from pH 1 to pH 2.5. When the technique was applied to dissolving of the iron oxide rust, it was found that the iron oxides existing in the rust, which are mainly goethite (α-FeOOH), lepidocrocite (γ-FeOOH) and iron hydroxide ($Fe(OH)_3$) can be dissolved faster than with hematite.

KEY WORDS : Iron Oxide Rusts, Oxalic Acid, Dissolution, Induction Period

1. Introduction

The dissolution of metal oxides is of practical importance as it can be used to clean iron oxide ore on the iron metal surface and remove the iron from mineral concentrates (Kim et al., 1997 ; Lee et al., 1997 ; Tsimas, 1995). Oxalic acid is a reagent commonly used in dissolving iron oxide and has been studied extensively. The basic concept was put forward by Engell (1956), Valverde and Wagner (1976) and later was reviewed by Diggle (1973). Blesa and co-workers (1987) studied the mechanism of oxalic acid dissolution of magnetite at 30 ℃ and found that the reaction is controlled by an electrochemical transfer between the Fe (Ⅱ)-and Fe (Ⅲ) oxalate complexes. The optimum pH was found to be around 2.5, above which the dissolution will decrease in rate. The dissolution of magnetite and hematite by other carboxylic acid was also studied in great details by many other investigators (Afonso et al., 1990 ; Sellers and Williams, 1984 ; Blesa et al., 1994 ; Panias et al., 1996).

The dissolution of iron oxide by oxalic acid involves complexation of the dissolved iron (either Fe (Ⅱ) or Fe (Ⅲ)) by oxalate and a redox mechanism. In this case, oxalate acts as a complexant and a reductant in the dissolution process. Both hydrogen ions and oxalate appear to be involved in the dissolution process, whereas the addition of Fe (Ⅱ) seems to accelerate the initial induction. This indicates that the slow induction step is affected by the complexation of oxalate with the Fe (Ⅱ) species. In the latest work, Panias et al. (1996) concluded that the dissolution consists of three distinctive steps: (a) adsorption of organic acid on the iron oxide surface, (b) non-reductive dissolution and (c) reductive dissolution. The reductive dissolution takes place in two stages of induction and autocatalytic reaction.

The interaction of UV light in photochemical reaction between goethite and oxalic acid was also studied by Cornell and Schindler (1987). It was found that UV irradiation seems to promote the release of Fe (Ⅲ) oxalate from the reaction surface.

Past investigations, however, did not deal with natural materials found in ores or in iron oxide rust materials. This work is different from others since it is to evaluate the efficiency of oxalic acid in dissolving iron oxide selected from iron ore and from iron oxides rust materials.

2. Experimental

2・1 Materials and reagents

The sample used in this experiment was hematite (Fe_2O_3, obtained from a U. S. A mine). An adequate amount of rust was also collected from waterworks zinc plated tubes selected and ground by tungsten carbide Jaw crusher (Leatch Co. Ltd). The samples were wet-separated by －100/＋140 mesh (105～149 μm) sieves, and dried at 100 ℃ for 24 hours to be used in dissolution experiments. Chemical analysis of samples, using X-ray fluorescence spectrometry and Atomic absorption spectrophotometer, confirmed the composition of 98.2 % Fe_2O_3, < 1 % of SiO_2 and Al_2O_3. Magnetite (Fe_3O_4, 99.33 %), used in comparative dissolution, was prepared under the

* Received September 2, 1998 : accepted publication July 26, 1999
1. M. Sc., Additional Full Time Lecture, Chodang Univ. and Special Researcher, Eng. Research Inst. of Chonnam Nat'l Univ., Korea
2. Dr., Principal Researcher in KIST., Korea
3. Membership of MMIJ, Emeritus Prof., Dr., Chonnam Nat'l Univ., Korea
〔For correspondence〕 E-mail : leeso@chonnam.chonnam.ac.kr

same conditions. BET tests (N_2-sorption technique) revealed that the specific surface areas of samples were 5.35 m^2/g and 6.01 m^2/g, respectively. Oxalic acid ($H_2C_2O_4 \cdot 2H_2O$) 99 % was used, and the pH was controlled by the use of aqueous ammonia (NH_4OH).

2・2 Experimental methods

The dissolution tests were carried out in the 1 *l*-3 necked flask immersed in a water bath, and the dissolution characteristics were investigated as the functions of the dissolution reaction time, pH, concentration of oxalic acid and velocity of agitation.

The temperature of the bath was controlled within 0.5 ℃. The dissolution characteristics were investigated, while fixing the amount of samples to 3g/*l* and changing the concentration of oxalic acid from 0.048 mol / *l* to 0.476 mol / *l*, dissolution reaction temperature from 25 to 100 ℃, and initial pH from about 1.0 to 4.5. The agitation speed was fixed at 450 rpm throughout the tests.

The dissolution rates were measured by calculating the dissolution efficiency of Fe with reaction time, and during the experiments, 2 m*l* of dissolved solution was withdrawn to analyze Fe by the atomic absorption spectrophotometry at the predetermined time intervals. The surface of particles dissolved by a function of initial pH was examined by the scanning electron micrographs.

3. Results and Discussion

The sample used when analysed using X-ray diffractometer, showed the presence of three iron oxide phases as shown in **Fig. 1**, namely goethite (α-FeOOH), lepidocrocite (γ-FeOOH) and iron trihydroxide ($Fe(OH)_3$). Chemical analysis (**Table 1**) shows that the iron content reaches 90.3 % while other major elements such as Zn, Al, Na, Mg, etc. are less than 2 % each.

Table 1 Chemical composition of the samples

Element	Fe	Zn	Al	Na	Mg	Ca
Assay (wt. %)	90.3	0.43	0.85	1.74	0.17	1.83

The dissolution rate of rust materials was compared with the dissolution of hematite under different conditions and the results will be discussed in the following sections.

3・1 Effect of oxalic acid concentration

The dissolution of iron oxide, either as hematite or iron rust materials increased with an increase of oxalic acid concentration. **Figures 2** (a) and (b) show the dissolution characteristics of both materials over a range of acid concentration from 0.048 mol/*l* to 0.476 mol/*l*. At a concentration of 0.095 mol/*l*, the dissolution rate of hematite is low, but this does not significantly affect the iron oxide rust materials as 84 % of dissolution within 60 min.

The dissolution rate is higher with iron oxide rust and complete reaction also take place within 60 min. for 0.250 mol/*l* oxalic acid or higher. It can be clearly seen that the oxalic acid concentration has practical effect on the hematite or iron oxide rust materials dissolution because the increase of oxalate concentration increases the hydrogen ion concentration in solution. In the case of this results, the significant difference in both types of dissolution is the absence of the induction period in which the ferrous ion generation takes place mainly at the beginning of the dissolution process through a heterogeneous reductive process (Panias et al., 1996), observed with iron oxide rust materials. In addition, the reactivities between iron oxides and oxalic acid can be explained in the thermodynamical aspects. And so the Gibbs free energy changes of the overall reactions on the oxalic acid leaching of iron oxides are calculated by Hess law (Cornell and Schwertmann, Panias et al., 1996) with thermodynamic data shown in equation (1) to (3).

$$Fe_2O_3 + 6\,HC_2O_4^- = 2\,Fe(C_2O_4)_3^{3-} + 3\,H_2O$$
$$\Delta G^\circ_{298} = -26.67\ \text{kJ/mol} \cdots\cdots (1)$$

$$\alpha\text{-FeO}\cdot\text{OH} + 3\,HC_2O_4^- = 2\,Fe(C_2O_4)_3^{3-} + 2\,H_2O$$
$$\Delta G^\circ_{298} = -43.54\ \text{kJ/mol} \cdots\cdots (2)$$

$$\gamma\text{-FeO}\cdot\text{OH} + 3\,HC_2O_4^- = 2\,Fe(C_2O_4)_3^{3-} + 2\,H_2O$$
$$\Delta G^\circ_{298} = -54.54\ \text{kJ/mol} \cdots\cdots (3)$$

The free energy changes imply that iron oxide rust (α-FeO·OH or γ-FeO·OH) becomes naturally spontaneous compared to hematite (eq. 1), which means that iron oxides

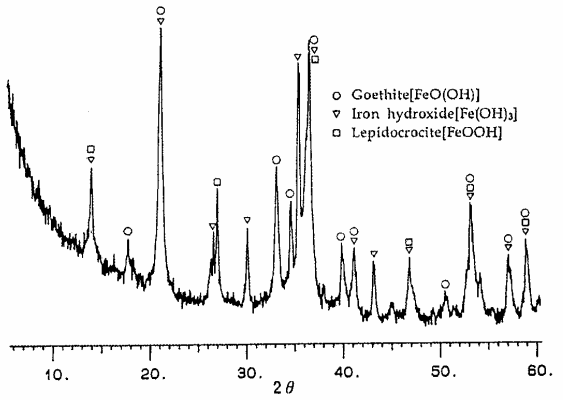

Fig. 1 XRD patterns for sample showing peaks belonging to different iron oxide phase.

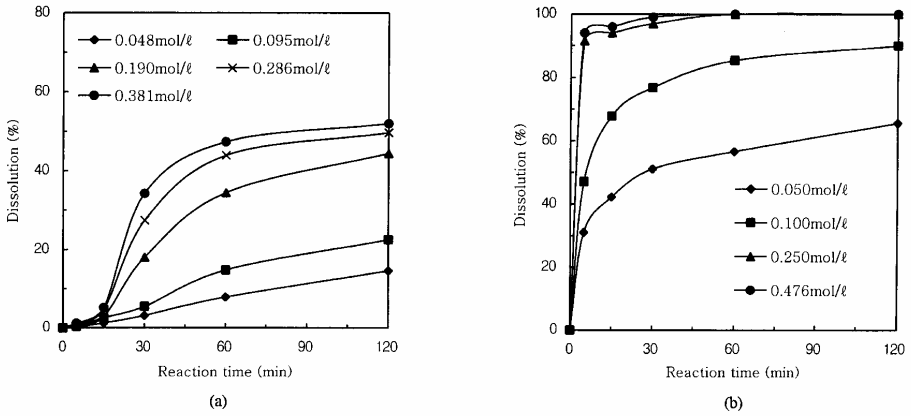

Fig. 2 Effect of oxalic acid concentration on the dissolution of (a) hematite and (b) iron oxide rust (temperature : 100 ℃, initial pH : 2.5, impeller speed : 450 rpm and particle size : 105～149 μm).

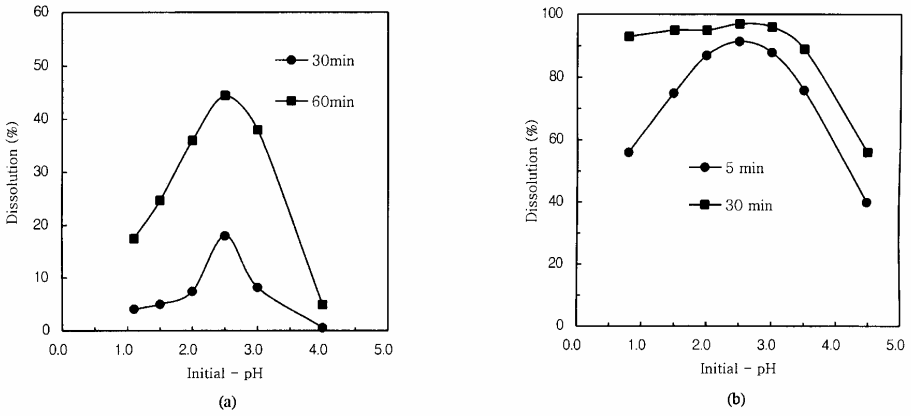

Fig. 3 The effect of initial pH on dissolution of (a) hematite at 100 ℃ with 0.190 mol/l oxalic acid concentration and (b) iron oxide rust at 95 ℃ with 0.250 mol/l oxalic acid concentration (initial pH : 2.5, impeller speed : 450 rpm and particle size : 105～149 μm).

with loose crystallinity like α-and/or γ-FeO·OH may be much more easily dissolved than hematite.

3・2 Effect of pH

The effect of pH on the dissolution of hematite was studied at 100 ℃ with 0.190 mol/l oxalic acid concentration and iron oxide rust materials at 95 ℃ with 0.250 mol/l oxalic acid concentration, and with pH values varying between 1 and 4.5. The results are shown in **Figs. 3** (a) and (b). With the temperature fixed, the acidity of varied pH is very important in determining the rate of dissolution, and it has influence on the protolytic of solution and complexation equilibria ; the rate of reaction (Blesa et al., 1994). That is to say, when oxalic acid dissociate, $H_2C_2O_4$ and $HC_2O_4^-$ show the same degree of 50 % in the range of pH 1, $HC_2O_4^-$ reach the maximum of 90 % in the range of pH 2.3, $HC_2O_4^-$ and $C_2O_4^{2-}$ show the same degree in the range of pH 3.5 and when the increase to over pH 3.5, $C_2O_4^{2-}$ exist as major ion in solution (Oh et al., 1998 ; Panias et al., 1996).

As inferred from the result, the dissolution rate was significantly affected by pH for both iron oxide rust materials and hematite. The dissolution rate is accelerated at the range of pH 2.5, while in more and less acidic solutions, that was decreased as shown the bell-shaped curves. The solution chemistry of oxalic acid shows that the concentration of $HC_2O_4^-$ is maximized at pH 2.5 (Blesa et al., 1994 ; Panias et al., 1996 ; Oh et al., 1998). The oxalic molecule is stable in strong acid solution while oxalate ion ($C_2O_4^{2-}$) becomes more stable in weak acid and alkaline pH range. So iron oxide should be attacked by hydrogen ion and formed as stable oxalate complex. The reaction steps could be divided into equation (4) to (6).

$$HC_2O_4^- = H^+ + C_2O_4^{2-} \quad \cdots\cdots (4)$$

$$Fe_2O_3 + 6\,H^+ = 2\,Fe^{3+} + H_2O \quad \cdots\cdots (5)$$

$$Fe^{3+} + 3\,C_2O_3^{2-} = Fe(C_2O_4)_3^{3-} \quad \cdots\cdots (6)$$

At last the overall reaction is presented as equation (1). These sequential reactions mean that the hydrogen ion and oxalate ion are neccessary in order to dissolve the iron oxides. It can be easily guessed that hydrogen oxalate ion ($HC_2O_4^-$)

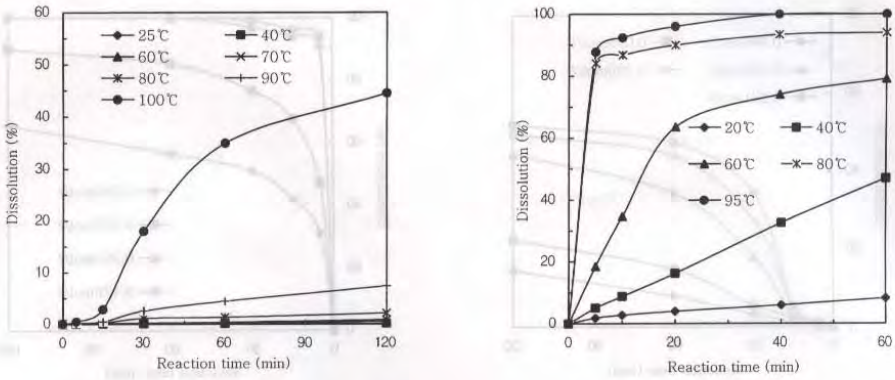

Fig. 4 The effect of temperature on the dissolution of (a) hematite at 0.190 mol/l oxalic acid concentration and (b) iron oxide rust at 0.250 mol/l oxalic acid concentration (initial pH : 2.5, impeller speed : 450 rpm and particle size : 105～149 μm).

plays important role for dissolution of iron oxides, which says the pH near 2.5 is optimal.

3・3 Effect of temperature

To study the effect of temperature on hematite and iron oxide rust materials dissolution, tests were conducted at 25～100 ℃ under the condition of a constant pH of 2.5, oxalic acid concentration of 0.190 mol/l and 0.250 mol/l, respectively.

Figures 4 (a) and (b) show the effect of temperature. Dissolution rate is seen to be dependent on temperature. For hematite at 90 ℃, the dissolution is slow to 14 % at 120 min., while at 100 ℃ it is fast and reaches up to 46 % at the same reaction time. The result can be explained as follows. The reaction is controlled by non-reductive dissolution which removes only the more reactive sites of the oxide surface at high temperature by the activated hydrogen ion in solution (Blesa et al., 1994). But, at lower temperatures below 90 ℃, the reaction was not proceeded with a reasonable dissolution rate at all. It shows that the dissociation of oxalic acid is dependent on the reaction temperature and the increase of temperature enhances the activity of oxalate species in solution, because the oxalic acid was not completely dissociated at low temperature and in acidic pH range as weak acid.

On the other hand, Fig. 4 (b) shows that there is no delayed effect of the induction period in this series because, during the dissolution process, the lability of Fe (Ⅲ)-O bond of hematite is lower than that of iron oxide rust by crystallinity produced in natural condition. Furthermore, it can be verified from the kinetic data which is based on Arrhenius equation. The values of activation energy of hematite and iron oxide rust calculated from Fig. 4 (a) and (b) show 1.5×10^2 kJ/mol and 59 kJ/mol, respectively.

3・4 Surface of the particles

Figure 5 shows the surface of dissolved particles by scanning electron micrographs under the reaction condition of (a and b) hematite at 100 ℃ with 0.190 mol/l oxalic acid concentration and (c and d) iron rust at 95 ℃ with 0.250 mol/l oxalic acid concentration.

The nature of the surface changes during dissolution. Hematite particle shows (a) the regular pits for ming at initial reaction and (b) the pits are enlarged as a result of attack at grain boundaries at the increasing of reaction time. However, the iron rust particle shows somewhat different dissolving types as forming (c) regular pits or (d) showing the rod-like types and plate structure by the dissolution of grain boundary (Lee et al., 1998). It shows that the significant difference in both types of dissolution can be considered the absence of the induction period observed in iron oxide rust materials.

4. Conclusions

The study has confirmed that the oxalic acid can be used to dissolve various iron oxide phases. One of the direct appli-

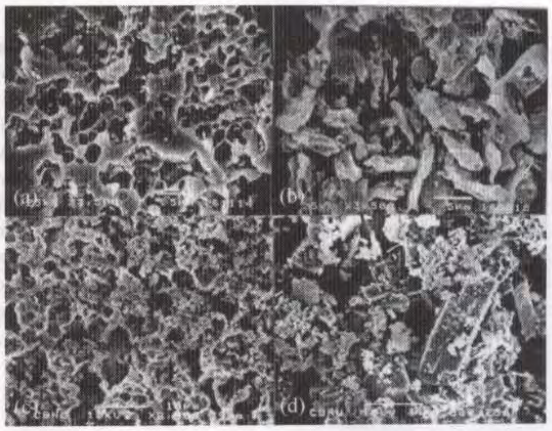

Fig. 5 Scanning electron micrographs of the dissolved (a and b) hematite at 100 ℃ with 0.190 mol/l oxalic acid concentration and (c and d) iron oxide rust at 95 ℃ with 0.250 mol/l oxalic acid concentration (impeller speed : 450 rpm, particle size : 105～149 μm and intial pH : 2.5). (a) reacted for 5 min, (b) 120 min, (c) 5 min, (d) 15 min.

cations is that the technique can be used to remove iron oxide rust from the metal surfaces as one method for cleaning. The dissolution of iron oxide rust which contains goethite, iron trihydroxide and lepidocrocite is faster compared that observed for hematite without a slow induction period at the beginning of the dissolution process. The dissolution process is affected by the pH of the initial solution, oxalic acid concentration and temperature. Especially, the temperature and initial pH of solution controlled the dissolution rate of hematite rather than that of iron oxide rust. The nature of the particle surface changes during dissolution and the hematite particle shows regular pits for ming, but the iron oxide rust particles shows different dissolving type. The values of activation energy of hematite and iron oxide rust calculated, show 1.5×10^2kJ/mol and 59 kJ/ mol, respectively.

Reference

Afonso, M. S., Morando, P. J., Blesa, M. A., Banwart, S. and Stumm, W. (1990) : J. Colloid Interface Sci., Vol. 138, No. 1, p. 74−82

Blesa, M. A., Marinovich, H. A., Baumgartner, E. C. and Maroto, A. J. G. (1987) : Inorg. Chem., Vol. 26, p. 3713−3717

Blesa, M. A., Morando, P. J. and Regazzoni, A. E. (1994) : Chemical Dissolution of Metal Oxides, CRC Press, p. 269

Cornell, R. M. and Schindler, P. W. (1987) : Clays Clay Miner., Vol. 35, No. 5, p. 347−352

Cornell, R. M. and Schwertmann, U. (1996) : The Iron Oxides, VCH Publishers, New York (USA), p. 175

Diggle, J. W. (1973) : In Oxides and Oxide Films, ed. J. W. Diggle (Marcel Dekker, New York, Vol. 2, p. 281

Dean, J. A, (1992) : Lange's Handbook of Chemistry, McGraw-Hill, Inc., 14 th Ed., p. 6.1

Engell, H. J. (1956) : Z. Phus. Chem. (N. F.), Vol. 7, p. 158 (CE-trans. 6891)

Kim, S. G., Kwon, K. J., Lee, H. Y. and Oh, J. K. (1997) : J. of The Korean Inst. of Mineral and Energy Resources Eng., Vol. 34, p. 94−101

Lee, S. O., Kim, W. T., Oh, J. K. and Shin, B. S. (1997) : J. of MMIJ, Vol. 113, p. 847−851

Lee, S. O., Kim, S. G., Oh, J. K. and Shin, B. S. (1998) : J. of The Korean Inst. of Mineral and Energy Resources Eng., Vol. 35, p. 520−526

Oh, J. K. and Shin, B. S., et al. (1998) : 96 R-NM 01-P-06 (a Report of Research in Korea)

Panias, D., Taxiarchou, M., Paspaliaris, I. and Kontopoulos, A. (1996) : Hydrometallurgy, Vol. 42, p. 257−265

Panias, D., Taxiarchou, M., Douni, I., Paspaliaris, I. and Kontopoulos, A. (1996) : Canidian Metallurgical Quarterly, Vol. 35, No. 4, p. 363−373

Sellers, R. M. and Williams, W. J. (1984) : Faraday Discuss. Chem. Soc., Vol. 77, p. 265−274

Tsimas, S. G. (1995) : Trans. Instn. Min. Metall., Vol. 104, p. 110−116

Valverde, N. and Wagner, C. (1976) : Ber. Bunsenges. Phys. Chem., Vol. 80, No. 4, p. 330−333

しゅう酸による iron oxide rust materials の溶解

李 成 五[1]　呉 鍾 基[2]　申 芳 燮[3]

鉄酸化物の溶解は，金属表面の洗浄および産業鉱物から鉄分の除去などにおいて非常に重要な湿式製錬工程である。本研究ではしゅう酸を使用して各々の初期 pH，反応温度，濃度の変化によって天然の鉄鉱石であるヘマタイト（赤鉄鉱）の溶解度を調査した。酸化鉄の溶解は反応温度 25～60 ℃においてゆっくり進行したが，90 ℃以上では溶解度が急激に増加した。また 0.048～0.476 mol/l ではしゅう酸濃度の増加によって溶解度が増加した。さらに pH の変化においても，pH 1.5～2.5 の増加により，溶解度は急激に増加したが，pH 2.5 以上では溶解度が鈍化するという現象を示した。以上の方法によって鉄酸化物である iron rust ($Fe_xO_y \cdot xH_2O$) に存在する goethite（針鉄鉱 α-FeOOH）と lepidocrocite（リン鉄鉱 γ-FeOOH）と水酸化鉄（$Fe(OH)_3$）がヘマタイトより早く溶解するという特性を示した。

1．碩士　草堂大学校兼任専任講師　全南大工業技術研究所　特別研究員（韓国）
2．工博　韓国科学技術研究院　責任研究員（韓国）
3．正会員　工博　全南大学校工科大学　名誉教授（韓国）
キーワード：iron oxide rusts, ヘマタイト, しゅう酸, 溶解, 誘導時間

資源と素材 (Shigen-to-Sozai)
Vol. 115 p. 820－824 (1999)

論文

Removal of Ferric Ions from Iron (Ⅲ) Oxalato Complexes Reacted with Calcium Hydroxide in Solution*

by Sung-Oh LEE[1], Myong Jun KIM[2], Jong-Kee OH[3] and Bang-Sup SHIN[4]

Calcium hydroxide was used to remove ferric ions from waste iron (Ⅲ) oxalato complexes in solution which were generated from the chemical leaching of clay minerals with oxalic acid, and other industrial processes. In this study, the iron (Ⅲ) oxalato complex solution which was prepared with iron (Ⅲ) chloride and oxalic acid, was studied on various factors such as temperature, oxalic acid concentration, initial pH and amount of calcium hydroxide. The pH of the solution depended on the concentration of calcium hydroxide. More than 0.054mol/l of calcium hydroxide was needed for the treatment of 0.010mol/l of Fe dissolved in 0.100mol/l of oxalic acid at 25 ℃. $Fe(OH)_3$ was formed from the iron (Ⅲ) oxalato complex solution by $Ca(OH)_2$, and this reaction was completed within 15 minutes. The concentration of calcium hydroxide added was dependant upon the initial pH and Fe concentration in the oxalic acid solution. When the precipitated sludge was reused repeatedly two or more times, the efficiency decreased sharply due to the inert nature of $CaC_2O_4 \cdot H_2O$ and a small amount of $Ca(OH)_2$. The reaction temperature did not play an important role on the removal of iron from the ferric oxalato complex solution, but the temperature was effective in removing Fe (Ⅲ) and Al (Ⅲ) from the clay leaching solution by adjusting the pH to alkaline range using calcium hydroxide.

KEY WORDS : Iron (Ⅲ) Oxalato Complexes, Calcium Hydroxide, Leaching of Oxalic Acid, Waste Water Treatment

1. Introduction

Large amounts of solution with iron (Ⅲ) oxalato complexes have been wasted from the cleaning process of metallic surfaces, chemical leaching of clay minerals, and the radioactive waste treated with organic acids (Ladd and Miller, 1988 ; Lee et al., 1997 ; Moon et al., 1997). The removal and recovery processes of metal ions from the waste water containing metal complexes are major subjects in the viewpoint of keeping water clean from contamination and recycling of valuable metals. The waste waters containing iron (Ⅲ) oxalato complexes generated from chemical leaching of clay materials and tube flushing solutions are stable in various pH ranges due to the stable nature of complex ions. The main metal components in the waste water generated from the chemical leaching of clay were Fe (Ⅲ), Ca (Ⅱ), Mg (Ⅱ) and Al (Ⅲ) in the range of pH 2.5～3.5 (Lee et al., 1998).

Recently, the treatment of industrial waste water by using calcium hydroxides was reported (Noyes, 1993 ; Tehobanoglous and Rurton, 1993). However, there were few reports on the treatment of waste water containing complexes such as $M^{m+}(C_2O_4)_n^{m-2n}$ (m and n = 1, 2 ,3).

This study has investigated the removal of ferric ions from an iron oxalato complex solutions using calcium hydroxides. The water regenerated in this process was reused to the system. Sludge mainly composed of $CaC_2O_4 \cdot H_2O$ could be used for other process.

Experimental conditions such as the effects of temperature, the concentration of oxalic acid, the concentration of Fe (Ⅲ) ion and the initial pH were investigated to clarify the behavior of Fe (Ⅲ), according to the addition of calcium hydroxides. The result was applied to a chemical leaching solution of clay minerals containing oxalic acid (Lee et al., 1997).

2. Experimental

2・1 Chemicals

The oxalato-ferric complex solution was prepared by dissolving oxalic acid ($H_2C_2O_4 \cdot 2H_2O$, EP grade) and iron chloride ($FeCl_3 \cdot 6H_2O$) into deionized water. Calcium hydroxide ($Ca(OH)_2$) was used as a neutralizer and sodium hydroxide (NaOH) as a pH modifier. All chemicals and reagents used in this study were of analytical grade.

2・2 Experimental procedures

A three-necked flask, 1 l in volume, was employed with a stirrer as a reactor in a temperature-controlled water bath.

* Received January 18, 1999 : accepted publication August 9, 1999
1. M. Sc., Additional Full Time Lecture, Chodang Univ., and Special Researcher, Eng. Research Inst. of Chonnam Nat'l Univ., Korea
2. Dr., Assistant Prof., Dept. of Mineral and Energy Resources Eng., Chonnam Nat'l Univ., Korea
3. Dr., Principal Researcher in KIST., Korea
4. Membership of MMIJ, Emeritus Prof., Dr., Chonnam Nat'l Univ., Korea
〔For correspondence〕 E-mail : leeso@chonnam.chonnam.ac.kr

The experimental conditions were as follows :

[Reaction conditions]

- Reaction temperature : 27, 40, 60, 85 ℃
- Concentration of oxalic acid(OxA) : 0.05, 0.1, 0.3mol/l
- Concentration of calcium hydroxide : 0.027, 0.040, 0.054, 0.067, 0.081 mol/l
- Concentration of iron chloride ($FeCl_3 \cdot 6H_2O$) : 0.008, 0.01, 0.03, 0.06 mol/l
- Initial pH range : 1.55, 2.55, 3.52
- Agitation speed : 350 rpm

pH value changes of solution by calcium hydroxide addition were measured by means of a pH meter (TOA Co). The removal efficiency of Fe (Ⅲ) was calculated by measuring the Fe (Ⅲ) concentration in the residual solutions, withdrawing each of 2ml of the solution to analyze the Fe (Ⅲ) by the ICP Spectrometer (JOBIN-YVON Co.). The efficiency of removal (%) was calculated according to the following equation (1)

[The efficiency of removal, %,]

$$= \frac{100(C_i - C_f)}{C_i} \quad \cdots\cdots (1)$$

where C_i is the initial concentration of the total M (Ⅲ) ion in the solution and C_f is the final concentration of total M (Ⅲ) ion in the batch experiments.

In application tests using waste water generated from a chemical leaching of clay minerals with oxalic acid, the effect of reaction temperature and concentration of calcium hydroxide was studied.

3. Results and Discussion

3・1 The reaction of $Ca(OH)_2$ and iron (Ⅲ) oxalato complexes in solution

The formation of metal complexes from the reaction of Fe (Ⅲ) ion and oxalic acid was affected by the ionic activity of oxalate and pH-value of the solution. When the oxalic acid and Fe (Ⅲ) ion co-existed in the solution without other elements, they formed iron (Ⅲ) oxalato complexes as $Fe(C_2O_4)_n^{3-2n}$ (n = 1, 2, 3), as shown in equations (2), (3) and (4). However, the oxalic acid did not dissociate completely at the low pH-value and temperatures because it is a week acid. Thus, under these conditions, the active species are specified to be $HC_2O_4^-$ rather than $C_2O_4^{2-}$, forming the $FeH(C_2O_4)^{2+}$ complex ion followed in equation (5). These reactions may bring different results according to the various experimental conditions, and the equilibrium constants calculated with the ionic strength of 1.0 at 25 ℃ are shown in following equations (Martell and Smith, 1996 ; Panias et al., 1996).

$$Fe^{3+} + C_2O_4^{2-} \leftrightarrow Fe(C_2O_4)^{1+}(aq) \quad K_1 = 10^{7.58} \cdots (2)$$

$$Fe(C_2O_4)^{1+} + C_2O_4^{2-} \leftrightarrow Fe(C_2O_4)_2^{1-}(aq) \quad K_2 = 10^{6.23} \cdots\cdots (3)$$

$$Fe(C_2O_4)_2^{1-} + C_2O_4^{2-} \leftrightarrow Fe(C_2O_4)_3^{3-}(aq) \quad K_3 = 10^{4.79} \cdots\cdots (4)$$

$$Fe^{3+} + HC_2O_4^- \leftrightarrow FeH(C_2O_4)^{2+}(aq) \quad K_4 = 10^{9.53} \cdots\cdots (5)$$

In these reactions, when the pH value of the solution was adjusted in a range of 2.5～3.0, the most stable reaction could be seen in equation (4), as a result of the increasing of oxalate activity. When the pH-value decreased to below 2.5, the reaction of equation (5) would dominate in decreasing of oxalate activity, and could co-exist with the free oxalic acid (Panias et al., 1996 ; Martell and Smith, 1996). Therefore, the reaction of $Ca(OH)_2$ and iron (Ⅲ) oxalato complex in solution to remove the ferric ions are shown in following equations.

$$Ca(OH)_2 + H_2O \leftrightarrow Ca^{2+} + 2\,OH^- + H_2O \quad K_{sp} = 6.5 \times 10^{-6} \cdots\cdots (6)$$

$$Ca^{2+} + C_2O_4^{2-} \leftrightarrow CaC_2O_4 \quad K_f = 1.0 \times 10^3 \cdots\cdots (7)$$

$$FeH(C_2O_4)^{2+} + Ca(OH)_2 \leftrightarrow CaC_2O_4 + Fe^{3+} + H_2O + OH^- \quad K_f = 2.5 \times 10^7 \cdots\cdots (8)$$

$$Fe(C_2O_4)_3^{3-} + 3\,Ca(OH)_2 \leftrightarrow 3\,CaC_2O_4 + Fe(OH)_3 + 3\,OH^- \quad K_f = 1.5 \times 10^{16} \cdots\cdots (9)$$

According to the above equation, the overall reaction in an acidic solution under pH 2.5 can be expressed by equation (8) and whereas in the range of pH 2.5～3.0, by equation (9), because the oxalate species is activated in the solution (Dean, 1992 ; Brady and Holum, 1996). The calcium (Ⅱ) oxalate and iron (Ⅲ) hydroxide were simultaneously precipitated in the solution. XRD (X-ray diffraction) test of the product showed formation of $CaC_2O_4 \cdot H_2O$, but $Fe(OH)_3$ was not detected due to the very small amounts or amorphous nature.

3・2 Effect of the amount of calcium hydroxide added

Figure 1 shows the change of pH with the concentration of calcium hydroxide added, and the reaction time. The initial solution was prepared with 0.010 mol/l of Fe dissolved in 0.100 mol/l of oxalic acid solution, adjusting the initial pH-value of 2.5 at 25 ℃. Fig. 1 shows that the change of pH-value in the solution with 0.027 mol/l of calcium hydroxide added is very small, but when the amount of calcium hydroxide was increased to 0.054 mol/l, the pH-value reached to 7.5 within 5 minutes. Of special concern is the fact that the pH-value in the solution showed a dramatic increase up to 11 within 30 minutes by adding 0.067 mol/l of calcium hydroxide. This indicated that increase of pH-value by adding calcium hydroxide was attributed to dissociation of $Ca(OH)_2$ into Ca^{2+} and OH^-

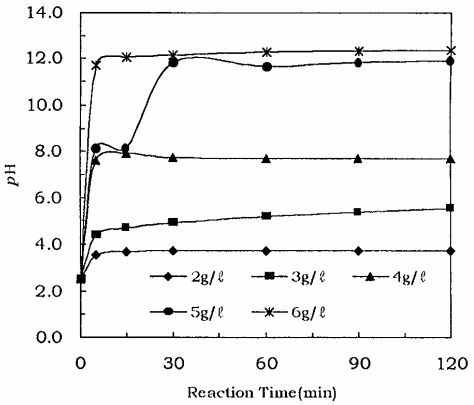

Fig. 1 The change of pH with the concentration of calcium hydroxide. (Oxalic acid conc. : 0.100 mol/l, Fe : 0.010 mol/l, pH : 2.5, Temp. : 25 ℃)

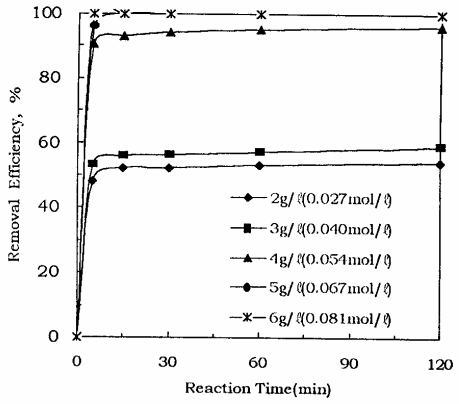

Fig. 2 The removal efficiency of Fe with the concentration of calcium hydroxide. (Oxalic acid conc. : 0.100 mol/*l*, Fe : 0.010 mol/*l*, pH : 2.5, Temp. : 25 ℃)

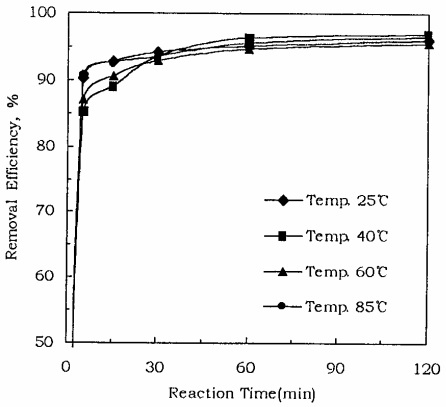

Fig. 3 The removal efficiency of Fe with the reaction temperature. (Calcium hydroxide conc. : 0.054 mol/*l*, Oxalic acid conc. : 0.100 mol/*l*, Fe : 0.010 mol/*l*, pH : 2.5)

in the solution by equation (6). Calcium and hydroxy ions react with oxalate and ferric ions into calcium oxalate and ferric hydroxide, respectively.

Figure 2 shows the removal efficiency of Fe with the concentration of calcium hydroxide added under common experimental conditions of other factors in Fig. 1. The concentration of Fe in the solution was decreased with the addition of calcium hydroxide, and the removal efficiency shows 50 % and 56 % within 5 minutes with 0.027 mol/*l* and 0.040 mol/*l* of calcium hydroxide, respectively. On the other hand, it was highly increased to 90 % within 5 minutes with 0.054 mol/*l*, and completed within 15 minutes with 0.067 mol/*l*. This indicates that the dissociation of ferric ion from the iron (Ⅲ) oxalato complexes was accelerated by the concentration of calcium hydroxide added, and its reaction was completed at the initial reaction time within 15 minutes.

3・3 Effect of reaction temperature

Figure 3 shows the removal efficiency of Fe and the effect of the reaction temperature when 0.010 mol/*l* of Fe is dissolved in 0.100 mol/*l* of oxalic acid solution with the initial pH-value of 2.5. Experiments were done changing temperature from 25 ℃ to 85 ℃, at the concentration of calcium hydroxide 0.054 mol/*l* was kept constant.

The removal efficiencies of Fe were about 90 and 90.5 % within 5 minutes at 25 ℃ and 85 ℃, respectively, but decreased to 85～86 % at 40～60 ℃. With an increase of reaction time to 120 minutes, the efficiency rised to about 96 % at all temperatures. This result means that the main reaction at a low temperature of 25 ℃ was controlled by the dissociation of calcium hydroxide, according to equation (6), because it was activated at room temperature rather than high temperature in an aqueous solution. On the other hand, the reaction at 85 ℃ was controlled by the activity of the free oxalate species in the solution to form the calcium oxalate and free oxalic acids undissociated in the solution. It shows that the reactivity of $Ca(OH)_2$ for the removal of ferric ion from the iron (Ⅲ) oxalato complex solution was not affected, or affected very little by the reaction temperature.

3・4 Effect of oxalic acid and Fe concentration

Figure 4 shows the removal efficiency of Fe under different oxalic acid concentrations with 0.054 mol/*l* of calcium hydroxide added at 25 ℃. The initial solution was prepared with 0.010 mol/*l* of Fe in various oxalic acid concentrations from 0.050 mol/*l* to 0.300 mol/*l* and the initial pH was adjusted to 2.5. The removal efficiency of Fe in 0.100 mol/*l* of oxalic acid solution showed 90 % within 5 minutes. The efficicency was increased to 99 % in the same duration when the oxalic acid concentration was decreased to 0.050 mol/*l*. This result is also seen in Fig. 5. Therefore, the increase of oxalic acid concentration in solution decreased the removal efficiency of Fe and increased the adding amount of calcium hydroxide under the same conditions.

3・5 Effect of initial pH and reuse of sludge

Figure 6 shows the effect of the initial pH-value with 0.010 mol/*l* of Fe dissolved in 0.100 mol/*l* of oxalic acid at 25

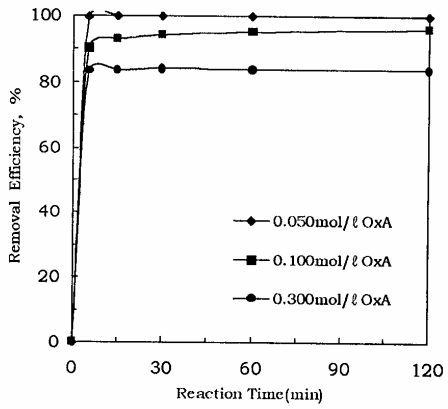

Fig. 4 The removal efficiency of Fe with the oxalic acid concentration. (Calcium hydroxide conc. : 0.054 mol/*l*, Fe : 0.010 mol/*l*, pH : 2.5, Temp. : 25 ℃)

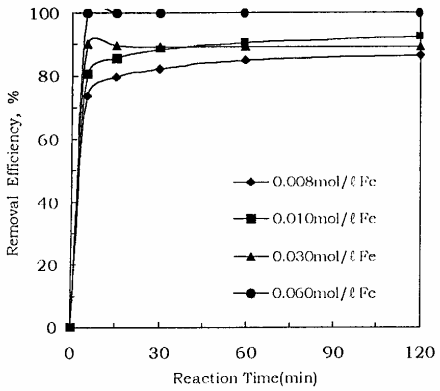

Fig. 5 The removal efficiency of Fe with the iron (Ⅲ) concentration. (Oxalic acid conc. : 0.100 mol/*l*, Calcium hydroxide conc. : 0.054 mol/*l*, pH : 2.5, Temp. : 25 ℃)

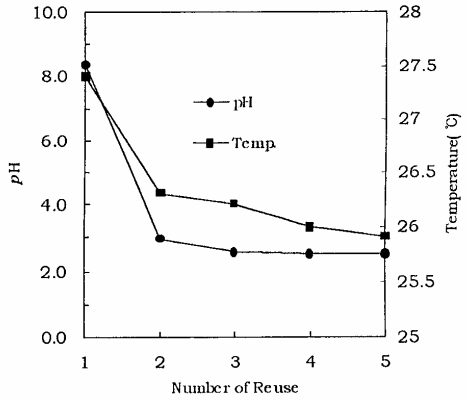

Fig. 7 The change of pH on number of reusing times of the precipitated sludge. (Oxalic acid conc. : 0.100 mol/*l*, pH : 2.5, Fe : 0.010 mol/*l*, Calcium hydroxide conc. : 0.067 mol/*l*, Reaction time : 15min., Temp. : 25 ℃)

℃. The initial pH-value of the initial solution was adjusted from 1.55 to 3.52. The pH-value, when the 0.054 mol/*l* of calcium hydroxide added to the solution, was sharply increased to 8.0～11.5 within 5 minutes and then the removal efficiency shows about 90～91 %. In a strongly acidic solution, the change of pH-value was low and the removal efficiency decreased to 59 %.

Figure 7 shows the change of pH on number of reusing times of the precipitated sludge. The sludge was filtered each time through 1.2 μm glass microfiber filters and dried at room temperature without removing iron hydroxide. When the sludge was reused two or more times, the activity was sharply decreased, showing a change of pH from 8.5 (the first use) to 3.2 (the second use), within the 15 minutes and at 0.067 mol/*l* of calcium hydroxide concentration. Sludge used several times was weakly affected by the change of pH in the solution because it consisted mainly of $CaC_2O_4 \cdot H_2O$ and the small amount of $Ca(OH)_2$ remained.

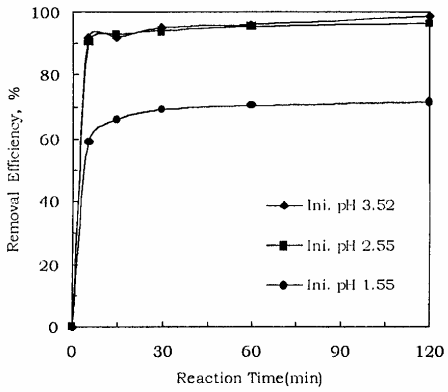

Fig. 6 The removal efficiency of Fe with the various initial pH. (Oxalic acid conc. : 0.100 mol/*l*, Fe : 0.010 mol/*l*, Calcium hydroxide conc. : 0.054 mol/*l*, Temp. : 25 ℃)

3・6 Application to the clay leaching solution

Figure 8 shows the removal efficiency of Fe and change of the pH-value with the concentration of calcium hydroxide to the clay leaching solution at 25 ℃ or 85 ℃. When the 0.338 mol/*l* of calcium hydroxide was added to the solution at 25 ℃, the removal efficiency of Fe shows about 2 % within 30 minutes at the final pH-value of 4.0. When the reaction temperature increased to 85 ℃, the efficiency increased to 99 % at the pH-value of 12.5. The clay leaching solution with oxalic acid contains Fe (Ⅲ), Al (Ⅲ), Ca (Ⅱ), Na(Ⅰ) and Mg (Ⅱ) ions, forming oxalato-metalic complexes such as $M^{m+}(C_2O_4)_n^{m-2n}$ (m and n = 1, 2 ,3). The removal efficiency of Fe and Al as a function of the reaction temperature shows in **Fig. 9**. In the case of artificial solution, the increase of the reaction temperature decreased the removal efficiency of ferric ion from iron (Ⅲ) oxalato complexes or did not affect it. But the leach solu-

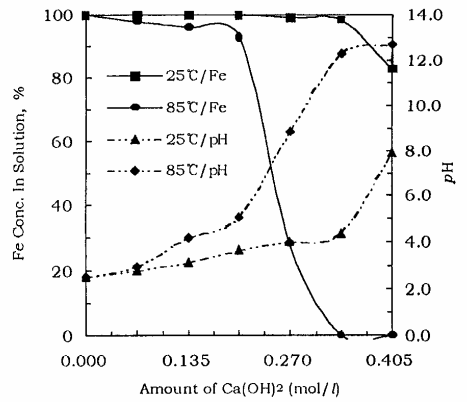

Fig. 8 The removal efficiency of Fe and change of pH with the concentration of calcium hydroxide. (Oxalic acid conc. : 0.100 mol/*l*, pH : 2.5, Fe conc. : 0.078 mol/*l* (4,350 mg/*l*), Reaction time : 30 min.)

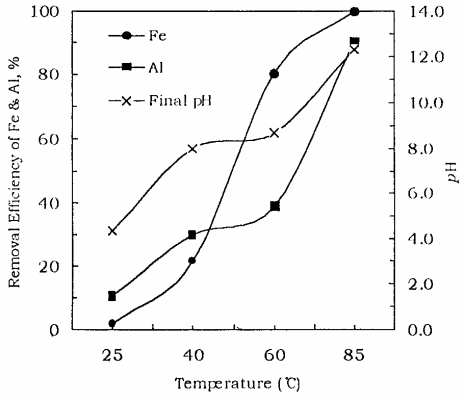

Fig. 9 The removal efficiency of Fe and Al with the reaction temperature. (Oxalic acid conc. : 0.100 mol/*l*, pH : 2.5, Calcium hydroxide conc. 0.338 mol/*l*, Reaction time : 30 min., Fe conc. : 0.078 mol/*l* (4,350 mg/*l*), Al conc. : 0.028 mol/*l* (750 mg/*l*)

tion increased the efficiency with the reaction temperature. Al ion was also removed according to the increase of pH and temperature. The solution can be recycled into the treatment and the sludge as $CaC_2O_4 \cdot H_2O$ produced from the processes is useful as materials for a flux of the tail and lightweight aggregate, and for cleaning process of SO_2 gas.

4. Conclusion

The change of pH-value in the solution depends on the concentration of calcium hydroxide added, more than 0.054 mol/*l* of which is needed for removing from Fe dissolved solution of 0.010 mol/*l* in 0.100 mol/*l* of oxalic acid. The formation of $Fe(OH)_3$ from the iron (Ⅲ) oxalato complex solution was completed during the initial reaction, within about 15 minutes. The concentration of calcium hydroxide added effects both pH-values and Fe concentration in the oxalic acid solution. When the sludge was used repeatedly, the activity was decreased, because it consists mainly of $CaC_2O_4 \cdot H_2O$ and the small amount of $Ca(OH)_2$ remained. The reaction temperature does not play an important role in the removal of iron from artificial ferric oxalato complex solutions, but the elevation of temperature increased the removal efficiency of both Fe (Ⅲ) and Al (Ⅲ) from the clay leaching solution by adjusting the pH-value to an alkaline range with calcium hydroxide.

References

Brady, J. E. and Holum, J. R. (1996) : Chemistry, The study of Matter and its Changes, 2 Ed., John Wiley & Sons Inc.

Dean, J. A. (1992) : Lange's Handbook of Chemistry, 14 Ed., Mcgraw-Hill, Inc.

Ladd, J. A. and Miller, M. J. (1988) : US Patent No. 5196580.

Lee, S. O., Kim, W. T., OH, J. K. and Shin, B. S. (1997) : J. of MMIJ, Vol. 113, p. 847−851

Lee, S. O., Oh, J. K. and Shin, B. S. (1999) : J. of MMIJ, Vol. 115, p. 815−819

Martell, A. E. and Smith, R. M. (1996) : Crystal Stability Constants, Vol. 3 ; Other Organic Ligands, Plenum Press, New York and London, p. 284−332

Moon, J. K., Park, S. Y., Jung, C. H., Lee, J. W. and Oh, Won. Z. (1997) : J. of Korean Inst. of Resources Recycling, Vol. 6, No. 3, p. 22−27

Noyes, R. (1994) : Unit Operation in Environmental Engineering, Noyes Publications

Panias, D., Taxiarchou, M., Douni, I., Paspaliaris, I. and Kontopoulos, A. (1996) : Canadian Metallurgical Quarterly, Vol. 35, No. 4, p. 363−373

Panias, D., Taxiarchou, M., Paspaliaris, I. and Kontopoulos, A. (1996) : Hydrometallurgy, Vol. 42, p. 257−265

Tehobanoglous, G. and Rurton, F. (1993) : Waste Water Engineering, 3rd Ed., Metcalf and Eddy, Inc.

消石灰の添加によるしゅう酸鉄(Ⅲ)錯体水溶液中の鉄イオンの除去

李 成五[1]　金 明俊[2]　吳 鍾基[3]　申 芳燮[4]

しゅう酸を利用した粘土の化学処理および他の産業工程から排出される廃しゅう酸鉄(Ⅲ)錯体を含む溶液中のFe(Ⅲ)イオンの除去に，中和剤として消石灰を用いる研究を行った。実験では，塩化鉄(Ⅲ)水溶液にしゅう酸を溶解してしゅう酸鉄(Ⅲ)水溶液を作成し，実験条件として液温，しゅう酸の濃度，Feの濃度，初期pHおよび消石灰添加量を変化させて行った。液中のpHは消石灰添加量に依存し，0.100 mol/*l* のしゅう酸に0.010 mol/*l* のFeの水溶液の場合では25℃で4 g/*l* 以上必要であった。溶液中の$Fe(OH)_3$沈殿生成は$Ca(OH)_2$の解離溶解性に依存するが，反応は15分以内で終了した。その際，消石灰使用量は溶液の初期pH，Fe濃度およびしゅう酸の濃度によって影響された。また，一度使用した消石灰の残渣を再使用したときには，その反応性は低下した。本実験においては人工のしゅう酸鉄水溶液における温度の影響はあまりないが，実際の粘土浸出液では温度の上昇とともに反応性は向上し，Feならびに Alの除去に効果的であることがわかった。

1．碩士　草堂大学校環境工学科　兼任専任講師　全南大工業技術研究所　特別研究員（韓国）
2．工博　全南大学校工科大学資源工学科　助教授（韓国）
3．工博　韓国科学技術研究院　責任研究員（韓国）
4．正会員　工博　全南大学校工科大学　名誉教授（韓国）
キーワード：しゅう酸鉄(Ⅲ)錯体，消石灰，しゅう酸の浸出，廃水処理

DISSOLUTION OF IRON OXIDE USING OXALIC ACID

Sung Oh Lee[1], Tam Tran[2], Yi Yong Park[3] and Myong Jun Kim[4]

[1] KC Corporation, Chonnam, Korea

[2] School of Chemical Engineering and Industrial Chemistry, University of New South Wales, Sydney, Australia

[3,4] Dept. of Civil, Geo & Environmental Eng., Chonnam National University, Gwangju, Korea

Correspondence author: Myong Jun Kim, junkim@chonnam.ac.kr

ABSTRACT

Iron oxide is the main contaminant of clay and silicate minerals used during the production of high quality ceramics. Its content has to be removed to generally less than 0.1% for achieving the required whiteness of 90% ISO or higher for clay and silicate materials. Oxalate has been used to dissolve iron oxide from various sources. The dissolution is affected by oxalate concentration, solution pH and temperature. The mineral phase is also critical in determining the reaction rate. Hematite is slow to dissolve whereas iron hydroxide and hydroxyoxides such as goethite and lepidochrosite can be easily dissolved. As the dissolution requires a pH controlled in the region 2.5-3.0 for maximum reaction rate, it is essential to create a hydroxide-oxalate mixture for use in the leaching process. The characteristics of NaOH-, KOH- and NH_4OH-oxalic acid mixtures were also determined in this study. Due to the precipitation of salts such as $Na_2C_2O_4$(s) and $NaHC_2O_4$(s) the NaOH-oxalic acid could act as pH buffer for the leaching. Such precipitation also reduces the concentration of the free bi-oxalate, $HC_2O_4^-$ required for the dissolution of iron oxide. KOH behaves the same as NaOH whereas NH_4OH precipitates the less stable salt $NH_4HC_2O_4$(s) which easily re-dissolves forming soluble oxalate species. Ammonium hydroxide is therefore the most suitable reagent that can be used for pH control during the leaching of iron oxide using oxalate.

INTRODUCTION

The production of high quality ceramics requires the iron oxide content of clay or silicates minerals be lowered to less than 0.1% to achieve an acceptable whiteness (higher than 90% ISO). Iron therefore has to be removed from these minerals by physical, physicochemical or chemical processing before being used. The use of different inorganic and organic acids for dissolving iron compounds has been evaluated in several studies in an attempt to replace the costly high-temperature chlorination technique. Sidhu and co-workers [1981] evaluated the dissolution of iron oxides and oxyhydroxides in hydrochoric and perchloric acids. Chiarizia and Hotwitz [1999] studied the dissolution of goethite in several organic acids belonging to the families of the carboxylic and diphosphonic acids in the presence of reducing agents. Ambikadevi and co-workers, [2000] tested several organic acids (such as acetic, formic, citric, ascorbic acid, etc.) and concluded that oxalic acid is the most efficient that can be used to dissolve iron oxide from ceramic minerals.

Oxalic acid was found to be the most efficient acid that can be used for dissolving most iron oxides as it presents a lower risk of contamination of the treated materials after calcinations. It also has a good complexing characteristics and high reducing power, compared to other organic acids. Many researchers have studied the use of oxalic acid to dissolve iron oxide as a result [Vaglio et al, 1998; Segal and Sellers, 1984; Jepson, 1988; Panias et al, 1996 and Cornell and Schindler, 1987]. Biological processes have also been evaluated, most recently by Mandal and Banerjee [2004] who presented their results of a study on the use of *Aspergillus niger* and their cultural filtrates for removing iron from a China clay. Using oxalic acid, the dissolved iron can be precipitated from the leach solution as ferrous oxalate, which can be further re-processed to form pure hematite by calcination [Taxiarchou et al, 1997a]

Ambikadivi and Lathithambika [2000] found oxalic acid (0.05-0.15M) to be the best extractant for removing iron from a kaolinite material finely ground to 90% passing 2

microns. The dissolution was found to increase with acid concentration within the range 0.05-0.15M studied. Both oxalate and hydrogen ion concentrations were increased in this case. The pH of the leach systems was not controlled nor any measurement given for the solution pH, making it harder to interpret their results. Using a 0.15M oxalic acid approximately 70% of the iron could be extracted from a kaolinite slurry (20%w/v) containing 0.93% iron oxide (of goethite and hematite phases) at 100^{o}C within 90 minutes. The iron oxide concentration in the leach is equivalent to 1.86g/L Fe_2O_3. The high loading and fine grind of the raw material could be the reasons explaining the faster iron dissolution found in their study compared to others reported by Taxiarchou et al [1997a, b].

The presence of Fe^{2+} was found to significantly enhance the leaching of iron extraction from silica sand at a temperature even as low as 25^{o}C [Taxiarchou et al, 1997a]. Ferrous oxalate however is oxidized quickly by air during the dissolution and in general an induction period of a few hours was observed unless a strong acidic environment (<pH1) or an inert atmosphere is maintained. Maintaining the high level of ferrous oxalate in the leach liquor using an inert gas will enhance the reaction kinetics according to these authors.

Most studies reported that the dissolution of magnetite and goethite by oxalic acid reached a maximum rate at around pH2.7-3.0, outside which range the dissolution rate dropped dramatically [Cornell and Schindler, 1987; Panias et al, 1996]. Dissolution of hematite was found to be slower than magnetite ($FeO.Fe_2O_3$) and other hydrated iron oxide such as goethite (α-FeOOH) and lepidochrosite (γ-FeOOH) and iron hydroxide ($Fe(OH)_3$).

The dissolution of iron oxide is believed to take place via a photo-electrochemical reduction process, involving a complicated mechanism of charge transfer between the predominant oxalate species, namely ferric oxalate, $Fe(C_2O_4)_3^{3-}$, ferrous oxalate, $Fe(C_2O_4)_2^{-}$ acting also as an auto-catalyst, the oxalate ligand on the iron oxide surface

[Taxiarchou et al, 1997b; Blesa et al, 1987]. In the absence of light the reaction proceeds slowly which complicates the reaction further.

The solution pH governs the distribution of various oxalate ions in the leach system. Below pH1.2, oxalic acid exists mainly as $H_2C_2O_4$, whereas $HC_2O_4^-$ is the most predominant species (mole fraction >0.92) at pH2.5-3.0. Above pH4, $C_2O_4^{2-}$ is the predominant species. The speciation of Fe(III) oxalate and Fe(II) oxalate is also governed by pH and total oxalate concentration [Panias et al, 1996]. For a solution having pH>2.5 and an oxalate concentration higher than 0.1M, the most predominant Fe(III)-oxalate species is $Fe(C_2O_4)_3^{3-}$. At these conditions (pH>2.5 and oxalate concentration higher than 0.1M) the predominant Fe(II) complex species is $Fe(C_2O_4)_2^{2-}$.

The dissolution process also has to be optimized with respect to oxalate concentration and pH to minimize the precipitation of ferrous oxalate. On Eh-pH diagrams (Sukhotin and Khentov, 1980) re-produced in Fig. 1, the predominance of FeC_2O_4(s) is clearly shown for the system containing 0.21M oxalate (right-sided graph). Without oxalate, Fe_2O_3 and Fe_3O_4 will be dissolved in acid forming Fe^{2+}, whereas in the presence of oxalic acid, solid FeC_2O_4(s) is the predominant species existing over a wide range of pH from acidic zone to pH>7 in the potential range where reductive dissolution of iron oxides takes place for 0.21M oxalate. This implies that solid FeC_2O_4(s) will be finally formed when the oxalate concentration is 0.21M (as shown in this graph) or higher.

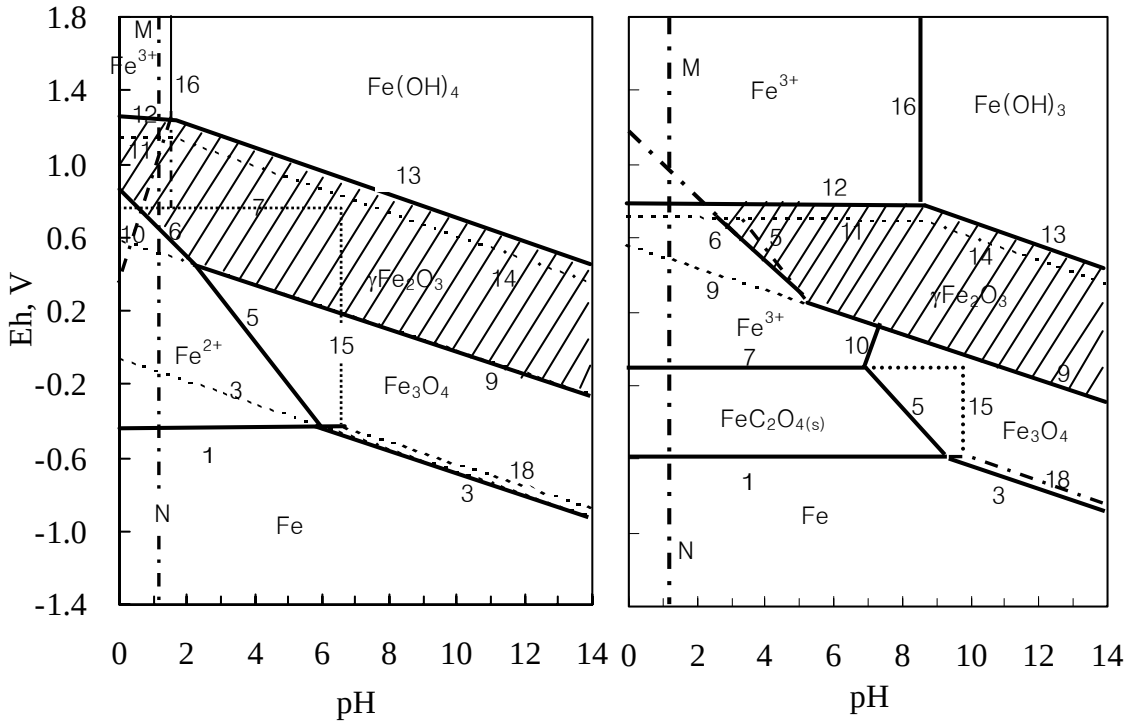

Fig. 1: Eh-pH diagrams for systems: (a) Fe-H_2O and (b) Fe-H_2O-0.21 M $H_2C_2O_4$ (from Sukhotin and Khentov, 1980).

The iron dissolution process therefore takes via an electrochemical process, summarised below:

Oxidation of oxalate to form carbonic acid or carbon dioxide,

$$HC_2O_4^- = H^+ + 2CO_2 + 2e^- \quad \text{(Eq. 1)}$$

Reduction of hematite forming Fe(II) oxalate,

$$2H^+ + Fe_2O_3 + 4HC_2O_4^- + 2e^- = 2Fe(C_2O_4)_2^{2-} + 3H_2O \quad \text{(Eq.2)}$$

The dissolution reaction is therefore:

$$H^+ + Fe_2O_3 + 5HC_2O_4^- = 2Fe(C_2O_4)_2^{2-} + 3H_2O + 2CO_2 \quad \text{(Eq. 3)}$$

The overall reaction indicates that species involved in the leaching would be hydrogen ions, oxalate and iron oxide particles. At the optimum pH2.5-3.0 temperature, concentration of oxalate, iron oxide mineralogy and its particle size will determine the

reaction kinetics. The charge transfer mechanism could also be assisted by the presence of Fe(II) as experienced in previous studies.

This paper presents results of a leaching study on the use of oxalate to dissolve iron oxide. Industrial clay samples were tested and compared with model and pure iron oxides (hematite and iron rust materials containing iron hydroxide and hydroxyoxides). Equilibrium studies were also conducted to determine the best reagent (NaOH, KOH or NH_4OH) that can be used for the control of the reaction pH.

EXPERIMENTAL

Leaching experiments were conducted using different iron oxides or iron-containing clay materials. The clay samples were obtained from Haeng Nam Chinaware Ltd, Korea who purchased their raw products from Jangsan Mine. Hematite and iron rust samples were ground and wet screened to obtain the 105-149 micron size range. For the raw clay the minus 149 micron size fraction was used for the test, of which the iron content was 1.06% Fe_2O_3 and contained mainly iron hydroxyoxide (FeOOH) and iron aluminium silicate. Hematite used in the study was 98.2% pure with main contaminants as silica and aluminium oxide. The iron rust materials contained 90.3% Fe_2O_3. XRD analysis of this material confirmed major phases of iron as goethite (α-FeOOH) and lepidochrosite (γ-FeOOH) and iron hydroxide ($Fe(OH)_3$). Iron rust and pure hematite were added at 3 g/L whereas for the clay material, a liquid/solid ratio of 4:1 to 10:1 was used. The 4:1 L/S ratio corresponded 25% w/v solid loading (or 2.1 g/L Fe_2O_3).

Leaching was conducted in batch tests on 250 mL scale. The liquor (250 mL volume) was first transferred to a round flask (1 litre capacity) which was heated to 100^{o}C using a heating mantle before the solid sample was added. Samples were taken from the reactor at different time intervals and the total iron was then determined by ICP analysis. All chemicals used in this study were of analytical grade.

RESULTS AND DISCUSSION

Leaching of iron oxides and iron containing clay

All leaching experiments in this study were conducted at 100^{o}C. The dissolution of the rust material and hematite at different concentrations of oxalic acid is shown in Figure 1.

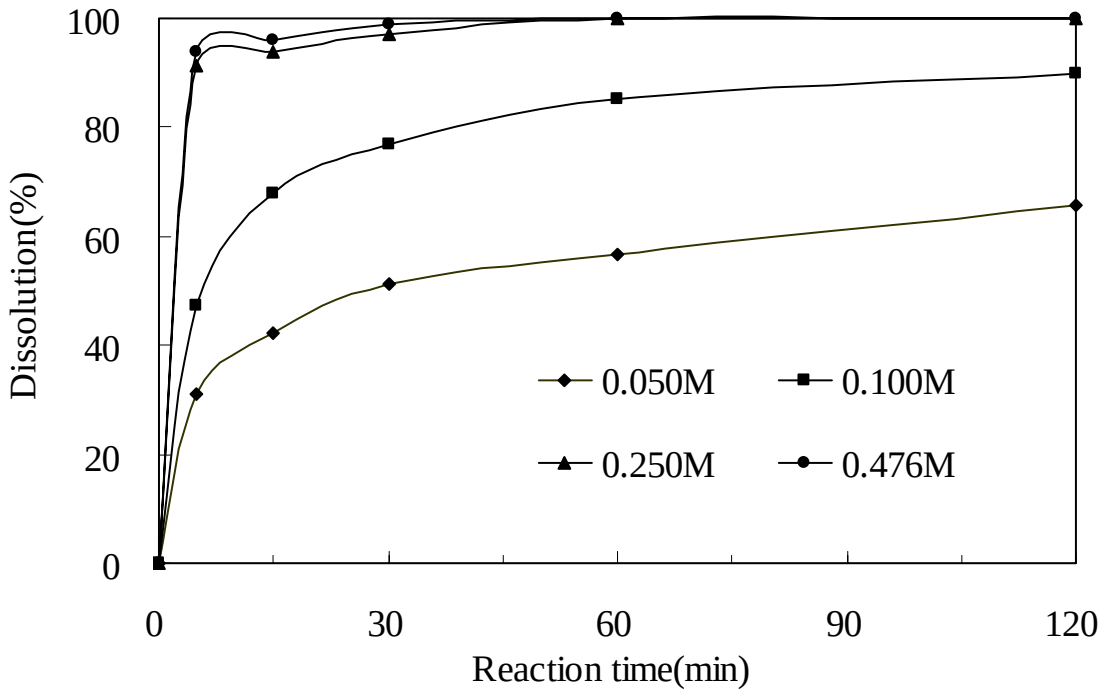

(A)

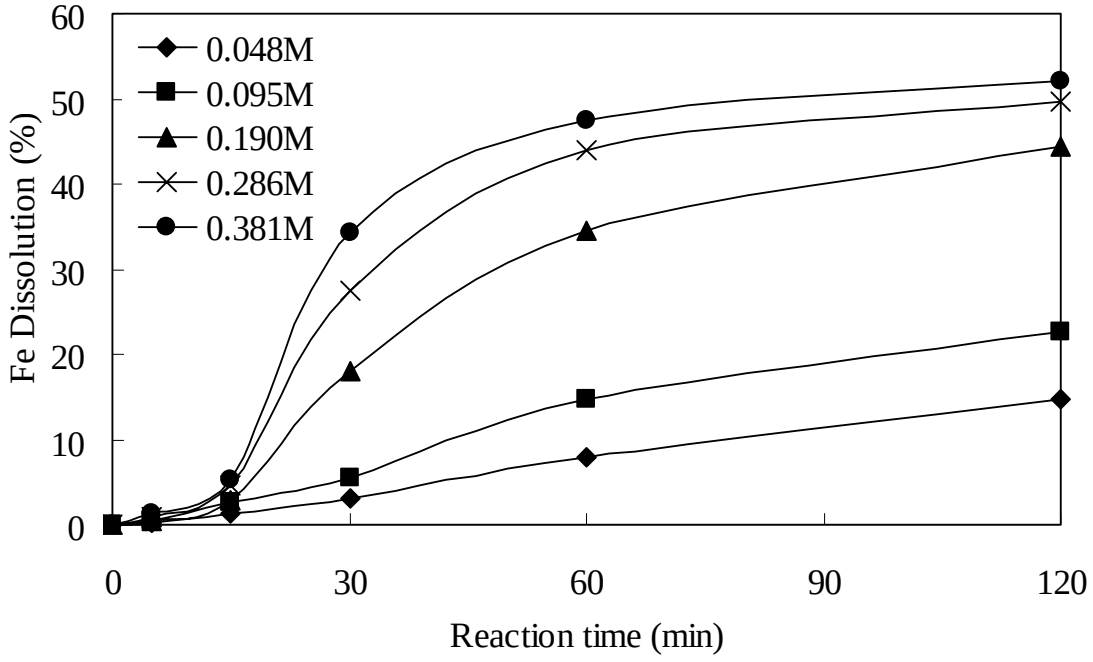

(B)

Fig. 2: Dissolution of at 100^{o}C and pH2.5 of (A) iron rust materials and (B) pure hematite at various oxalic acid concentrations. Solid loading: 3g/L (0.0187mol/L).

Non-hematite iron oxides in the iron rust were found to dissolve faster than hematite, confirming previous studies by other workers (Fig. 2(A) and 2(B)). At stoichiometric ratio (oxalate/iron oxide) of 5:1 as per Eq. 3, a concentration of 0.048-0.05M represents only 50-60% of the stoichiometric requirement for oxalate. Therefore for experiments reported in Fig. 2, except for this concentration, all others had enough or excessive acid for the dissolution. The dissolution of hematite seemed to be either affected by a passivation mechanism due to the formation of ferrous oxalate on the oxide surface or be governed by its precipitation from the bulk solution. After 30 minute of leaching dissolution of iron reached a plateau corresponding to <50% iron dissolution, especially at a high oxalate concentration (>0.286M). However for the iron rust samples containing hydroxyoxides, the reaction reached over 90% within 30 minute, indicating that bulk precipitation of ferrous oxalate was not the mechanism causing the low dissolution of hematite.

The leaching of the clay sample also showed the effect due to a high solid loading (Fig. 3). At a L/S ratio of 5:1 or lower (ie. higher solid loading), the dissolution seemed to slow down compared with the results observed at higher L/S ratios (ie. lower solid loading). A high L/S ratio also corresponds to a higher molar ratio of oxalate/iron oxide and the results obtained are predictable for heterogeneous systems, except for the fact that the dissolution was independent of L/S ratios higher than 6.7:1

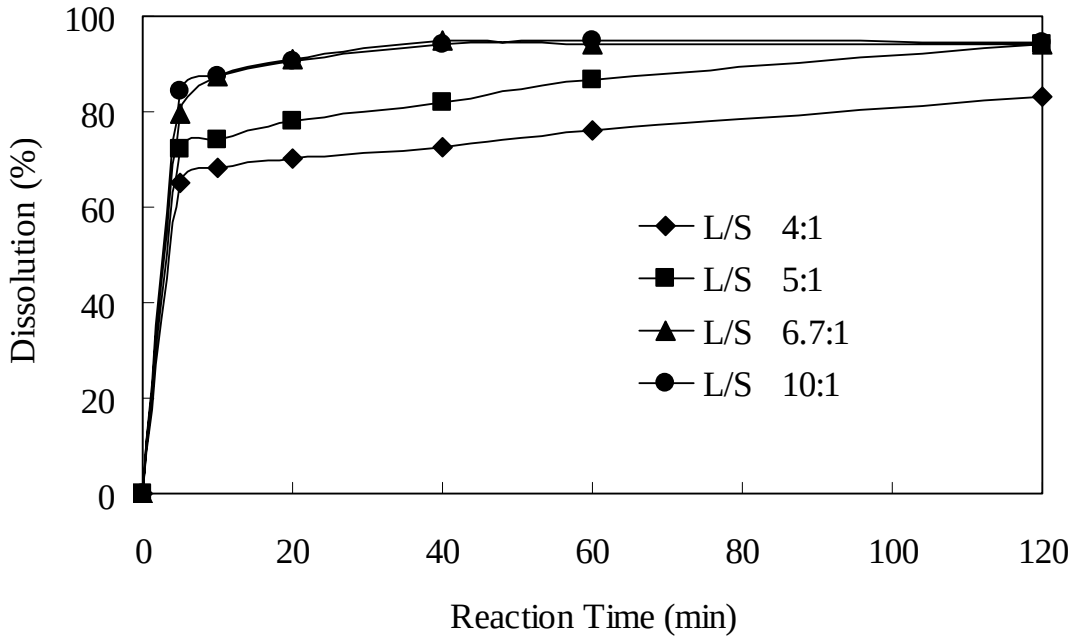

Fig. 3: Dissolution of iron-containing clay at different L/S ratios (100^{o}C, 0.38M oxalic acid, no pH control)

A higher oxalic acid concentration caused adverse effect on the dissolution of iron from the clay material tested at a L/S ratio of 5:1 corresponding to a solid loading of 20% w/v (Fig. 4). As the clay mineral contained 1.06% Fe_2O_3 mainly as iron hydroxyoxide (FeOOH) and iron aluminium silicate, the level of iron oxide in the pulp was 2.1 g/L Fe_2O_3. A slower rate was observed at a higher oxalic acid concentration, although the reaction did reach 90% or higher, independently of concentration.

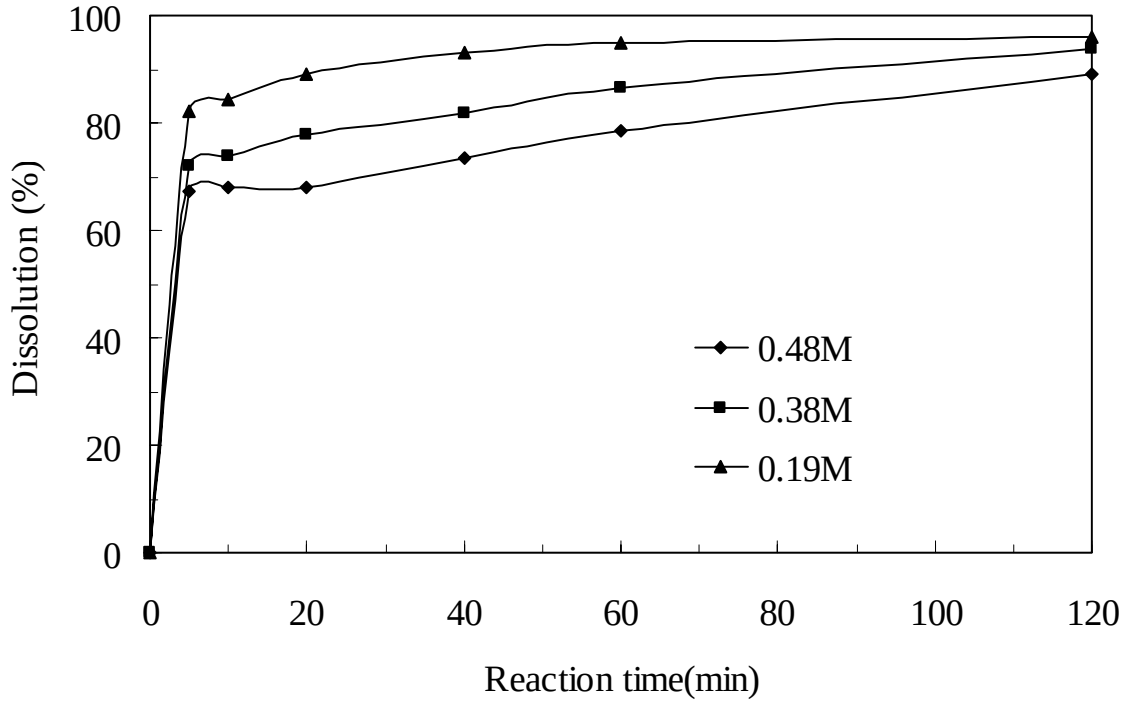

Fig. 4: Dissolution of iron from clay at different oxalic acid concentrations (100^{o}C, L/S ratio 5:1, no pH control).

Table 1 shows the small variation of pH of the range of oxalic acid concentration used in the study. The variation of acid concentration used for leaching causes little effect to the solution pH due to the stability of the neutral species $H_2C_2O_4$ at pH<1.2, of which fraction is 50% speciation at this pH. At pH1.0, the fraction of this species increases to 70% [Pourbaix, 1958, Huang, 2000].

Table 1: pH's of different oxalic acid concentrations at 25^{o}C and 100^{o}C.

Oxalic acid, M	25^{o}C	100^{o}C
0.19	1.51	1.26
0.38	1.37	1.07
0.48	1.38	1.01

Effect of pH

For non-hematite iron oxides (iron rust materials), the initial dissolution rate (at 5 minute) was observed to reach a maximum at pH2.5 (Fig. 5(B)). Full iron extraction (>90%) however was reached after 30 minute independently of pH as long as the pH was maintained at pH<3.0. However for hematite the dissolution seemed to be governed by pH which was found to also reach a peak at pH2.5, above and below which the reaction rate would decrease (Fig. 5(A)).

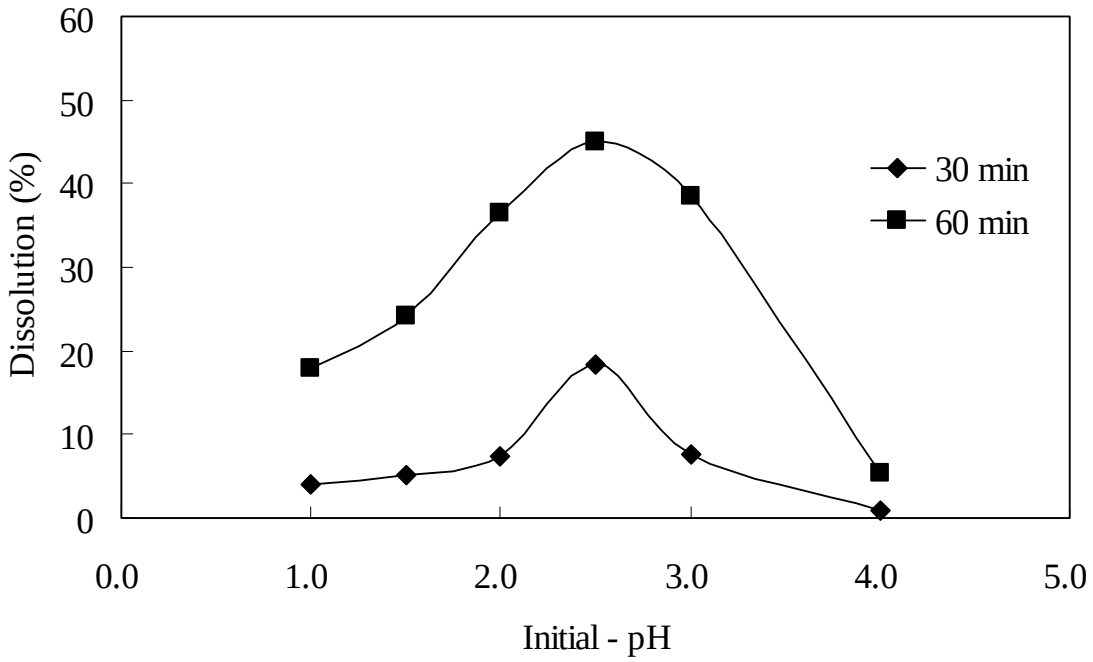

(A)

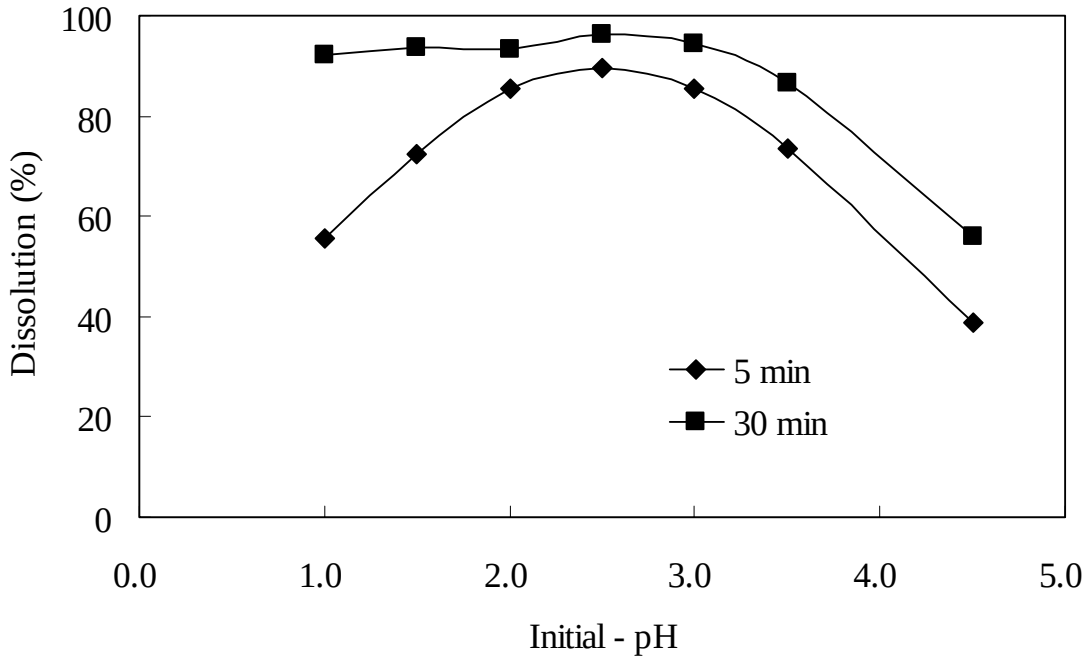

(B)

Fig. 5: Iron dissolution at various times, showing the effect of pH for (A) hematite (100^oC, 0.19M oxalic acid, 3g/L hematite) and (B) iron rust materials (95^oC, 0.25M oxalic acid, 3g/L iron rust)

These results indicated that the dissolution of hematite was slow compared to other iron oxides. For non-hematite oxides, the chemical (non-reductive) reaction between the oxide with the predominant species $HC_2O_4^-$ (mole fraction highest at >0.95) at pH2.5 seems to assist the overall reaction rate.

The above results are in accordance with other studies on the dissolution of different forms of iron oxides. By studying the electrochemical dissolution of hematite (α-Fe_2O_3), maghemite (γ-Fe_2O_3), goethite (α-FeOOH) and lepidochrocite (γ-FeOOH) in hydrochloric and oxalic acid using voltammetry, Cepria and his co-workers [2003] found that the hydroxy-oxides of FeOOH could be dissolved also via soluble Fe(III) species at 0.6-0.8V (vs Ag-AgCl), whereas hematite and maghemite dissolved only via direct reduction of the solid at -0.55V to -0.60V (vs Ag-AgCl). This fundamental study

confirms the electrochemical nature of hematite reductive dissolution. It further explains why hydroxyl-oxides such as goethite or lepidochrocite can dissolve in oxalic acid via reduction and complexation [Stumm and Furrer, 1987] whereas hematite dissolves mainly via solid reduction [Banwart et al, 1989].

Either NaOH or NH_4OH can be used to buffer the solution pH. An addition of hydroxide to oxalic acid first caused the precipitation of insoluble salts. During the leaching process, such precipitate would control the solution pH's as any consumption of hydrogen ions would cause the equilibrium to shift. This would result in the solids to re-dissolve and stabilize such pH changes.

Fig. 6 shows the variation of pH at different levels of addition of NaOH to various solutions of oxalic acid (from 0.20 to 1.0M oxalic acid). For the 0.2M, 0.6M and 1.0M oxalic acid, a total addition of 40mL, 60mL and 100mL, respectively of 1.0M NaOH caused the precipitation of $NaHC_2O_4(s)$ at a 1:1 molar ratio (buffer region A1, B1 and C1, respectively) to reach completion. The pH would be buffered in this precipitation zone (pH1-4) as shown and in this pH range the predominant species is $HC_2O_4^-$ [Panias et al, 1996]. The solubility of Na $HC_2O_4(s)$ is 17g/L and 210g/L at 25 and 100^{o}C, respectively [CRC Handbook of Chemistry and Physics, 1982]. As further NaOH was added, another less soluble precipitate was also formed at pH>4.0 where oxalate ion predominates, namely $Na_2C_2O_4(s)$ of which the solubilities are 37g/L and 63.3 g/L at 25 and 100^{o}C, respectively. The 'end point" was reached at A2, B2 and C2, when the reaction between NaOH and oxalic acid reached completion as shown in Fig. 6. Theoretically at these "end points" of the reaction, 2 moles of NaOH would have reacted with 1 mole of oxalic acid ($H_2C_2O_4.\ 2H_2O$), according to the reaction represented by Eq. 4, before re-dissolution of the precipitate takes place:

$$H_2C_2O_4 \cdot 2H_2O_{(aq)} + 2NaOH_{(aq)} \rightarrow Na_2C_2O_{4(s)} + 4H_2O_{(aq)} \qquad \text{(Eq. 4)}$$

Due to the slow dissolution of the precipitate slight extra acid was used (overshooting of the end point determination). Nevertheless the clear buffer zone (A1, B1 and C1) was demonstrated in each case as shown in Fig. 6.

A similar behaviour was observed for KOH as shown in Fig. 7, where buffer zones were observed between pH1-4. . However, for the NH_4OH system (Fig. 8), although the precipitate would re-dissolve quickly with further addition of ammonia, especially at low concentration of oxalic acid (0.2M), there is only one “end point” corresponding to the 1:1 reaction (Eq. 5) as a result.

$$H_2C_2O_4 \cdot 2H_2O_{(aq)} + NH_4OH_{(aq)} \rightarrow (NH_4)HC_2O_{4(s)} + 4H_2O_{(aq)} \qquad \text{(Eq. 5)}$$

The 1:1 requirement for the NH_4OH-oxalic acid system indicates that there are stable soluble ammonia-bioxalate complexes (holding back one hydrogen ion) compared to the other two systems of NaOH- and KOH-oxalic acid. The solubilities for $(NH_4)_2C_2O_4(s)$ of 25.4g/L and 118g/L at 25 and 50^oC, respectively (CRC Handbook of Physisc and Chemistry, 1982) are higher than for their counterparts of the NaOH-oxalic acid system. Although the ammonia-bioxalate $NH_4HC_2O_4(s)$ solid is very soluble (no figure on solubility given in the CRC Handbook of Physics and Chemistry, 1982) its re-dissolution must form stable ammonium-bioxalate complexes.

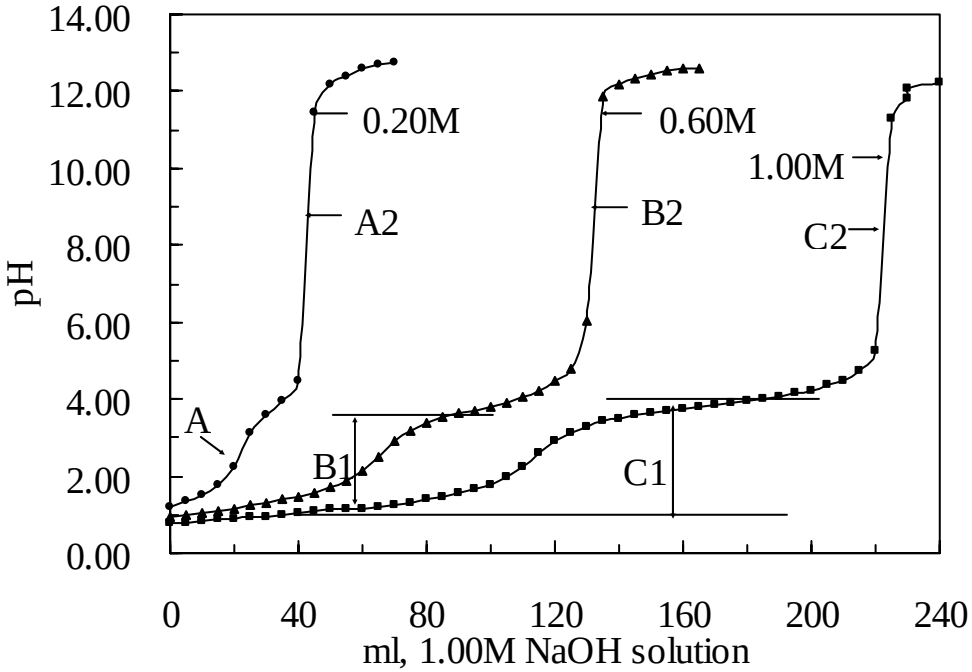

Fig. 6: Variation of the solution pH as 1M NaOH was added to 10 mL of various solutions of 0.2, 0.6 and 1.0M oxalic acid (27^{o}C), showing precipitation (pH buffer) zones (A1, B1 and C1) and end points A2, B2 and C2.

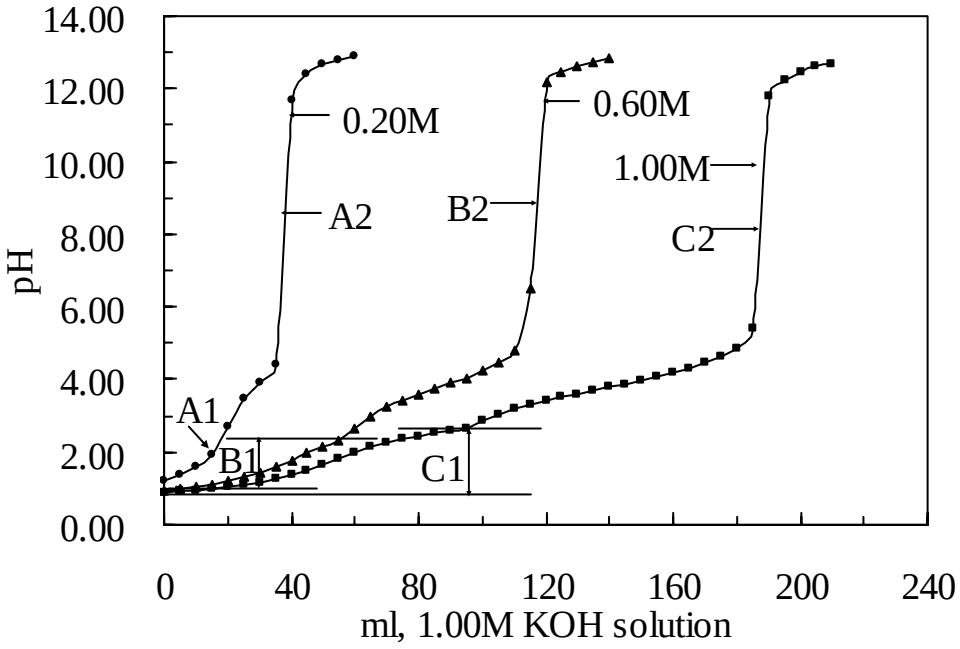

Fig. 7: Variation of the solution pH as 1M KOH was added to 10 mL of various solutions of 0.2, 0.6 and 1.0M oxalic acid (27^{o}C), showing precipitation (pH buffer) zones (A1, B1 and C1) and end points A2, B2 and C2.

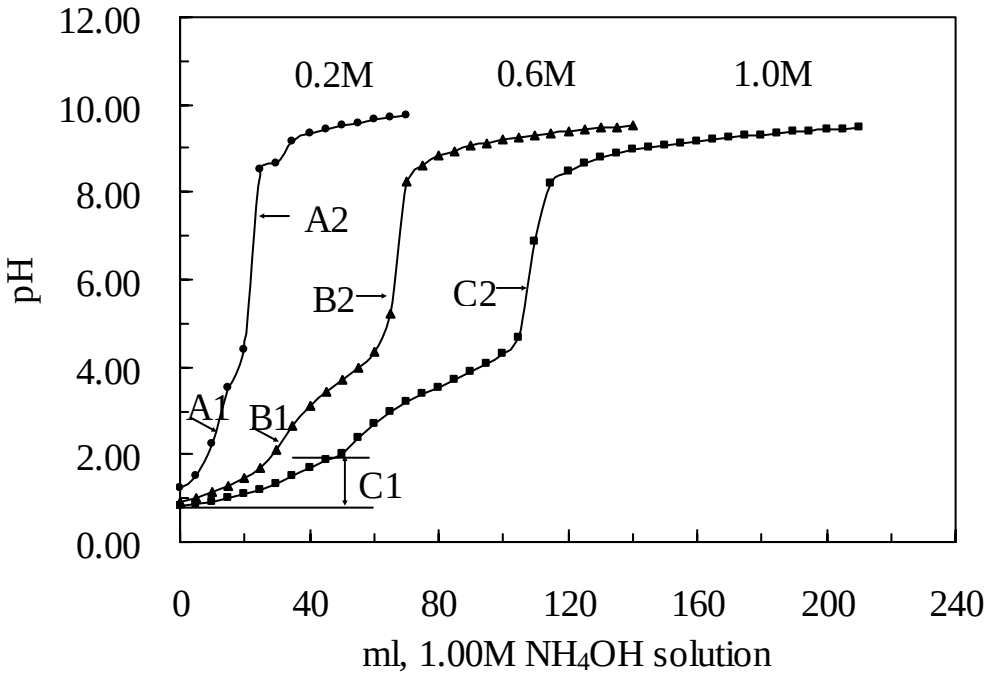

Fig. 8: Variation of the solution pH as 1M NH_4OH was added to 10 mL of various solutions of 0.2, 0.6 and 1.0M oxalic acid (27^{o}C), showing precipitation (pH buffer) zones (A1, B1 and C1) and end points A2, B2 and C2.

There was a slight shift in the buffer zone when the temperature was raised (Fig. 9 and Fig. 10). The zone for precipitation at 50^{o}C was less than that at 27^{o}C. At 80^{o}C almost no precipitate was formed as its solubility increased as expected. The pH buffer zone was shortened as a result for both NaOH-oxalic acid and NH_4OH-oxalic acid systems (Fig. 8). The stoichiometry of the systems (ie. 2:1 for NaOH-oxalic acid and 1:1 for NH_4OH-oxalic acid) was unchanged at higher temperatures.

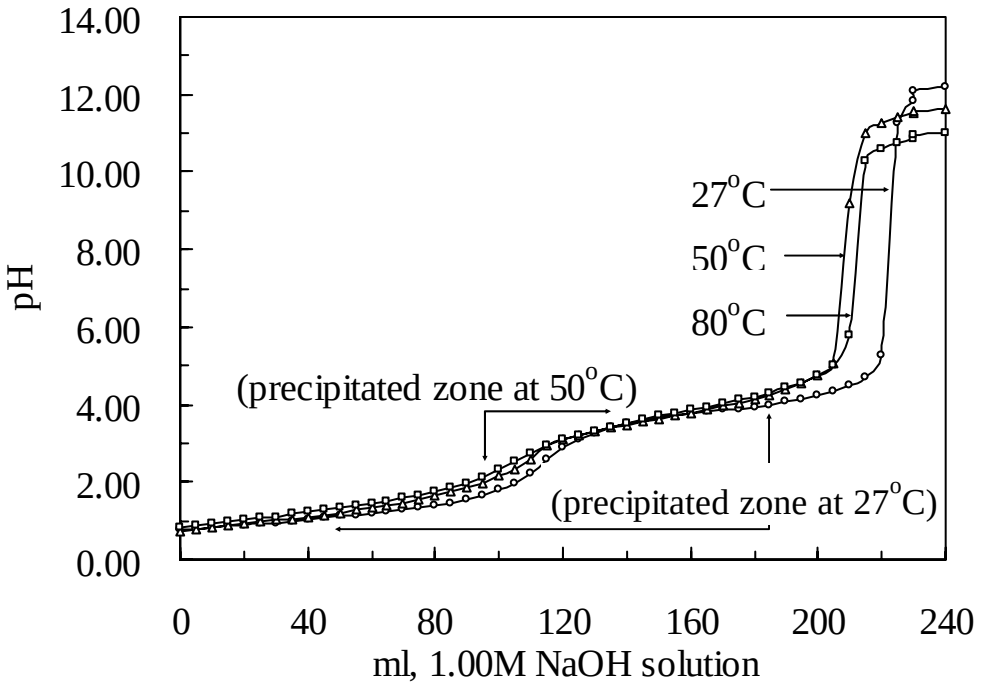

Fig. 9: Variation of the solution pH as 1M NaOH was added to 10 mL of various solutions of 1.0M oxalic acid (27, 50 and 80°C), showing precipitation (pH buffer) zones and end points.

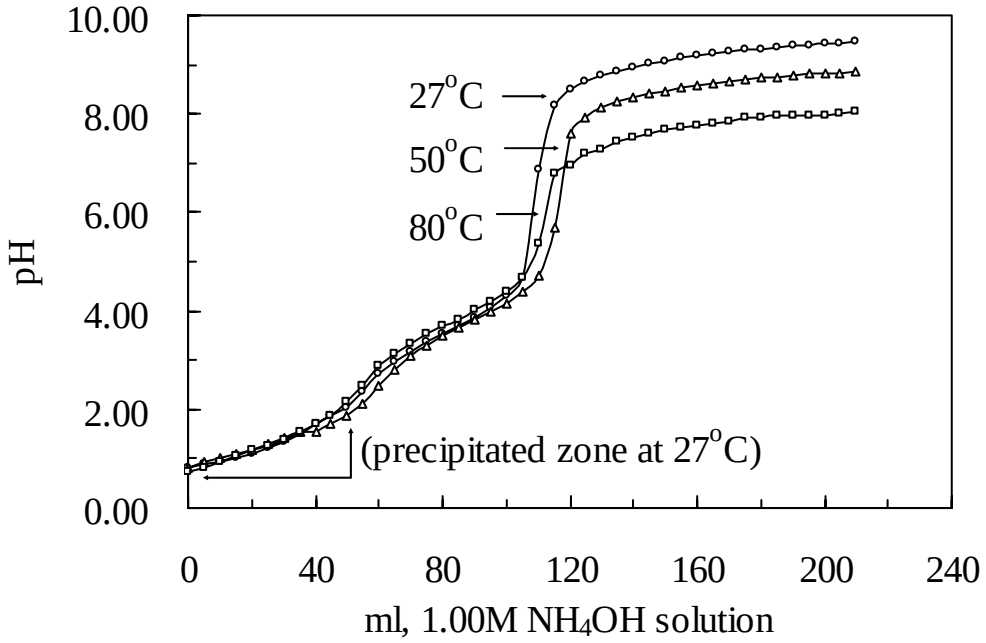

Fig.10: Variation of the solution pH as 1M NH_4OH was added to 10 mL of various solutions of 1.0M oxalic acid (27, 50 and 80^oC), showing precipitation (pH buffer) zones and end points.

The NH_4OH-oxalic acid mixture therefore is the best system for use in the leaching process if the pH needs to be adjusted. Soluble oxalate species should exist at higher concentrations in this system compared to NaOH- or KOH-oxalic acids as the Na-oxalate or K-oxalate solids are less soluble. The different speciation of both NaOH-oxalic acid and NH_4OH-oxalic acid is confirmed as free oxalate species were determined as shown in Fig. 11 after various amounts of NaOH or NH_4OH were added to 1.0M oxalic acid. The ammonia-oxalate precipitate re-dissolves quickly and at pH>4.0 all oxalate species (free or complex) are soluble in the mixture. On the other hand, for the NaOH-oxalic acid system, the level of soluble oxalate species is much lower in the solution compared to the NH_4OH-oxalic acid system.

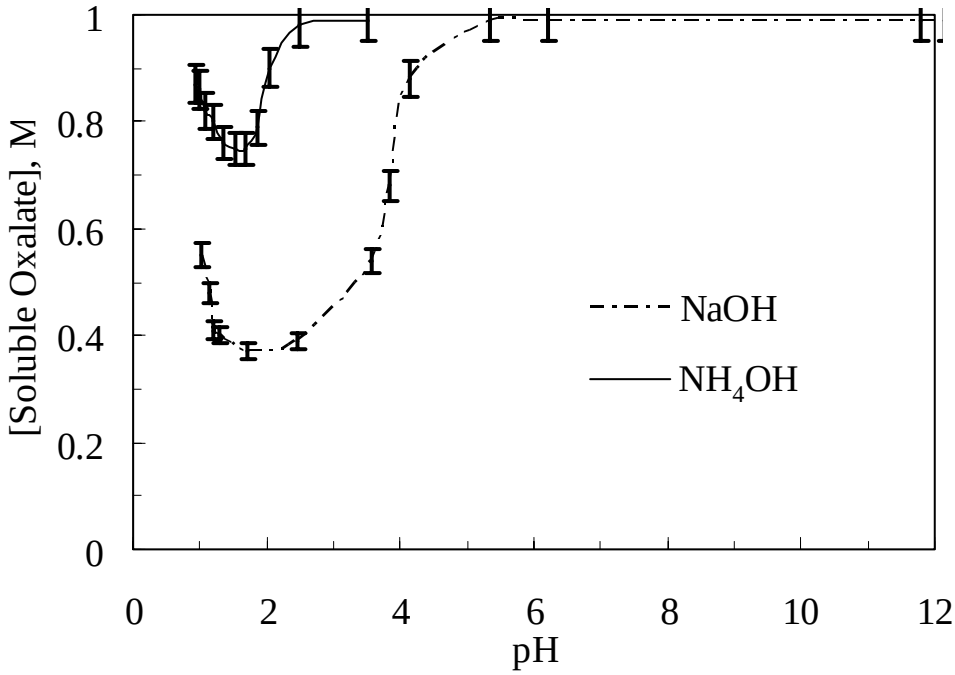

Figure 11: The speciation of soluble oxalate ion in 1.0 M $H_2C_2O_4 \cdot H_2O$ at different pH's after continuous addition at 27^oC of 1.0M NaOH and 1.0M NH_4OH solutions.

CONCLUSIONS

Oxalic acid was used to dissolve iron oxide from hematite, synthetic iron rust (containing iron hydroxide and hydroxyoxide) and a clay material. The critical effect of solution pH was confirmed with optimum dissolution taking place at pH2.5-3.0. A precipitation of ferrous oxalate, either on the oxide surface or in the bulk also affects the level of iron dissolved from hematite where its dissolution was limited to less than 50% at 100^{o}C. Over 90% of the iron rust material was also dissolved.. Also over 90% of iron was dissolved from the clay material containing mainly iron hydroxyoxide and iron aluminium silicate. A higher acid concentration had an adverse effect on the dissolution rate in this case.

When a control of pH was required, NH_4OH offers the best solution to be used for the neutralization as more soluble oxalate species (free or complexed with ammonia) was found in the leachant. On the other hand NaOH and KOH form stable and less soluble species which decrease the level of soluble oxalate species in the solution, rendering it less effective for iron oxide dissolution.

REFERENCES

Banwart, S., Davies, S. and Stumm, W., 1989, The role of oxalate in accelerating the reductive dissolution of hematite(α-Fe_2O_3) by ascorbate, Colloids and Surfaces, Vol. 39, p. 303-309.

Cepria, G., Uson, A., Perez-Arantegui, J. and Castillo, J.R., 2003, Identification of iron (III) oxide and hydroxyl-oxides by voltammetry of immobilized microparticles, Analytical Chim. Acta, 477, 157-168.

Chiarizia, R. and Horwitz, E. P., (1991), New Formulations for Iron Oxides Dissolution, Hydrometallurgy, Vol. 27, p. 339-360.

Cornell, R. M. and Schindler, P. W., (1987), Photochemical Dissolution of Goethite in Acid/Oxalate Solution, Clays Clay Miner., Vol. 35, No. 5, p. 347-352.

CRC Handbook of Chemistry and Physics, Ed: Weast R. and Astle, M.J., pub: CRC Press, Florida, USA

Huang, H. H., (2000), Examples in Stabcal-Stability Calculation for Aqueous Systems, software produced by Montana Tech (USA)

Mandal, S.K. and Banerjee, P.C., 2004, Iron leaching from China clay with oxalic acid: effect of different physico-chemical parameters, Int. J. Miner. Process., 74, 263-270.

Panias, D., Taxiarchou, M., Paspaliaris, I. and Kontopoulos, A., (1996), Mechanisms of Dissolution of Iron oxides in Aqueous Oxalic Acid Solutions: Hydrometallurgy, Vol. 42, p. 257-265.

Pourbaix, M. (1958), Atlas of Electrochemical Equilibria in Aqueous Solution, Pergamon Press.

Segal, M. G. and Sellers, R. M., (1984), Advances in Inorganic and Bioinorganic Mechanisms, Ed : Sykes, A. G., Academic Press : London, Vol. l. No. 3, p. 97.

Sidhu, P. S., Gilkes, R. J., Cornell, R. M., Posner, A. M. and Quirk, J. P., (1981), Dissolution of iron Oxides and Oxyhydroxides in Hydrochloric and Perchloric Acids, Clays Clay Min., Vol. 29, p. 269-276

Stumm, W. and Furrer, G., 1987, The dissolution of oxides and aluminum silicates: Examples of surface-coordination-controlled kinetics, In: Stumm, W., (Ed.), Aquatic Surface Chemistry J., Wiley and Sons, New York, p. 197-219.

Sukhotin, A. M. and Khentov, A. I., 1980, Anodic Behavior of Iron Oxides and Repassivation of Iron in Acid Solutions, Elektrokhimiya, Vol. 16, No. 7, p. 1037-1041.

Taxiarchou, M., Panias, D., Douni, I., Paspaliaris,I. and Kontopoulos, A., 1997a, Removal of iron from silica sand by leaching with oxalic acid, Hydrometallurgy, 46, 215-227.

Taxiarchou, M., Panias, D., Douni, I., Paspaliaris,I. and Kontopoulos, A., 1997b, Dissolution of hematite in acidic oxalate solutions, Hydrometallurgy, 46, 215-227.

Vaglio, F., Passariello, B., Barbaro, M., Plescia, P. and Marabini, A. M., (1998), Drum Leaching Tests in the Iron Removal from Quartz using Oxalic Acid and Sulphuric Acids, Int. J. Mineral Processing, Vol.54, p.183-200.

STUDY ON THE KINETICS OF IRON OXIDE LEACHING BY OXALIC ACID

Sung Oh Lee[1], Tam Tran[2], Yi Yong Park[3] and Myong Jun Kim[4]

[1] KC Corporation, Chonnam, Korea

[2] School of Chemical Engineering and Industrial Chemistry, University of New South Wales, Sydney, Australia

[3,4] Dept. of Civil, Geo & Environmental Eng., Chonnam National University, Gwangju, Korea

ABSTRACT

The presence of iron oxides in clay or silica raw materials is detrimental to the manufacturing of high quality ceramics. Although iron has been traditionally removed by physical mineral processing, acid washing has been tested as it is more effective, especially for extremely low iron (of less than 0.1% w/w). However, inorganic acids such as sulphuric or hydrochloric acids easily contaminate the clay products with SO_4^{2-} and Cl^-, and therefore should be avoided as much as possible. On the other hand, if oxalic acid is used, any acid left behind will be destroyed during the firing of the ceramic products. The characteristics of dissolution of iron oxides were therefore investigated in this study.

The dissolution of iron oxides in oxalic acid was found to be very slow at temperatures within the range 25-60^{o}C, but its rate increases rapidly above 90^{o}C. The dissolution rate also increases with increasing oxalate concentration at the constant pH values set within the optimum range pH2.5-3.0. At this optimum pH, the dissolution of fine pure hematite (Fe_2O_3) (105-140 μm) follows a diffusion-controlled shrinking core model. The rate expression expressed as $1-(2/3)x-(1-x)^{2/3}$ where x is fraction of iron dissolution was found to be proportional to $[oxalate]^{1.5}$.

The addition of magnetite to the leach liquor at 10% w/w hematite was found to enhance the dissolution rate dramatically. Such addition of magnetite allows coarser hematite in the range 0.5-1.4mm to be leached at a reasonable rate.

INTRODUCTION

Iron oxides are detrimental impurities if they exist at high levels in clay or silica minerals which are used extensively in the manufacturing of high quality ceramics and refractories. For the production of high quality ceramics, the iron oxide content of clay minerals has to be lower than 0.1% to achieve an acceptable whiteness of around 90%. Iron therefore is removed from these minerals by physical, physicochemical or chemical processing before being used. Current processes for lowering the iron content of these raw materials are costly and environmental unfriendly. Chemical processing to remove the contaminated iron oxides from clay and silica minerals is considered as it is most cost-efficient [Cornell and Schwertmann 1996; Blesa et al, 1994].

The use of different inorganic and organic acids for dissolving iron compounds has been evaluated in several studies. Sidhu and co-workers [1981] evaluated the dissolution of iron oxides and oxyhydroxides in hydrochoric and perchloric acids. Lim-Nunez and Gilkes [1987] used synthetic metal-containing goethite and hematite in their evaluation while Borghi and co-workers [1989] studied the effect of EDTA and Fe(II) during the dissolution of magnetite. The industrial use of sulphuric and other inorganic acids to remove iron oxide from high purity clay or sand minerals, however, is limited as the trapped acid after treatment can potentially contaminate the raw materials used for ceramic making. In order to find an appropriate alternative, Chiarizia and Hotwitz [1999] studied the dissolution of goethite in several organic acids belonging to the families of the carboxylic and diphosphonic acids in the presence of reducing agents. Ambikadevi and co-workers, [2000] evaluated the effectiveness of several organic acids (such as acetic, formic, citric, ascorbic acid, etc.) used for removing iron from kaolinitic clay.

Oxalic acid was found to be the most promising because of its acid strength, good complexing characteristics and high reducing power, compared to other organic acids. Using oxalic acid, the dissolved iron can be precipitated from the leach solution as ferrous oxalate, which can be further re-processed to form pure hematite by calcination [Taxiarchou et al, 1997a]. Oxalic acid can be obtained cheaply as a by-

product from other industrial processes and any remaining oxalate in the treated materials will decompose to carbon dioxide during the firing stage of ceramic making. Many researchers have studied the use of oxalic acid to dissolve iron oxide as a result [Vaglio et al, 1998; Segal and Sellers, 1984; Frenier and Growcock, 1984; Jepson, 1988; Panias et al, 1996, Blesa et al, 1987; Cornell and Schindler, 1987]. Biological processes for iron removal have also been evaluated based on the use of several types of fungi, some being oxalic acid producing. Mandal and Banerjee [2004] recently presented their results of a study on the use of *Aspergillus niger* and their cultural filtrates for removing iron from a China clay, including an extensive review of previous work conducted in this area.

In all cases, the reaction temperature was found to be critical as confirmed by many workers. Most reaction systems studied had to be conducted above 90^{o}C to achieve a reasonable dissolution rate. As an example, it was found by Taxiarchou et al [1997b] that it took close to 40h to dissolve 80% of a pure hematite slurry (97% purity, 0.022% w/v or 0.21g/L Fe_2O_3) at pH1. Even at 90^{o}C it required close to 10 hours to achieve 95% dissolution of iron of the above slurry at pH1. However, no information was given on the particle size distribution of the hematite powder used to shed light into the reasons why the dissolution rate was quite slow in this case.

Taxiarchou and co-workers [1997a] used 0.1-0.5M oxalic acid (pH1-5) to dissolve iron from a 20% w/v slurry of a coarse silica sand (83% of particle size in the range 0.18-0.35 mm, containing 0.029% Fe_2O_3). The iron oxide concentration in the leach is equivalent to 0.058 g/L Fe_2O_3. These authors found that the maximum iron extraction of only 40% within 3 hours at temperatures in the range 90-100^{o}C. At 0.5M oxalate and all temperatures (25, 60 and 80^{o}C) the dissolution of iron was faster at a lower pH in the range pH1-5 studied. At pH1 and 80^{o}C the limited total iron dissolution (25% extraction after 180 hours) however is independent of oxalate concentration in the range 0.1-0.5M, although during the early stage of leaching a higher oxalate concentration did enhance the dissolution rate. The coarse grind and low original iron content in the leach could be the reason for the low iron removal overall. In this study, the two major phases reported were iron oxides (no identification of major phases given) and chromium ferrites. A small amount of iron (5.5%) was also present in the silica sand as magnetite.

Ambikadivi and Lathithambika [2000] found oxalic acid (0.05-0.15M) to be the best extractant for removing iron from a kaolinite material finely ground to 90% passing 2 microns. The dissolution was found to increase with acid concentration within the range 0.05-0.15M studied. Both oxalate and hydrogen ion concentrations were increased in this case. The pH of the leach systems was not controlled nor any measurement given for the solution pH, making it harder to interpret their results. Using a 0.15M oxalic acid approximately 70% of the iron could be extracted from a kaolinite slurry (20%w/v) containing 0.93% iron oxide (of goethite and hematite phases) at 100^{o}C within 90 minutes. The iron oxide concentration in the leach is equivalent to 1.86g/L Fe_2O_3. The high loading and fine grind of the raw material could be the reasons explaining the faster iron dissolution found in this study compared to others reported by Taxiarchou et al [1997a, b].

Lee and co-workers [1997] used 0.19-0.48M oxalic acid to dissolve hydrated iron oxide and iron aluminium silicate from a clay material which was separated into two size fractions. Iron dissolution reached 90% for a 20% slurry within 60 minutes using 0.19M oxalic acid for the finer fraction (<150 microns) containing 0.56% Fe_2O_3. The coarser fraction (>150 microns) containing 1.06% Fe_2O_3 achieved a lower iron removal, reaching a steady state of only 78% after 1 hour of leaching. Both treatment yielded clay materials of acceptable iron content (approximately 0.1%) and required whiteness (90% ISO). Although the pH was not measured or controlled it was expected that the liquor pH is <pH1 at the oxalic acid concentration range studied (0.19-0.48M).

The presence of Fe^{2+} was found to significantly enhance the leaching of iron extraction from silica sand at a temperature even as low as 25^{o}C [Taxiarchou et al, 1997a]. Ferrous oxalate however is oxidized quickly by air during the dissolution and in general an induction period of a few hours was observed unless a strong acidic environment (<pH1) or an inert atmosphere is maintained. Maintaining the high level of ferrous oxalate in the leach liquor using an inert gas will enhance the reaction kinetics according to these authors.

The above studies on a wide variety of iron oxides seem to present conflicting information on the oxalic acid leaching system. Taxiarchou and co-workers' studies [1997a, b] on hematite and iron oxides other than magnetite contradict with others who reported that dissolution of magnetite and goethite by oxalic acid reaches a maximum rate at around pH2.7-3.0, outside which range the dissolution rate dropped dramatically [Cornell and Schindler, 1987; Panias et al, 1996]. Lee and co-workers [1999] confirmed that the leaching of 3 g/L pure hematite (98.2% purity, 105-140 micron size range) using 0.048-0.48M oxalic acid at 80-100^{o}C passed through a maximum peak at pH2.5. Dissolution of hematite was found to be slower than magnetite ($FeO.Fe_2O_3$) and other hydrated iron oxide such as goethite (α-FeOOH) and lepidochrosite (γ-FeOOH) and iron hydroxide ($Fe(OH)_3$).

The dissolution of iron oxide is believed to take place via a photo-electrochemical reduction process, involving a complicated mechanism of charge transfer between the predominant oxalate species, namely ferric oxalate, $Fe(C_2O_4)_3^{3-}$, ferrous oxalate, $Fe(C_2O_4)_2^{-}$ acting also as an auto-catalyst, the oxalate ligand on the iron oxide surface [Taxiarchou et al, 1997b; Blesa et al, 1987]. In the absence of light the reaction proceeds slowly which complicates the reaction further.

It has been agreed by several workers [Panias et al, 1996; Oh et al, 1998] that the optimum pH for dissolving iron oxide is pH2.5-3.0. The solution pH governs the distribution of various oxalate ions in the leach system. Below pH1.5, oxalic acid exists mainly as $H_2C_2O_4$, whereas $HC_2O_4^{-}$ is the most predominant species (mole fraction >0.92) at pH2.5-3.0. Above pH4, $C_2O_4^{2-}$ is the predominant species. The speciation of Fe(III) oxalate and Fe(II) oxalate is also governed by pH and total oxalate concentration [Panias et al, 1996]. For a solution having pH>2.5 and an oxalate concentration higher than 0.1M, the most predominant Fe(III) complex ion existing is $Fe(C_2O_4)_3^{3-}$. At these conditions (pH>2.5 and oxalate concentration higher than 0.1M) the predominant Fe(II) complex species is $Fe(C_2O_4)_2^{2-}$.

Earlier workers [Panias et al, 1996; Taxiarchou et al, 1997a,b] suggested a reaction mechanism involving an autocatalytic process involving Fe(II) which can be represented by the following reaction:

$$Fe(III)\text{-}O_{(solid)} + 2H^{+} + L^{n-} + [Fe(II)\text{-}L]_{aq}^{(n-2)-} \rightarrow H_2O + [Fe(II)\text{-}L]_{(solid)}^{(n-1)-} + [Fe(III)\text{-}L]_{aq}^{(n-3)-}$$

(Eq. 1)

The subsequent steps involved electron transfer in which the ligand is oxidized and the soluble $[Fe(III)\text{-}L]_{aq}^{(n-3)-}$ is reduced to $[Fe(II)\text{-}L]_{aq}^{(n-2)-}$ in the process. The autocatalytic dissolution of $>[Fe(II)\text{-}L]_{(solid)}^{(n-1)-}$ by soluble Fe(III) complex also takes place forming Fe(II) oxalate and activates the surface of the iron oxide solid.

Many past studies evaluated the dissolution of iron from host minerals such as silica sand or clay materials. Emphasis was placed on the reaction temperature and solution chemistry such as pH, Fe(II) and oxalate concentration while little attention was paid on the characteristics of iron oxide such as mineral phase, surface area and particle size used during leaching, which are equally important in governing the heterogeneous reaction kinetics. The interpretation of these data for plant application is therefore limited, especially in view of the slow dissolution of hematite compared to other iron oxides. This study was therefore conducted to evaluate the characteristics of dissolution of hematite and how its dissolution kinetics could be improved by adding magnetite into the leach.

EXPERIMENTAL

The oxalate leachant was prepared by dissolving known quantities of oxalic acid in distilled water. Ammonium hydroxide was added slowly to adjust the pH to the value required. The liquor (250 mL volume) was then transferred to a round flask (1 litre capacity) which was brought to test temperatures using a heating mantle before the iron oxide sample (3-4 g/L iron oxide) was added. Each reaction run was conducted for 2 hours and samples were taken out at 10, 30, 60 and 120 minutes for iron analysis. For each sample, 1ml of liquor was withdrawn from the reactor into a 25ml of volumetric flask. This was followed by addition of 1ml of 1M ammonium acetate, 1ml of 10% hydroxylamine hydrochloride and 10ml of 0.3% phenanthroline. Samples were then subjected to Fe(II) analysis by absorption measurement at 510nm (adsorption peak for Fe(II)-phenanthroline complex), following a calibration curve produced with standards prepared using the same technique. Total iron was then

determined by ICP analysis. All chemicals used in this study were of analytical grade. Hematite sample used in the study was 98.2% pure with main contaminants as silica and aluminium oxide. The hematite material was wet-screened using appropriate sieves and several size fractions between fine (105-149 μm) and coarse sizes (0.5-1.4mm) were isolated. Magnetite used for the study had a purity of 99.3%. The solution pH was controlled at pH2.5 or pH3.0 using ammonium hydroxide.

RESULTS AND DISCUSSION

Although several studies have demonstrated the effect of various parameters influencing the leaching reaction, strict control of the experimental conditions, especially on particle size was not implemented. The modeling of the reaction kinetics from these data therefore is restricted. Another issue of concern is that iron oxide can be dissolved in oxalate via two mechanisms, either via chemical dissolution where Fe(III) oxalate will be formed first, or if a reductive dissolution is more predominant, then Fe(II) oxalate is the major product.

Dissolution of hematite

A study on the electrochemical dissolution of hematite (α-Fe_2O_3), maghemite (γ-Fe_2O_3), goethite (α-FeOOH) and lepidochrocite (γ-FeOOH) in hydrochloric and oxalic acid using voltammetry [Cepria et al, 2003] indicated that the hydroxy-oxides of FeOOH can be reduced also via soluble Fe(III) species at 0.6-0.8V (vs Ag-AgCl), whereas hematite and maghemite dissolves only via direct reduction of the solid at -0.55V to -0.60V (vs Ag-AgCl). These potentials were determined as peaks on voltammograms conducted with stationary electrodes made from these iron oxides and hydroxyl-oxides. This fundamental study on the electrochemical behaviour of different types of iron oxides confirms the electrochemical nature of hematite reductive dissolution. It further explains why it is easier to dissolve hydroxyl-oxides such as goethite where dissolution can take place via both reduction (solid and aqueous species) and complexation [Stumm and Furrer, 1987] whereas hematite dissolves mainly via solid reduction [Banwart et al, 1989]. Oxalate can easily be a reductant for such a process, as shown in its Eh-pH diagram [Pourbaix, 1958].

For all conditions studied, analysis of the samples taken through out the course (2 hours) of the reaction confirmed that there was no Fe(III) existing in the solution. This implied that the dissolution of hematite was via a reductive mechanism. The overall reaction was therefore a redox reaction, formed by two half cells:

Oxidation of oxalate to form carbonic acid or carbon dioxide:

$$HC_2O_4^- = H^+ + 2CO_2 + 2e^- \quad \text{(Eq. 2)}$$

Reduction of hematite forming Fe(II) oxalate:

$$2H^+ + Fe_2O_3 + 4HC_2O_4^- + 2e^- = 2Fe(C_2O_4)_2^{2-} + 3H_2O \quad \text{(Eq. 3)}$$

The dissolution reaction is therefore:

$$H^+ + Fe_2O_3 + 5HC_2O_4^- = 2Fe(C_2O_4)_2^{2-} + 3H_2O + 2CO_2 \quad \text{(Eq. 4)}$$

The overall reaction indicates that species involved in the leaching would be hydrogen ions, oxalate and iron oxide (hematite particles). At the optimum pH2.5-3.0 temperature, concentration of oxalate and the particle size (and/or surface area) of hematite will determine the reaction kinetics. The charge transfer mechanism could also be assisted by the presence of Fe(II) as experienced in previous studies.

The dissolution of hematite by oxalic acid at pH2.5 and 100^{o}C is shown in Fig. 1. The presence of the induction period (first 15 minutes) was also observed in this case, especially at a high oxalate concentration. The stoichiometric requirement (5:1 molar ratio) for dissolving 0.0184 mole/L Fe_2O_3 is 0.092 mole oxalate/L in this case. Therefore the concentration range of oxalic acid studied corresponded to 0.52x, 1.03x, 2.06, 3.11x and 4.14 times the stoichiometric requirement, indicating that except for the experiment at 0.048M oxalate, all other conditions had more than enough acid required for the dissolution.

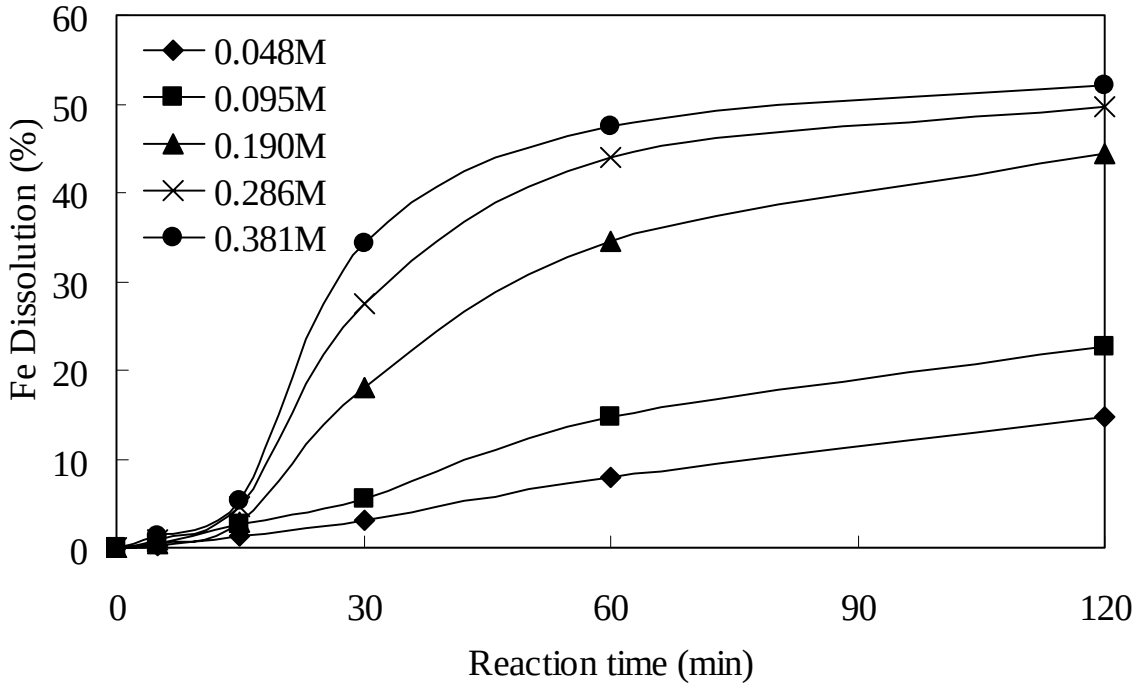

Fig. 1: Dissolution of hematite at various oxalic acid concentrations (0.048-0.381M) (105-140 μm size range, 100°C, 0.0184 mole/L Fe_2O_3, pH2.5).

Yet the dissolution stalled after 30 minutes, leading to less than 50% dissolution after 2 hours. Considering the excess of acid used, the decreasing rate of dissolution indicates that the hematite surface must have been blocked by a product layer.

The dissolution of hematite by oxalic acid (2.06x stoichiometric requirement) at different temperatures is shown in Fig. 2. The finding on the effect of temperature by other workers was confirmed in that a reasonable reaction rate can only be achieved at temperatures above 80°C.

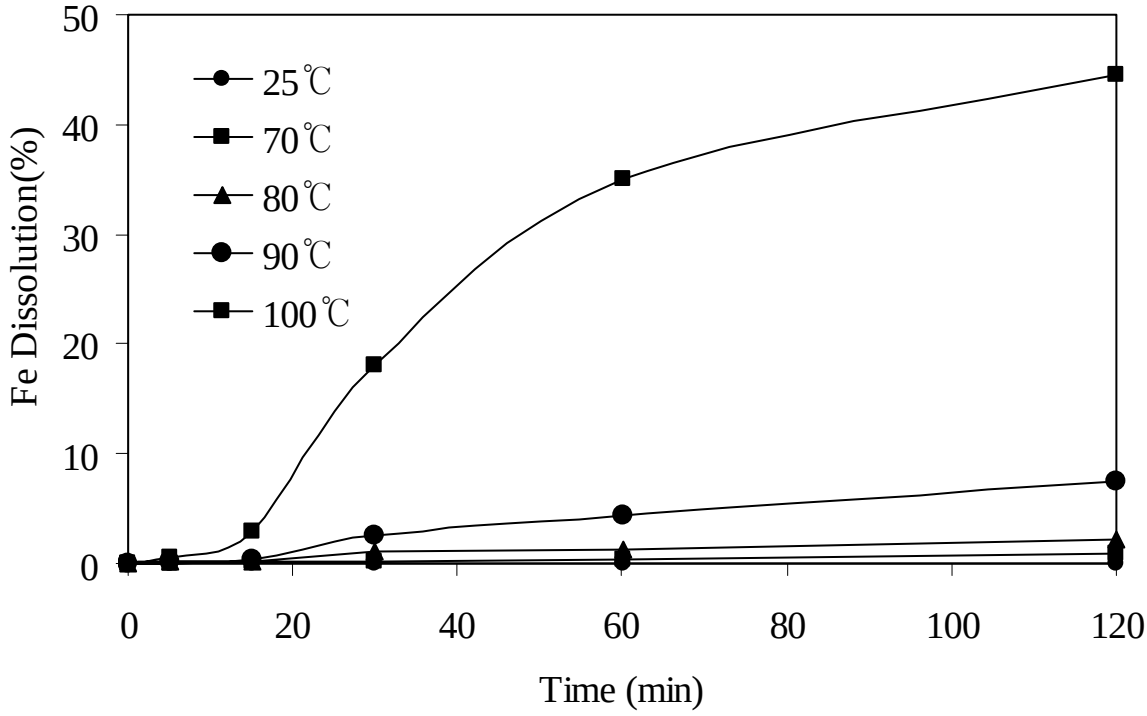

Fig. 2: Effect of temperature on the dissolution of hematite(25-100°C) (0.0187 mol/L Fe_2O_3, 0.19M oxalic acid, pH2.5).

These controlled experiments yielded reliable data for reaction kinetic modeling. For heterogeneous systems the reaction kinetics is usually based on the shrinking core model. For such systems, the solid particles are assumed to be spherical which shrink as the reaction interface move to the inner core of the particles. The reaction kinetics can then be controlled by either (i) the diffusion of reactants through a product layer formed during the reaction, or (ii) the kinetic step of the electrochemical reaction involved during leaching

An attempt was made to fit the above kinetic data for pure hematite into a shrinking-core model. For a reaction controlled by the diffusion through an inert product layer, the rate expression (named PLD expression) for the system studied at a constant pH2.5 [Levenspiel, 1972] is as follows:

$$\text{(PLD):} \qquad 1-(2/3)x - (1-x)^{2/3} = (V/r_o^2)\, k\, [Ox]^m\, t \qquad \text{(Eq. 5)}$$

where:

x	;	fraction of dissolution
V	:	volume of solution, cm^3
r_o	:	initial average radius of the particles, cm
[Ox]	:	oxalate concentration, mol/L

Plots of PLD expression vs time of data from Figs. 1 yield straight lines with regression coefficient R^2 higher than 0.90 for most conditions except for higher concentrations of oxalate where deviation from linearity was observed after 60 minutes. The same plot (Fig. 2) showing the effect of temperature in the range 70-100^oC in which data could be measured accurately also yields straight lines with regression coefficient R^2>0.95.

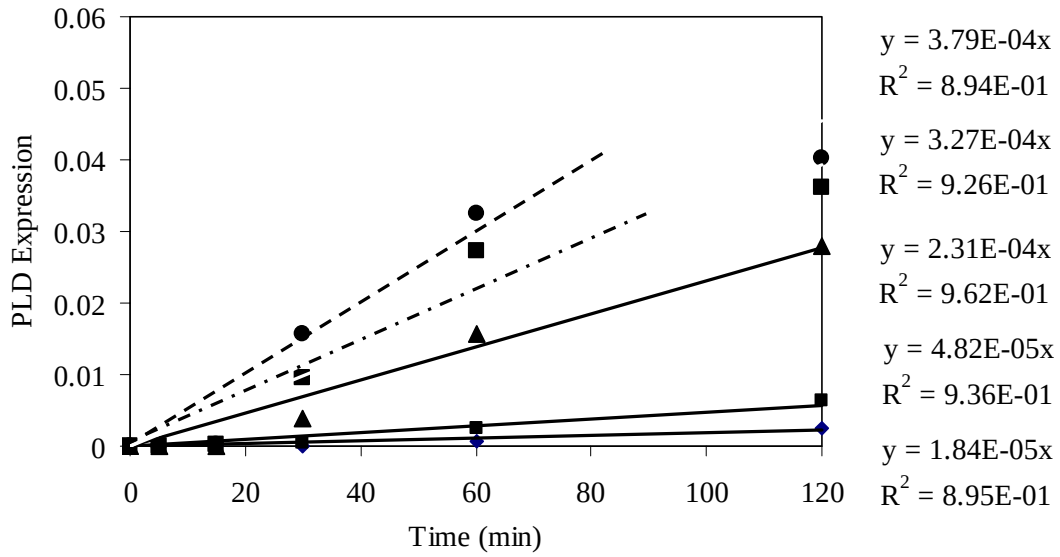

Fig. 3: Plot of PLD expressions vs time for the dissolution of hematite at different oxalate concentrations (0.048M, 0,095M, 0.19M, 0.286M and 0.381M) (0.0187 mole/L Fe_2O_3, pH2.5, 100^oC).

The slopes of the above lines (slope1) were calculated corresponding to (V/r_o^2) k $[Ox]^m$, from which a plot of log(slope1) vs log[Ox] was constructed (V/r_o^2 is constant in this case) A straight line from this plot (R^2 of 0.97) yielded the value of m=1.5 for the rate equation (Eq. 5) above (Fig. 4).

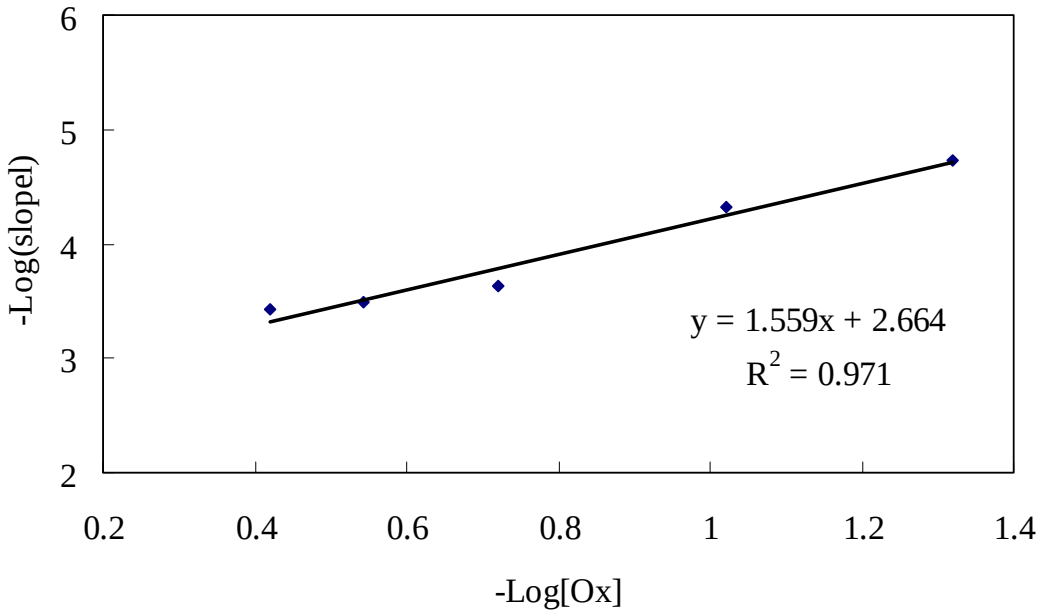

Fig. 4: Plot of slope1 (V/r_o^2 k $[Ox]^m$) vs log[Ox] showing the slope m as 1.5 for rate equation Eq. 5.

An Arrhenius plot was constructed showing the variation of Log(slope1) vs (1/T) where T is temperature (T in K) in the range 70-100^{o}C, yielding a straight line as shown in Fig. 5, from which slope the activation energy was found to be 140kJ/mole hematite dissolved. This activation energy seems to be much higher than those expected for liquid diffusion (where values around 25 kJ/mol were determined) or for diffusion through a porous media (activation energy up to 50 kJ/mol). The implication for such high value is discussed in the next section.

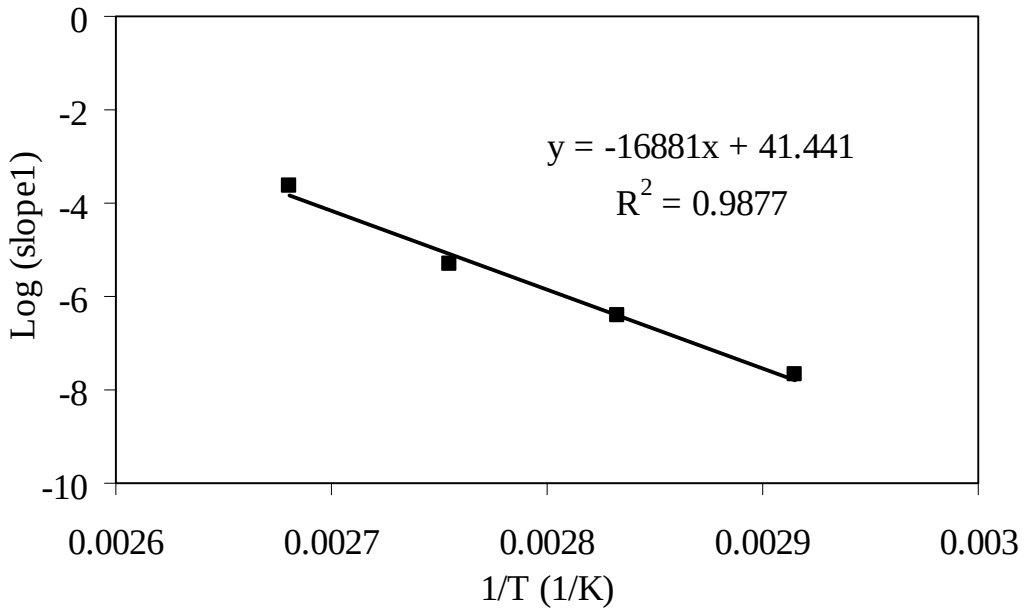

Fig. 5: Arrhenius plot for the dissolution of hematite (70-100^{o}C, 0.0187 mol/L Fe_2O_3, 0.19M oxalic acid, pH2.5.

Although the initial dissolution of hematite expressed as Eq. 2 does not show the formation of a solid layer product, it is believed that the changes in solution chemistry at the reaction interface promote the formation of FeC_2O_4(s), which has a K_{sp} value of 2.0×10^{-7} (corresponding to an equilibrium concentration of oxalate or Fe(II) of 4.5×10^{-4} mol/L at saturation). As the reaction proceeds, the pH at the solid-solution interface must have risen well above pH4.0 from the pH2.5-3.0 of the bulk solution due to the consumption of hydrogen ions for the dissolution. As the pH rises above pH4, oxalate would mainly exist as $C_2O_4^{2-}$. This is compounded by the fact that soluble Fe(II) produced by the dissolution process would accumulate near the reaction interface, therefore creating favourable conditions for the formation of solid ferrous oxalate. At 40% dissolution, the amount of Fe(II) formed already reached 0.015M Fe(II) (that is 40% of 0.0187mole/L x 2 stoich.).

On Eh-pH diagrams re-produced in Fig. 6, the predominance of $FeC_2O_{4(s)}$ is clearly shown for the system containing 0.21M oxalate (right-sided graph). Without oxalate, Fe_2O_3 and Fe_3O_4 will be dissolved forming Fe^{2+}, whereas in the presence of oxalate solid $FeC_2O_{4(s)}$ is the predominant species existing over a wide range of pH from acidic zone to >pH7 in the potential range where dissolution of iron oxides takes

place. This implies that solid $FeC_2O_{4(s)}$ will be finally formed when the oxalate concentration is 0.21M (as shown in this graph) or higher.

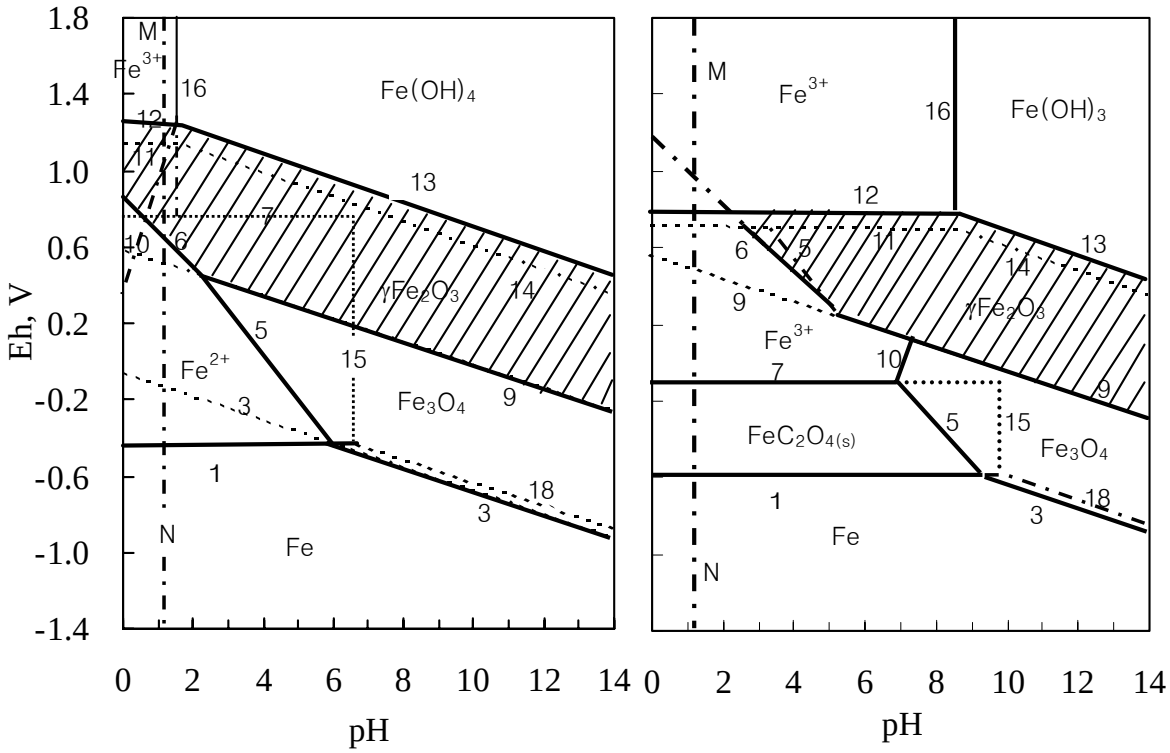

Fig. 6: Eh-pH diagrams for systems: (a) Fe-H_2O and (b) Fe-H_2O-0.21 M $H_2C_2O_4$ (from Sukhotin and Khentov, 1980).

Dissolution of hematite/magnetite mixtures

Industrial practices require the processing of materials which are not always ground to micron sizes as in most fundamental studies. Due to the slow reaction rate most studies did not evaluate the dissolution of coarse hematite in the mm size ranges. This study therefore evaluated materials ground and sized into different fractions in the range 0.50-1.4mm.

The slow start of the reaction (induction period) was also observed (Fig. 7) during the dissolution of pure hematite at 100^{o}C. The total dissolution only reached 2-3% after 2 hours of leaching.

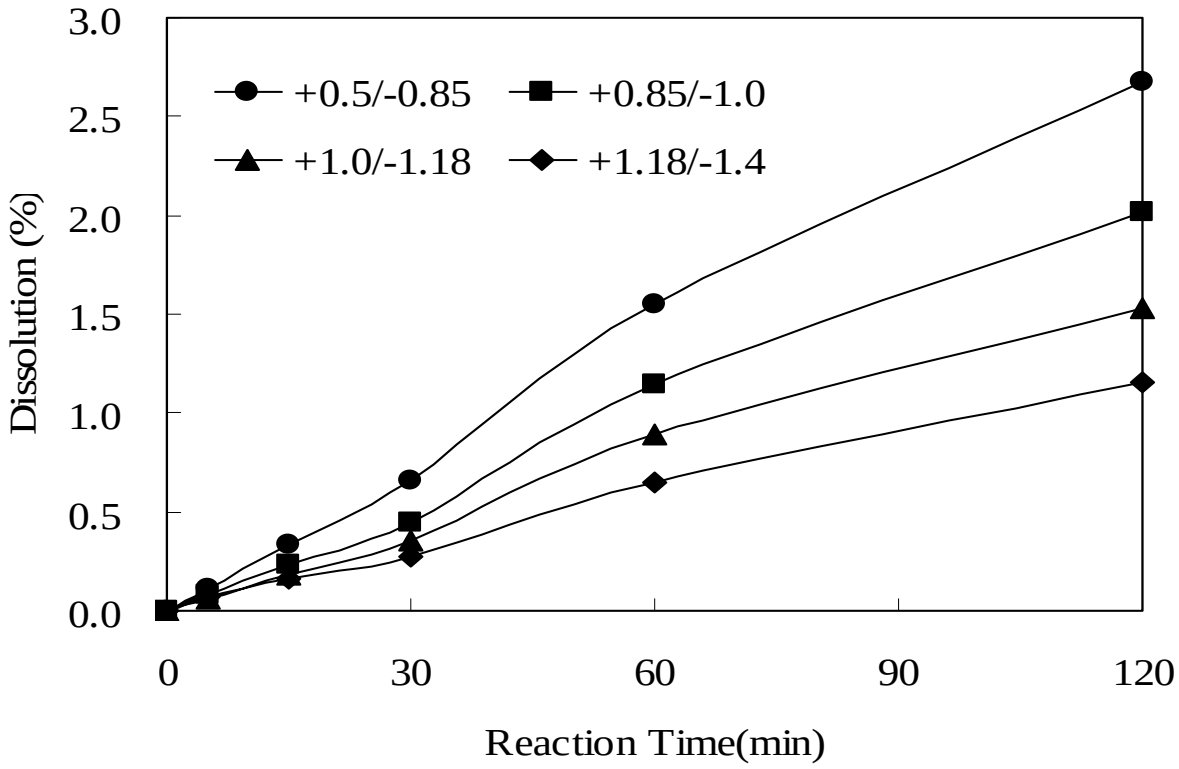

Figure 7. Dissolution vs time plots for different size fractions(mm) of hematite at 100°C, 5:1 oxalate/iron oxide molar ratio (stoichiometric requirement), pH 3.0, 0.025 mol/L Fe_2O_3).

However a significant improvement of the dissolution rate was observed as magnetite was added to the leach system as shown in Fig. 8. Dissolution reached 15-25% within 2 hours when approximately 10% of magnetite (w/w) was added under the same conditions. The dissolution of iron oxide mixtures did not follow the slow induction period as with pure hematite, indicating the beneficial effect of FeO in the leach system.

Other coarser grind was also leached at a reasonable rate as shown in Fig. 8. The "product layer diffusion control" nature of the reaction kinetics was also confirmed for the dissolution of hematite-magnetite mixtures as shown in Fig. 9 for the different size fractions tested. Linearity of all lines plotted on Fig. 9 is confirmed with good regression where coefficients R^2 are generally >0.97.

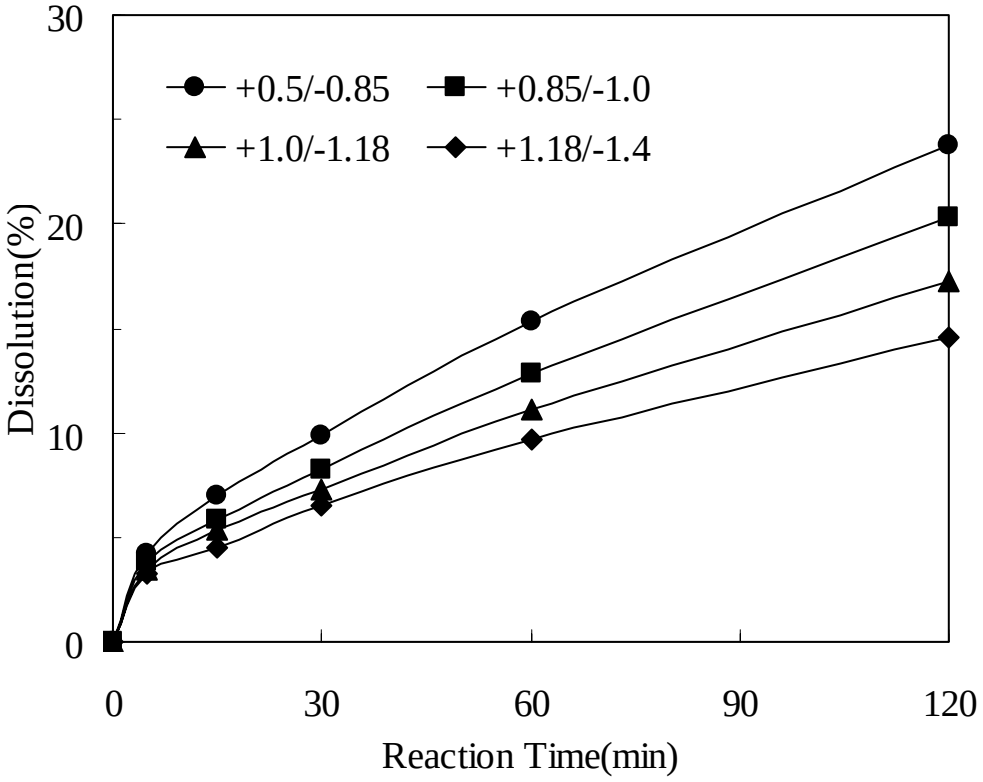

Figure 8. Dissolution vs time plots for mixtures of hematite/magnetite at different size ranges at 100°C, 5:1 oxalate/iron oxide molar ratio (stoichiometric requirement), pH 3.0, 0.025 mol/L (4g/L) Fe_2O_3 + 0.0022mole/L(0.4 g/L) Fe_3O_4.

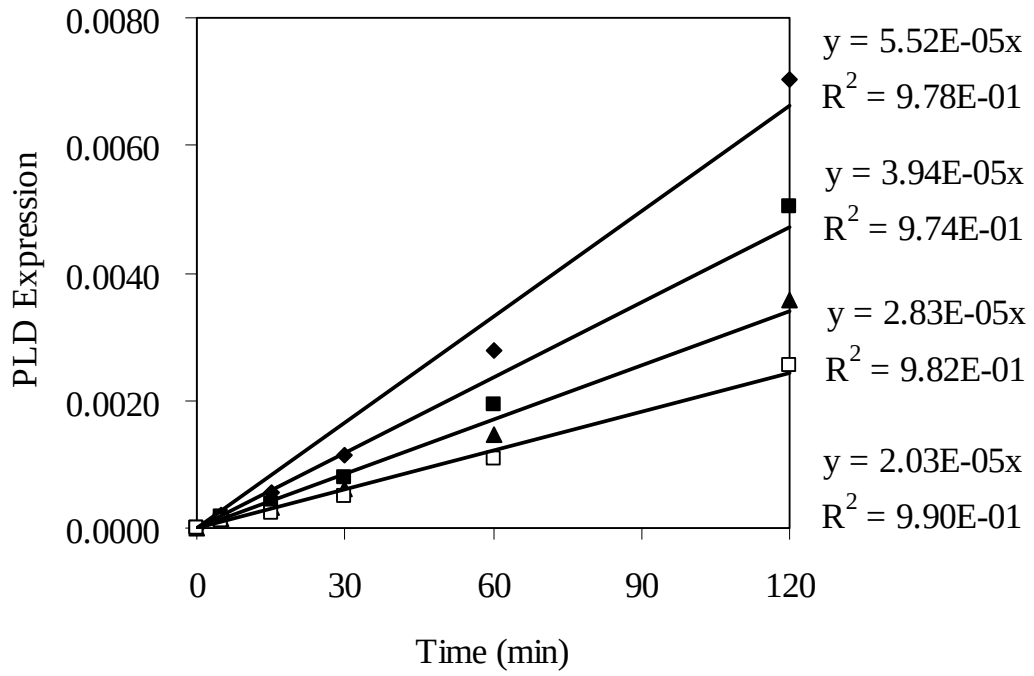

Fig. 9: Plots of PLD expression vs time for the dissolution of hematite-magnetite mixtures of different size fractions (-0.5+0.85mm, -0.85+1.0mm, -1.0+1.18mm, 11.18+1.4mm) at 100°C, 5:1 oxalate/iron oxide molar ratio (stoichiometric requirement), pH 3.0, 0.025 mol/L (4g/L) Fe_2O_3 + 0.0022mole/L(0.4 g/L) Fe_3O_4.

The critical effect of temperature was also observed as shown in Fig. 10. For the -0.5+0.85 mm size range, the reaction proceeded reasonably well only at 100^{o}C. The linearity of PLD plots with regression coefficient R^2 within 0.91-0.99 was also observed as shown in Fig. 11, confirming the controlling mechanism as diffusion through a product layer.

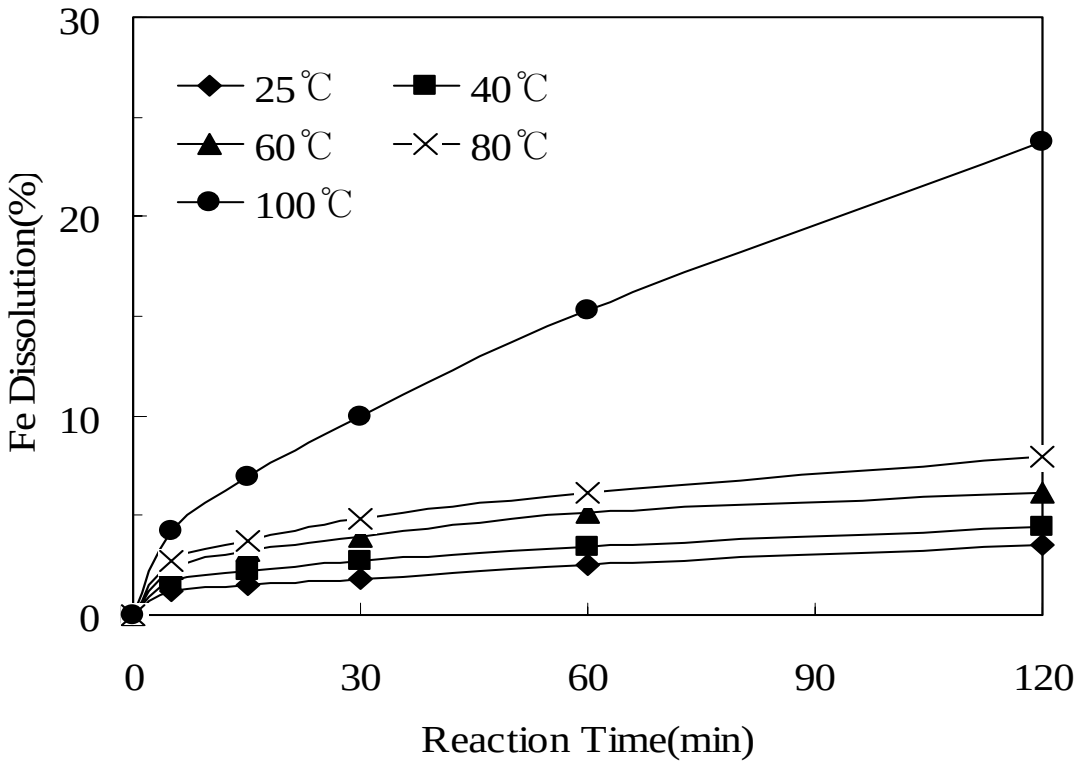

Fig. 10: Dissolution of hematite-magnetite mixture (-0.50+0.81mm size fraction) at different temperatures (70,80, 90 and 100^{o}C), 5:1 oxalate/iron oxide molar ratio (stoichiometric requirement), pH 3.0, 0.025 mol/L (4g/L) Fe_2O_3 + 0.0022mole/L(0.4 g/L) Fe_3O_4.

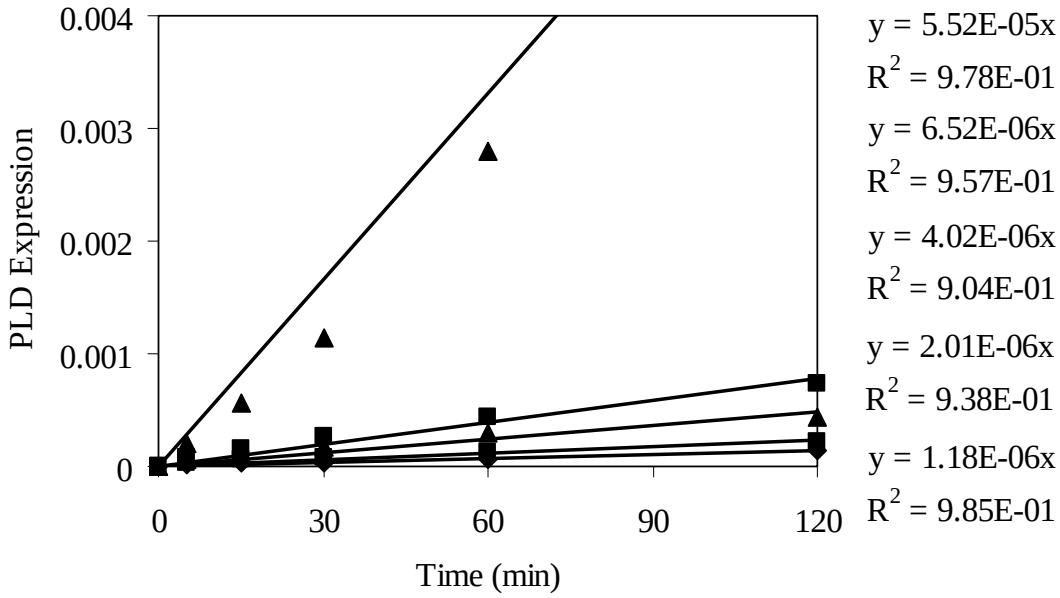

Fig. 11: Plots of PLD expression vs time for the dissolution of hematite-magnetite (-0.50+0.81mm size fraction) at different temperatures: 25, 40, 60, 80 and 100^{o}C, 5:1 oxalate/iron oxide molar ratio (stoichiometric requirement), pH 3.0, 0.025 mol/L (4g/L) Fe_2O_3 + 0.0022mole/L(0.4 g/L) Fe_3O_4.

The effect of temperature could also be seen in detail from the Arrhenius plot (Fig. 12) in which the slopes of straight lines from Fig. 11 are plotted against 1/T (T in degree K). There seems to be a change in slope of the Arrhenius plot corresponding to an increase in activation energy of the leaching. Linearity seems to fit best for the temperature range 25-80^{o}C. The activation energy for the dissolution of hematite-magnetite mixtures by oxalate at pH3.0 was found to be 12.2 kJ/mol in this temperature range. Above this temperature range, the activation energy seems to increase dramatically by the sharp upward turn in the Arrhenius plot. Taking the last 2 points of the Arrhenius plot (at 80 and 100^{o}C) for the calculation, a value of 50.7 kJ/mole was obtained. The only reason which caused this shift could the gradual building up of the passivating layer of iron oxalate (FeC_2O_4) with time when a conversion of >20% was reached.

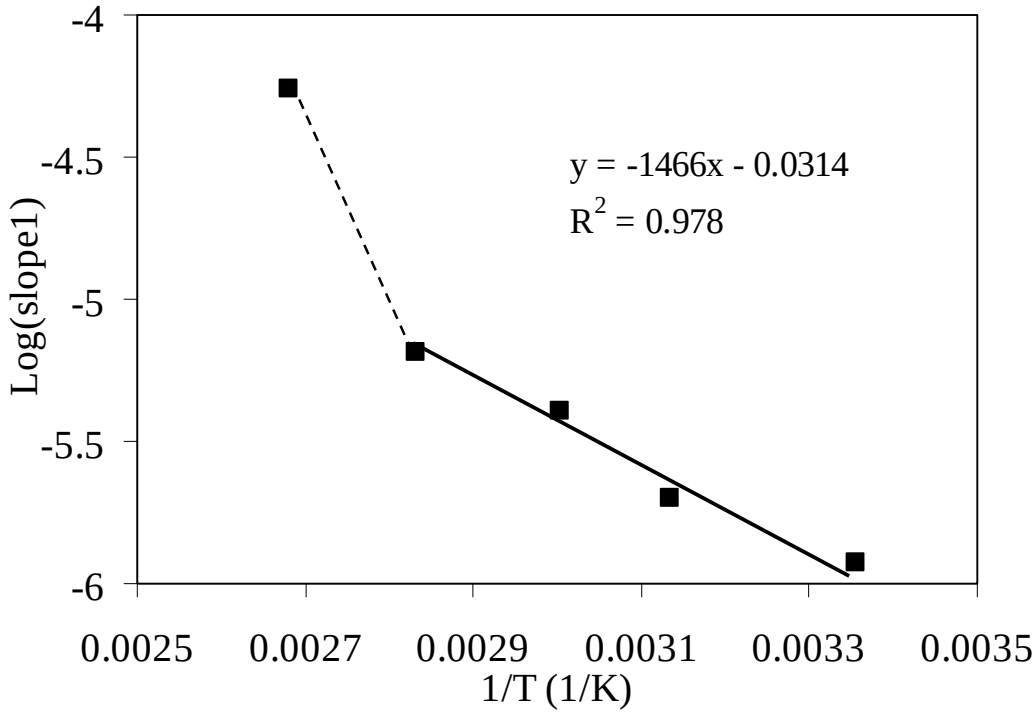

Fig. 12: Arrhenius plot for the dissolution of hematite-magnetite (-0.50+0.81mm size fraction) at different temperatures: 25, 40, 60, 80 and 100^{o}C, 5:1 oxalate/iron oxide molar ratio (stoichiometric requirement), pH 3.0, 0.025 mol/L (4g/L) Fe_2O_3 + 0.0022mole/L(0.4 g/L) Fe_3O_4). Values of Slope1 are taken from Fig. 9.

CONCLUSIONS

Kinetic studies using hematite and magnetite showed improvement achieved when both are used in a mixture. The dissolution of hematite at pH2.5-3.0 follows a "product layer diffusion control" shrinking core model. The rate expression relating conversion to time which can be expressed as:

$$1-(2/3)x - (1-x)^{2/3} = (V/r_o^2)\, k\, [Ox]^m\, t$$

shows linearity for pure hematite systems, where m is 1.5. This model also fits the systems in which a mixture of hematite and magnetite was used.

The dissolution rate was significantly improved when magnetite was added to the leaching system. Reasonable reaction rates could only be achieved at high temperatures (80-100°C). Coarse hematite (in the particle size range 0.50-1.45mm) could only be dissolved at a reasonable rate only when magnetite was added.

REFERENCES

Ambikadevi, V. R. and Lalithambika, M., (2000), Effect of Organic Acids on Ferric Iron Removal from Iron-stained Kaolinite, Applied Clay Science Vol. 16, p.133-145.

Banwart, S., Davies, S. and Stumm, W., 1989, The role of oxalate in accelerating the reductive dissolution of hematite(α-Fe_2O_3) by ascorbate, Colloids and Surfaces, Vol. 39, p. 303-309.

Blesa, M. A., Marinovich, H. A., Baumgartner, E. C. and Maroto, A. J. G., (1987), Mechanism of Dissolution of Magnetite by Oxalic Acid - Ferrous Ion Solutions, Inorg. Chem., Vol. 26, p. 3713-3717.

Blesa, M. A., Morando, P. J. and Regazzoni, A. E., (1994), Chemical Dissolution of Metal Oxides, CRC Press Inc. p. 269-308.

Borghi, E.B., Regazzoni, A.E., Maroto, A.J.G. and Blesa, M.A., 1989, Reductive Dissolution of Magnetite by Solutions Containing EDTA and Fe(II): J. Colloid Interface Sci., Vol. 130, No. 2, p. 299-310.

Cepria, G., Uson, A., Perez-Arantegui, J. and Castillo, J.R., 2003, Identification of iron (III) oxide and hydroxyl-oxides by voltammetry of immobilized microparticles, Analytical Chim. Acta, 477, 157-168.

Chiarizia, R. and Horwitz, E. P., (1991), New Formulations for Iron Oxides Dissolution, Hydrometallurgy, Vol. 27, p. 339-360.

Cornell, R. M. and Schindler, P. W., (1987), Photochemical Dissolution of Goethite in Acid/Oxalate Solution, Clays Clay Miner., Vol. 35, No. 5, p. 347-352.

Cornell, R. M. and Schwertmann, U., (1996), The Iron Oxides, VCH Publishers, New York (USA), p. 175.

Frenier, W. W. and Growcock, F. B., (1984), Mechanism of Iron Oxides Dissolution, A Review of Recent Literature, Corrosion NACE Vol. 40, p. 663-668.

Jepson, W. B., (1988), Structural Iron in Kaolinites and in Associated Ancillary Minerals, In; Stucki, J. W., Goodman, B. A. and Schwertmann, U., (Eds), Iron in Soils and Clay Minerals, D. Reidel Publ. Co., Dordrecht, Holland, NATO ASI Ser, Vol. 217, p. 467-536.

Lee, S.O., Kim, W.T., Oh, J.K. and Shin B.S., 1997, Iron removal of clay mineral with oxalic acid, J. of Min. Met. Inst of Japan, 113, 847-851.

Lee, S.O., Oh, J.K. and Shin B.S., 1999, Dissolution of iron rust materials using oxalic acid, J. of Min. Met. Inst. of Japan, 115, 815-819.

Levenspiel, O., 1972, Chemical Reaction Engineering, Pub: Wiley International, New York.

Lim-Nunez, R. and Gilkes, R. J., (1987), Acid Dissolution of Synthetic Metal-containing Goethites and Hematites, In: Schultz, L. G., Van Olphen, H. and Mumpton, F. A., (Eds), Proc. Int. Clay Conf. Denver, (1985), Clay Min. Soc. Bloomington, Indiana, p. 197-204.

Mandal, S.K. and Banerjee, P.C., 2004, Iron leaching from China clay with oxalic acid: effect of different physico-chemical parameters, Int. J. Miner. Process., 74, 263-270.

Panias, D., Taxiarchou, M., Paspaliaris, I. and Kontopoulos, A., (1996), Mechanisms of Dissolution of Iron oxides in Aqueous Oxalic Acid Solutions: Hydrometallurgy, Vol. 42, p. 257-265.

Pourbaix, M. (1958), Atlas of Electrochemical Equilibria in Aqueous Solution, Pergamon Press.

Segal, M. G. and Sellers, R. M., (1984), Advances in Inorganic and Bioinorganic Mechanisms, Ed : Sykes, A. G., Academic Press : London, Vol. l. No. 3, p. 97.

Sidhu, P. S., Gilkes, R. J., Cornell, R. M., Posner, A. M. and Quirk, J. P., (1981), Dissolution of iron Oxides and Oxyhydroxides in Hydrochloric and Perchloric Acids, Clays Clay Min., Vol. 29, p. 269-276

Stumm, W. and Furrer, G., 1987, The dissolution of oxides and aluminum silicates: Examples of surface-coordination-controlled kinetics, In: Stumm, W., (Ed.), Aquatic Surface Chemistry J., Wiley and Sons, New York, p. 197-219.

Sukhotin, A. M. and Khentov, A. I., 1980, Anodic Behavior of Iron Oxides and Repassivation of Iron in Acid Solutions, Elektrokhimiya, Vol. 16, No. 7, p. 1037-1041.

Taxiarchou, M., Panias, D., Douni, I., Paspaliaris,I. and Kontopoulos, A., 1997a, Removal of iron from silica sand by leaching with oxalic acid, Hydrometallurgy, 46, 215-227.

Taxiarchou, M., Panias, D., Douni, I., Paspaliaris,I. and Kontopoulos, A., 1997b, Dissolution of hematite in acidic oxalate solutions, Hydrometallurgy, 46, 215-227.

Vaglio, F., Passariello, B., Barbaro, M., Plescia, P. and Marabini, A. M., (1998), Drum Leaching Tests in the Iron Removal from Quartz using Oxalic Acid and Sulphuric Acids, Int. J. Mineral Processing, Vol.54, p.183-200.